Heinrich Heine
Universität
Düsseldorf

Native-state characterization of the melanocortin system

Inaugural-Dissertation

for the attainment of the title of doctor

in the Faculty of Mathematics and Natural Sciences

at the Heinrich Heine University Düsseldorf

Ci Chu

2024

Native-state characterization of the melanocortin system

Inaugural-Dissertation

for the attainment of the title of doctor

in the Faculty of Mathematics and Natural Sciences

at the Heinrich Heine University Düsseldorf

presented by

Ci Chu

from Henan, China

Düsseldorf, April 2024

from the institute for Physical Biology

at the Heinrich Heine University Düsseldorf

Published by permission of the

Faculty of Mathematics and Natural Sciences at

Heinrich Heine University Düsseldorf

Supervisor: Dr. Manuel Etzkorn

Co-supervisor: Prof. Dr. Gunnar Schröder

Date of the oral examination: 15.03.2024

At the end of the storm

There is a golden sky

Contents

Summary 3

Zusammenfassung 4

Abbreviations 5

List of publications connected to this thesis 6

1. Introduction 7

1.1 G-protein-coupled-receptors (GPCRs) 7

1.1.1 General introduction of GPCRs 7

1.1.2 Allosteric modulation of GPCRs 11

1.2 Human melanocortin-4 receptor (MC4R) 16

1.2.1 MC4R ligands 16

1.2.2 MC4R allosteric regulation 21

1.2.3 MC4R structural properties 22

1.3 Membrane-mimicking systems 23

1.4 Objectives 24

2. Membrane mimicking systems and their applications 25

3. Electroneutral polymers for membrane protein studies 41

3.1 Abstract 42

3.2 Introduction 42

3.3 Associated results 44

3.4 Conclusions 46

4. Characterization of MC4R in native-lipid environment 47

4.1 Abstract 48

4.2 Introduction 48

4.3 Methods 50

4.4 Results and discussion 54

4.5 Conclusions 63

5. Development of novel polymers for membrane protein studies 64

5.2 Abstract 65
5.3 Introduction 65
5.4 Methods 67
5.5 Results and discussion 70
5.6 Conclusions 77
6. Conclusions and perspectives 78
Supplementary Information 79
Acknowledgments 84
Bibliography 85
Eidesstattliche Versicherung 120

Summary

G-protein-coupled-receptors (GPCRs) are highly dynamic and undergo conformational rearrangements induced by the binding of extracellular stimuli, leading to different conformations during activation which in turn interact with intracellular signal transducers and initiate downstream signaling pathways. The functional and structural studies of GPCRs *in vitro* require the extraction from cellular membrane using membrane-mimiking systems. One of the most widely applied membrane mimetics for the solubilization and purification of GPCRs is detergent that has been extensively used for the structural characterization of GPCRs. However, detergents are also known to destabilize GPCRs. Therefore, alternative methods have been developed including lipid bilayer nanodiscs formed by membrane scaffold proteins (MSPs) which provide a more stable environment for the functional and structural studies of GPCRs. Still MSP nanodiscs require the extraction of GPCRs via detergents, and the process of optimizing the reconstitution of GPCRs into MSP nanodiscs is time-consuming and labor-intensive. The functional activities of GPCRs, such as ligand binding and G protein coupling, are regulated by different properties of surrounding phospholipid bilayer, such as hydrophobic mismatch, bilayer thickness, lateral pressure, membrane fluidity, curvature and composition, which are missing or difficult to mimic using detergent micelles or synthetic phospholipids. Of note, the amphiphilic copolymers have attracted great interest and offer several advantages, including the detergent-free extraction and purification of membrane proteins within their surrounding native phospholipids from cellular membrane, leading to the formation of native lipid-bilayer nanodiscs. Among them, the electronetural polymer Sulfo-DIBMA stands out for its interference-free characterization of protein-protein and protein-lipid interactions. While the relatively low extraction efficiency of Sulfo-DIBMA may restrict its application in NMR measurements, which usually require a large amount of proteins.

The melanocortin-4 receptor (MC4R) plays a critical role in the regulation of energy homeostasis and feeding behavior. It is known that the physiological ions strongly affect the function of MC4R, but little is known about the regulation of these metal ions on MC4R in different environments. Herein, in order to evaluate the influence of environment on the functional integrity of MC4R, we performed the solubilization and purification of MC4R expressed in Sf9 cells using different membrane mimicking systems, including detergent micelles, MSP nanodiscs and Sulfo-DIBMA native membrane nanodiscs. The ligand binding affinity for MC4R was examined in various membrane mimetics in the absence and presence of divalent cations. Our data demonstrated that the functional integrity of MC4R is well-preserved in lipid bilayer, especially in the Sulfo-DIBMA native membrane nanodiscs. Moreover, the environment plays an importment role in the allosteric modulation of MC4R.

Given the advantages of native membrane nanodiscs for *in vitro* functional and structural studies of GPCRs without requiring detergents or artificial lipids, and the preservation of lipid-bilayer architecture and packing (e.g., Sulfo-DIBMA), we further introduced and tested a series of new DIBMA variants. We found that the new mPEG$_4$-DIBMA variant exhibits high solubilization efficiency, and does not interfere with ligand-lipid interactions, providing us more choices for the studies of GPCRs in native lipid-bilayer environment using different technologies.

Zusammenfassung

G-Protein-gekoppelte Rezeptoren (GPCRs) sind hochdynamisch und unterliegen konformationellen Umordnungen, die durch die Bindung extrazellulärer Reize hervorgerufen werden. Dadurch entstehen verschiedene Konformationen während der Aktivierung, die wiederum mit intrazellulären Signaltransduktoren interagieren und nachgeschaltete Signalwege initiieren. Die funktionellen und strukturellen Studien von GPCRs in vitro erfordern die Extraktion aus der zellulären Membran unter Verwendung von membranmimetischen Systemen. Eines der am weitesten verbreiteten Membranmimetika für GPCRs sind Detergenzien, welche ausgiebig für die strukturelle Charakterisierung von GPCRs verwendet wurde. Dabei kann das Detergens jedoch in den Transmembranhelix-Bündel eindringen und die GPCRs destabilisieren. Daher wurden alternative Methoden entwickelt. Die durch Membran-Scaffolding-Proteine (MSPs) gebildeten Lipiddoppelschicht-Nanodiscs wurden ebenfalls weit verbreitet eingesetzt und bieten eine stabilere Umgebung für funktionelle und strukturelle Studien von GPCRs. Die Extraktion von GPCRs erfordert jedoch weiterhin den Einsatz von Detergens, und der Prozess der Optimierung der Rekonstitution von GPCRs in MSP-Nanodiscs ist zeitaufwendig und arbeitsintensiv. Die funktionellen Aktivitäten von GPCRs, wie die Ligandenbindung und die G-Protein-Kopplung, werden durch verschiedene Eigenschaften der umgebenden Phospholipiddoppelschicht reguliert, wie z. B. hydrophober Missmatch, Dicke der Doppelschicht, lateraler Druck, Membranfluidität, Krümmung und Zusammensetzung, die in Detergensmizellen oder synthetischen Phospholipiden fehlen oder schwer zu imitieren sind. Amphiphile Copolymere haben großes Interesse geweckt und bieten mehrere Vorteile, einschließlich der detergensfreien Extraktion und Reinigung von Membranproteinen zusammen mit ihren umgebenden nativen Phospholipiden aus der zellulären Membran, was zur Bildung von nativen Lipiddoppelschicht-Nanodiscs führt. Unter ihnen zeichnet sich das amphiphile Polymer Sulfo-DIBMA durch seine störungsfreie Charakterisierung von Protein-Protein- und Protein-Lipid-Interaktionen aus. Während die relativ geringe Extraktionseffizienz von Sulfo-DIBMA ihre Anwendung in NMR-Messungen einschränken kann, die in der Regel eine große Menge an Proteinen erfordern.

Der Melanocortin-4-Rezeptor (MC4R) spielt eine entscheidende Rolle bei der Regulation der Energiehomöostase und des Essverhalten. Es ist bekannt, dass physiologische Ionen die Funktion von MC4R stark beeinflussen, aber wenig ist darüber bekannt, wie die Regulation dieser Metallionen auf MC4R in verschiedenen Umgebungen erfolgt. Hierbei haben wir, um den Einfluss der Umgebung auf die funktionale Integrität von MC4R zu bewerten, MC4R, welcher in Sf9-Zellen exprimiert wurden, unter Verwendung verschiedener Membranmimetiksysteme, darunter Detergensmizellen, MSP-Nanodiscs und Sulfo-DIBMA-Nativmembran-Nanodiscs, untersucht. Die Affinität von Ligandenbindung für MC4R wurde in verschiedenen Membranmimetika in Abwesenheit und Gegenwart von zweiwertigen Kationen untersucht. Unsere Daten zeigten, dass die funktionale Integrität von MC4R in der Lipiddoppelschicht gut erhalten ist, insbesondere in den Sulfo-DIBMA-Nativmembran-Nanodiscs. Darüber hinaus spielt die Umgebung eine wichtige Rolle bei der allosterischen Modulation von MC4R.

Angesichts der Vorteile von nativen Membran-Nanodiscs für in vitro funktionelle und strukturelle Studien von GPCRs ohne den Einsatz von Detergenzien oder künstlichen Lipiden sowie der Erhaltung der Lipiddoppelschichtarchitektur und -anordnung (z. B. Sulfo-DIBMA) haben wir eine Reihe neuer DIBMA-Varianten eingeführt und getestet. Wir stellten fest, dass mPEG4-DIBMA eine hohe Effizienz aufweist und nicht mit Ligand-Lipid-Interaktionen interferiert, was uns mehr Möglichkeiten für die Untersuchung von GPCRs in einer nativen Lipiddoppelschichtumgebung unter Verwendung unterschiedlicher Technologien bietet.

Abbreviations

Only the terms that are highly relevant to this work were included below. More details can be found in the text.

AgRP	Agouti-related protein
ACTH	Adrenocorticotropic hormone
α-MSH	α-melanocyte stimulating hormone
Ago-PAMs	Agonist-positive allosteric modulators
ASD	Allosteric Database
CMC	Critical micelle concentration
CPP	Critical packing parameter
CMT	Critical micelle temperature
CHS	Cholesterol hemisuccinate
cAMP	Cyclic adenosine monophosphate
DLS	Dynamic light scattering
DSC	Differential scanning calorimetry
DMPC	1,2-dimyristoyl-*sn*-glycero-3-phosphocholine
DDM	*n*-Dodecyl-β-D-maltopyranoside
DIBMA	Diisobutylene/maleic acid
ECD	Extracellular domain
ECRs	Extracellular regions
ECL2	Extracellular loop 2
ECL3	Extracellular loop 3
GPCRs	G-protein-coupled-receptors
HFRW	His-Phe-Arg-Trp
MPs	Membrane proteins
MCRs	Melanocortin receptors
MC1R	Melanocortin-1 receptor
MC4R	Melanocortin-2 receptor
MC3R	Melanocortin-3 receptor
MC4R	Melanocortin-4 receptor
MC5R	Melanocortin-5 receptor
MRAP1	Melanocortin-2-receptor accessory protein 1
MRAP2	Melanocortin-2-receptor accessory protein 2
MST	Microscale thermophoresis
MDS	Microfluidic diffusional sizing
MSPs	Membrane scaffold proteins
NAMs	Negative allosteric modulators
NDs	Nanodiscs
NanoDSF	Nano differential scanning fluorimetry
NMR	Nuclear Magnetic Resonance
PAMs	Positive allosteric modulators
SMA	Styrene/maleic acid
TEM	Negative-stain transmission electron microscopy
T_m	Phase transition temperature
THIQ	Tetrahydroisoquinoline

List of publications connected to this thesis

Manuscript 1:

Native-state NMR characterization of membrane systems (*Manuscript submitted*)

Ci Chu, Thibault Viennet, Manuel Etzkorn

Manuscript 2:

Electroneutral Polymer Nanodiscs Enable Interference- Free Probing of Membrane Proteins in a Lipid-Bilayer Environment

Glueck, D., Grethen, A., Das, M., Mmeka, O. P., Patallo, E. P., Meister, A., Rajender, R., Kins, S., Räschle, M., Victor, J., Chu. C., Etzkorn, M., ... & Keller, S. *(2022). Small, 18(47), 2202492. DOI: 10.1002/smll.202202492.*

Manuscript 3:

Functional insights into human Melanocortin-4 Receptor (MC4R) in Native Lipid-Bilayer Nanodiscs (*Manuscript in preparation*)

Ci Chu, Carolyn Vargas, Simon Sommerhage, Gunnar F. Schröder, Sandro Keller, Manuel Etzkorn

Manuscript 4:

Capturing G protein-coupled receptors (GPCRs) into native lipid-bilayer nanodiscs using new diisobutylene/maleic acid (DIBMA) copolymers (*Manuscript submitted*)

Ci Chu, Carolyn Vargas, Maria Carolina Barbosa, Simon Sommerhage, Gunnar F. Schröder, Sandro Keller, Manuel Etzkorn

1. Introduction

1.1 G-protein-coupled-receptors (GPCRs)

1.1.1 General introduction of GPCRs

G-protein-coupled-receptors (GPCRs) are the largest superfamily of cell surface membrane proteins in mammalian cells. All GPCRs share the conserved architecture of seven transmembrane (7TM) helical domains. Approximately 800 membranes are encoded by 2% of the human genome and targeted by approximately 475 small-molecule medicines (more than 30% of all approved drugs by the Food and Drug Administration (FDA) binding to 108 GPCRs) on the market, making them the largest intensively studied targets for drug development and highlighting their vital roles in human health and disease [1,2]. According to the amino acid sequence similarities and physiological features, GPCRs identified in vertebrates and invertebrates have been categorized into six classes, of which only four classes are found in human GPCR family, i.e., class A (rhodopsin-like receptors), class B (B1/secretin and B2/adhesion receptors), class C (glutamate receptors) and class F (frizzled or smoothened receptors). In the GRAFS classification system, human GPCRs have been divided into five families based on the phylogenetic tree, including glutamate (G), rhodopsin (R), secretin (S), frizzled/taste2 (F) and adhesion (A). GPCRs have been implicated in a plethora of diseases, such as cancer, obesity and Alzheimer's disease [3–5]. Besides, GPCRs are highly dynamic and perform conformational changes during activation, making them the most promiscuous druggable receptors [6]. GPCRs are highly dynamic and recognize a variety of extracellular stimuli, such as photons, hormones, peptides, proteins, lipids, neurotransmitters, purines, amines, chemokines and ions, leading to conformational rearrangements during activation which in turn interact with intracellular signal transducers, such as heterotrimeric G proteins ($G\alpha_i$, $G\alpha_q$, $G\alpha_s$ and $G\alpha_{12/13}$), G protein-coupled receptor kinases (GRKs) and β-arrestins, thus initiate downstream signaling pathways through the cellular second messengers such as cyclic adenosine monophosphate (cAMP) and mediate a wide variety of physiological processes [7].

The Class A rhodopsin-like family containing 719 members, is the largest group of GPCRs in humans and mainly divided into two subgroups, i.e., sensory receptors activated by smell or light, and non-sensory receptors activated by ligands, such as peptides, hormones and neurotransmitters. The class A family is characterized by its short disordered N-terminal domain (< 50 amino acids) such as the human β_2-adrenergic receptor (β_2AR) [8–10], but with exceptions such as the glycoprotein hormone receptors (GPHRs) which have a large and well-ordered N-terminal extracellular leucine-rich repeats (LRRs) hormone binding domain where the hormone can be gripped in a "hand-clasp" manner by the extracellular domain (ECD) [11–13]. Activation of class A subfamily receptors involves the rearrangement of the conserved structural motifs, such as the D/ERY motif in intracellular end of TM3, the CWxP in the middle of TM6, the NPxxY in intracellular end of TM7 and the Na^+ pocket. In addition, several highly conserved residues, such as $Arg^{3.50}$, $Trp^{6.48}$ and $Trp^{7.53}$ (superscript numbers correspond to the Ballesteros-Weinstein nomenclature [14]), seem to act as micro-switches regulating GPCR signaling [15,16]. Due

to their abundance and extensive physiological and pathological functions, more than 150 class A GPCRs are targets by therapeutic agents [17,18].

The Class B receptors are divided into secretin and adhesion subfamilies. The secretin receptors are further classified into five subfamilies, including (i) five glucagon receptors (GCGRs), (ii) two vasoactive intestinal peptide receptors (VIPRs) and the pituitary adenylate cyclase-activating peptide receptor (PAC1), (iii) two parathyroid hormone receptors (PTHRs), (iv) two corticotropin-releasing factor receptors (CRFRs), (v) three amylin receptors (AMYRs), CT gene-related peptide (CGRP) receptor and two adrenomedullin receptors (AM1 and AM2) [19]. They are characterized by some common structural features, including the large ECD (~120-160 amino acids) involved in the recognizing and binding of the C-terminal half (α-helix) of peptide hormone, the TMD (~310-420 amino acids) which provides a binding pocket for the N-terminal portion of peptide hormone and intracellular C-terminal domain [19]. One of the most important and well-characterized glucagon receptor subfamily members is glucagon-like peptide 1 receptor (GLP-1R), which plays a critical role in the glucose homeostasis regulated by the secretion of insulin and treatment of type 2 diabetes [20]. The crystal structure of the full-length human GLP-1R bound by a modified agonist peptide and the cryo-EM structure of GLP-1 peptide bound rabbit GLP-1R-Gs complex reveal a relatively conserved binding mode of peptide, providing deeper insights into the receptor-Gs interface [21,22]. Comparison between activated GLP-1R and activated β_2AR reveals that GLP-1R is activated by agonist by means of a distinct "two-domain" binding mechanism which is the hallmark of class B receptor activation model, whereas both class A and B receptors adopt the similar way to accommodate the α5-helix of Ras-like domain of Gs protein, i.e., the notable outward movement of TM6. The crystal structure of inactive full-length human GLP-1R reveals that the dynamic ECD might favor a distinct closed conformation. The binding of C-terminal peptide hormone to ECD induces the "separation" of ECD from extracellular side of TMD, allowing the binding of the N-terminus of peptide to the binding pocket of TMD, trigger the activation of receptor and subsequent intracellular signaling cascades [23]. The secretin subfamily receptors possess significant therapeutic potential, being targeted by 34 drugs [17].

Adhesion G protein-coupled receptors (ADGRs) are divided into nine subfamilies based on their phylogenetic analysis of TMD and extracellular domain [24]. ADGRs and secretin GPCRs were incorporated into class B family considering their similar structures, especially both containing ECDs. The unique features of ADGRs have been extensively characterized. For instance, according to the cleavage-based compartmentation of receptor architecture. ADGRs consist of two fragments, i.e., N-terminal fragment (NTF)/extracellular regions (ECRs) and C-terminal fragment (CTF). Of note, the ECRs of ADGRs frequently involved in a number of biological processes, such as cellular adhesion, migration and cell-cell fusion, contain a vast array of subdomains, such as hormone-binding domain, leucine-rich repeat (LRR), EGF-like domain, cadherin repeat and olfactomedin-like domain which vary widely in the length of residues [25]. The crystal structures of α-Latrotoxin receptor CIRL/latrophilin 1 (CL1, ADGRL1) and Brain angiogenesis inhibitor 3 (BAI3, ADGRB3) reveal two domains, i.e., the Hormone receptor domain (HormR, ~70 amino acids) at N-terminus and the highly conserved GPCR autoproteolysis inducing domain (GAIN, ~320 amino acids) which is located proximal to the N-terminus of TMD (TM1) and mediates the constitutive self-cleavage of receptors [26]. The GAIN domain consists of the N-terminal A subdomain composing of 6 α-helices and C-terminal B subdomain composing 13 β-strands and 2 α-helices. Both subdomains are jointly responsible for the autoproteolysis. Strikingly, as the molecular hallmark of ADGRs,

the GPCR proteolysis site (GPS, ~40 amino acids) motif comprising the last five β-strands of B subdomain is not an autonomously folded unit but forms a single folded domain with the N-terminus sequence of TM1 termed stalk region (~20 amino acids) which is a part of GAIN domain. It was suggested that the auto-cleavage occurs at the internal consensus site His Leu/Thr (HL/T) through a nucleophilic attack mechanism between the last 2 β-strands (β-strand 12 and β-strand 13), resulting in the formation of NTF and CTF [24,26]. Interestingly, there are some noncleavable ADGRs, such as ADGRC1, ADGRF2 and ADGRF4, due to the incomplete GAIN domain. ADGRA1 (GPR123), an exception in mammalian ADGRs, does not have a GAIN domain and therefore does not have a GPS motif [27]. It was proposed that the ECD, as an inhibitor, hampers the activation of receptors. The highly conserved β-strand 13 of GPS and stalk region might function together as a tethered agonist inducing the activation of receptor signaling upon the dissociation or displacement of ECD mediated by the ligand binding [28]. The precise activation mechanism of ADGRs remains elusive. According to the signal activation-based spatial configuration, four mechanisms have been proposed [29,30]. As the second largest subfamily of GPCRs in humans, the ADGRs subfamily plays a critical role in physiological functions and has been linked to human health and a variety of diseases, possessing great potential for drug discovery. To date, no drugs have been approved to specifically target any members of this subfamily. Nevertheless, different strategies have been developed to regulate receptor function via recognizing various druggable sites, such as N-terminal extracellular domains targeted by antibody, GAIN domain targeted by protease modulators, tethered peptide site targeted by peptide molecules, 7TM domain and C-terminal PDZ (PSD95/Dlg1/Zo-1) binding motif targeted by small molecule modulators [30].

The Class C receptors are divided into five subfamilies, including one calcium-sensing receptor (CaSR) [31,32], three taste type 1 receptors ($T1R_{1-3}$) [33,34], two gamma-aminobutyric acid type B receptors ($GABA_{B1}R$ and $GABA_{B2}R$) [35,36], eight metabotropic glutamate receptors ($mGluR_{1-8}$) [37], one GPCR/class C/group 6/subtype A (GPRC6A) [38] and a few orphan receptors. Based on the sequence homology, the metabotropic glutamate receptors (mGluRs) have been further subclassified into three groups: group I ($mGlu_1$ and $mGlu_5$) are mainly localized in postsynaptic location and couples to G_q protein, group II ($mGlu_2$ and $mGlu_3$) and group III ($mGlu_4$, $mGlu_6$, $mGlu_7$ and $mGlu_8$) are mostly localized in presynaptic area and couples to $G_{i/o}$ protein [37]. The class C receptors differ from other GPCRs by the large ECD and constitutive dimerization. Of note, the ECD of most of class C receptors consists of a conserved Venus fly trap (VFT) domain characterized by the bi-lobed structure which forms a cleft, providing the orthosteric binding site for endogenous ligands [39], and a cysteine-rich domain (CRD) connecting the VFT and TMD, except for $GABA_B$ receptors [40]. The critical role of mandatory homo-/heterodimerization of class C GPCRs in receptor activation has been extensively documented and widely accepted, making it a distinct and complexity subfamily for physiological and functional studies. The intersubunit disulfide bridge formed by conserved cysteine residues located in VFT domain has been found responsible for the receptor covalent dimerization [41–44], while the cysteine mutation experiment has revealed that truncated $mGluR_1$ still remains a stable non-covalent dimer via a core hydrophobic interface contributed by the upper and lower lobes of VFT domain, particularly by the upper part [45], which has been conformed in the solved structures, such as isolated $mGlu_1$ VFT [39] and full-length $mGlu_5$ [46]. Furthermore, mutation of Cysteine-129 in VFT domain of $mGlu_5$ interferes with the covalent dimerization of receptor but does not affect the receptor function [47]. Interestingly, mutation of Cysteine-121 in VFT domain of $mGlu_2$ disturbs the covalent linkage

between two monomers and reduces the apparent affinity of glutamate. It is further proposed that this intersubunit disulfide bond formed by Cysteine-121 stabilizes the active state of receptors. In contrast, receptor dimerization has been significantly impaired by the mutations located in the hydrophobic interface of the upper lobe of VFT domain [48]. Even though the role of oligomerization of class A and B GPCRs still has some controversy and remains to be clarified in detail, the homo-/heterdimerization or higher-order oligomers/complexes of class C receptors has been extensively studied [49]. The mGlu receptors have been thought to form strict homodimeric complex. However, they can also form heterodimers, rendering the complexity of the receptor oligomerization [48,50]. In contract to mGlu receptors, $GABA_B$ receptors consist of three principal subunits, including $GABA_{B1a}$, $GABA_{B1b}$ and $GABA_{B2}$, forming two heterodimers, i.e. $GABA_{B(1a,2)}$ and $GABA_{B(1b,2)}$. Of note, $GABA_{B1a}$ contains two unique sushi domains (SD) at the N-terminal extracellular region involved in the $GABA_{B(1a,2)}$ trafficking to axonal and interaction with extracellular binding proteins [51]. The heterodimerization of $GABA_B$ receptors has been extensively characterized [52]. However, the cryo-EM structure of the full-length $GABA_{B1b}$ homodimer has expanded our understanding of the functional relevance of oligomerization and signal transduction [53]. The activation mechanism of class C receptors has been proposed such as the open-close model and extensively reviewed [54–57]. The advances made from biochemical, biophysical and structural biology approaches have greatly expanded our understanding of the function of class C receptors in human diseases and provided opportunities for drug development and therapy. The class C receptors have been targeted by 16 drugs approved by FDA [18].

The Class F receptors consist of one smoothened (SMO) and ten frizzled (FZD_{1-10}) isoforms, differ from class A, B and C GPCRs by their unique functional and structural features. The structure of FZDs is characterized by a highly conserved N-extracellular cysteine rich domain (CRD) and a hydrophilic linker with varied length connecting the CRD and TMD. It is worth noting that class F receptors lack the DRY motif at the C-terminal region of TM3 and the NPxxxY motif at the end of 7TM which are common motifs in class A receptors and known to be essential for G protein binding and selectivity. In addition, the short α-helix 8 playing an fundamental role in G protein coupling couldn't be formed in FZD1, FZD2 and FZD7 due to the lack of cysteine residues at the C-terminus [58]. FZDs play crucial roles in cellular processes, such as cell polarity, proliferation, migration, differentiation, and embryonic development. FZDs have been found to be associated with human diseases, such as cancers, neurological and metabolic disorders [59,60]. As cell surface receptors, FZDs recognize Wingless/Int1 (WNT) proteins, a large family of secreted glycoproteins containing 19 members in mammals and transduce the extracellular signals into cells by interacting with the intracellular proteins such as Dishevelled (DVL). Three signaling pathways of FZDs have been described and characterized, including WNT/planar cell polarity (non-calsscial/canonical WNT/PCP) pathway related to the receptor mutation, canonical WNT/β-catenin pathway and WNT/Ca^{2+} pathway based on the G protein coupling [58,61]. Of note, accessory proteins, such as low density lipoprotein receptor related protein 5/6 (LRP5/6), tyrosine kinases ROR1/2 (ROR) and receptor-like tyrosine kinase (RYK), play a vital role in the ligand binding process through forming heterodimeric complex with FZDs [60]. In addition, several non-FZD receptors, such as parathyroid hormone receptors (PTHRs), leucine-rich repeat-containing GPCRs (LGR4/5/6), adhesion GPCRs (GPR124/125) and cadherin EGF LAG seven-pass G-type receptors (CELSR1/2/3), have been found involved in the regulation of WNT/β-catenin signaling [62].

1.1.2 Allosteric modulation of GPCRs

Most ligands or drugs currently on the market are designed using traditional discovery strategies to target and bind directly to the primary active sites (also known as orthosteric binding sites) of proteins, such as enzymes, transporters, ion channels, and GPCRs. This binding often results in the activation or inhibition of the target's function [63,64]. Molecules that bind to the orthosteric binding sites of GPCRs are termed canonical orthosteric ligands, including endogenous and synthetic agonists, antagonists and inverse agonists, and the binding location of orthosteric ligands varies by receptor classes [65] (Fig.1). For class A GPCRs, the binding pocket for ligands, such as neutransmitters and hormones, is found within the seven-transmembrane (7TM) domain (for example β_2-adrenergic receptor/β_2AR, PDB code: 7BZ2) [66]. In the case of class B GPCRs, the large orthosteric ligands, such as glucagon, secretin and calcitonin, are recognized by both extracellular domain (ECD) and 7TM domain (for example the glucagon-like peptide-1 receptor/GLP-1R, PDB code: 5VAI) [22]. In the case of class C receptors, the binding pocket for small molecules, such as γ-aminobutyric acid (GABA), calcium, glutamate and aromatic amino acids, is located in the large bilobate extracellular region/Venus flytrap (VFT) domain; for example metabotropic glutamate receptor 5/mGlu5, PDB code: 6N51) [67]. The class F receptors contain a highly conserved N-extracellular cysteine rich domain (CRD) and a hydrophilic linker connecting the CRD and 7TM region, which provide the binding site for ligands (for example the human smoothened receptor/SMO, PDB code: 5V57) [68]. Despite the high affinity of orthosteric ligands for the active sites in *in vitro* experiments, adverse side effects are often reported in the clinical trials and even caused by the administration of approved drugs, which are mostly due to the comparable orthosteric binding pockets encoded by the highly conserved amino acids in structurally homologous receptor subtypes and even in distinct proteins that could recognize chemically similar ligands [64]. For example, the five acetylcholine muscarinic receptors (mAChRs) play critical roles in the regulation of many physiological process [69]. However, side effects have been observed due to the presence of highly similar binding sites shared among the mAChRs for ligands or drugs that are specifically designed for a particular receptor subtype [70].

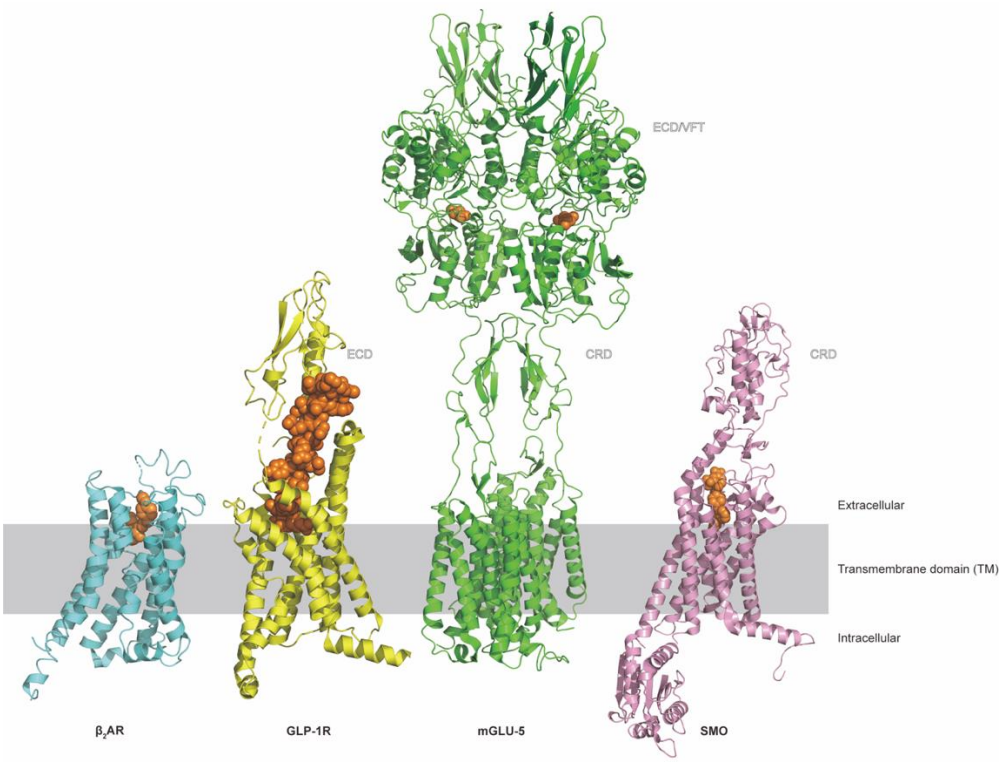

Fig. 1 Comparison of the extracellular regions and the orthosteric ligand binding sites of different GPCRs shown as cartoon model and colored separately, i.e., β_2AR (cyan, class A), GLP-1R (yellow, class B), mGlu5 (green, class C) and SMO (pink, class F). Ligands are shown as spheres and colored orange.

Of note, the orthosteric molecules function in a coarse adjustment manner, leading to direct non-progressive activation (agonist) or inhibition (antagonists) of receptors. In addition, extensive endeavors have been undertaken to design highly selective and effective ligands for a wide array of GPCRs. Over the past decades, an appealing approach for rational drug design has gained significant attention as a promising strategy for the screening and development of novel therapies [71]. This approach is based on the binding of molecules to the allosteric binding sites on receptors, which are topologically distinct from the orthosteric binding pockets. Allosteric binding sites exhibit lower evolutionary conservation compared to orthosteric binding pockets, yet they are conformationally linked [71]. Molecules that bind to allosteric sites are termed allosteric modulators, including allosteric enhancers (potentiators) and allosteric antagonists (inhibitors), which fine turn the physiological functions of receptor by stabilizing receptor conformation and shifting system equilibrium thereby influencing the behavior of orthosteric ligands, including their affinity, efficacy and GPCR subtype selectivity. As a result, this allosteric modulation leads to the enhancement or inhibition of recptor signaling responses [72–75]. Such molecules are subdivided into different types based on their activities [76], including the positive allosteric modulators (PAMs) which potentiate the effects (affinity and/or efficacy) of orthosteric agonists by binding at allosteric site on receptor leading to the enhanced receptor activation in the presence of orthosteric agonissts, the negative allosteric modulators (NAMs, also referred to noncompetitive antagonists) which noncompetitively decrease the effects (affinity and/or efficacy) of orthosteric agonists, and the neutral allosteric modulators which occupy the allosteric site and function as competitive antagonists of both PAMs and NAMs, preventing their binding at the same allosteric site, yet have no effects on the activity of orthosteric ligands, as well as the agonist-

positive allosteric modulators (Ago-PAMs) which function both as PAMs of the endogenous agonists and agonists on their own inducing the activation of receptors in the absence of orthosteric agonists [76–79]. In addition, allosteric modulators are also able to regulate the downstream signaling pathways (for example the coupling of receptor to G protein) through the allosteric interaction between the orthosteric ligand binding site and effector binding site [80].

Allosteric modulators can be either exogenous molecules such as natural and/or synthetic compouds, or endogenous molecules such as peptides, proteins, metal ions, lpids, autoantibodies and amino acids [74].

Exogenous allosteric modulators. As an innovative pharmacological approach, allosteric modulators exhibit few side effects, good selectivity in GPCR subtypes, and have been explored for the treatment of a range of neurological and psychiatric disorders, such as anxiety, schizophrenia, depression, Parkinson's and Alzheimer's diseases [74,76,81,82]. Much effort has been made to design allosteric modulators targeting different types of protein over the past decades, resulting in a growing number of potentially upcoming drugs in different phases of clinical trials. There have more more than 82,000 allosteric molecules reported and included in the Allosteric Database (ASD), which pairs with approximately 2,000 targets involved in 187 disease conditions [83]. It is also worth mentioning that several allosteric drugs, such as Cinacalcet, Etelcalcetide, Evocalcet and Maraviroc, have been approved for marketing (Fig. 2). These drugs target different GPCR subfamilies and binding sites, exhibiting improved specificity and fewer side effects compared to orthosteric drugs, making this field of GPCR allosteric modulation even more promising [84].

The Calcium-sensing receptor (CaSR) belongs to class C GPCRs, which is characterised by a large N-terminal extracellular domian (ECD) comprised of a venus flytrap (VFT) domain linked to the 7TM domian through the cysteine-rich domain (CRD) [40]. CaSR plays a crucial role in the regulation of extracellular calcium homeostasis primarily through the secretion of parathyroid hormone (PTH) and calcitonin, thereby influencing a spectrum of importent physiologial preocesses [85]. Many diseases are associated with the dysfunction of CaSR [32,86]. In addition to the physiological ligand Ca^{2+}, CaSR can also be activated by numerous other molecules known as calcimimetics, including type I calcimimetics such as the inorganic and organic polycations that bind to the ECD and functin as orthosteric agonists of CaSR, and type II calcimimetics that bind to the allosteric binding site of CaSR and function as PAMs potentiating the action of Ca^{2+} (Fig. 2) [87,88]. Cinacalcet (also known as Mimpara in Europe or Sensipar in North America and Australia) was the first approved allosteric modulator in 2004 (a PAM of CaSR) for the treatment of secondary hyperparathyroidism (2HPT) in adult patients with chronic kidney disease (CKD) on hemodialysis or peritoneal dialysis and hypercalcemia in patients with parathyroid carcinoma. Cinacalcet can directly lower the PTH levels by increasing the sensitivity of CaSR to extracellular Ca^{2+} [89–92]. Etelcalcetide (trade name Parsabiv), a eight-amino acid calcimimetic PAM of CaSR, was approved in 2016 and 2017 by EU and FDA, respectively, for the treatment of 2HP in adult patients with CKD on hemodialysis, which increases the activation of CaSR through extracellular Ca^{2+}, resulting in the inhibition of PTH secretion [93]. The new effective oral positive allosteric CaSR agonist Evocalcet (trade name Orkedia) was launched in 2018 in Japan for the treatment of 2HPT in patients on dalysis, which suppresses parathyroid cell function and exhibits fewer gastrointestinal adverse effects than Cinacalcet [94–96]. In the active state of CaSR, two PAM Cinacalcet (or Evocalcet) molecules bind to the 7TM domains of CaSR homodimer, but adopt distinctly

different extended and bent conformations in two protomers [97]. In contrast to Cinacalcet and Evocalcet, two identical copies of Etelcalcetide bind to the bilobed (LB2) interface located in the ECD, which are stabilized by the interactions formed with enriched negatively charged residues. The cryo-EM structurs of calcilytic molecules (NAMs) and calcimimetic molecules (PAMs) bound receptor reveal the symmetric inhibition and asymmetric activation of CaSR homodimer [97]. The chemokine (C-C motif) receptor 5 (CCR5) is a member of family A GPCR, which recognizes the chemokines and plays a vital role in immunity and inflammation [98]. The negative allosteric molecule Maraviroc (also referred to Selzentry in the USA or Celsentri in Europe) was entered the market in 2007 for the treatment of human immunodeficiency virus type 1 (HIV-1) infection (Fig. 2). As a specific, reversible and noncompetitive antagonist of CCR5, Maraviroc selectively binds to CC5R and prevents the virus from entering the host cells by blocking the interaction between CCR5-tropic HIV-1 glycoprotein (gp) 120 and CCR5 [99–101]. The recently reported cryo-EM structures of G protein coupled CCR5 and the previous solved inative crystal structure of Maraviroc bound CCR5 provide insights into the mechanism of ligand recognition and receptor activation, as well as the negative allosteric regulation of Maraviroc [102,103].

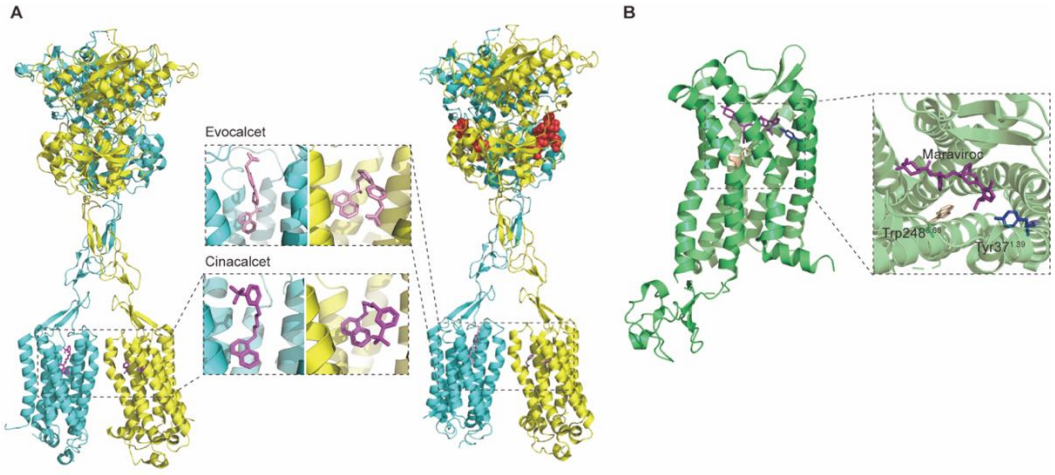

Fig. 2 Allosteric binding pockets of the approved exogenous allosteric drugs. (A) Cryo-EM structures depict the active-state CaSR bound by positive allosteric modulators, i.e., Cinacalcet (shown as stick representation and colored lightmagenta; PDB code: 7M3F), Evocalcet (shown as stick representation and colored pink; PDB code: 7M3G) and Etelcalcetide (shown as sphere representation and colored red; PDB code: 7M3G). Cinacalcet and Evocalcet bound within 7TM adopt distinct extended (left) and bent (right) conformations, leading to different interactions with two protomers of CaSR. This asymmetric activation of CaSR promotes the binding of G protein with the protomer (shown as cartoon representation and colored cyan) bound by extended positive allosteric modulator [97]. (B) X-ray crystal structure of the inactive state CCR5 (shown as cartoon representation and colored green) bound by negative allosteric modulator Maraviroc (shown as stick representation and colored purple; PDB code: 4MBS). The Maraviviroc binds within the cavity of CCR5 transmembrane domains and inhibits the activation of CCR5 probably through the intreactions with $Tyr37^{1.39}$ (colored blue) and $Trp248^{6.68}$ (colored wheat), which are involved in the binding of chemokine [102].

Endogenous allosteric modulators. In addition to exogenous allosteric regulators, many endogenous modulators have also been investigated and shown to participate in GPCR allosterism acting as PAMs or NAMs, including receptor activity-modifying proteins (RAMPs) [104,105], lipids (such as cholesterol [106,107]), amino acids (such as Phe, Trp and Tyr), peptides (such as γ-glutamyl peptide/γ-Glu-Cys-Gly [108,109], melanostatin/Leu-Pro-Gly [110], 5-hydroxytryptamine-moduline/Leu-Ser-Ala-Leu [111], pepcan-12/Arg-Val-

Asp-Pro-Val-Asn-Phe-Lys-Leu-Leu-Ser-His [112,111] and pepducins [113]), GPCR-targeted antoantibodies [114] and ions [115]. In addition, the binding of G protein to the intracellular face of GPCR can also promote the conformational changes of the extracellular face in an allosteric manner, which in turn influences the orthosteric ligand binding site, leading to the increased or decreased affinity of agonists or antagonists [116]. Thus, it is reasonable to speculate that some orphan GPCRs in question possessing allosteric sites with unknown exogenous regulators may be regulated by hitherto unappreciated endogenous modulators.

Of these modulators, the physiological cations play a significant role in GPCR-mediated intracellular signaling transduction [117]. Sperically, the high-resolution crystal structure of A_{2A} adenosine receptor ($A_{2A}AR$) reveals a sodium-binidng pocket (Na^+/water cluster) coordinated by several highly conserved residues, including Asp52$^{2.50}$, Ser91$^{3.39}$, Trp246$^{6.48}$ and Asn284$^{7.49}$, as well as water moleculers, in the middle of 7TM domain [118,119]. As a negative allosteric modulator, Na^+ stabilizes the inactive state of receptor, whereas the binding of agonist induces the structural rearrangements of receptor including the Na^+ binding pocket, leading to the collapse of Na^+/water cluster and acitivation of GPCR [120]. The crystallographic studies of β_1-adrenoceptor (β_1AR), protease-activated receptor 1 (PAR1) and δ-opioid receptor (δ-OR) also show that Na^+ stabilizes the receptor in an inactive conformational state, suggesting that the Na^+ binding pocket appears to be a common feature of most non-olfactory class A GPCRs [120–123]. The divalent cations also contribute to the regulation of GPCR signaling. Ca^{2+} is known to function as an endogenous orthosteric agonist of calcium-sensing receptor (CaSR), which regulates the secretion of parathyroid hormone (PTH) and maintains the Ca^{2+} homeostasis [124]. A study regarding the parathyroid hormone receptor (PTHR) reveals the positive allosteric actons of Ca^{2+}. The acidic amino acids within the ECL1 of PTHR play a key role in the allosteric regulation of Ca^{2+} [125]. In the case of class A GPCRs, the allosteric effects of Ca^{2+} and Mg^{2+} have been observed from earlier studies, such as $A_{2A}AR$ and muscarinic M2 receptor [126,127]. A resent NMR study with respect to the effects of cations on $A_{2A}AR$ also reveals that Ca^{2+} and Mg^{2+} are able to function as positive allosteric modulators, enhancing the agonist binding affinity and shifting the equilibrium towards the active-state conformation, whereas Na^+ acts as the negative allosteric modulator stabilizing the inactive state of receptor [128]. Moreover, as a second most abundant biologically relevant transition metal ion, Zn^{2+} is able to make strong interactions with Cys, His, Glu and Asp residues, and has been proposed to play a vital role in many biochemical reactions in the human body and confirmed as allosteric modulator of a number of GPCRs [129–131]. A study regarding the bovine rhodopsin receptor reveals several binding sites for Zn^{2+}, including one with high affinity located in 7TM domian and coordinated by the highly conserved residues Glu122$^{3.37}$ and His211$^{5.46}$. Moreover, the physiological and supraphysiological concentrations of Zn^{2+} exert completely distinct effects on the receptor [132–134]. At the human β_2-AR, Zn^{2+} is able to increase the agonist binding and enhance the cAMP accumulation acting as a positive allostric modulator. The mutanenesis experiments localize the binding site on β_2-AR for Zn^{2+} consisting of Glu255$^{5.64}$, Cys265$^{6.27}$ and His269$^{6.31}$ [135,136]. A study concerning human CXCR4 chemokine receptor unveils the increased binding of antagonist AMD3100 to Asp262$^{6.58}$ in the extracellular end of TM6 by Zn^{2+} [137]. While, at the dopamine receptors, Zn^{2+} inhibits orthosteric ligand (antagonist) binding acting as a negative allosteric modulator in a dose-dependent and reversible manner (for rat and D2R) or in the presence of other distinct allosteric sites bound by Na^+ and methylisobutylamiloride (for rat D4R) [138,139]. Two histidine residues (His394$^{6.55}$ and His399$^{6.60}$) towards the extracellular end of TM6 of rat D2 receptor facilitate the formation of Zn^{2+} binding site [140]. In addition, a

biphasic effect of Zn^{2+} has also been observed in human metabotropic serotonin receptors (5-HT), wherein Zn^{2+} exhibits allosteric potentiation and inhibition of orthosteric ligand binding to 5-HT1A at sub-micromolar and submillimolar concentrations, respectively [141]. Moreover, a recent structural and functional study has demonstrated the negative allosteric mudulation of Zn^{2+} on huamn galanin 1 receptor (GALR1) likely by restricting the conformational change of TM6, and the Zn^{2+} effect can be abolished through the mutation of $His267^{6.55}$ located in TM6 below the agonist binding site. In contrast, GALR2 receptor was not affected by Zn^{2+} [142].

1.2 Human melanocortin-4 receptor (MC4R)

1.2.1 MC4R ligands

The human melanocortin-4 receptor (MC4R) is one of the members of human melanocortin receptor family (MCRs) which consists of five subtypes (MC1R to MC5R) and belongs to rhodopsin-like class A GPCR superfamily [143]. In particular, MC4R is found in peripheral tissues, intestinal L cells and predominantly expressed in the central nervous melanocortin system therefore together with MC3R referred to as the neural MCRs [144,145]. In the melanocortin pathway, food intake and energy homeostasis are primarily coordinated by the interaction of MC4R with different neuropeptides also termed melanocortins (Table 1) [146,147]. In contrast to other MCRs, MC2R is specifically activated by adrenocorticotropic hormone (ACTH) and interacts with the obligatory accessory protein (melanocortin receptor accessory protein 1, MRAP1) for its functional expression, trafficking and signaling. In addition, the melanocortin-2-receptor accessory protein 2 (MRAP2) plays a critical role in the regulation of MC4R signaling [148–150]. Naturally occurring MC4R loss-of-function (LOF) mutations are the most frequent cause of monogenic obesity and binge eating disorder [151,152], while some gain-of-function (GOF) variants have been found to be associated with low body mass index (BMI) and obesity related cardiometabolic diseases [153]. In addition to its central roles in the control of energy homeostasis and feeding behavior, the deficiency of MC4R is also involved in the regulation of blood pressure, cardiovascular function and type 2 diabetes mellitus, making it an attractive therapeutic target for the treatment of obesity and related diseases [154–159].

The activation of MC4R is induced by different agonists, leading to the increased energy expenditure and loss of appetite. The endogenous linear peptide agonists, including ACTH, α-melanocyte stimulating hormone (α-MSH), β-MSH and γ-MSH, are all derived from the post-translational processing/proteolytic cleavage of the precursor polypeptide proopiomelanocortin (POMC) by prohormone convertases (PCs) [160,161]. Among them, α-MSH is one of the most extensively studied peptides which activates all MCRs with the exception of MC2R. Much effort has been devoted to designing and synthesizing more potent, selective peptides and small molecules targeting MC4R. Extensive structure-activity studies based on the fragment of α-MSH have led to the discovery of many synthetic analogs. Some of them are currently being developed, optimized, and tested in clinical trials. Specially, the synthetic 13-amino-acid linear peptide 4-Norleucine (Nle^4), 7-D-phenylalanine ($D\text{-}Phe^7$)-α-melanocyte stimulating hormone (also termed afamelanotide, Scenesse, [Nle^4, $D\text{-}Phe^7$]-α-MSH, NDP-α-MSH, melanotan I and MT I, superscript numbers correspond to the peptide position number based on α-MSH, see table

1) possesses a prolonged biological activity and high affinity in nanomolar range at all MCRs except the MC2R and has been approved by European Union in 2014 and FDA in 2019 to stimulate the melanin production in dermal cells by binding to MC1R and prevent phototoxicity in adults with erythropoietic protoporphyria (EPP) showing acceptable side effects [162,163]. In addition, the activation of MCRs by MSH analogues shows different binding affinity towards specific receptor subtypes. In particular, with respect to MC4R, the binding affinity has been studied and evaluated as follows: NDP-α-MSH > α-MSH = ACTH > β-MSH > γ-MSH [164,165]. All of these endogenous and synthetic agonists share a conserved central core tetrapeptide His-L/DPhe-Arg-Trp (HFRW) pharmacophore, where the terms L and D refer to the configurational stereochemistry of the Phenylalanine side chain. Site-directed mutagenesis experiments reveal that extensive interactions, such as salt bridge, CH···O hydrogen bonds, π-π stacking, hydrophobic and aromatic-aromatic, formed between the receptor transmembrane helix residues and HFRW motif play a crucial role in the regulation of receptor activation [166–169]. It should be emphasized that the reverse β-turn secondary structure on HFRW motif functions as a scaffold in the receptor binding site for orienting the angle of amino acid side chains in the suitable orientation and thus is found to contribute to the agonist recognition and binding, making it an important cornerstone to design more potent and selective ligands or small molecules for specific MCR subtypes and pharmacological treatment of related diseases [170,171].

Due to the high sequence homology between MCRs, most of the linear peptide agonists have low selectivity towards specific MCR subtype and cause undesirable side effects. Numerous efforts have been dedicated to the study of novel therapeutics. Notably, considerable progress has been achieved in the development of macrocyclic peptide ligands modified from the natural products over the years, which compose of natural amino acids (and analogues) and possess several favorable pharmacological properties, such as the high metabolic stability, binding affinity, target selectivity and biocompatibility, thus have attracted special attention as drug candidates for promising therapeutic modality [172,173]. A variety of macrocyclization strategies, such as head-to-tail, head-to-side chain, side chain-to-tail and side chain-to-side chain, have been used to cyclize linear peptides based on different reactions such as amide bond, disulfide bridge, thioacetal, thioether, ether, carbon-carbon and triazole-ring fromation [174]. Several peptide and non-peptide ligands have been evaluated in clinical trials (for more information see review [175]). Among them, Melanotan II (MT II) is a small synthetic cyclic heptapeptide analogue of endogenous ligand of α-MSH, which contains a lactam bridge formed between Aspartic Acid (Asp^5) and Lysine (Lys^{10}) for peptide cyclisation. MT II exhibits prolonged and potent inhibition of food intake and thus induces weight loss, nevertheless, side effects have also been found because Melanotan II is a non-selective agonist of MCRs, including MC4R [176–179]. The substitution of C-terminal amino group of MT II by a hydroxyl group has led to the discovery of Bremelanotide (also known as Vyleesi), which exhibits non-selective agonist activities at different MCRs but with high affinity for MC4R and has been approved in 2019 for the treatment of premenopausal women with Hypoactive Sexual Desire Disorder (HSDD) [180,181]. Setmelanotide, also known as Imcivree, RM-493, BIM-22493 and IRC-022493, is an eight-amino-acid cyclic peptide analogue of α-MSH containing D-Alanine ($D\text{-}Ala^5$) and D-phenylalanine ($D\text{-}Phe^7$) in the core melanocortin sequence, which preferentially binds to and activates MC4R with inhibition constant (K_i) of 2.1 nM and 50% effective concentration (EC_{50}) of 0.27 nM in respect of cAMP accumulation by stimulating Gs signalling pathway, being higher affinity and more potent than α-MSH with 20- and 15-fold, respectively. In addition, Setmelanotide shows

20- and 5000-fold less potent in activating MC1R, MC3R and MC5R (EC_{50} of 5.8 nM, 5.3 nM and more than 1600 nM, respectively), and does not active MC2R [182,183]. Setmelanotide reduces hunger and leads to substantial weight loss in severely obese individuals caused by the loss-of-function mutation-related biallelic deficiency including POMC or proprotein convertase subtilisin/kexin type 1 (PCSK1) and leptin receptor (LEPR) deficiency which are rare genetic disorders of obesity leading to the disruption of MC4R pathway and resulting in extreme hyperphagia and severe early-onset obesity [184,185]. The clinical trials show that Setmelanotide is well tolerated with some common adverse events, such as injection site reactions, nausea and hyperpigmentation, however it does not cause severe side effects, such as increased heart rate and blood pressure [186–189]. Setmelanotide has been approved by FDA in 2020 for chronic weight management in adult and pediatric patients with obesity caused by the ultrarare genetic POMC, PCSK1 and LEPR deficiency. In addition, Setmelanotide has also been extended and granted by FDA in 2022 for the treatment of obese patients with Bardet–Biedl syndrome (BBS) which is a rare genetic disorder with a wide range of symptoms [190–192].

Table 1. Ligands targeting melanocortin receptors.

Peptide	Sequence of ligands (by α-MSH numbering)
α-MSH	Ac-Ser^{1}-Tyr^{2}-Ser^{3}-Met^{4}-Glu^{5}-His^{6}-Phe^{7}-Arg^{8}-Trp^{9}-Gly^{10}-Lys^{11}-Pro^{12}-Val^{13}-NH_2
ACTH (1-39)	Ser-Tyr-Ser-Met^{4}-Glu^{5}-His^{6}-Phe^{7}-Arg^{8}-Trp^{9}-Gly-Lys-Pro-Val-Gly-Lys-Lys-Arg-Arg-Pro-Val-Lys-Val-Tyr-Pro-Asn-Gly-Ala-Glu-Asp-Glu-Ser-Ala-Glu-Ala-Phe-Pro-Leu-Glu-Phe-OH
β-MSH	Asp-Glu-Gly-Pro-Tyr-Arg-Met^{4}-Glu^{5}-His^{6}-Phe^{7}-Arg^{8}-Trp^{9}-Gly-Ser-Pro-Pro-Lys-Asp-OH
γ-MSH	Tyr-Val-Met^{4}-Gly^{5}-His^{6}-Phe^{7}-Arg^{8}-Trp^{9}-Asp-Arg-Phe-OH
NDP-α-MSH	Ac-Ser-Tyr-Ser-Nle^{4}-Glu^{5}-His^{6}-D-Phe^{7}-Arg^{8}-Trp^{9}-Gly-Lys-Pro-Val-NH_2
Melanotan II	Ac-Nle^{4} cyclo[Asp^{5}-His^{6}-D-Phe^{7}-Arg^{8}-Trp^{9}-Lys^{10}]-NH_2
Bremelanotide	Ac-Nle^{4} cyclo[Asp^{5}-His^{6}-D-Phe^{7}-Arg^{8}-Trp^{9}-Lys^{10}]-OH
Setmelanotide	Ac-Arg^{3} cyclo[Cys^{4}-D-Ala^{5}-His^{6}-D-Phe^{7}-Arg^{8}-Trp^{9}-Cys]-NH_2
SHU9119	Ac-Nle^{4} cyclo[Asp^{5}-His^{6}-D-2-Nal^{7}-Arg^{8}-Trp^{9}-Lys^{10}]-NH_2
	Note: The central pharmacophore His-Phe-Arg-Trp (HFRW) colored red. Nle: lipophilic Norleucine; D-Phe: stereoisomer D-phenylalanine; D-2-Nal: D-2-naphthylalanine. Position 4: Methionine (Met) is often replaced with lipophilic residue Norleucine (Nle), acidic residue Aspartic Acid (Asp) or non-polar residue Cysteine (Cys) which is normally used for peptide cyclization based on the disulfide bond formation. Position 5: The preferred residue at this position is neutral or acidic, such as D-Alanine (D-Ala), Glutamic acid (Glu) and Aspartic acid (Asp). Position 6: No preference has been found for a specific residue at this position. Position 7: The chirality change of Phenylalanine (D-Phe) has been found given more ligand potency.

Besides the linear and cyclic peptide ligands, intense efforts have been made to develop highly active and selective small non-peptide ligands either based on the natural melanocortin peptides for example the β-turn conformation of HFRW consensus sequence which plays a key role in peptide recognition or the high-throughput screening of organic compounds. Haskell-Luevano et al. performed the screening of a small molecule library based on β-turn structure and first reported the discovery of the non-peptide small heterocyclic compounds which

are able to strongly stimulate Mouse MC1R (mMC1R) with the exception of mMC3R and mMC4R [193]. Notably, the first non-peptide small molecule agonist tetrahydroisoquinoline (THIQ) aimed at MC4R was designed and synthesized by Patchett et al. THIQ exhibits remarkable potency and selectivity, leading to substantial reduction in food intake [194]. Subsequently, the optimization based on THIQ structure has led to the discovery of many derivatives for example MB243 which can also reduce the food intake and augment erectile activity [175,195]. Due to their metabolic stability and versatile modifiability, non-peptide small molecules provide a promising scaffold for the development of novel drugs targeting MC4R with exceptional potency, selectivity, and safety. Furthermore, in addition to the small peptidic and non-peptide agonists, a study has reported that a large bone-derived hormone/protein, lipocalin-2, can cross the blood-brain barrier and binds to MC4R in the paraventricular and ventromedial neurons of the hypothalamus acting as an agonist [196]. To date, no structural information has been disclosed for the lipocalin-2/MC4R complex. However, it is foreseeable that this huge hormone protein may interact with MC4R in a novel manner completely different to the agonists discussed above.

The regulation of energy homeostasis involves not only agonists but also antagonists or inverse agonists that possess opposing effects at MC4R (Fig. 3). The POMC neurons within the hypothalamic arcuate nucleus (ARC) are activated by leptin and release α-MSH which activates MC4R in paraventricular nucleus (PVN) and negatively influences feeding behavior, resulting in suppression of food intake and increase of energy expenditure. In contrast, the inhibition of MC4R activity can be positively regulated by endogenous antagonists/inverse agonists, specifically by agouti-related protein (AgRP) that coexists with neuropeptide Y (NPY) released by NPY/AgRP (γ-aminobutyric acid, GABA) neurons which are also located in ARC and release the inhibitory neurotransmitter GABA, leading to increased food intake [197]. As a potent orexigenic peptide, NPY is able to stimulate food intake and the corresponding appetite stimulating responses are mediated through NPY receptors, such as Y1 and Y5 [198,199]. Many diseases of negative energy balance, such as cachexia, anorexia nervosa, self-starvation and failure to thrive in Prader-Willi Syndrome (PWS) infants, can be prevented and alleviated via the administration of AgRP, indicating its important role in the regulation and treatment of metabolic dysfunctions [200–204].

AgRP is encoded by AGRP gene in humans and identified in 1997. AgRP is 25% identical to human agouti signaling protein that antagonizes MC1R which is involved in the regulation of pigmentation. As a potent endogenous antagonist of MC3R and MC4R, the orexigenic neuropeptide AgRP is primarily produced in the arcuate nucleus of hypothalamus and plays essential roles in the regulation of feeding behavior and energy homeostasis [205–207]. In particular, AgRP also functions as an inverse agonist at MC4R and suppresses the constitutive activity of MC4R through a mechanism independent of MC4R agonist ligands. While, the action of AgRP on MC4R can be blocked by SHU9119 which is a potent antagonist of MC3R and MC4R, as well as partial agonist of MC5R [208,209]. The mature human AgRP consists of two domains containing 112 residues after cleavage of the N-terminal signal peptide sequence. In particular, the cysteine-rich C-terminal domain of AgRP, corresponding to AgRP(87-132), possesses the receptor binding affinity and selective antagonistic activity. The NMR structure analysis indicates that AgRP(87-132) active domain contains N-terminal, central and C-terminal loops, which is stabilized by five disulfide bonds and forms an inhibitor cysteine knot (ICK) fold motif. Interestingly, the flexible and highly dynamic N-terminal domain of AgRP lacks the well-defined structure and negatively suppresses the antagonist activity of AgRP(87-132) but does not significantly affect its structural

characteristics. In addition, the RFF (Arg-Phe-Phe) triplet located on the β-hairpin of AgRP(87-132) central loop has been proven to be the active sequence of AgRP, playing a key role in MCRs binding. It is also proposed that the binding selectivity of AgRP for MC3R and MC4R is conferred by the N-terminal loop of AgRP(87-132) [210–212]. Moreover, the AgRP(87-120) lacking the C-terminal loop and small cyclic decapeptide Yc[CRFFNAFC]Y synthesized based on the CRFFNAFC residues in the β-hairpin of central loop function as inverse agonists at human MC4R revealing the functional determinants of inverse agonism [213]. Additionally, the more potent and selective antagonists have been designed and synthesized based on the structure-activity relationship (SAR) studies, which will accelerate progress toward the treatment of metabolic diseases [214].

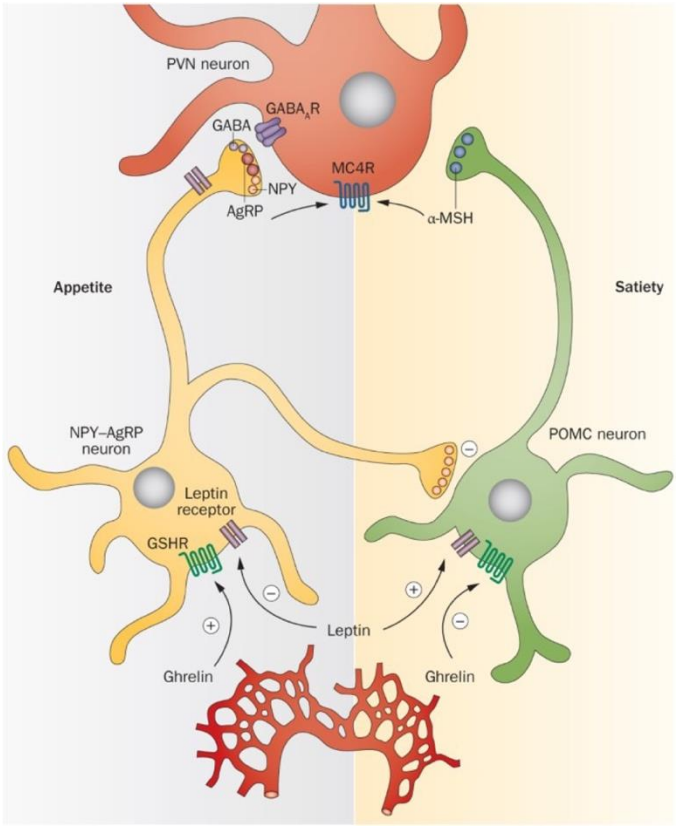

Fig. 3 Schematic representation of the melanocortin system in the arcuate nucleus of the hypothalamus (ARC). The orexigenic NPY/AgRP (GABA) and anorexigenic POMC neurons form a coordinated first-order sensory regulatory network and both project to the second-order target PVN neurons to positively and negatively regulate the food intake and energy expenditure, respectively, as well as other physiological functions. The binding of leptin and ghrelin to their respective receptors in NPY/AgRP (GABA) and POMC neurons results in distinct activation (+) and inhibition (-) effects. The POMC neuron is activated by the binding of leptin, leading to the release of α-MSH which binds to MC4R resulting in satiety. While the NPY/AgRP (GABA) neuron is inhibited by leptin but primarily stimulated by ghrelin which is an orexigenic endogenous peptide for GHSR and secreted from stomach [215]. In addition, the NPY/AgRP (GABA) neurons can also project to POMC cell bodies and inhibit the POMC neurons [216]. Furthermore, the gene expression of hypothalamic AgRP and POMC can be downregulated and upregulated by leptin, respectively, leading to the decreased production of AgRP and increased release of α-MSH, and eventually result in decreased energy intake [217,218]. GSHR, growth hormone secretagogue receptor (ghrelin receptor); NPY, neuropeptide Y; AgRP, agouti-related protein; GABA, γ-aminobutyric acid; PVN, paraventricular nucleus; GABAAR, γ-aminobutyric acid receptor; MC4R, Melanocortin 4 Receptor; α-MSH, α-melanocyte stimulating hormone; POMC, proopiomelanocortin. Figure from [219].

1.2.2 MC4R allosteric regulation

Biological and pharmacological studies have implicated that a number of endogenous regulators have been investigated and shown to participate in GPCR allosterism acting as PAMs or NAMs, including G proteins, β-arrestins, receptor activity-modifying proteins (RAMPs), lipids, amino acids, peptides, GPCR-targeted antoantibodies and ions [220]. Of these modulators, metal ions are required for the lignad binding to a number of GPCRs and GPCR-mediated signaling transduction [117,221,222]. A study has demonstrated that the specific binding of radioligand ^{125}I-NDP-α-MSH to MC4R requires the presence of calcium [223]. Further evidence for the putative cations binding has been provided by the investigation of the thermal stability measurements of MC4R in complex with different ligands, such as the agonists α-MSH and NDP-α-MSH, antagonist SHU9119 and inverse agonist AgRP(83-132), in response to Mg^{2+}, Zn^{2+} and Ca^{2+}, whereas only Ca^{2+} increases the thermalstability of MC4R in complex with SHU9119 and NDP-α-MSH [224]. Ca^{2+} can also increase ^{125}I-NDP-α-MSH binding to MC4R with a EC_{50} of 3.7 μM acting as a positive allosteric modulator. In contrast, Ca^{2+} has no impact on the AgRP(82-132) binding. Of note, the precise Ca^{2+} binding site was first described in the MC4R-SHU9119 crystal structure and the calcum ion was coordinated by three negatively charged amino acids Glu100$^{2.60}$, Asp122$^{3.25}$ and Asp126$^{3.29}$ in MC4R and two backbone-carbonyl oxygen atoms in SHU9119 (Asp^{5} and D-2-naphthylalanine/D-2-Nal^{7} residues) (Fig. 4) [224]. Moreover, recent studies with respect to the functional and structural characterizations of MC4R also demonstrate the important roles of Ca^{2+} in the agonist binding, the regulation of MC4R activation and signaling. Particularly, both peptides (α-MSH, NDP-α-MSH, Bremelanotide and Setmelanotide) and small non-peptide moleculer (THIQ) agonist ligands bound active state MC4R cryo-EM structures unambiguously confirm the presence of Ca^{2+} ion between TM2, TM3 and agonist, and share the same Ca^{2+} coordination (i.e., coordinated by Glu100$^{2.60}$, Asp122$^{3.25}$ and Asp126$^{3.29}$ in MC4R as observed in MC4R-SHU9119 complex crystal structure and different backbone-carbonyl oxygen atoms in ligands) (Fig. 4) [225,226]. In addition, as a neuromodulator, Zn^{2+} also plays a critical role in the functional regulation of melanocortin receptors. Although the exact binding site of Zn^{2+} on MC4R remains unclear. However, previous studies have demonstrated that Zn^{2+} can act both as a partial agonist and a positive allosteric mudulator for the action of peptide agonists (NDP-α-MSH and α-MSH) on MC1R and MC4R, suggesting the presence of Zn^{2+} binding site on the receptor [227–229]. Furthermore, a recent publication reveals that Zn^{2+} functions as a positive allosteric modulator for ligand binding and exhibits agonistic properties in relation to the constitutive activity of MC4R at physiologically relevant low micromolar concentrations, whereas Cu^{2+} acts as an inverse agonist and inhibits the constitutive activity of MC4R [230].

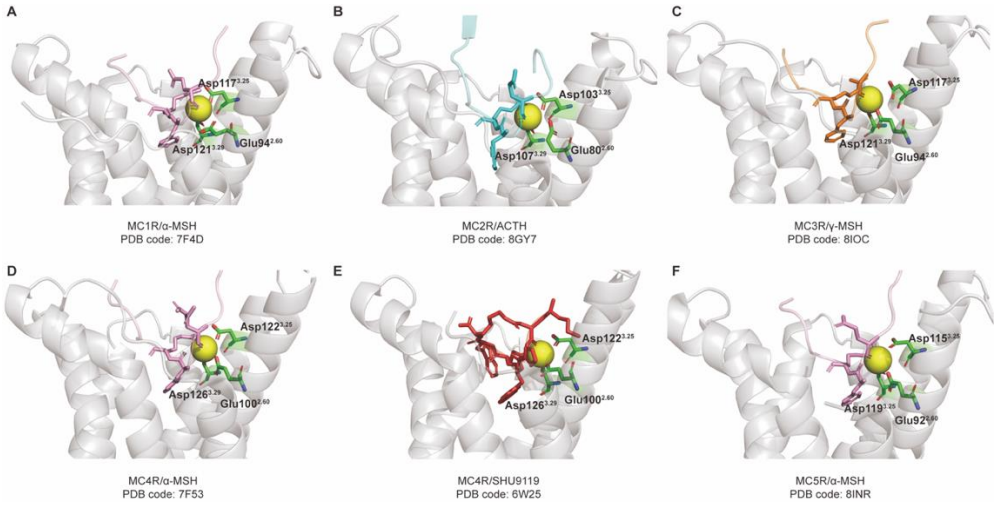

Fig. 4 Conformational comparison of the Ca^{2+} binding sites among MCRs. Ca^{2+} is shown as sphere colored yellow. All MCRs share same Ca^{2+} coordination ($Glu^{2.60}$, $Asp^{3.25}$ and $Asp^{3.29}$) when bound ligands containing HFRW motif (see table 1).

1.2.3 MC4R structural properties

MC4R is among the few GPCRs displaying distinct structural features compared with most other class A GPCRs. Usually, the extracellular loop 2 (ECL2) containing over 15 amino acids is the largest ECL in class A GPCRs and contains different secondary structural elements (Fig. 5), such as the β-hairpin formed by two β-sheets found in rhodopsin and CXCR4, the short α-helix stabilized by an intra-helical disulfide found in β_2AR and the short loop found in dopamine receptor 3 (D3R), thus adopting varying conformations [231]. ECL2 plays a vital role in the extracellular region of receptor and contributes to the ligand binding cavity, thereby influencing the ligand selectivity, ligand binding affinity, allosteric modulation, receptor activation and downstream intracellular signaling. For example, ECL2 can form a structured extracellular cap covering the binding pocket of the covalently bound or lipid ligands, or keep away from the binding cavity to facilitate the entrance of diffusible ligands such as the large peptide to the transmembrane domain bundle [231–233]. However, MCRs including MC4R have a very short ECL2 containing just three to four amino acids without defined secondary structural elements compared with other class A GPCRs [229], resulting in the formation of a relatively open and extracellular solvent-accessible ligand binding pocket for large peptides (Fig. 5), which has been recently confirmed by the inactive and active MC4R structures [224–226]. Particularly, two hydrogen bonds have been observed from the inactive state MC4R structure between $Ser188^{ECL2}$, and Arg^{8} and Trp^{9} in antagonist SHU9119 [224]. The agonist bound active state MC4R structures reveal the involvement of $Ser188^{ECL2}$ in the formation of hydrogen bonds with Arg^{8} in endogenous agonist α-MSH, Trp^{9} in linear agonist NDP-α-MSH, Trp^{9} in cyclic agonist bremelanotide and Trp^{9} in cyclic agonist Setmelanotide, respectively. In addition, $Ser188^{ECL2}$ also contributes to the formation of a hydrophobic pocket that accommodates the non-peptide agonist THIQ for binding to MC4R [225,226]. Moreover, these studies also confirm that MC4R does not possess a conserved disulfide bridge usually found in a number of GPCRs including class A and class B, which connects ECL2 and the extracellular tip of TM3 ($Cys122^{3.25}$), which constrains the conformational changes of this region during receptor activation [231]. In contrast, MC4R contains a non-conserved negatively charged amino acid aspartate

(Asp122$^{3.25}$) in TM3 which is involved in the formation of ligands and calcium ion binding network. Furthermore, all five MCRs share three highly conserved cysteines, including Cys271^{ECL3}, Cys277^{ECL3} and Cys279^{ECL3} [225,226,234–237]. Among them, Cys271^{ECL3} and Cys277^{ECL3} form an intra-loop disulfide bound within ECL3, while Cys279^{ECL3} forms another disulfide bound with N-terminal Cys40$^{N\text{-}ter}$ which is observed in the agonist bound MC4R cryo-EM structures but not in the antagonist SHU9119 bound MC4R crystal structure. A missense mutation at ECL3 (Cys271^{ECL3} to Arg271^{ECL3}) reduces the ligand binding affinity and cell surface expression of receptors. An unusual functionally disastrous disulfide bridge within ECL3 of this mutant formed by Cys279^{ECL3} with Cys277^{ECL3} instead of Cys40$^{N\text{-}ter}$ contributes to the loss of the properly folded ECL3, leading to the malfunction of MC4R [238]. Taken together, all of these compelling pieces of evidence emphasize the significant impact of the extracellular loops on the functional properties of MC4R.

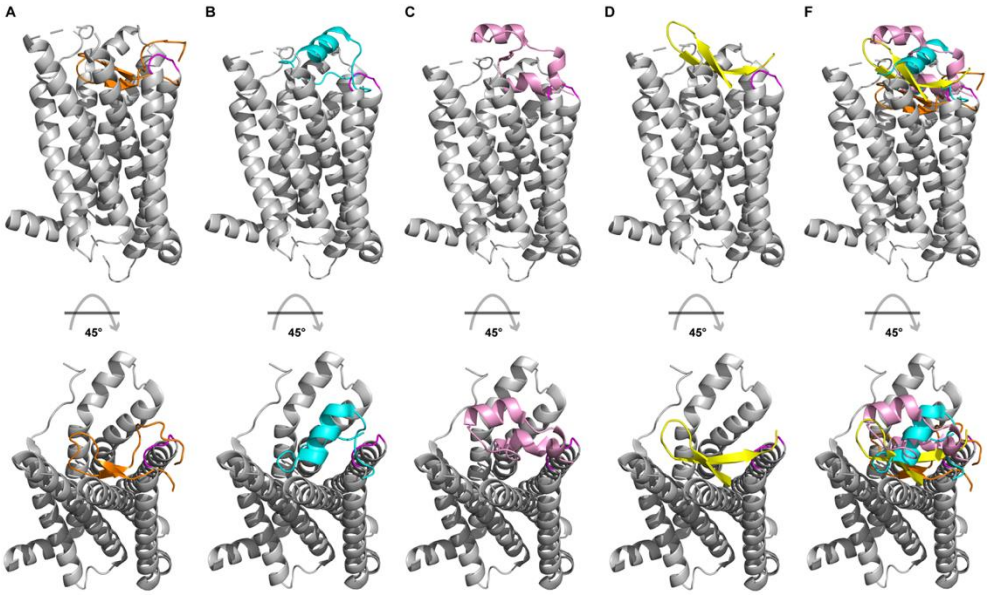

Fig. 5 The conformational diversity of extracellular loop 2 (ECL2) in several class A GPCRs. (A-D) The ECL2 of MC4R colored magenta (PDB code: 7F53) is compared with ECL2 of rhodopsin colored orange (A; PDB code: 3CAP), β_2AR colored cyan (B; PDB code: 2RH1), A_{2A}R colored pink (C; PDB code: 2YDO) and CXCR4 colored yellow (D; PDB code: 3OE0). (F) The overlay of all ECL2 of five GPCRs. Only the transmembrane helices of MC4R are shown for clarity.

1.3 Membrane-mimicking systems

The structural and functional characterization of membrane proteins including GPCRs have been performed using different membrane mimetics, including organic solvents [239–242], amphipols [243,244], detergent micelles [245], bicelles [246], nanodiscs [247], liposomes [248,249] and co-polymers [250]. A comprehensive discussion of the different membrane-mimicking systems is provided in chapter 2.

1.4 Objectives

A number of membrane proteins are susceptible to denaturation when extracted from their native lipid environment by detergents. Alternative methods have been developed, such as MSP nanodiscs and amphiphilic copolymers. Specially, the amphiphilic copolymers enable the direct extraction of functional membrane proteins along with their surrounding lipids and form native lipid-bilayer nanodiscs. The work shown in this thesis focused on the functional characterization of MC4R and development of novel amphiphilic copolymers. In more detail, the objectives of this thesis can be specified as follows:

1) Evaluate the pros and cons of the currently used membrane-mimicking systems for the functional and structural studies of membrane proteins (chapter 2).

2) Explore the potential of newly synthesized electroneutral polymer Sulfo-DIBMA for *in vitro* studies of GPCRs-ligand interactions in native lipid-bilayer environment (chapter 3).

3) Characterize the functional integrity and allosteric regulation of MC4R in different environments, including detergent micelles, MSP1D1 nanodiscs and Sulfo-DIBMA native membrane nanodiscs (chapter 4).

4) Characterize the potential of newly synthesized amphiphilic copolymers for GPCR studies derived from DIBMA via partial amidation of the carboxylate pendant groups with various biocompatible amines, including Arg-DIBMA, Dab-DIBMA, Meg-DIBMA and $mPEG_4$-DIBMA (chapter 5).

2. Membrane mimicking systems and their applications

This chapter reflects the content of the following manuscript.

Native-state NMR characterization of membrane systems (*Manuscript submitted*)

Ci Chu[a], Thibault Viennet[b]*, Manuel Etzkorn[a,c,d] *

[a]Institute of Physical Biology, Heinrich Heine University Düsseldorf, Düsseldorf, Germany

[b]Department of Chemistry and iNANO, Aarhus University, Aarhus, Denmark

[c]Institute of Biological Information Processing (IBI-7: Structural Biochemistry), Forschungszentrum Jülich, Jülich, Germany

[d]Jülich Center for Structural Biology (JuStruct), Forschungszentrum Jülich, Jülich, Germany

Abstract

Structure and function of proteins can be strongly affected by the surrounding environment. In this respect the generation of a 'native-state', i.e., a condition that adequately captures the relevant features of the target protein during the experimental characterization, is generally desired. It is, however, evident that a considerable number of important protein systems, especially including membrane proteins, require complex environments to allow a native-state characterization. Focusing on membrane systems, this chapter discusses various aspects of generating native-state conditions and appropriate NMR-based methods that can provide insights into the increasingly complex environments that accompany them.

Background

Membrane proteins (MPs), such as integral membrane proteins (IMPs), lipid-anchored proteins, and peripheral membrane proteins, play crucial roles in regulating a wide variety of physiological processes. To understand their signaling properties and enable rational development of novel drugs, it is essential to obtain atomic-resolution insights into structure and dynamics of MPs in an environment that adequately maintains their functionally relevant conformation(s). An appropriate combination of biochemical and biophysical approaches that is able to provide these insights and thus enables a 'native-state characterization' of the respective system is the aspired goal of most studies. Unfortunately, challenges in sample preparation, stability and/or applicability of suitable biophysical techniques often restrict native-state characterizations of MPs.

Traditionally, X-ray crystallography has been used as a powerful method to determine a large number of high-resolution atomic structures of MPs. However, the preparation of high-resolution diffracting crystals is often time-consuming and notoriously difficult [251]. Alternatively, cryo-electron microscopy is a great tool for structural characterization of large MPs in different membrane mimetics [252,253]. To facilitate sample handling, enable prolonged measurement times, and/or to increase the achievable structural resolution, many studies exploited the benefits of protein engineering and/or specific synthetic environments to stabilize/lock MPs in particular conformational states and/or to increase thermal stability [254–257]. Yet, one central parameter of many MP signaling pathways is the dynamic modulation of multiple conformational states, such as found in GPCR systems [258–260]. Consequently, an accurate quantitative determination of the population of the different conformational states of a GPCR and its modulation by extracellular stimuli is arguably one of the most valuable read-out parameters to assess the impact of new drug candidates. Nuclear Magnetic Resonance (NMR) is one of the very few techniques capable of not only providing structural information into highly dynamic MPs, but also to offer quantitative information about the populations of different conformational states in dynamic equilibrium [261]. However, since these populations will very likely be affected by receptor modification/stabilization as well as non-native membrane environments, it will be of fundamental importance to carry out the respective experiments under native-state conditions. Overall, it may thus be envisioned that future rational drug design strategies may be inspired by a suitable combination of dynamic processes characterized by native-state NMR and structural snapshots obtained from cryo-EM and X-ray crystallography. In the following we will discuss current approaches and future requirements for the desired native-state NMR characterizations of MPs.

Membrane environment

The surrounding phospholipids' characteristics and bilayer structure contribute to the preservation of the structural and functional integrity of MPs through different physical properties such as thickness, charge, lateral pressure, hydrophobic mismatch, membrane fluidity and curvature [262–265]. For example, the tilt and rotational angles of MPs' transmembrane α-helices can be affected by the lipid-protein interactions, leading to modulation of the functional properties of MPs [266]. In general, most of the structural and biophysical characterization of MPs have been conducted in membrane mimicking systems (membrane mimetics) such as organic solvents [239–242], amphipols [243,267], detergent micelle [245], bicelles [246], nanodiscs [247] and liposomes [248,249]. The following section will focus on commonly used membrane mimetics for solution NMR studies (Fig. 6).

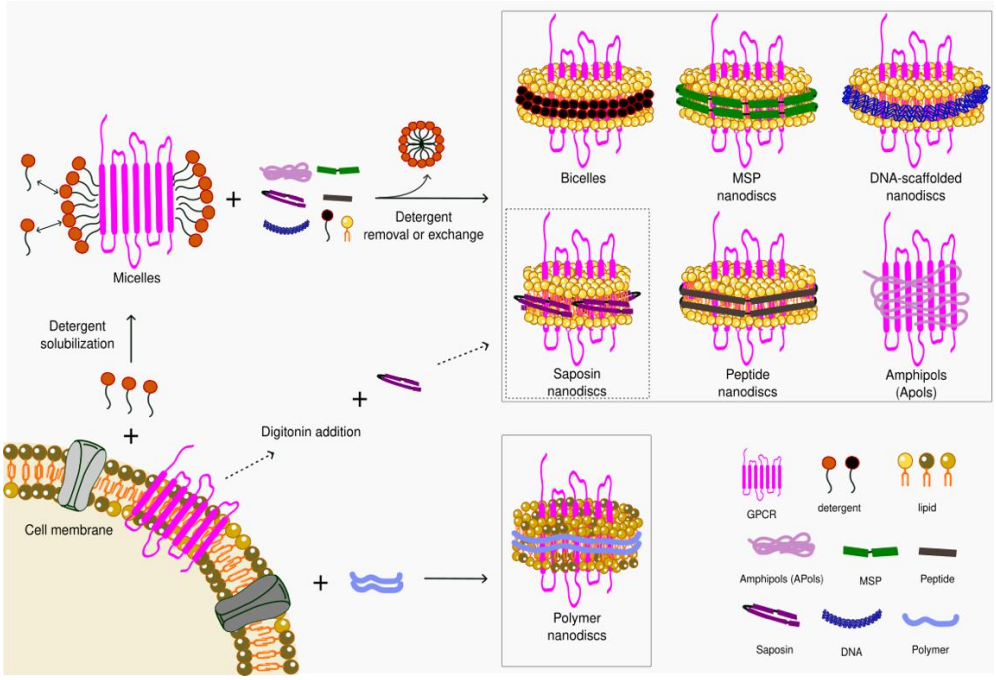

Fig. 6 Schematic presentation of various commonly used membrane mimicking systems for functional and structural studies of MPs.

Detergents. In general, the most popular applied membrane mimetics for solubilization and purification of MPs have been derived from micelle forming detergents. A wide variety of detergents have been developed and synthesized over the past decades, which have made impressive achievements in the characterization of MP structures [268]. In addition to the critical micelle concentration (CMC) needed to form the desired micelle particles, parameters such as the critical packing parameter (CPP), micelle aggregation number, cloud point, critical micelle temperature (CMT) and hydrophilic-lipophilic balance (HLB), influence the selection of proper detergents for the biophysical and structural characterization of MPs [245,269]. The CPP is useful to predict the preferred geometry of detergent micelles, such as spherical, cylindrical and inverted or reverse micelles, as well as flexible and planar bilayers [270]. The aggregation number is defined as the average number of detergent molecules present in a micelle when the CMC has been reached, which is correlated to the CPP and affects the micelle size and shape. Detergents with larger aggregation number are likely to form ellipsoid micelles, while

detergents with smaller aggregation number tend to form spherical micelles. The aggregation number of a detergent is related to its hydrocarbon chain length and to the size of its hydrophilic head group. In general, the longer the hydrocarbon chain length, the larger the aggregation number. The bigger the hydrophilic head group, the smaller the aggregation number. For solution NMR the aggregation number and thus the molecular mass of the micelle, which typically ranges from 20 to 100 kDa [271], is one central parameter. However, also the micelle shape, and thus the CPP, may induce anisotropic effects potentially influencing NMR properties. The cloud point is used to describe the temperature above which the detergent solution forms two distinct phases ("detergent-rich" and "detergent-poor") from the isotropic micellar solution, which is one of the issues frequently encountered during the crystallization of protein-detergent complexes and affected by the buffer conditions such as pH, salt concentration and additives [272]. Due to the increased molecular tumbling rate and related favorable spin relaxation rates, higher temperatures are often desirable for NMR experiments. In this respect, the cloud point and the CMT which is defined as the temperature above which isotropic micelles are formed, should also be considered for selection of suitable detergents for solution NMR studies.

Detergents are mainly classified into three categories according to the property of their hydrophilic head groups, i.e., ionic, nonionic and zwitterionic detergents [271,273]. The ionic detergents contain small, cationic or anionic charged hydrophilic head groups and relatively short hydrophobic alkyl chains, which are commonly used as surfactants to study the folding of MPs, such as the negatively charged sodium dodecyl sulfate (SDS). As an extremely effective ionic detergent, SDS exhibits excellent performance for solubilization and has been successfully used in the NMR measurement of stable proteins or peptides such as Magainin2 [274] or to study unfolded states [275]. Regarding the latter, SDS tends to denature MPs by breaking the hydrophobic interactions in the protein core or between the protein and biological membrane, resulting in the loss of biological activity. Most of the detergents currently used for purification and structural characterization of MPs are either nonionic or zwitterionic detergents possessing neutral charged hydrophilic head groups, which are considered to be 'mild' and to preserve the structural integrity and activity of isolated MPs. A selection of commonly used detergents is given in Table 2. If required, detergents can also be combined with e.g., cholesterol hemisuccinate (CHS) to stabilize the membrane-mimicking environment for purification and/or increased MP activity [276].

For the structural characterization of MPs by solution NMR, the preferred detergents should form small, homogeneous micelles and tumble rapidly to elongate relaxation times of the observed spins. Some zwitterionic detergents have been successfully used for α-helical and β-barrel MPs, such as LDAO [277], dihexanoyl- and diheptanoyl-phosphocholine (DHPC) [278–281], decyl-phosphocholine (DePC) [282], and dodecyl-phosphocholine (DPC) [283–288]. Overall, due to their comparably small size, detergent systems may offer the best NMR-spectral properties resulting in favorable features for NMR-based studies of structure and dynamics of the target MP. However, the price for this is a rather artificial environment lacking many aspects of native membranes. In this respect, the used detergent molecules may introduce destabilizing effects or alter the MP's structure due to different physicochemical properties including different chemical composition, hydrophobic mismatch, internal dynamics, lateral pressure, curvature and fast molecular exchange processes. Furthermore, the constant presence of monomeric detergent molecules may interfere e.g., with ligand binding or other functional features and thus prevent a native-state characterization of the system.

Table 2. Commonly used detergents. [a]Different values have been reported.

	Detergent		Micelle size (kDa)	Mw (Da)	CMC (wt %/mM)	Refer-ences
Non-ionic	DDM	n-Dodecyl-β-D-maltoside	72	510.6	0.0087/0.17	[289]
	DM	n-Decyl-β-D-maltoside	40	482.6	0.087/1.8	[290]
	OG	n-Octyl-β-D-glucoside	25	292.4	0.53/20	[291]
	NG	n-Nonyl-β-D-glucopyranoside	90	306.4	0.2/6.5	[290]
	$C_{12}E_8$	Polyoxyethylene 8 dodecyl ether	66	538.7	0.005/0.11	[271]
	$C_{12}E_9$	Polyoxyethylene 9 dodecyl ether	83	582.8	0.003/0.05	[289]
	UDM	n-Undecyl-β-D-maltopyra-noside	50	496.59	0.029/0.59	[292]
	LMNG	Lauryl maltose neopentyl gly-col	91 or 393[a]	1005.19	0.001/0.01	[290]
Zwitterionic	CHAPS	3-[(3-cholamidopropyl)dime-thylammonio]-1-propanesul-fonate	6	614.88	0.5/8	[271,293]
	CHAPSO	3-[(3-cholamidopropyl)dime-thylammonio]-2-hydroxy-1-propanesulfonate	7	630.88	0.5/8	[293]
	LDAO	lauryldimethylamine-N-oxide	21.5	229.4	0.023/1-2	[289]
	DPC	n-Dodecyl-phosphocholine (Fos-choline-12)	19	351.46	0.047/1.5	[294]

Bicelles. In contrast to detergent micelles, bicelles contain a planar lipid bilayer formed by long-chain phospholipids, such as dimyristoylphosphatidylcholine (DMPC), surrounded by a rim of either detergents or short-chain phospholipids (most commonly CHAPSO or DHPC) [295]. Bicelles were first introduced by Prestegard and co-workers for NMR measurements [296,297]. The size of bicelles depends on the molar ratio between the long-chain lipids and detergents (or short-chain lipids) used, which is defined as q parameter: q = concentration of long-chain lipid / (concentration of detergent above its CMC). The radius R of bicelles is defined as: $R = 1/2\ krq\ (\pi + (\pi^2 + 8k/q)^{1/2})$, where r is the radius of the rim of short-chain lipids (r equals 2 nm when using DHPC), k is the difference between the head-group areas of short-chain and long-chain lipids (k equals 0.6 when using DHPC and DMPC) [298,299]. In general, 'detergent-rich' isotropic bicelles with a low q value (~0.25-0.5) exhibit fast tumbling and can maintain rapid lipid reorientational diffusion, making them the bicelle of choice for solution NMR [300–302]. Some structures of peptides and MPs in isotropic bicelles have been determined by solution NMR, such as penetratin [303], dynorphins [304], the dimeric transmembrane domain of the receptor tyrosine kinase EphA [305], BNip3 [306], and the growth factor receptor ErbB2 [307], the integrin αIIbβ3 transmembrane complex [308], and the phototaxis receptor sensory rhodopsin II [279]. In addition to the q values, the morphology of bicelles can also be affected by total lipid concentration, lipid composition and temperature, which can induce transition from isotropic bicelles to vesicles [309,310]. Overall, the application of bicelles for solution NMR can provide a step towards more native-like conditions. In this respect, bicelles offer a planar-lipid-bilayer platform that can be conveniently adapted to study for example the influence of distinct lipid compositions on the function and structure of MPs, such as cholesterol, fatty acids and sphingolipids [311–313]. However, the presence of destabilizing effects by (monomeric) detergents, increased sizes, limited set of compatible lipids and detergents, and limited stability/tolerability for temperature, pH, and ionic strength, may still interfere with the generation of a native state.

Protein and peptide stabilized lipid-bilayer nanodiscs. Small lipid bilayers can also be stabilized in a detergent-free environment by amphipathic proteins or peptides. The resulting discoidal particles are normally referred to as lipid-bilayer nanodiscs (NDs).

MSP-based nanodiscs. The most common type of nanodiscs uses the so-called membrane scaffold proteins (MSPs). MSPs are derived from truncated forms of human Apolipoprotein A-I (ApoA-I), which can efficiently wrap around and stabilize a small patch of phospholipid bilayer. MSP nanodiscs can accommodate a wide range of lipid composition including 1-palmitoyl-2-oleoyl-glycero-3-phosphocholine (POPC), 1-palmitoyl-2-oleoyl-sn-glycero-3-phospho-L-serine (POPS), 1-palmitoyl-2-oleoyl-sn-glycero-3-phosphoglycerol (POPG), 1,2-dipalmitoyl-sn-glycero-3-phosphocholine (DPPC), 1,2-dimyristoyl-sn-glycero-3-phosphocholine (DMPC), 1,2-dimyristoyl-sn-glycero-3-phosphoglycerol (DMPG). MSP nanodiscs are disc-like particles that have defined size and high solubility in aqueous solutions, making it an ideal detergent-free system to perform functional and structural studies of MPs [314,315]. Nanodiscs contain two copies of the MSP, each stabilizing one leaflet of the bilayer. MSPs comprise repeated amphipathic α-helices that interact through salt bridges and zipper-like patterns of cation-π interactions. Preparation is generally straightforward, although some pitfalls need to be avoided (reviewed elsewhere [316]). It typically involves mixing the selected MSP variant with detergent solubilized phospholipids and, if desired, detergent solubilized MPs followed by suitable detergent removal initiating the self-assembly process (Fig. 6) [317–321]. The size of MSP nanodiscs ranges from 6 to 16 nm in diameter depending on the length of the MSP variants used [247,322–324]. The MSP-nanodisc system has been specifically optimized for solution-NMR applications by introducing shorter MSP variants, such as the MSPD1Δ5 [323], to increase molecular tumbling [323,325] and by covalently circularizing the scaffold proteins by sortase A, leading to so-called cNDs, to increase homogeneity and thermal stability [326]. A growing number of exciting NMR results could be obtained on different incorporated target proteins using a broad range of MSP-variants, for example reviewed in [327,328]. Noteworthy, the MSP-ND system in combination with solution-NMR readouts also offers an appealing platform to study the lipid-specific membrane binding modes of (soluble) proteins [329]. Advantages of the MSP-ND system include its high stability, solubility and homogeneity, the absence of detergents, the high tolerability for different lipids and lipid mixtures, as well as the possibility to adjust the particle size according to the specific needs.

In addition to NMR applications, these advantages have naturally stimulated numerous studies on the function and structure of MPs in a bilayer environment using small-angle X-ray or neutron scattering [330–333] and cryo-EM [334–337], including the cNDs system [338]. Still, the MSP-ND system requires detergent extraction/solubilization of the target MP and subsequent transfer of the MP into a lipid bilayer that typically comprises a non-native lipid composition. These features may interfere with the generation of a native-state due to denaturing effects of the detergents and/or an artificial lipid composition. While variations of the lipid compositions can be made, finding a suitable lipid composition with optimal NMR characteristics can be a tedious and time-consuming process [316,328,339].

Saposin-based nanodiscs. In addition to MSP, another class of proteins named saposins has been used to form NDs. The cysteine-rich α-helical sphingolipid activator glycoprotein family contains four homologous members (saposin A, B, C and D) which function as non-enzymatic modulators of lipid homeostasis and are

derived from the precursor protein prosaposin [340]. Saposin nanodiscs are formed by two saposin A proteins surrounding the lipid bilayer in a head-to-tail arrangement [341]. Due to the lipid-binding and self-assembling properties of saposin A, Frauenfeld and co-workers investigated the feasibility of reconstituting detergent solubilized MPs into saposin A based lipid-bilayer particles (also known as Salipro nanoparticles) in physiological conditions for the structural investigation of MPs in a detergent-free environment [342].

In comparison to the relatively laborious screening process for selecting suitable MSP variants, Salipro nanoparticles offer a more straightforward approach by mixing saposin A and lipids in different ratios to accommodate MPs with varying sizes. The Salipro system has been frequently used for functional [343] and in particular also cryo-EM studies [342,344–346]. More recently, Drulyte et al. introduced a new one-step approach for direct solubilization of MPs from cell pellets into Salipro. Of note, the cell pellets were first treated with the mild detergent digitonin, which increases the cell membrane fluidity, making the lipids and MPs more accessible for following reconstitution by saposin A proteins [347]. So far, a limited number of applications of the Salipro system for solution NMR have been reported, including the investigation of the feasibility of NMR studies of MPs in saposin nanodiscs, such as isotope-labeled β-barrel protein OmpX (16.5 kDa), phototaxis receptor sensory rhodopsin II (pSRII) (26.4 kDa) and turkey β1-adrenergic receptor (β_1AR) (36 kDa) [348]. Preservation of the MPs biological function as well as reasonably high quality 2D [^{1}H,^{15}N]- and [^{1}H,^{13}C]-SOFAST-HMQC spectra indicated that saposin nanodiscs have good potential for MPs studies by NMR [348]. The saposin nanodisc system mirrors most advantages and disadvantages of the MSP-ND system. In direct comparison the ease of size tunability may favor the saposin system for distinct application, while homogeneity and stability, in particular of the cND system, could be favorable in MSP-ND system. Furthermore, potential interaction between the saposin A protein with incorporated MPs should be taken into consideration [342].

Peptide nanodiscs. Small amphipathic peptides have also been used to prepare discoidal phospholipid bilayer particles. The α-helical peptide 18A (Ac-Asp-Trp-Leu-Lys-Ala-Phe-Tyr-Asp-Lys-Val-Ala-Glu-Lys-Leu-Lys-Glu-Ala-Phe-NH_2) derived from Apolipoprotein A-I (ApoA-I) is commonly used to prepare peptide nanodiscs (hereafter termed peptidisc) [349]. The Ala, Phe, Tyr, Leu and Val residues form the hydrophobic/lipophilic side of the amphipathic helix, while the opposite hydrophilic/polar side is composed of negatively charged (Asp and Glu) and positively charged (Lys) residues. The interaction between positively charged residues and negatively charged phosphate groups of phospholipids can be exploited to directly solubilize membranes without extra addition of detergents [350,351]. Two amphipathic α-helical peptides are arranged in an antiparallel fashion on the belt of a phospholipid bilayer patch covering the lipid fatty acyl chains [352]. The size of peptidiscs can be controlled by varying the lipid to peptide molar ratio, as is the case with saposin nanodiscs and co-polymer nanodiscs (discussed below). Fluorescence resonance energy transfer (FRET) experiments indicated that collision-mediated lipid exchange, probably caused by mismatches and dynamic exchange in the continuous belt, can occur between peptidiscs [351]. Furthermore, it has been suggested that above the phase transition temperature of the used lipids, translocation of the peptide from the particle belt to the liquid-crystalline bilayer phase of phospholipid can occur [353]. Also, changes in the particle size over time have been reported, corroborating the highly dynamic behavior of 18A peptidiscs [354]. The potential benefits of the 18A system in respect to ease of handling and size adaption, may therefore come at the prize of reduced (thermal) stability.

To stabilize the system, a self-polymerizing amphiphilic peptide with a cysteine-glycine flexible linker at N-terminus and a benzyl thioester (COSBn) at C-terminus (known as ASPP1, NH_2-Cys-Gly-Asp-Trp-Leu-Lys-Ala-Phe-Tyr-Asp-Lys-Val-Ala-Glu-Lys-Leu-Lys-Glu-Ala-Phe-COSBn) have been introduced [355]. ASSP1 can self-polymerize and spontaneously formed nanodiscs when incubated with (synthetic) phospholipid bilayers in the absence of detergents, which exhibit excellent stability in varying conditions. The size of ASPP1 peptidiscs can also be easily controlled by adjusting the peptide:lipid ratio [355]. In addition, Carlson et al. presented a rapid and cost-effective peptidisc system formed by nanodisc scaffold peptides (NSPr), which is made by two copies of the reverse version of 18A peptide linked by proline residue and exhibits outstanding solubilization efficiency of different MPs that have been transferred from purified detergent micellar conditions [356]. In recent years, the peptidisc systems have been successfully used for the structural determination of MPs by means of cryo-EM, such as PlexinC1/A39Rcomplex [357], HIV envelope glycoprotein [358], human dual oxidase 1 complex [359], yeast ABC transporter Pdr5 [360] *Acinetobacter baumannii* ATP synthase [361] and human Sec61 complex [362]. Noteworthy, the versatile and robust features of the DNA (origami) nanotechnology [363–366] can be exploited to expand the scaffolding features of protein-based NDs [367] and control MP oligomerization in NDs [368]. In addition, the generation of protein-free smaller membrane nanoparticles known as DNA-encircled bilayers (DEBs) has been reported [369]. In general, DNA-scaffolded and DNA-encircled NDs offer appealing features for NMR-structural studies such has homogeneity, size-tunability, and possible absence of other proteins/peptides. While exciting new developments and applications can be expected in this area, the laborious and cost intensive preparation may be restrictive for systems that do not require the benefits of this technique.

Co-polymer nanodiscs. Amphiphilic copolymers are an emerging class of synthetic polymers capable of directly extracting and/or stabilizing lipid bilayers. In contrast to most other nanodiscs technologies, usage of co-polymers can avoid the intermediate step of detergent solubilization of MPs and directly extract the functional MPs along with surrounding native lipids from the cellular membrane to form planar native lipid-bilayer nanodiscs. One of the most prominent systems is the negatively charged styrene/maleic acid (SMA) co-polymer. In particular SMA(2:1), which bears the hydrophobic styrene group and hydrophilic maleic acid group with an average ratio of 2.3 and has been widely used to isolate MPs, such as GPCR, ABC transporters, reaction centre-light harvesting 1 (RC-LH1) complex and nucleoside transporter [370–375].The formation of nanoscale SMA lipid particles (SMALPs) relies on the polymer's insertion into the membrane by hydrophobic and electrostatic interactions [376–378]. However, the efficiency of solubilization and ease of characterization of MPs with SMA(2:1) are largely affected by buffer conditions. At low pH and/or in the presence of divalent cations such as Mg^{2+} and Ca^{2+}, SMALPs tend to precipitate [379,380]. These issues have been addressed by the synthesis of zwitterionic SMA (zSMA), which exhibits enhanced buffer compatibility [381]. Often the UV absorption caused by the aromatic styrene moiety hampers the determination of encapsulated MPs concentration and other downstream biochemical experiments [381,382]. As a non-styrene containing co-polymer, Diisobutylene/maleic acid (DIBMA) does not bear the aromatic group and exhibits good solubility, resulting in the formation of DIBMA lipid particles (DIBMALPs). In addition, DIBMA is able to tolerate high concentration of divalent cations [383,384]. Due to their promising potential to study different aspects in the MP-research field, a variety of derivatives have been synthesized, such as the positively charged SMI [385], PMA [386], SMA-QA [387] and

SMAd-A [388]; and the negatively charged stilbene maleic acid (STMA) [389], Glyco-DIBMA [390], SMA-SH [391], SMA-EA [387] and acrylic acid styrene (AASTY) [392] systems (Fig. 7).

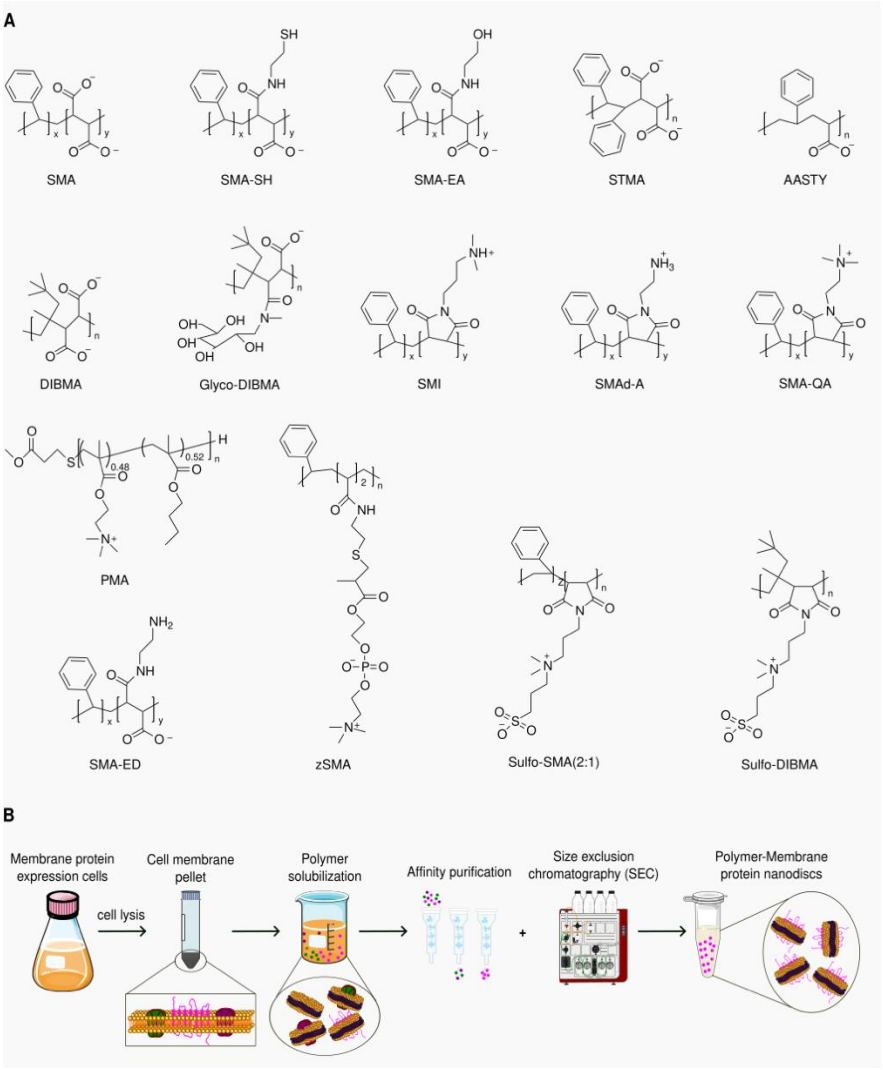

Fig. 7 The common and recently synthesized amphipathic polymers for MP studies. A) Chemical structures of polymers. SMA, styrene maleic acid; SMA-SH, styrene maleic acid with sulfhydryl group; SMA-EA, styrene maleic acid ethanolamine; STMA, stilbene–maleic anhydride; AASTY, poly(acrylic acid-co-styrene); DIBMA, diisobutylene maleic acid; SMI, poly(styrene-co-maleimide); PMA, polymethacrylate; SMA-QA, styrene maleimide quaternary ammonium; SMAd-A, styrene maleimideamine; SMA-ED, styrene maleic acid ethylenediamine. B) Schematic of MPs purification by amphipathic polymers.

While the extracted lipid patches in theory provide a direct native-like environment for the target MP, the high charge density of the surrounding polymers introduces clear restrictions. For example, strong charge-driven interactions of (soluble) binding partners with the polymer-belt may interfere with functional studies of the target MP. More recently, Glueck et al. have introduce the zwitterionic co-polymer Sulfo-DIBMA, which still exhibits excellent solubilization efficiency, high pH and divalent cation stability, and is able to accommodate large MPs and MP complexes with varying sizes, while largely reducing unwanted interactions within the tested systems [393]. This may be essential to generate native-state conditions for *in vitro* measurement of ligand-GPCR binding affinities under physiologically relevant conditions by suitable biophysical methods, such as microfluidic

diffusional sizing (MDS), microscale thermophoresis (MST), isothermal titration calorimetry (ITC), bio-layer interferometry (BLI) and surface plasmon resonance (SPR) [394–398]. Sulfo-DIBMA native membrane nanoparticles have also been used for initial cryo-EM structural studies of the encapsulated MPs [399]. Furthermore, DIBMA and SMA co-polymers have been successfully used for the structural characterization of MscS-like channel YnaI and Cytochrome bc_1 complexes by means of cryo-EM [400,401]. SMA co-polymers have also been used as vehicle for the transport of purified MP into lipid cubic phase (LCP) for crystallization [402].

So far, NMR studies have mainly used polymer nanodiscs comprising synthetic lipids to exploit their size tunability including the ability to form macro-nanodiscs that align with the magnetic field, thus functioning as novel alignment medium for determination of residual dipolar couplings and/or chemical shift anisotropy measurements [403–406]. Furthermore, the ability of NMR-based structural studies of MPs extracted from native membranes has been demonstrated for the bacterial cation diffusion facilitator CzcD from *E. coli*'s cytoplasmic membrane using SMA polymers in combination with solid-state NMR [407]. While these studies lay the foundation for high-resolution and quantitative NMR characterizations of MPs in a native state, increased sample heterogeneity and particle sizes, paired with challenges in isotope labeling in often-required eukaryotic expression systems, will benefit from a suitable strategy that combines vital advances in NMR methodology to provide the aspired results.

NMR methodology

The usage of increasingly complex membrane mimicking environment requires dedicated NMR-methods that are tailored to the respective environment and desired readout. The following section summarizes a selection of suitable techniques.

Methyl labeling. One NMR method that is coming of age as a powerful technique to study large molecular machines and membrane proteins is the detection of methyl groups. $^{13}CH_3$ groups are particularly good NMR sensors due to the combination of fast rotation of the methyl protons around the CH_3 axis and the degeneration of the three magnetically equivalent protons. Moreover, the methyl TROSY experiment has been developed that relies on the methyl group's favorable interferences of single- and triple-quantum cross-relaxation paths to further enhance resolution and sensitivity [408]. Pulse sequences have been developed using methyl group NMR sensors for structure characterization (3D HHC, HCC and 4D HCCH NOESY experiments) [409–411] and dynamics (nuclear spin relaxation including of the ^1H triple-quantum coherence [412,413], forbidden coherence transfer (FCT) [414], CPMG relaxation dispersion [415], CEST [416]. Similarly, the assignment pipeline of CH_3 groups has become easier with the introduction of structure-based assignment algorithms paired with NOESY experiments, and usage of optimal-control designed experiments able to distinguish Leu from Val signals [417].

Arguably one of the most powerful NMR experiments for detection of methyl groups is the band-selective optimized flip-angle short-transient (SOFAST) [^{13}C-^1H]-HMQC [418]. It is compatible with the methyl-TROSY approach and SOFAST provides a gain in measurement time of up to 5-fold due to accelerated sampling (shorter recycle delays). The setup exploits the pool of ^1H magnetization (e.g., non-methyl ^1H spin in protonated proteins, water, detergents, lipids, etc.) that are left 'untouched' (longitudinal), thus acting as a cross-relaxation sink to accelerate the methyl ^1H magnetization relaxation, enabling considerably shorter inter-scan delays. For large

proteins such as MPs in their membrane mimetic systems, the pulse sequence can be tuned to minimize losses due to transverse relaxation. In this regard, a minimum of pulses and shortening of delays can be used, which include (i) the optimization of the INEPT transfer step taking the adverse effects of magnetization buildup and transverse relaxation into account and (ii) the start of signal acquisition already prior the (complete) final refocusing of ^{1}H anti-phase magnetization, which in combination with a delayed decoupling, allows a considerable increase in signal-to-noise but requires dedicated processing due to distorted line shapes [419,420].

In protonated proteins, where the TROSY effect is difficult to exploit, isotope filtering can be used at the end of the first INEPT by flipping back all not-used ^{1}H magnetization along the z-axis, thus participating in the SOFAST effect. The XL-ALSOFAST-HMQC setup combines these benefits in one experiment and thus enables considerably increased sensitivity in large protonated systems [419]. For deuterated systems the TROSY-delayed decoupling (dd)-HMQC setup has been recently reported that uses a similar strategy but exploits the strong TROSY effect in these samples [419].Both pulse sequences will effectively contribute to improving the NMR accessibility of MPs in increasingly native environments.

In addition to optimized pulse sequences, a critical aspect for methyl NMR naturally is the incorporation of suitable isotope labeling pattern in the target protein. Generally, the aim is often to introduce, in addition to the desired (^{13}C,^{1}H) labeled methyl group, also a deuterated background to reduce spin-spin couplings and further enhance resolution and sensitivity. Stereo-specific metabolic precursors have been used to generate isolated $^{13}CH_3$ spin systems in Ile, Leu and Val residues [421,422]. This has proven very successful for proteins that can be expressed recombinantly in bacteria, but is difficult to realize for proteins, such as entire classes of membrane proteins, that can only be reliably expressed in eukaryotic or cell-free systems. Using dedicated methodology, cell-free protein production has been used to expressed ILV selective methyl labeled SREBP transmembrane segment [423]. A rather demanding workflow has been used in which first a protein is expressed in bacteria using selective metabolic precursors followed by its digestion to create a selective labeled amino acid mix that is ultimately used for cell-free expression. Alternatively, a modified cell-free system with the addition of enzymes able to process the metabolic precursors for Val and Leu was used to express selective $^{13}CH_3$ labeled progesterone receptor [424] that was recently optimized resulting in the “Stablelabel” approach [425].

As far as eukaryotic expression systems are concerned, yeast strains such as *P. pastoris* as well as *K. lactis* have been utilized to incorporate the metabolic precursor for Ile (alpha-Keto-butyric acid) as well as prelabeled amino acids [426–429]. Some of these strains can survive deuteration and express functional GPCRs, as shown for the adenosine A_{2A} receptor in both micelles and nanodiscs, using labeling of Ile methyl groups [430] or methionine residues [431]. Alternatively, ^{13}C-methylation of Lys residues has been employed to introduce $^{13}CH_3$ groups in the β_2-adrenergic and μ-opioid receptors expressed in *S. frugiperda* (Sf9) insect cells, but these result in non-natural probes [432,433]. In addition, insect cells have been used to introduce isotope-labeled Met [434–437] or Ala [438] in the β_2-adrenergic and P2X4 purinergic receptors reconstituted in micelles and nanodiscs by adding selectively isotope-labeled amino acids and deuterated algal mix to an amino acid deficient insect cell growth medium. The NMR signal was boosted by judicious ‘local deuteration’, i.e., addition of deuterated amino acids in the vicinity of the methyl group of interest. Incorporation of ^{2}H to 80% was achieved for a group of eight residue types (CFILTVWY) [438]. This approach was successful for Met (85% incorporation) where the metabolic

scrambling is minimal in eukaryotic cells but required addition of trans-aminase inhibitors to achieve selective $^{13}CH_3$ labeling of Ala residues (45% incorporation).

Recently, we reported usage of affordable stereo-specifically labeled Leu that can be incorporated in proteins, including MPs, expressed in insect cells or cell-free systems [439]. The local deuteration pattern inside the pre-synthetized Leu partially alleviate the need for background deuteration providing a gain of about 40% in relaxation times compared to a not deuterated environment. The absence of ^{13}C spins on the neighboring carbons furthermore circumvents restrictions associated with homonuclear ^{13}C-^{13}C scalar couplings and usage of constant-time encoded experiments. We anticipate that this new approach will facilitate the suitable incorporation of $^{13}CH_3$ NMR sensors in proteins expresses in eukaryotic systems and thus contribute to enable new native-state characterizations of MPs.

^{19}F NMR. An attractive NMR methodology for the investigation of membrane proteins makes use of the special properties of ^{19}F nuclei. Fluorine NMR presents interesting advantages related to the high gyro-magnetic ratio of ^{19}F, its 100% natural isotopic abundance and its high sensitivity to changes in chemical environment (chemical shift space). Moreover, its absence in most biomolecules provides a background-free approach even in cellular applications. This comes with the drawback that ^{19}F has a strong chemical shift anisotropy, leading to high relaxation rates. However, this issue can be partially alleviated by making use of the rotational dynamics in trifluoro-methyl groups [440] or by using the interference between the ^{19}F CSA and the ^{13}C-^{19}F dipole-dipole coupling for TROSY selection in aromatic ^{13}C-^{19}F spin systems [441]. Assignment of ^{19}F signals remains a challenge and still heavily relies on site-directed mutagenesis, although pulse sequences have been developed to correlate ^{19}F to neighboring nuclei in some cases like in the HOESY [442] and HCCF-COSY [443] experiments. Finally, the toolbox of ^{19}F NMR has been expanded towards characterization of molecular dynamics with the development of ^{19}F relaxation [444,445] and relaxation-dispersion [446] experiments.

A very successful approach for ^{19}F NMR characterization of membrane proteins is the introduction of trifluoromethyl groups in purified samples through chemical ligation with a single or a small set of Cys residues. For instance, several positions in the β_2-adrenergic receptor have been labeled with 2,2,2-trifluoroethanethiol (TET) to observe conformational changes in the cytoplasmic ends of helices VI and VII and understand its allosteric regulation [447–449]. A single TET-modified Cys residue has also been utilized as an NMR sensor to investigate the influence of lipid composition on the conformational equilibrium of the $A_{2A}AR$ receptor in MSP-nanodiscs. The presence of anionic lipids was found to induce conformational changes of similar magnitudes to those induced by drugs. Other probes based on ^{19}F-functionalized aromatic rings, such as 2-bromo-4-(trifluoromethyl)acetanilide (BTFA) have been used to study the effect of nanobody binding on the β_2-adrenergic receptor's conformation [450]. Furthermore, multiple ^{19}F-reactants were tested for their chemical-shift sensitivities to the environment and 2-bromo-N-(4-(trifluoromethyl)phenyl)acetamide (BTFMA) was found to be the best reporter label [451]. BTFMA proved successful in the conformational investigation of the β_2-adrenergic receptor [452] and the A_{2A} adenosine receptor [453], including a preparation in MSP-nanodiscs [454]. Of note, the tradeoff between the higher chemical shift sensitivity of ^{19}F-aromatic probes and their potential to reliably report on the desired conformational changes, is likely a sample-dependent choice to make for each new study. For example, it has been reported that reliable detection of ring current effects as reporters of membrane protein

conformational changes are primarily obtained for aliphatic [^{19}F] methyl groups proteins [455]. Chemical modification of Cys residues is feasible for samples produced in eukaryotic systems but has the disadvantage of introducing unnatural probes that may disrupt the normal conformational landscape of proteins. Furthermore, it often requires mutations of (all not observed) native Cys to Ser residues with difficult to predict effects on the target protein.

Instead, direct incorporation of ^{19}F probes into proteins of interest can be achieved in *E. coli* by using large excess of fluorinated amino acids in a minimal culture medium (M9). Consequently, only a minor modification, i.e., replacement of one native ^{1}H by the desired ^{19}F, can be realized. This has been readily achieved for 5-^{19}F-Trp [456] and 4-^{19}F-Phe [457] that was incorporated in glucagon to study its binding mode to glucagon receptor (GCGR). Incorporation levels of fluorinated aromatic amino acids can be enhanced by adding glyphosate to the culture medium (which blocks metabolic aromatic amino acid synthesis) and supplementing Phe, Tyr and Trp in lower amounts. This was critical for samples with more expensive ^{19}F-^{13}C Tyr probe that can be used to make use of the TROSY effect [441]. Moreover, direct incorporation of ^{19}F aromatic amino acids in proteins expressed in mammalian (HEK293T) cells was recently demonstrated and ^{19}F NMR was performed in-cell [458]. This approach shows great promise for the study of membrane systems in their native environments, with minimal modification of the target protein.

Often it may also be beneficial to label just a single site in the target protein with ^{19}F to avoid issues related to spectral crowding, ambiguous assignments, etc. Genetic code expansion in *E. coli* utilizing Amber codon repurposing was used to introduce a 3,5-difluorotyrosine site-specifically in β-arrestin and observe its binding mode to GPCR phospho-peptides by ^{19}F NMR [459]. In a more recent study, the Amber codon strategy was successfully used to introduce the unnatural amino acid 3′-trifluoromenthyl-phenylalanine into the cannabinoid receptor 1 expressed in Sf9 insect cells [460].

While the above sections have focused on solution NMR applications, ^{19}F NMR has also been used in the study of membrane proteins by solid-state NMR, where ^{19}F-^{19}F diffusion are particularly powerful and can quantify distances up to 2 nm. Such approaches were applied to the influenza M2 protein [461], the HIV fusion protein gp41 [462] and the bacterial drug transporter EmrE [463]. Furthermore, ^{19}F NMR can benefit from fast magic angle spinning (MAS) and Dynamic Nuclear Polarization (DNP) in the solid-state, as demonstrated for the HIV capsid protein [464]. The specific usage of DNP for proteins in native environments is discussed in the next section.

Targeted and localized DNP. DNP can enhance sensitivity of NMR by orders of magnitude by transferring the higher polarization of electrons to the nuclei of interest. Such a hyperpolarization has for example already been used for complex cellular and/or membrane systems [465–467]. DNP generally relies on introducing radicals carrying unpaired electron spins with specific magnetic properties as source of the hyperpolarization. An entire area of research on developing efficient, water-soluble, and biocompatible radicals has emerged [468–470]. In general, DNP provides an exciting way, not only to increase sensitivity, but also to bring selectivity to NMR experiments by engineering modified radicals that will specifically direct hyperpolarization to a target protein. Selective hyperpolarization can be realized via radicals that are brought in close proximity to the target protein

either by directly attaching them covalently or using endogenous interacting radicals such as specific metal ions. These scenarios are normally referred to as localized DNP. Hijacking the selectivity of biological interactions, a (bi)radical can also be covalently bound to a ligand of the target protein, which upon binding can direct the hyperpolarization to the ligand-protein complex. The latter scenario is also referred to as targeted DNP [471,472].

Localized-DNP approaches in which DNP radicals have been site-specifically attached to the protein of interest via Cys covalent linkage, include (i) Ubiquitin functionalized with a Gd^{3+}-DOTA moiety [473], (ii) Anabaena sensory Rhodopsin functionalized with a methanethiosulfonate-modified TOTAPOL (ToSMTSL) [474], and (iii) the ion channel KcsA with a similarly modified AMUPOL radical [475]. Although this is a straightforward and useful strategy to achieve selective hyperpolarization, it requires suitable point mutations of the target protein and suitable environments for the radical-labeling reaction.

Alternatively, (artificial) membrane systems can be selectively enhanced through usage of lipids chemically modified with radicals, for instance a C16-functionalized variant of the radical TOTAPOL (DPPC-TOTAPOL) termed PALMIPOL [476]. This approach has been shown to increase hyperpolarization by a factor of 4 compared to conventional soluble radical for Proteorhodospin in liposomes [477]. Similarly, DPPC-TEMPO lipids have been used to hyperpolarize the KL_4 lipophilic peptide inside lipid bilayers and study its membrane partitioning properties [478]. The distribution of radical-functionalized lipids in the bilayer is critical to optimize hyperpolarization but difficult to achieve in practice, which is a major limitation of that approach.

Directing the hyperpolarization via functionalizing an interaction partner of the target protein can separate the radical-labeling reaction from the target protein preparation. Consequently, the investigation of the target protein in a cellular context may become more accessible. Using a functionalized high affinity ligand of dihydrofolate reductase (TMP-T) it was shown that spectral bleaching and chemical perturbation could be reduced, and that selective hyperpolarization over the background could be realized [479]. We also achieved selective hyperpolarization of Bcl-xL thanks to a TOTAPOL-functionalized Bak peptide [471]. We demonstrated that, providing one can deuterate the environment to avoid ^{1}H-^{1}H spin diffusion effects, highly selective hyperpolarization of the target protein can be achieved even in the complex environment of a cell lysate.

The development of localized and targeted DNP approaches provides an exciting avenue for the characterization of proteins in their native environments, including in-cell. In a proof-of-concept experiment, introduction of the spin-label unnatural amino acid 2,2,6,6-tetramethyl-N-oxyl-4-amino-4-carboxylic acid (TOAC) in an antimicrobial peptide directly through solid-phase peptide synthesis allowed for DNP investigation of the peptide in intact bacterial cells [480,481]. Also, recombinantly expressed isotopically labeled proteins can be delivered into intact, non-isotopically labeled mammalian cells in native concentrations and be investigated by DNP [482]. With careful consideration of the radical stability in cells [483,484], its partition inside cells and cell compartments [485] and of the cell's intactness during sample delivery, freezing and magic-angle spinning procedures [486], we expect localized and targeted DNP to become a valid avenue for in-cell characterization of membrane systems in the future.

Conclusions and perspectives for native-state characterization of challenging MPs

In the following we will use GPCRs as an example to outline the motivation, requirements, and feasibility of a native-state NMR strategy. GPCRs comprise the largest superfamily of cell surface proteins in mammalian cells. Approximately 800 GPCRs are encoded by ~2% human genome [487]. GPCRs are highly dynamic and undergo conformational rearrangements induced by the binding of a plethora of extracellular stimuli, leading to different conformations during activation which in turn interact with intracellular signal transducers and initiate downstream signaling pathways. This dynamic equilibrium and its modulation are among the most important read-out parameters to understand GPCR signaling and potential effects by new drug candidates. Pioneering studies, including [434,437,452,488–490] (among many others reviewed for example in [258,263,443,491]), have impressively demonstrated that NMR belongs to the very few techniques that is capable of providing this read out. However, it is also apparent that this read out can be influenced by the frequently used mutations that are introduced to stabilize the receptor as well as by the surrounding lipid environment. Therefore, usage of a native-state condition is essential to obtain the desired insights. In this respect it can be speculated that the native-lipid membrane extraction via suitable polymer-disc systems offers two advantages, i.e. (i) the native lipid environment is preserved and (ii) the sample preparation procedure is entirely detergent-free. It can be envisioned that both features will increase the receptor's general stability potentially reducing the need for stabilizing mutations.

Despite their crucial importance in the development of pharmaceuticals, studies into the function and structure of GPCRs by NMR remain challenging, largely owing to the low-level expression and typically high costs of isotopically labeled medium. While the expression level of endogenous GPCRs is low, several heterologous expression systems have been successfully used to produce isotope-labeled GPCRs [492]. In addition to mammalian system such as HEK293 cells, the *Spodoptera frugiperda* cells such as Sf9, Sf21 and *Trichoplusia ni* (High Five) have been successfully used for MP expression. These insect-cell expression systems are able to produce functional GPCRs at comparatively high yields (approximately 0.5 mg per liter of cell culture) [489,491,493]. Affordable isotope-labeling protocols using labeled algal extract [494–496] and yeast extract as well as stereo-specific methyl labeled Leucine [439] have been developed. In general, these approaches should be able to produce sufficient amounts of the target GPCR for native-state characterization. At the same time, the availability of new sets of (electroneutral) polymers [393], capable of solubilizing MPs in their native lipid environment, may allow to stabilize GPCRs in a native-like state, ideally evading the need for stabilizing mutations, while still allowing ligand binding studies. Consequently, the long-lasting limits in generation of sufficient amounts of isotope labeled target GPCR in a native-like environment may just have been resolved.

Still, the intended sample, i.e., wild-type GPCR in native-membrane discs, will likely display increased heterogeneity, conformational dynamics and an overall increased particle size as for example compared to NMR-optimized MSP nanodiscs. To counter these features, it is essential to exploit appropriate NMR methodology such as methyl[196] or ^{19}F labeling to reduce effects of (heterogenous) sizes combined with dedicated new pulse sequences such as the XL-ALSOFAST-HMQC [419] or the TROSY-ddHMQC [420]. In parallel to the above outline solution-NMR strategy, the usage of (DNP-enhanced) solid-state NMR may provide additional insights into specific structural features. Due to the reduced spectral resolution in (low temperature) DNP, this approach presumably needs to involve specific isotope labeling and/or selective hyperpolarization techniques to obtain the

desired insights. However, DNP-enhanced solid-state NMR will likely have the capability to obtain atomic-resolution insights into wild-type GPCRs in native eucaryotic membranes or even whole-cell preparations.

In conclusion, the field of NMR-based GPCR research has entered an exciting period in which the available tools are paving the way to reliable atomic-resolution and quantitative insights into the structural features and highly relevant dynamic equilibria of these key receptors in their native state.

3. Electroneutral polymers for membrane protein studies

This chapter reflects content of the following publication focusing on our contribution that involves the microfluidic diffusional sizing (MDS) measurement of the electroneutral polymers, including Sulfo-DIBMA, which are amenable to protein/lipid interaction studies.

Electroneutral Polymer Nanodiscs Enable Interference-Free Probing of Membrane Proteins in a Lipid-Bilayer Environment

Glueck, D., Grethen, A., Das, M., Mmeka, O. P., Patallo, E. P., Meister, A., Rajender, R., Kins, S., Räschle, M., Victor, J., Chu. C., Etzkorn, M., ... & Keller, S.

Small 18.47 (2022): 2202492. DOI: 10.1002/smll.202202492.

3.1 Abstract

Membrane proteins can be examined in near-native lipid-bilayer environments with the advent of polymer-encapsulated nanodiscs. These nanodiscs self-assemble directly from cellular membranes, allowing in vitro probing of membrane proteins with techniques that have previously been restricted to soluble or detergent-solubilized proteins. Often, however, the high charge densities of existing polymers obstruct bioanalytical and preparative techniques. Thus, the authors aim to fabricate electroneutral-yet water-soluble-polymer nanodiscs. By attaching a sulfobetaine group to the commercial polymers DIBMA and SMA(2:1), these polyanionic polymers are converted to the electroneutral maleimide derivatives, Sulfo-DIBMA and Sulfo-SMA(2:1). Sulfo-DIBMA and Sulfo-SMA(2:1) readily extract proteins and phospholipids from artificial and cellular membranes to form nanodiscs. Crucially, the electroneutral nanodiscs avert unspecific interactions, thereby enabling new insights into protein-lipid interactions through lab-on-a-chip detection and in vitro translation of membrane proteins. Finally, the authors create a library comprising thousands of human membrane proteins and use proteome profiling by mass spectrometry to show that protein complexes are preserved in electroneutral nanodiscs.

3.2 Introduction

Membrane proteins constitute ≈23% of the human proteome and account for over 60% of current drug targets [497]. Despite their evident importance in biology and medicine, membrane proteins are challenging to analyze in vitro because it is difficult to extract them from a lipid membrane gently; that is, without perturbing the protein's native structure and function. Over recent years, membrane mimics offering a lipid bilayer [498], such as membrane-scaffold protein (MSP) nano-discs [314], have been used with great success. However, these methods also require conventional detergents in time-consuming and potentially deleterious initial steps [373].

Overcoming these pitfalls, amphiphilic copolymers such as diisobutylene/maleic acid (DIBMA) [383] and styrene/maleic acid (SMA) [499] have emerged as alternatives to purifying integral membrane proteins [392,500]. These polymers induce formation of nanodiscs composed of a lipid-bilayer patch surrounded by a polymer belt [501–503]. The proteins simply remain embedded in their native lipid-bilayer patch as part of the DIBMA or SMA nanodiscs, and detergents are not required [273]. Nonetheless, the high charge densities of both DIBMA and SMA lead to unspecific interactions with charged proteins and lipids. Such unspecific interactions interfere with labile protein–protein and protein–lipid interactions and also with enzymatic (especially ribosomal) activities [504]. Furthermore, they obstruct many preparative and analytical techniques, such as protein electrophoresis and cell-free protein translation [373,505]. Thus, creating electroneutral polymers for lipid-bilayer nanodiscs has become an attractive goal. One approach toward electroneutrality has been to incorporate phosphocholine pendant groups into the zwitterionic copolymer zSMA, which was synthesized de novo [381,382]. While zSMA has shown promise for biological applications, the multistep nature of its synthesis has so far prevented its widespread use in membrane-protein applications. A considerably simpler synthetic approach was to modify commercially available SMA backbones with ionizable pendant groups. Although chemically straightforward, the resulting polymers are water-soluble only when they carry a net charge [388]. With this simplified approach in mind, we

hypothesized that a sulfobetaine moiety would provide the desired electroneutrality without sacrificing solubility. Sulfobetaine is zwitterionic at biologically relevant pH values, so we reasoned that its polymer chains and nanodiscs should also be electroneutral. In addition, sulfobetaine is found in popular buffers (in particular, Good's buffers), attesting to its high water solubility and excellent biocompatibility.

Here, we present two new electroneutral—yet water-soluble—polymers, Sulfo-DIBMA and Sulfo-SMA(2:1), formed by attaching sulfobetaine to the commercially available polymers DIBMA and SMA(2:1), respectively (Fig. 8). We show that the new polymers quantitatively solubilize phospholipid bilayers and extract proteins from cellular membranes to form electroneutral nanodiscs. The electroneutrality of the new nanodiscs allows charge sensitive protein–lipid interactions to be reliably detected and quantified—for the first time—by using the new lab-on-a-chip method, microfluidic diffusional sizing (MDS). The unique combination of electroneutral nanodiscs and MDS reveals protein–lipid interactions that are otherwise overshadowed by unspecific electrostatic effects in the case of charged nanodiscs. We further highlight the benefit of these electroneutral polymers for cell-free translation and in vitro folding of membrane proteins. Like MDS, cell-free protein translation has so far been incompatible with polymer-encapsulated nanodiscs because of interference due to unspecific electrostatic interactions. Moreover, we demonstrate that the proteins extracted by the sulfo-polymers can be directly analyzed by electrophoresis with no need for prior polymer removal. We exploit these properties for creating soluble libraries comprising thousands of human membrane proteins embedded in a nanoscale lipid-bilayer environment that preserves the integrity of protein complexes and is amenable to proteome profiling by mass spectrometry.

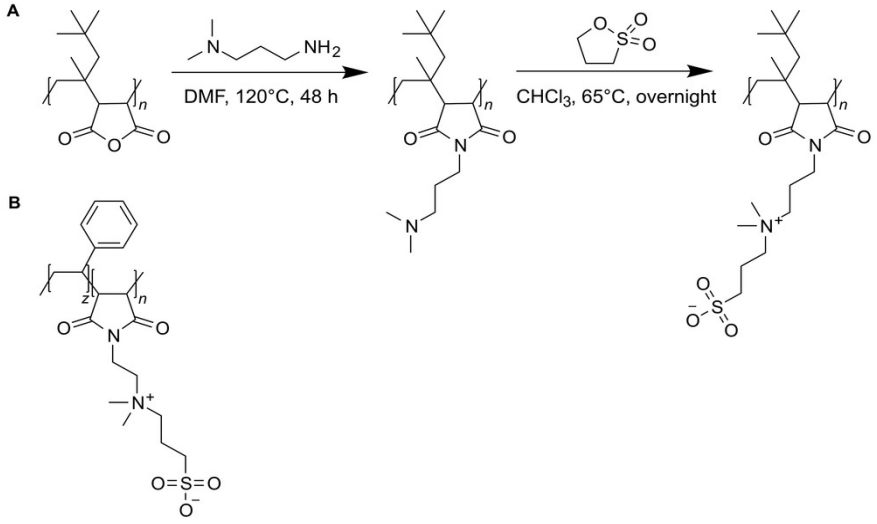

Fig. 8 Synthetic route for the electroneutral sulfo-polymers. (A) Sulfo-DIBMA formation from maleimide copolymer and 1,3-propane sultone. (B) Sulfo-SMA(2:1) structure.

3.3 Associated results

Charge-sensitive protein–lipid interactions are involved in many physiologically relevant but barely understood processes. For example, the binding and (mis)folding of proteins on lipid membranes are thought to underlie amyloid-plaque formation in neurodegenerative diseases [506]. Therefore, understanding protein–lipid interactions may have important implications for biology and medicine. However, these interactions cannot be studied with existing polymer nanodiscs (such as those based on DIBMA and SMA) because their polyionic polymer chains interfere with such charge-sensitive interactions. We assessed the usefulness of Sulfo-DIBMA and Sulfo-SMA(2:1) polymers for probing protein–lipid interactions by means of microfluidic diffusional sizing (MDS), a recent lab-on-a-chip technique that requires only microliter volumes of sample [507–511]. MDS can detect binding of proteins to lipid bilayers by measuring changes in the effective hydrodynamic size of the protein upon membrane binding. Since vesicles tend to exceed the hydrodynamic-size range applicable for MDS, smaller lipid-bilayer nanoparticles are needed for analyzing protein–lipid interactions. Hence, Sulfo-DIBMA and Sulfo-SMA(2:1) nanodiscs are ideal candidates for this kind of assay.

To assess which polymers are able to probe charge-sensitive protein–lipid interactions, we first studied the membrane interactions of α-synuclein, a protein that plays a pivotal role in neurodegenerative diseases [512]. Physiologically, this water-soluble protein binds to presynaptic vesicles, which presumably aids synaptic release [512]. α-synuclein has a high affinity to anionic lipids, whereas interactions with zwitterionic lipids are weak [513]. Consequently, lipid-specific binding modes, predominantly those involving formation of amphipathic α-helices, have been detected using liposomes [514,515] and MSP nanodiscs [329]. Due to its well-established lipid-binding properties, α-synuclein here served as a positive control for our assay (Fig. 9A). Thus, we titrated α-synuclein with nanodiscs formed from the different polymers and harboring either zwitterionic DMPC or anionic DMPG (1,2-dimyristoyl-sn-glycero-3-phospho-(1'-rac-glycerol)). Upon titration with anionic DMPG encapsulated by either Sulfo-DIBMA or Sulfo-SMA(2:1), the hydrodynamic size of α-synuclein increased from 7 nm to about 16 nm, which is consistent with binding of the protein to these nanodiscs (Fig. 9B). Upon titration with zwitterionic DMPC encapsulated by either of the two electroneutral polymers, however, α-synuclein did not bind to the nanodiscs, as evidenced by its unchanged hydrodynamic size. In stark contrast, titration with nanodiscs formed from polyanionic DIBMA or SMA always revealed binding of α-synuclein to the nanodiscs irrespective of the charge of the encapsulated lipid, obscuring any lipid-specific effects. Thus, our data clearly demonstrate that the expected lipid specificity of this interaction is detected only for nanodiscs formed from electroneutral Sulfo-DIBMA or Sulfo-SMA.

Following our positive control, we examined the less-well-characterized binding of the peptidic adrenocorticotropic hormone (ACTH) to DMPC and DMPG nanodiscs [516]. As for other secretory peptides, binding to anionic lipids is thought to facilitate directed intracellular transport by vesicles [517]. Indeed, we observed that ACTH strongly preferred anionic DMPG over zwitterionic DMPC in both Sulfo-SMA(2:1) and Sulfo-DIBMA nanodiscs (Fig. 9C and 9D). Here again, this lipid specificity was lost when ACTH was exposed to nanodiscs encapsulated by polyanionic SMA(2:1) or DIBMA, which gave rise to unspecific interactions irrespective of the chemical nature of the lipid constituent (Fig. 9C). With the aid of Sulfo-DIBMA nanodiscs, we

probed the charge-sensitive membrane interactions of ACTH over several orders of magnitude of lipid concentrations (Fig. 9D). Thus, MDS measurements enabled us to reliably detect even the rather weak interaction of ACTH (Fig. S1) with DMPG lipids. Finally, we used monomeric guanine nucleotide-binding protein subunit β1 (GB1) as a negative control. Because GB1 in its monomeric form does not interact with DMPC or DMPG, the protein should be inert toward Sulfo-nanodiscs regardless of their lipid constituents [518]. As expected, GB1 showed no increase in size in the presence of Sulfo-SMA(2:1) nanodiscs. Taken together, these three examples demonstrate that the new, electroneutral polymers do not interfere with charge-sensitive protein–lipid interactions and—for the first time—enable sensitive membrane-interaction assays in a microfluidic format.

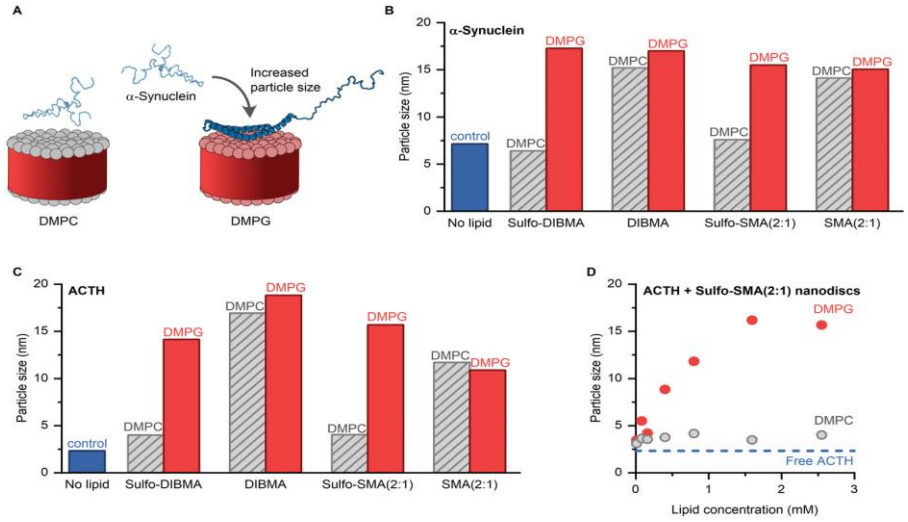

Fig. 9 Electroneutral nanodiscs enable probing of lipid-specific protein–lipid interactions via MDS. A) Schematic showing that α-synuclein selectively binds to and folds at anionic membrane surfaces, such as DMPG, resulting in a protein–nanodisc assembly with increased hydrodynamic size [519]. By contrast, α-synuclein should not interact with nanodiscs having electroneutral surfaces, such as DMPC. B) Particle size of α-synuclein in the absence and presence of DMPC or DMPG nanodiscs formed from Sulfo-DIBMA, DIBMA, Sulfo-SMA(2:1), or SMA(2:1). C) Particle size of ACTH in the absence and presence of DMPC or DMPG nanodiscs formed from Sulfo-DIBMA, DIBMA, Sulfo-SMA(2:1), or SMA(2:1). ACTH showed strong selectivity for DMPG lipids in Sulfo-DIBMA and Sulfo-SMA(2:1) nanodiscs but not in nanodiscs made from negatively charged DIBMA or SMA(2:1). D) Particle size of ACTH upon titration with Sulfo-SMA(2:1) nanodiscs containing zwitterionic DMPC or anionic DMPG.

3.4 Conclusions

The electroneutral polymers introduced herein offer considerable advantages for membrane-protein research because they significantly extend the range of bioanalytical and preparative methods compatible with lipid-bilayer nanodiscs. Sulfo-DIBMA and Sulfo-SMA(2:1) can be readily obtained by a simple modification of commercial polyanionic precursors, allowing their low-cost and straightforward production in nonspecialized laboratories. Electroneutral polymer nanodiscs can then self-assemble directly from cellular membranes, enabling embedded proteins to be probed in vitro without ever being removed from their lipid-bilayer environment.

4. Characterization of MC4R in native-lipid environment

The previous chapter demonstrates that the electroneutral polymer Sulfo-DIBMA does not interfere with protein/lipid interactions, suggesting its potential utility in characterizing protein/protein interactions in native lipid nanodiscs. The following chapter focuses on the investigation the ligand binding properties and allosteric modulation by divalent cations of MC4R in different membrane mimicking systems, including the Sulfo-DIBMA native membrane nanodiscs. Chapter 4 reflects the content of the following manuscript:

Functional insights into human Melanocortin-4 Receptor (MC4R) in Native Lipid-Bilayer Nanodiscs (*Manuscript in preparation*)

Ci Chu,[a] Carolyn Vargas,[b,c,d] Simon Sommerhage,[e] Gunnar F. Schröder,[e] Sandro Keller,[b,c,d*] Manuel Etzkorn[a,e,f*]

[a]Heinrich Heine University Düsseldorf, Faculty of Mathematics and Natural Sciences, Institute of Physical Biology, Universitätsstr. 1, 40225 Düsseldorf, Germany

[b]Biophysics, Institute of Molecular Biosciences (IMB), NAWI Graz, University of Graz, Humboldtstr. 50/III, 8010 Graz, Austria

[c]BioTechMed-Graz, Graz, Austria

[d]Field of Excellence BioHealth, University of Graz, Austria

[e]Institute of Biological Information Processing (IBI-7: Structural Biochemistry), Forschungszentrum Jülich, Jülich, Germany

[f]Jülich Center for Structural Biology (JuStruct), Forschungszentrum Jülich, Jülich, Germany

4.1 Abstract

The human melanocortin-4 receptor (MC4R) is a unique GPCR, which is regulated not only by endogenous agonists, but also endogenous antagonists or inverse agonists. MC4R is involved in energy homeostasis and feeding behavior, and its dysfunction leads to a variety of diseases. It is known that the physiological ions strongly affect the functional activity of MC4R, but little is known about the regulation of these metal ions on MC4R in different environments. Detergent micelles, MSP nanodiscs, and Sulfo-DIBMA/native membrane nanodiscs provide us with three membrane-mimicking systems to gain insights into the influence of the environment on the ligand binding to MC4R and extend our understanding of the allosteric modulation of divalent cations. Our data demonstrated that the functional integrity of MC4R is well-preserved in lipid bilayer, especially in Sulfo-DIBMA/native membrane nanodiscs. In all membrane mimetics, Ca^{2+} and Cu^{2+} functioned as a positive and a negative allosteric modulator potentiating and inhibiting the ligand binding affinity, respectively. Interestingly, Zn^{2+} exhibited environment-dependent biphasic effect, acting as a positive and a weak negative allosteric modulator for ligand binding to MC4R embedded in detergent micelles and lipid bilayer, respectively.

4.2 Introduction

G-protein-coupled-receptors (GPCRs) are the largest superfamily of cell surface membrane proteins in human genome and targeted by more than 30% of all approved drugs by Food and Drug Administration, making it the largest intensively studied targets for drug development and highlighting their vital roles in human health and disease [1,2]. Although all GPCRs sharing the conserved architecture of seven transmembrane (7TM) helical domains, their sequence homology remains very low and are divided into four major classes including class A (rhodopsin-like), B (secretin-like and adhesion), C (glutamate) and F (Frizzled), [520]. More than 700 GPCRs belong to class A and share several highly conserved motifs in their 7TM domains, including D/ERY motif in the intracellular end of TM3, CWxP in the middle of TM6, NPxxY in the intracellular end of TM7 and the hydrogen bond network. In addition, several highly conserved residues, such as $Arg^{3.50}$, $Trp^{6.48}$ and $Trp^{7.53}$ (superscript numbers correspond to the Ballesteros-Weinstein nomenclature [14]), seem to act as micro-switches regulating GPCR signaling [15,16]. MC4R is one of the members of human melanocortin receptor family (MCRs) that consists of five subtypes (MC1R to MC5R), and belongs to class A GPCR [143]. In particular, MC4R is found in peripheral tissues, intestinal L cells and predominantly expressed in the central nervous melanocortin system therefore together with MC3R referred to as neural MCRs [144,145]. In the melanocortin pathway, food intake and energy homeostasis are primarily coordinated by the interaction of MC4R with neuropeptides also termed melanocortins [146,147]. Naturally occurring MC4R loss-of-function (LOF) mutations are the most frequent cause of monogenic obesity and binge eating disorder [151,152], while some gain-of-function (GOF) variants have been found to be associated with low body mass index (BMI) and obesity related cardiometabolic diseases [153]. In addition to its central roles in the control of energy homeostasis and feeding behavior, the deficiency of MC4R is also involved in the regulation of blood pressure, cardiovascular function and type 2 diabetes mellitus, making it an attractive therapeutic target for the treatment of obesity and related diseases [155–159]. As a pharmacological puzzle, MC4R exhibits unique properties, including the regulation by endogenous agonists such

as adrenocorticotropic hormone (ACTH), α-melanocyte stimulating hormone (α-MSH), endogenous antagonists/inverse agonists (specifically agouti-related protein, AgRP) [161,197], and melanocortin-2-receptor accessory protein 2 (MRAP2) [148,150,521], as well as the ability to couple with ion potassium channel Kir7.1 in a G protein-independent manner [522].

Most ligands or drugs currently on the market are designed using conventionally discovery strategies binding directly to the primary active sites (also known as orthosteric binding sites), leading to non-progressive activation (agonists) or inhibition (antagonists) of target receptors in a coarse adjustment manner [63,64]. Molecules that bind to the orthosteric binding sites of GPCRs are termed canonical orthosteric ligands, including endogenous and synthetic agonists, antagonists and inverse agonists, and the binding location of orthosteric ligands varies by receptor classes [65]. Of note, GPCRs can also interact with a variety of extracellular molecules which function as allosteric modulators by binding to the lower evolutionary pockets on the receptor that are topologically distinct from the orthosteric binding sites but remain conformationally linked [71]. These allosteric modulators are able to fine turn the physiological functions of receptors by stabilizing receptor conformation and shifting system equilibrium, thereby influencing the binding behavior of orthosteric ligands, such as the affinity, efficacy and GPCR subtype selectivity. As a result, this allosteric modulation leads to the enhancement or inhibition of ligand binding and signaling responses [72–75]. Such allosteric molecules are subdivided into different types based on their activities [76], including positive allosteric modulators (PAMs) which potentiate the effects of orthosteric agonists, negative allosteric modulators (NAMs, also referred to noncompetitive antagonists) which noncompetitively decrease the effects of orthosteric agonists, neutral allosteric modulators which occupy the allosteric sites and function as competitive antagonists of both PAMs and NAMs, preventing their binding at the same allosteric sites, yet have no effects on the activity of orthosteric ligands, as well as agonist-positive allosteric modulators (Ago-PAMs) which function as both PAMs of the endogenous agonists and agonists on their own, leading to the activation of receptors in the absence of orthosteric agonists [76–79]. Biological and pharmacological studies have implicated that a number of endogenous regulators have been investigated and shown to participate in GPCR allosterism acting as PAMs or NAMs, including G proteins, β-arrestins, receptor activity-modifying proteins (RAMPs), lipids, amino acids, peptides, GPCR-targeted antoantibodies and ions [220]. Of these modulators, metal ions are required for the lignad binding to a number of GPCRs and GPCR-mediated signaling transduction [117,221,222]. Previous study has demonstrated that the specific binding of radioligand ^{125}I-NDP-α-MSH to MC4R requires the presence of Ca^{2+} [223]. In addition, Zn^{2+} has been found to stimulate the signal transduction and enhance the ligand potency on MC4R and MC1R [227]. A study regarding the regulation of constitutive activity of MC4R reveals that Zn^{2+} functions as a positive allosteric modulator for orthosteric ligand binding and exhibits agonistic properties at physiologically relevant low micromolar concentrations, whereas Cu^{2+} acts as an inverse agonist and inhibits the activity of MC4R [230].

In general, the extraction of membrane proteins including GPCRs from cellular membrane for *in vitro* studies are widely carried out with the aid of detergents, which form membrane-mimetic micelles by displacing the native membrane lipids for stabilizing isolated membrane proteins in an aqueous environment. In addition, the lipid bilayer nanodiscs formed by membrane scaffold proteins (MSPs) have also been widely used, which allow the control of lipid composition and nanodisc size using defined lipid mixture and different MSP variants [314]. However, the membrane protein isolation still necessitates the use of detergents, and the process of optimizing

the reconstitution of membrane proteins into MSP nanodiscs is time-consuming and labor-intensive [523]. Moreover, the functional activities of GPCRs such as ligand binding and G protein coupling are regulated by various properties of surrounding phospholipid bilayer such as hydrophobic mismatch, bilayer thickness, lateral pressure, membrane fluidity, curvature and composition, which are missing or difficult to mimic using synthetic phospholipid mixture in detergent micelles or MSP nanodiscs [262,264,265,524]. Amphiphilic copolymers are a new alternative tool for membrane proteins studies, which are able to directly extract the membrane proteins from cellular membrane with surrounding native phospholipids and form nanodiscs suitable for subsequent functional and structural studies of membrane proteins [400]. Notably, the utilization of electroneutral Sulfo-DIBMA polymer has recently been described [393]. Its outstanding properties, including electroneutrality, high stability toward a range of pH values and divalent cations, and decent solubilization efficiency, render it an ideal choice for membrane protein studies in their native lipid environment. In the current work, we used various biochemical and biophysical techniques to study the effects of different membrane mimicking systems (i.e., detergent micelles, MSP nanodiscs and Sulfo-DIBMA/native membrane nanodiscs) and several divalent cations, including Ca^{2+}, Zn^{2+} and Cu^{2+}, on the function of MC4R. We found that Sulfo-DIBMA is able to extract MC4R with surrounding native phospholipids forming homogeneous nanoparticles. The native lipid environment (Sulfo-DIBMA) enhanced the thermal stability of MC4R. In addition, the functional integrity of MC4R was well-preserved by the lipid-bilayer. Furthermore, We observed that Ca^{2+} enhances the binding of orthosteric agonists to MC4R acting as a positive allosteric modulator, whereas Cu^{2+} inhibits the ligand binding functioning as a negative allosteric modulator. Interestingly, we also observed that Zn^{2+} exhibits a biphasic effect on the orthosteric agonist binding, and this effect is environment-dependent.

4.3 Methods

Peptide ligand preparation. The human adrenocorticotropic hormone truncated construct ACTH (1-23) containing a cysteine residue at C-terminus was cloned into pET-16b vector containing a 6xHis tag at N-terminus, followed by B1 domain of Streptococcal protein G (GB1 fusion protein) and tobacco etch virus (TEV) cleavage site. *Escherichia coli* strain BL21 (DE3) cells were used for peptide expression. Cells were cultured in 2xYT medium at 37 °C, supplemented with 100 µg/ml Ampicillin. The expression was inducted with 1 mM isopropyl-β-D-thiogalactopyranoside (IPTG) upon the optical density 600 (OD_{600}) reached 0.6. 5 h after induction, cells were harvested by centrifugation at 3,000 *g*, 15 min (Avanti J-26S XP, Beckman Coulter) and were resuspended in a lysis buffer containing 50 mM sodium phosphate, pH 7.5, 300 mM NaCl, 1 mM dithiothreitol (DTT), supplemented with EDTA free oCmplete protease inhibitor cocktail tablet (Roche), then lysed by sonication on ice (Bandelin, Germany). The lysate was centrifuged at 120,000 *g,* 4 °C for 20 minutes. Supernatant was incubated with Ni-NTA resin (Macherey-nagel, Germany) at 4 °C overnight. Resin was loaded onto gravity column and washed with 10 column volumes (CVs) of lysis buffer, and 10 CVs lysis buffer supplemented with 20 mM imidazole. Bound proteins were eluted with 10 CVs lysis buffer supplemented with 250 mM imidazole. Fractions containing peptides were pooled and dialyzed against lysis buffer using 3.5K MWCO SnakeSkin dialysis tubing (Thermofischer) at 4 °C overnight. The fusion protein was removed by the addition of home-made TEV protease. Cleaved peptides were further purified by Superdex 16/600, 30 pg column (GE Healthcare) with a running buffer

containing 20 mM ammonium bicarbonate (Sigma). Peptide labeling by thiol-reactive ATTO-488 Maleimide (ATTO-TEC, Germany) was carried out according to the manufacturer's instructions. The labeled peptides were further purified using high-pressure liquid chromatography (HPLC) using Zorbax SB300 C8 4.6 x 250 mm analytical column (Agilent Technologies).

Molecular cloning of MC4R and expression. The thermostable variant of MC4R was modified by introducing 5 mutations ($E49^{1.37}V$, $N97^{2.57}L$, $S99^{2.59}F$, $S131^{3.34}A$ and $D298^{7.49}N$) to wild-type MC4R (a generous gift of Prof. Dr. Raymond C. Stevens, iHuman Institute at ShanghaiTech University [224]), and inserted into pFastbac1 vector containing a HA signal sequence followed by a twin-strep tag and TEV cleavage site at N-terminus. In addition, the MC4R mutant was also inserted into a pFastbac1 vector containing a HA signal sequence followed by a Flag tag at N-terminus, HRV3C cleavage site, eYFP and 10xHis tag at C-terminus. Receptor was expressed in *Spodoptera frugiperda* (Sf9) cells. Recombinant baculovirus of MC4R was generated by transfecting Sf9 cells cultured in Sf-900 III SFM medium (Thermo Fisher Scientific) at 27°C with bacmid (Bac-to-Bac system, Thermo Fisher Scientific) using FuGENE HD Transfection Reagent (Promega, Germany) according to manufacturer's instructions. Sf9 cells were infected by recombinant baculovirus at a density of 4 x 10^6 cells/mL. 72 h after infection, cells were harvested by centrifugation at 3000 *g*, 4 °C for 30 min and stored at – 80 °C.

Preparation of MC4R embedded in detergent micelles. Sf9 cell pellets containing expressed MC4R were resuspended in a lysis buffer containing 50 mM HEPES, pH 7.5, 200 mM NaCl, 20 mM KCl, 5 mM β-mercaptoethanol (β-ME) supplemented with cOmplete EDTA-free protease inhibitor cocktail tablet, then lysed by sonication on ice. The cell membrane was harvested by ultracentrifugation at 180,000 *g*, 4 °C for 40 min (Beckman) and solubilized using 1% (*w/v*) n-dodecyl-β-D-maltopyranoside (DDM; Cube Biotech), 0.2% (*w/v*) cholesteryl hemisuccinate (CHS; Sigma) in 50 mM HEPES, pH 7.5, 500 mM NaCl, 2 mM β-ME, supplemented with biolock biotin locking solution (750 µL for 1 L cell culture) and cOmplete EDTA-free protease inhibitor cocktail tablet. The mixture was incubated at 4 °C for 3 to 4 h. Insoluble material was removed by ultracentrifugation at 120,000 *g*, 4 °C for 30 min, and clarified supernatant was incubated with Strep-Tactin XT superflow resin (IBA Lifesciences, Germany) for 2 h at 4 °C. Resin was loaded onto a gravity flow column, washed with 10 CVs buffer containing 50 mM HEPES, pH 7.5, 500 mM NaCl, 2 mM β-ME, 1% (*w/v*) DDM and 0.2% (*w/v*) CHS, followed by 10 CVs buffer containing 50 mM HEPES, pH 7.5, 200 mM NaCl, 0.1% (*w/v*) DDM, 0.02% (*w/v*) CHS and 100 µM TCEP. The bound material was eluted with 10 CVs buffer containing 50 mM HEPES, pH 7.5, 200 mM NaCl, 0.02% (*w/v*) DDM, 0.004% (*w/v*) CHS, 100 µM TCEP and 50 mM biotin (Sigma). Sample containing MC4R was collected and concentrated using 30 KDa MWCO concentrator (Amicon) and loaded onto Superdex 200 Increase 10/300 GL column (GE Healthcare) with running buffer containing 50 mM HEPES, pH 7.5, 200 mM NaCl, 0.02% (*w/v*) DDM, 0.004% CHS (*w/v*) and 100 µM TCEP. Fractions containing purified MC4R embedded in detergent micelles were pooled and concentrated using 30 KDa MWCO concentrator (Amicon), flash-frozen in liquid nitrogen and stored at – 80 °C.

Preparation of MC4R embedded in MSP1D1 nanodiscs. The purification of MSP1D1 protein was carried out as described previously with slight modifications [314,317,523] . *E. coli* BL21 (DE3) cells containing the recombinant plasmid (pET28a-6xHis-TEV-MSP1D1) were cultured in 2xYT medium supplemented with 50 µg/mL Kanamycin at 37 °C until OD600 reached 0.6. The expression of MSP1D1 was induced by the addition of

1 mM IPTG. 5 h after induction, cells were harvested and resuspended in a lysis buffer containing 50 mM Tris-HCl, pH 8.0, 500 mM NaCl supplemented with 6 M Guanidinhydrochlorid (GuHCl; Sigma) and cOmplete protease inhibitor cocktail tablet, then lysed by sonication on ice. Cell debris were removed by centrifugation at 40,000 *g,* 4 °C for 40 min. The supernatant was incubated with Ni-NTA resin at 4 °C overnight. Resin was loaded onto a gravity column and washed sequentially with lysis buffer, lysis buffer supplemented with 1% (*v/v*) Triton X-100, lysis buffer supplemented with 60 mM sodium cholate, lysis buffer supplemented with 20 mM imidazole and lysis buffer supplemented with 50 mM imidazole. Bound material was eluted with lysis buffer supplemented with 250 mM imidazole. Eluted proteins containing MSP1D1 were pooled and dialyzed against 1000-fold dialysis buffer containing 50 mM Tris-HCl, pH 7.4, 100 mM NaCl using 10K snakeskin dialysis tubing (Thermo Scientific). Sample was incubated with home-made TEV protease at 4 °C for 16 h, afterwards, incubated with Ni-NTA resin at 4 °C for 2 h. Flow through containing His tag free MSP1D1 was concentrated using 10 KDa MWCO concentrator (Amicon).

Purified MC4R embedded in detergent micelles were mixed with MSP1D1 protein and zwitterionic lipid 1-palmitoyl-2-oleoyl-sn-glycero-3-phosphocholine (POPC; Avanti) solubilized in 20 mM HEPES, pH 7.5, 100 mM NaCl, 0.5 mM EDTA and 100 mM sodium cholate (Sigma) in a molar ratio of 1:10:600. Sample was incubated at 4 °C for 2 h. The self-assembly process was initiated by the addition of BioBeads SM-2 (Bio-Rad). The assembly mixture was first treated with 10% (*w/v*) of BioBeads with gentle shaking for 15 min at 4 °C, followed by the addition of another 20% (*w/v*) of BioBeads incubated for 2 h at 4 °C. Afterwards, BioBeads were removed and possible residual nanodiscs were eluted by washing BioBeads once with 200 µl 20 mM HEPES, pH 7.4, 100 mM NaCl and 0.5 mM EDTA. Sample was then treated with another 50% (*w/v*) BioBeads with gentle shaking overnight at 4 °C. In order to remove residual detergents, 50% (*w/v*) fresh BioBead were added to the assembly mixture and incubated for 4 h at 4 °C. Empty nanodiscs were removed by incubating with Strep-Tactin XT 4Flow high capacity resin (IBA Lifesciences, Germany) for 2 h at 4 °C. Resin was loaded onto a gravity flow column, washed with 20 mM HEPES, pH 7.4, 100 mM NaCl, 0.5 mM EDTA. Bound proteins were eluted with 50 mM biotin in 20 mM HEPES, pH 7.4, 100 mM NaCl and 0.5 mM EDTA, concentrated using 30 KDa MWCO concentrator (Amicon) and loaded onto Superdex 200 Increase 10/300 GL column with running buffer 50 mM HEPES, pH 7.5, 200 mM NaCl. Fractions containing homogeneously and monodisperse assembled MSP1D1/POPC/MC4R nanodiscs were collected and concentrated using 30 KDa MWCO concentrator (Amicon), flash-frozen in liquid nitrogen and stored at – 80 °C.

Preparation of MC4R embedded in Sulfo-DIBMA nanodiscs. Sf9 cell pellets containing expressed MC4R were resuspended in a lysis buffer containing 50 mM HEPES, pH 7.5, 200 mM NaCl, 20 mM KCl and cOmplete EDTA-free protease inhibitor cocktail tablet, then lysed by sonication on ice. Cell membrane was harvested by ultracentrifugation at 180,000 *g*, 4°C for 40 min, and resuspended in a solubilization buffer containing 50 mM HEPES, pH 7.8, 500 mM NaCl, 2.5% (*w/v*) electroneutral polymer Sulfo-DIBMA [525], biolock biotin locking solution and cOmplete EDTA-free protease inhibitor cocktail tablet, incubated overnight at 4 °C. The supernatant was collected by ultracentrifugation at 120,000 *g,* 4 °C for 30 min, incubated with Strep-Tactin XT superflow resin at 4 °C for 2 h. Resin was loaded onto a gravity flow column, washed with 50 mM HEPES, pH 7.8, 500 mM NaCl. Bound proteins were eluted with 50 mM biotin in 50 mM HEPES, pH 7.8, 500 mM NaCl. Sample was concentrated using 30 KDa MWCO concentrator (Amicon) and loaded onto Superdex

200 Increase 10/300 GL column with running buffer 50 mM HEPES, pH 7.5, 200 mM NaCl. Fractions containing MC4R embedded in Sulfo-DIBMA/native membrane nanodiscs were pooled and concentrated using 30 KDa MWCO concentrator (Amicon), flash-frozen in liquid nitrogen and stored at – 80 °C.

Negative-stain transmission electron microscopy (TEM). TEM specimens were prepared by spreading 4 µL MSP1D1/POPC/MC4R nanodiscs and Sulfo-DIBMA/MC4R native membrane nanodiscs, respectively, onto freshly glow-discharged grids (15 mA, 25 s at 0.39 mbar) coated with carbon support film on copper. 5 s after incubation, excess suspension was blotted off using filter paper. Grids were washed using 5 µL MilliQ water, followed by staining twice with 5 µL 2% (*w/v*) aqueous uranyl acetate solution. Excess suspension was blotted off after ~15 s incubation using filter paper. Afterwards, specimens were air-dried and the morphology of MSP1D1/POPC/MC4R nanodiscs and Sulfo-DIBMA/MC4R native membrane nanodiscs were examined on a Talos L120C transmission electron microscopy equipped with 4k × 4K Ceta CMOS camera (Thermo Fisher Scientific).

Thermal stability measurement. The thermal stability of MC4R embedded in either detergent micelles or Sulfo-DIBMA/native membrane nanodiscs was measured with the aid of Nano differential scanning fluorimetry (NanoDSF) technique [526,527]. The changes of intrinsic tyrosine or tryptophan fluorescence intensity of MC4R at 350 nm and 330 nm wavelengths caused by the exposure of buried aromatic side chains to hydrophilic chemical environment upon unfolding are monitored and recorded by NanoDSF. The melting temperature (T_m) can be then extracted from the fluorescence transition curves obtained from the fluorescence ratio (F350 nm/F330 nm) as a function of temperature. Samples were loaded into high-sensitivity capillaries (NanoTemper, Germany) and measured in triplicate using Prometheus NT.48 (NanoTemper, Germany) in a linear thermal ramp of 1 °C/min from 20 °C to 95 °C using 50% excitation power. The melting temperatures (T_m) corresponding to the maximum values of the first derivative of NanoDSF curve were identified using Prometheus NT.Control software (NanoTemper, Germany).

Ligand binding affinity measurement. The binding affinities between ACTH (1-23) and MC4R embedded in detergent micelles, MSP1D1/POPC nanodiscs and Sulfo-DIBMA/native membrane nanodiscs in the absence and presence of divalent cations were measured with MicroScale Thermophoresis (MST) using Monolith NT.115 system (NanoTemper, Germany) [528]. The concentration of labeled ACTH (1-23) was kept constant (16 nM), while the unlabeled MC4R embedded in detergent micells, MSP1D1/POPC nanodiscs and Sulfo-DIBMA/native membrane nanodiscs was titrated with a 1:1 dilution series. Samples were filled into monolith premium capillaries (MO-K025, NanoTemper, Germany). The thermophoretic movement was measured at 50% LED power, 50% MST power, 30 s Infrared (IR) laser on and 5 s laser off at 25 °C. Fluorescence was excited at 460-480 nm and emission was detected at 515-530 nm. The MO.Affinity analysis software (NanoTemper, Germany) was used to analysis MST results and extract dissociation constant (K_d) values.

The potential unspecific interactions between ACTH (1-23) and native membrane were examined by means of Microfluidic diffusional sizing (MDS) using Fluidity One-W system (Fluidic Analytics, Cambridge, United Kingdom) [529]. In brief, the purified uninfected Sf9 cell membrane was disrupted using dounce homogenizer and resuspended in a buffer containing 50 mM HEPES, pH 7.5, 200 mM NaCl, 2.5% (*w/v*) Sulfo-DIBMA (or

2.5% (*w/v*) DIBMA) supplemented with cOmplete EDTA-free protease inhibitor cocktail tablet, then incubated at 4°C overnight and harvested by centrifugation at 120,000 *g,* 4 °C for 30 min. The supernatant containing native membrane nanodiscs in Sulfo-DIBMA (or DIBMA) was examined using dynamic light scattering (DLS). A Zetasizer Nano S equipped with a He–Ne laser having a wavelength of 633 nm (Malvern Panalytical, UK) was used to perform DLS measurements using 70-µL microcuvette (Brand, Wertheim, Germany). The sample was thermostatted for 5 min at 25 °C prior to measurement and the detection scattering angle was fixed at 173°. Polymer/native membrane nanodiscs were incubated with ACTH (1-23), and loaded into a disposable MDS chip.

4.4 Results and discussion

Previous studies have shown that electroneutral Sulfo-DIBMA is able to induce the self-assembly of well-defined nanodiscs by using synthetic lipids or native membrane from Hela cells [393]. We first evaluated the effects of different conditions on the solubilization efficiency of integral transmembrane proteins from native cellular membrane into nanodiscs by Sulfo-DIBMA. For this purpose, we used the insect cells infected by MC4R-eYFP baculovirus (Fig. 10A). Purified insect membrane (20 mg/mL, wet mass/volume) was exposed to different concentrations of Sulfo-DIBMA. The amounts of extracted receptor were quantified by measuring the emission intensity of eYFP. We found that Sulfo-DIBMA completely extracted the receptor from insect cellular membrane at the polymer concentration of 2% (*w/v*) and pH 8.0 after either 4 h or 16 h incubation (Fig. 10B). To assess the effects of ionic strength, the cellular membrane was exposed to increasing concentrations of NaCl in the presence of 2% (*w/v*) Sulfo-DIBMA. The highest solubilization efficiency was obtained at around 400 mM NaCl. Interestingly, the higher the concentration of NaCl (above 400 mM at pH 7.4 or above 500 mM at pH 8.0), the lower the extracted protein (Fig. 10C).

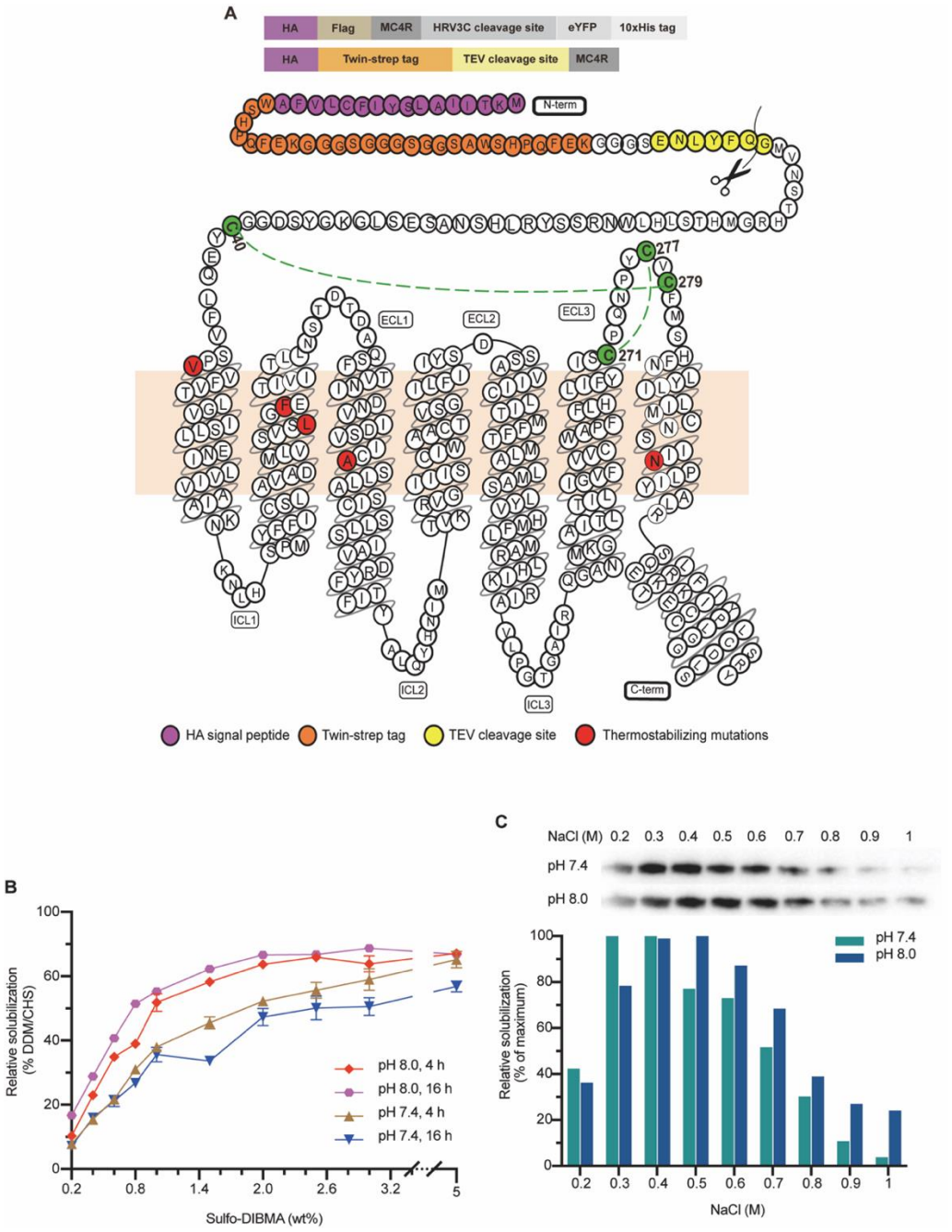

Fig. 10. Characterization and solubilization of receptor. (A) Schematic representation of MC4R-eYFP and MC4R constructs used for solubilization experiment and receptor purification, respectively. The snake plot of MC4R has been colored to show the location of signal peptide, twin-strep tag, thermostabilizing mutations and two disulfide bonds (Cys271 and Cys277 form an intra-loop disulfide bound within extracellular loop 3 (ECL3), while Cys279 forms another disulfide bound with N-terminal Cys40, both shown as green dotted lines). (B) Solubilization test of MC4R-eYFP from insect cellular membrane using Sulfo-DIBMA (normalized to 1% DDM (*w/v*) and 0.2% (*w/v*) CHS). All experiments were performed at 50 mM HEPES, 200 mM NaCl, pH 7.4 or 8.0, and different concentrations of Sulfo-DIBMA. The mixture of membrane and polymer was incubated at 4 °C for 4 h or 16 h. The supernatant was collected by centrifugation at 120,000 *g*, 4°C for 30 min and the solubilization efficiency was evaluated by measuring the emission intensity of eYFP. Error bars indicate the mean ± standard deviation of two independent experiments, each repeated in triplicate. (C) Western blotting analysis (anti-Flag) of the effects of ionic strength on the solubilization efficiency of Sulfo-DIBMA.

In this study, we performed the purification of MC4R from 1L Sf9 cell culture using 2.5% (*w/v*) Sulfo-DIBMA at pH 8.0 in the presence of 500 mM NaCl and detergent (Fig. 11C-D, S2 and S3). To evaluate whether Sulfo-DIBMA produces homogeneous sample that will be compatible with currently used methods for functional and structural studies of membrane proteins, we examined the size and morphology of the size-exclusion chromatography purified MC4R embedded in MSP1D1/POPC nanodiscs and Sulfo-DIBMA/native membrane nanodiscs with the aid of negative-stain transmission electron microscopy (TEM). The results demonstrated the formation of homogeneously sized Sulfo-DIBMA/MC4R native membrane nanodiscs with an average diameter of ~10 nm which are similar to that assembled by MSP1D1 (Fig. 11G and 11H).

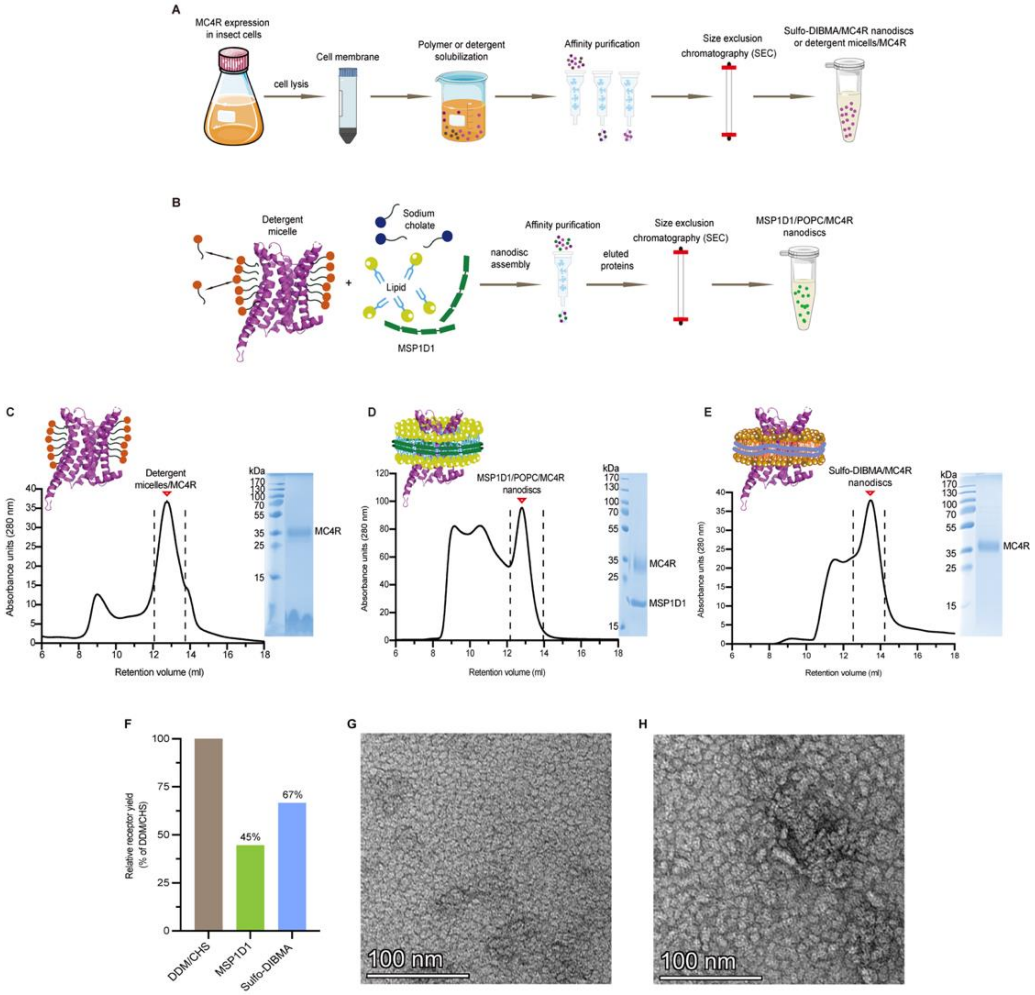

Fig. 11. Assembly of MC4R in different membrane mimicking systems. (A and B) Schematic representation of MC4R purification and assembly of MC4R in lipid bilayer nanodiscs using MSP1D1 protein. Representative analytical size-exclusion chromatography profiles (superdex 200 Increase 10/30 column) and corresponding SDS-PAGE gels for MC4R embedded in detergent micelles (C), MSP1D1/POPC nanodiscs (D) and Sulfo-DIBMA/native membrane nanodiscs (E). (F) Yield of purified MC4R using different membrane mimetics (~ 0.25 mg or ~ 200 µL, 30 µM) MC4R can be purified from 1L Sf9 cell culture using DDM/CHS). Negative-stain TEM images of Sulfo-DIBMA/MC4R native membrane nanodiscs (G) and MSP1D1/POPC/MC4R nanodiscs (H).

Recent ^{19}F-NMR experiments on $A_{2A}AR$ and the structure determination of NTS-NTSR1-G protein complex in lipid nanodiscs both highlight the important role of phospholipids in the regulation of GPCR activation [261,530]. In order to gain more insights into the influence of different environments on the thermalstability of MC4R, we performed nano differential scanning fluorimetry (NanoDSF) experiments. The NanoDSF measurements showed an increased thermostability of MC4R embedded in Sulfo-DIBMA/native membrane nanodiscs compared to in detergent micelles which do not preserve a lipid bilayer (Fig. 12), with a transition temperature (T_m) about 6 °C higher. This observation agrees with previous studies showing GPCRs are more stable in lipid environment [531].

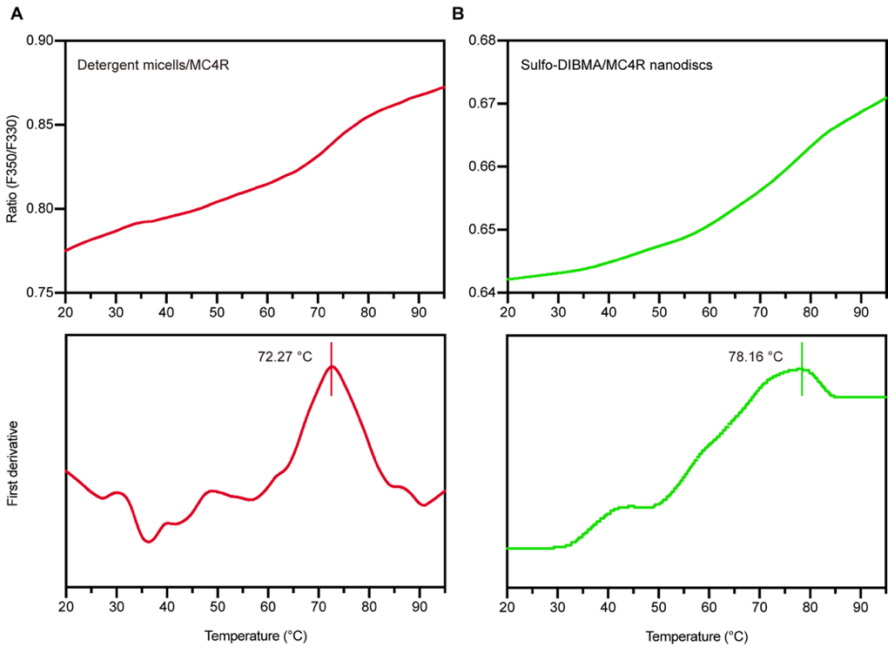

Fig. 12 Influence of different membrane mimicking systems on the thermalstability of MC4R. (A and B) NanoDSF results demonstrated that the native lipid bilayer formed by Sulfo-DIBMA provides a more stable *in vitro* environment for extracted MC4R. Both detergent micelles/MC4R and Sulfo-DIBMA/MC4R native membrane nanodiscs were diluted to get a final concentration of 4 µM for NanoDSF measurements using 50 mM HEPES, pH 7.5, 200 mM NaCl, 0.02% (*w/v*) DDM, 0.004% (*w/v*) CHS, 100 µM TCEP, and 50 mM HEPES, pH 7.5, 200 mM NaCl, respectively.

In addition, in order to study the effects of different membrane mimicking systems on the functional integrity of MC4R, we performed the ligand binding measurements using microscale thermophoresis (MST). Our MST results exhibited a compromised ligand binding affinity when MC4R is embedded in detergent micelles (K_d of ACTH (1-23): 280.38 ± 42.72 nM) compared to in HEK293 cell membrane (K_i of α-MSH: 19 nM, which has the same binding affinity as ACTH) (Fig. 13A and S1) [165,532]. While the binding affinities of ACTH (1-23) were 56.25 ± 2.77 nM in MSP1D1/POPC nanodiscs and 30.36 ± 5.33 nM in Sulfo-DIBMA/native membrane nanodiscs, respectively, indicating the functional integrity of MC4R is well-preserved by lipid bilayer, especially in native membrane environment (Fig. 13B and 13C).

In order to examined why the ligand binding behavior was significantly influenced by the receptor embedded environments especially the detergent micelles, we further performed the binding measurements between ACTH (1-23) and DDM/CHS micelles using MST (Fig. 13D). The results showed that ACTH (1-23) exhibits weak unspecific interactions with detergents when the detergent concentration is below the critical micelle concentration (CMC, ~ 120 µM in the presence of 200 mM NaCl) of DDM (K_d =18.79 ± 0.27 µM). In addition, the data indicated the presence of a second binding mode involving the micellar particles with very low affinity (K_d = 46.78 ± 13.3 mM). As the ligand-receptor binding measurements were performed in the presence of 0.02% (*w/v*, ~ 392 µM) DDM, our results suggested that nonspecific interactions with monomeric DDM are saturated and weak interactions with micellar DDM are present, possibly affecting the levels of 'available' ACTH (1-23) when MC4R is embedded in detergent micelles. However, given the low affinities of these interactions ,we argue that this effect does not suffice to explain the larger change in binding affinity of the receptor in DDM micelles.

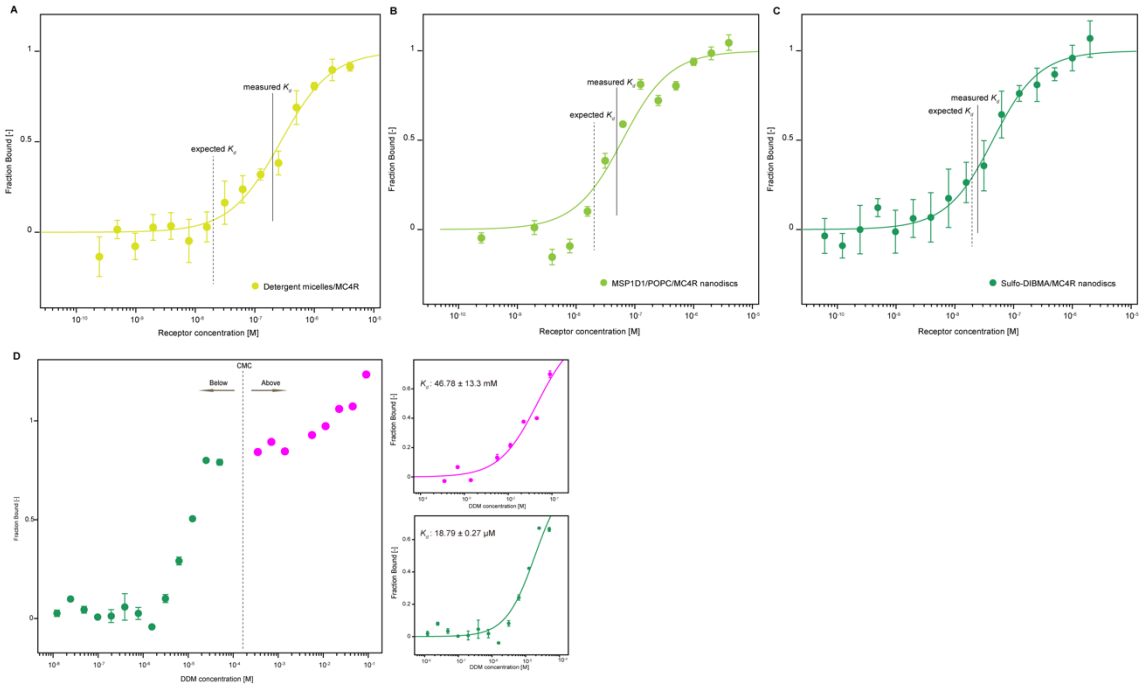

Fig. 13 Ligand binding measurements. (A-C) The effects of membrane mimetics, i.e., detergent micelles (K_d = 280.38 ± 42.72 nM, colored light yellow), MSP1D1/POPC nanodiscs (K_d = 56.25 ± 2.77 nM, colored light green) and Sulfo-DIBMA/native membrane nanodiscs (K_d = 30.36 ± 5.33, colored green) on the ACTH (1-23) ligand binding to MC4R were examined using microscale thermophoresis (MST). All experiments were carried out at 50 mM HEPES, pH 7.5, 200 mM NaCl, 0.02% (*w/v*) DDM, 0.004% (*w/v*) CHS, 100 µM TCEP for MC4R embedded in detergent micelles, and 50 mM HEPES, pH 7.5, 200 mM NaCl for MC4R embedded in MSP1D1/POPC nanodiscs and Sulfo-DIBMA/native membrane nanodiscs. The dotted and solid lines in panels A, B, and C represent the affinity of α-MSH in eukaryotic membrane fragments and the measured affinity of ACTH (1-23) in this study, respectively. (D) Interaction between ACTH (1-23) and detergents. Ligand binding to detergent micelles below the CMC (K_d = 18.97 ± 0.27 µM, colored green) and above the CMC of DDM (K_d = 46.78 ± 13.3 mM, colored magenta) in 50 mM HEPES, pH 7.5, 200 mM NaCl, 0.02% (*w/v*) DDM, 0.004% (*w/v*) CHS, 100 µM TCEP. Error bars indicate the mean ± standard deviation of two independent experiments, each repeated in triplicate.

In order to evaluate the potential unspecific interactions between either Sulfo-DIBMA or native membrane and ACTH (1-23) ligand, the polymer-encapsulated nanodiscs containing either zwitterionic phospholipid DMPC (known to not show unspecific interaction with ACTH (1-23) [393]) or purified Sf9 cell membrane were used to perform the microfluidic diffusional sizing (MDS) assay. The MDS results indicated that neither the Sulfo-DIBMA/DMPC nanodiscs nor Sulfo-DIBMA/native membrane nanodiscs interfere with the ligand binding (Fig. 14A), a prerequisite for reliably characterizing ligand-GPCR interactions, whereas DIBMA (the anionic counter-part of Sulfo-DIBMA) does interfere with the ligand binding (Fig. 14B) which is in agreement with previous studies [393].

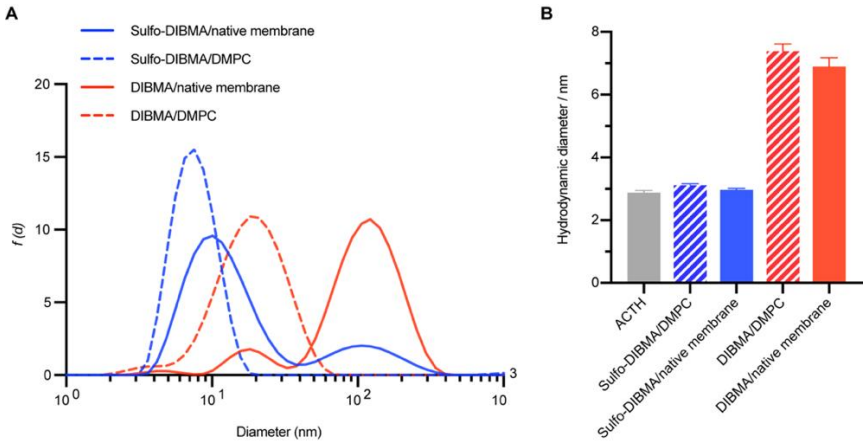

Fig. 14 Unspecific interaction measurements. (A) Intensity-weighted particle size distributions *f(d)* of 4 mg/ml DMPC large unilamellar vesicles (LUVs) and 25 mg/mL (wet mass/volume) purified Sf9 cell membrane treated with polymers at the polymer/DMPC mass ratio of 4 and polymer/native membrane mass ratio of 1, respectively, obtained from DLS. (B) Unspecific interactions between peptide and polymer/DMPC or polymer/native membrane nanodiscs obtained from (A) were measured by means of microfluidic diffusional sizing measurements (MDS). All experiments were carried out at 50 mM HEPES, pH 7.5, 200 mM NaCl. Error bars indicate the mean ± standard deviation of two independent experiments, each repeated in triplicate.

Of note, MC4R is among the few GPCRs displaying distinct structural features. Usually, the extracellular loop 2 (ECL2) containing over 15 amino acids is the largest ECL in class A GPCRs and plays a vital role in the formation of ligand binding cavity, thereby influences the ligand selectivity, ligand binding affinity, allosteric modulation and receptor activation. For example, ECL2 can form a structured extracellular cap covering the binding pocket of covalently bound or lipid ligand, or keep away from the binding cavity to facilitate the entrance of diffusible ligands, such as the large peptide, to the transmembrane domain bundle [231–233]. MCRs including MC4R have a very short ECL2 containing just three to four amino acids without defined secondary structural elements [225,226,234–237], resulting in the formation of a relatively open and extracellular solvent-accessible binding pocket for large peptides, which has been recently confirmed by the inactive and active MC4R structures (in detergent micelles) [224–226]. The MC4R structures in active state reveal the involvement of Ser188^{ECL2} in the formation of hydrogen bonds with different agonists which all share a conserved central core tetrapeptide His-Phe-Arg-Trp (HFRW) pharmacophore with ACTH (1-23) [225,226]. MC4R does not possess a conserved disulfide bridge usually found in a number of GPCRs including class A and class B (connecting ECL2 and Cys122$^{3.25}$ in the extracellular tip of TM3), which constrains the conformational changes of extracellular region

during receptor activation [231]. In contrast, MC4R contains a corresponding non-conserved negatively charged Asp122$^{3.25}$ in TM3 which is involved in the formation of ligands and calcium ion binding network. Thus, all of these compelling pieces of evidence emphasize the significant impact of the extracellular loops on the regulation of ligand binding to MC4R.

Detergent molecules can rapidly associate and dissociate from GPCR, potentially influencing the stability and conformational exchange of GPCR. Consequently, this dynamic interplay influences the accessibility and conformation of the ligand binding pocket and binidng kinetics. The high off-rate of detergent may promote rapid dissociation of the ligand from GPCR, potentially affecting the ligand binding affinity. A ^{19}F NMR experiment regarding the conformational changes of β_2AR in different detergent micelles reveals that DDM exhibits a high detergent off-rate (1.43×10^6 s^{-1}) that may directly facilitate the conformational exchange of distinct functional (such as active and inactive) states of β_2AR, whereas MNG-3 characterized by its CMC in the nanomolar range comparable to that of phospholipids, effectively restricts the exchange of functional states of β_2AR due to the low off-rate [533]. In addition, the molecular simulation experiments demonstrat that DDM does not tumble or penatrate into transmembrane helix bundle of A_{2A}R, however, unlike the POPC, the unbranched DDM cannot form a tightly packed micelle around the receptor and the absence of bifurcated hydrogen bonds between transmembrane domain helices and loops contributes to the increased flexibility of extracellular region, leading to reduced stability of receptor embeded in DDM micelles [534,535]. Thus, the alteration of the microenvironment may contribute to the increased ligand binding affinity when MC4R is embedded in lipid bilayer (Fig. 13B and 13C). Moreover, the composition of detergent micelles, such as CHS, plays a critical role in retaining the functional integrity of the receptor. The absence of CHS may not cause a significant change in the structural core segment of the receptor (i.e., ligand binding pocket), but results in a complete loss of the ligand binding activity [536,537]. Thus, one can speculate that MC4R embedded in DDM/CHS micelles still retains its functional fold for ligand binding as observed from the MST measurement (Fig. 13A) and cryo-EM structures [226,226], but may possesses indistinguishable subtle conformational differences when compared to in lipid bilayer environment (Fig. 13B and 13C). Taken together, it is reasonable to infer that the physical properties of the environment may play a critical role in the activation of MC4R, ultimately resulting in different ligand binding behaviors.

Studies of divalent cations on the ligand binding and signal tracduction of a number of GPCRs have highlighted their critical roles in the regulation of physiological processes. Studies with respect to A_{2A}AR and muscarinic M2 receptors unveils the allosteric effects of Ca^{2+} and Mg^{2+} [126,127]. A resent NMR study regarding the effects of cations on A_{2A}AR also demonstrates that Ca^{2+} and Mg^{2+} are able to function as positive allosteric modulators enhancing the agonist binding affinity and shifting the equilibrium towards the active-state conformation [128]. As a second most abundant biologically relevant transition metal ion, Zn^{2+} is able to make strong interactions with Cys, His, Glu and Asp residues, and has been proposed to play a vital role in many biochemical reactions in the human body and confirmed as allosteric modulator of a number of GPCRs [129–131]. A study regarding the bovine rhodopsin receptor reveals several binding sites for Zn^{2+} including one showing high affinity located in transmembrane domian and coordinated by the highly conserved residues Glu122$^{3.37}$ and His211$^{5.46}$ [134]. At the human β_2-adrenergic receptor (β_2AR), Zn^{2+} is able to increase the agonist binding and enhance cAMP accumulation acting as a positive allostric modulator. The mutagenesis experiments localize the binding site for Zn^{2+} consisting of Glu255$^{5.64}$, Cys265$^{6.27}$ and His269$^{6.31}$ [135,136]. A study concerning human

CXCR4 chemokine receptor unveils the increased binding of antagonist AMD3100 to Asp262$^{6.58}$ by Zn^{2+} [137]. While, at the dopamine receptors, Zn^{2+} inhibits antagonist binding acting as a negative allosteric modulator in a dose-dependent and reversible manner (for rat D1R and D2R) or in the presence of other distinct allosteric site bound by Na^{+} and methylisobutylamiloride (for rat D4R) [138,139]. Two histidine residues (His394$^{6.55}$ and His399$^{6.60}$) towards the extracellular end of TM6 of rat D2 receptor facilitate the formation of Zn^{2+} binding site [140]. In addition, a recent structural and functional study has demonstrated the negative allosteric mudulation of Zn^{2+} on human galanin 1 receptor (GALR1) likely by restricting the conformational change of TM6, and the Zn^{2+} effect can be abolished through the mutation of His267$^{6.55}$ below the agonist binding site [142]. Moreover, a biphasic effect of Zn^{2+} has also been observed in human metabotropic serotonin receptors (5-HT), wherein Zn^{2+} exhibits allosteric potentiation and inhibition of orthosteric ligand binding to 5-HT1A at sub-micromolar and sub-millimolar concentrations, respectively [141].

In the case of MC4R, it is known that the physiologic cations are essential for ligand binding and MC4R mediated signal transduction [227,230,224–226]. More evdiences have been provided by the investigation of the thermalstability measurements of MC4R in complex with different ligands, such as the agonists α-MSH and NDP-α-MSH, antagonist SHU9119 and inverse agonist AgRP(83-132), in response to Mg^{2+}, Zn^{2+} and Ca^{2+}, whereas only Ca^{2+} increases the thermalstability of MC4R in complex with SHU9119 and NDP-α-MSH [224]. Ca^{2+} can also increase ^{125}I-NDP-α-MSH binding to MC4R with a EC_{50} of 3.7 μM acting as a positive allosteric modulator. The precise Ca^{2+} binding site has been first described in the crystal structure of MC4R/SHU9119 complex embedded in detergent micelles and Ca^{2+} is coordinated by Glu100$^{2.60}$, Asp122$^{3.25}$ and Asp126$^{3.29}$ in MC4R and two backbone-carbonyl oxygen atoms in SHU9119 [224]. Moreover, the cryo-EM structures of active state MC4R (embedded in detergent micelles) also unambiguously confirm the presence of Ca^{2+} between TM2, TM3 and agonist, which all share the same Ca^{2+} coordination in MC4R as observed in MC4R/SHU9119 complex [225,226]. Additionally, as a neuromodulator, Zn^{2+} plays a critical role in the functional regulation of melanocortin receptors. Despite the exact binding site of Zn^{2+} on MC4R still remains unclear, previous studies have demonstrated that Zn^{2+} can act both as partial agonist and positive allosteric mudulator for the action of peptide agonists (NDP-α-MSH and α-MSH) on MC1R and MC4R, suggesting the presence of Zn^{2+} binding site on the receptor [227–229]. In order to understand the effects of divalent cations on ACTH (1-23) binding to MC4R embedded in different membrane mimetics, we performed the ligand binding assay in the presence of 10 μM Ca^{2+}, Zn^{2+} and Cu^{2+}, respectively, with the aid of MST. In the case of MC4R embedded in detergent micelles, Ca^{2+} and Zn^{2+} did not induce significant changes showing slight enhancement and inhibition of the ACTH (1-23) binding affinity, respectively (Fig. 15A). However, the most significant changes induced by Ca^{2+} and Zn^{2+} were observed when MC4R embedded in lipid bilayer exhibiting pronounced increase in ligand binding affinity, particularly in Sulfo-DIBMA/native membrane nanodiscs (Fig. 15B and 15C). In addition, Cu^{2+} inhibited the ligand binding in all membrane mimetics, while Sulfo-DIBMA/native membrane nanodiscs appeared to be more resistant to this influence (Fig. 15A-C). Therefore, our results demonstrated that Ca^{2+} functions as a positive allosteric modulator and enhances the ACTH (1-23) binding affinity to MC4R in all membrane mimiking systems: ~1.9-fold increase in detergent micells, ~11.8-fold increase in MSP1D1/POPC nanodiscs and ~6.5-fold increase in Sulfo-DIBMA/native membrane nanodiscs, whereas Cu^{2+} inhibits the ACTH (1-23) binding affinity to MC4R in all membrane mimiking systems acting as a negative allosteric modulator: ~3.7-fold decrease in detergent micelles,

~9.9-fold decrease in MSP1D1/POPC nanodiscs and ~6.7-fold decrease in Sulfo-DIBMA/native membrane nanodiscs. Interestingly, Zn^{2+} exhibits biphasic effects functioning as either a positive allosteric modulator or a weak negative allosteric modulator for ligand binding, depending on the environments: ~1.3-fold decrease in detergent micells, ~5.6-fold increase in MSP1D1/POPC nanodiscs and ~9.7-fold increase in Sulfo-DIBMA/native membrane nanodiscs.

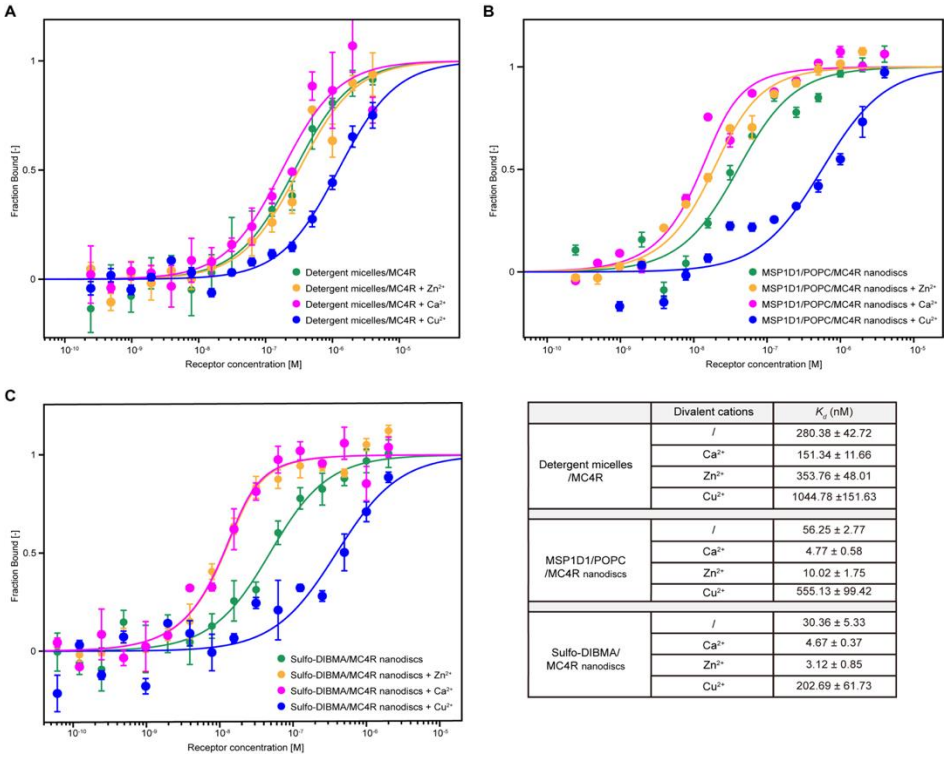

	Divalent cations	K_d (nM)
Detergent micelles /MC4R	/	280.38 ± 42.72
	Ca^{2+}	151.34 ± 11.66
	Zn^{2+}	353.76 ± 48.01
	Cu^{2+}	1044.78 ±151.63
MSP1D1/POPC /MC4R nanodiscs	/	56.25 ± 2.77
	Ca^{2+}	4.77 ± 0.58
	Zn^{2+}	10.02 ± 1.75
	Cu^{2+}	555.13 ± 99.42
Sulfo-DIBMA/ MC4R nanodiscs	/	30.36 ± 5.33
	Ca^{2+}	4.67 ± 0.37
	Zn^{2+}	3.12 ± 0.85
	Cu^{2+}	202.69 ± 61.73

Fig. 15 Allosteric modulation of ligand binding to MC4R by divalent ions. The effects of divalent cations on the ACTH (1-23) binding to MC4R in different environments including detergent micelles (A), MSP1D1/POPC nanodiscs (B) and Sulfo-DIBMA/native membrane nanodiscs (C), were examined using microscale thermophoresis (MST). Right, a table showing the K_d values obtained from A-C. The MST results demonstrated that the ligand binding of MC4R is allosterically modulated by divalent cations. All experiments were carried out at 50 mM HEPES, pH 7.5, 200 mM NaCl, 0.02% (*w/v*) DDM, 0.004% (*w/v*) CHS, 100 µM TCEP for MC4R embedded in detergent micelles, and 50 mM HEPES, pH 7.5, 200 mM NaCl for MC4R embedded in MSP1D1/POPC nanodiscs and Sulfo-DIBMA/native membrane nanodiscs. Error bars indicate the mean ± standard deviation of at least two independent experiments, each repeated in triplicate.

4.5 Conclusions

The extration of GPCRs from cellular membranes is usually carried out by using various detergents which generally serve as a gold standard for the purification and structural characterization of GPCRs. The MSP nanodiscs have also been widely used to assembly detergent extracted GPCRs into lipid bilayer and provide a more stable environment for *in vitro* studies of GPCRs. However, the reconstitution process is time-consuming and may potentially compromise the activity of GPCRs. While, polymer-encapsulated nanodiscs offer several advantages over above membrane mimetics, including the detergent-free extraction and purification of GPCRs within their surrounding native phospholipids environment. In this work, we examined the influence of different environments on the function of MC4R by incorporating MC4R into detergent micelles, MSP1D1/POPC nanodiscs and Sulfo-DIBMA/native membrane nanodiscs, respetively. We found that the lipid bilayer, particularly the native lipid environment (Sulfo-DIBMA), is more effective in preserving the functional integrity of MC4R *in vitro*, as evidenced by the heightened thermal stability and enhanced ligand binding affinity. Given the critical roles of divalent cations in the ligand binding and signal transduction of a number of GPCRs, we investigated the allosteric regulation of divalent cations on the ACTH (1-23) binding to MC4R embedded in different environments. We observed that the Ca^{2+} and Cu^{2+} act as a positive and a negative allosteric modulator on MC4R, leading to enhancement and inhibition of ACTH (1-23) binding affinity, respectively. Interestingly, the allosteric modulation of Zn^{2+} is environment-dependent. The increased ligand binding affinity was obaserved when MC4R embedded in lipid bilayer especially the native membrane, but decreased ligand binding affinity in detergent micelles. Our results demonstrated that the different environments play a role in shaping the function of GPCRs, including their ligand binding properties in the absence or presence of extracellular modulators. The formation of homogeneous Sulfo-DIBMA/native membrane nanodiscs with decent protein yield provides us a more straightforward way to perform the functional and structural characterization of membrane proteins in a well-defined but still native phospholipid-bilayer environment [399]. Furthermore, additional experiments should be conducted to ascertain the binding sites of metal ions on MC4R in its native environment.

5. Development of novel polymers for membrane protein studies

The previous chapter demonstrates the advantages of electroneutral polymer Sulfo-DIBNMA for *in vitro* functional studies of MC4R. The following chapter focuses on the characterization of a set of new polymers that may overcome remaining shortcomings of currently available systems. Chapter 5 reflects the content of the following manuscript:

Capturing G protein-coupled receptors (GPCRs) into native lipid-bilayer nanodiscs using new diisobutylene/maleic acid (DIBMA) copolymers (*Manuscript in preparation*)

Ci Chu,[a] Carolyn Vargas,[b,c,d] Maria Carolina Barbosa,[e] Simon Sommerhage,[f] Gunnar F. Schröder,[f] Sandro Keller,[b,c,d*] Manuel Etzkorn[a,f,g*]

[a]Heinrich Heine University Düsseldorf, Faculty of Mathematics and Natural Sciences, Institute of Physical Biology, Universitätsstr. 1, 40225 Düsseldorf, Germany

[b]Biophysics, Institute of Molecular Biosciences (IMB), NAWI Graz, University of Graz, Humboldtstr. 50/III, 8010 Graz, Austria

[c]BioTechMed-Graz, Graz, Austria

[d]Field of Excellence BioHealth, University of Graz, Austria

[e]Molecular Biophysics, Technische Universität Kaiserslautern (TUK), Erwin-Schrödinger-Str. 13, 67663 Kaiserslautern, Germany

[f]Institute of Biological Information Processing (IBI-7: Structural Biochemistry), Forschungszentrum Jülich, Jülich, Germany

[g]Jülich Center for Structural Biology (JuStruct), Forschungszentrum Jülich, Jülich, Germany

5.2 Abstract

Many membrane proteins, including G-protein-coupled receptors (GPCRs), are susceptible to denaturation when extracted from their native membrane by detergents. Therefore, alternative methods have been developed, including amphiphilic copolymers that enable the direct extraction of functional membrane proteins along with their surrounding lipids, leading to the formation of native lipid-bilayer nanodiscs. Among these amphiphilic copolymers, styrene/maleic acid (SMA) and diisobutylene/maleic acid (DIBMA) polymers have been extensively studied and successfully utilized to isolate various types of membrane proteins, including GPCRs. Despite their many benefits, SMA and DIBMA polymers also have significant drawbacks that limit their application. Most notably, both SMA and DIBMA carry high negative charge densities, which can interfere with protein–protein and protein–lipid interactions through unspecific Coulombic attraction or repulsion. Herein, we describe a series of new amphiphilic copolymers derived from DIBMA via partial amidation of the carboxylate pendant groups with various biocompatible amines. The nanodisc-forming properties of the new polymers were assessed using model membranes as well as in the context of extracting the melanocortin 4 receptor (MC4R), a prototypical class A GPCR. While each new DIBMA variant displays distinct features that may be favorable for selected applications, we identified a new PEGylated DIBMA variant called $mPEG_4$-DIBMA as particularly promising for the present purpose. On the one hand, $mPEG_4$-DIBMA abolishes unspecific interactions with the tested peptide ligand, a prerequisite for reliably characterizing GPCR–ligand interactions. On the other hand, $mPEG_4$-DIBMA outperforms other polymers such as SMA and DIBMA by achieving higher extraction efficiencies of MC4R from Sf9 insect cell membranes. Thus, this new nanodisc-forming polymer combines two key advantages that are crucial for investigating GPCRs in a well-defined but still native lipid-bilayer environment, thus paving the way for manifold future applications.

5.3 Introduction

G protein-coupled receptors (GPCRs), the largest superfamily of cell-surface proteins, share a conserved architecture of seven transmembrane helical domains (TMDs) and have been implicated in a plethora of diseases such as cancer, obesity, and Alzheimer's disease [3–5]. The isolation of GPCRs from cellular membranes for subsequent *in vitro* studies is traditionally carried out with the aid of detergents, which displace native lipids and form micelles as a membrane-mimetic environment to solubilize GPCRs. Lipid-bilayer nanodiscs formed by membrane scaffold proteins (MSPs) have also been widely used in studies of GPCRs [314], such as neurotensin receptor 1 (NTSR1) [538] and rhodopsin [539]. However, the stability of GPCRs often decreases upon solubilization by detergents, which is the first step for preparing MSP nanodiscs [314]. In addition, GPCR activities are regulated by various physical properties of the surrounding phospholipid bilayer such as lipid order, lateral pressure, bilayer thickness, hydrophobic mismatch, membrane fluidity, curvature, and lipid composition, which are altered in detergent micelles and difficult to mimic in synthetic lipid mixtures [524,262,264,265]. The lipid environment also plays critical roles in GPCR–ligand interactions, receptor coupling, and the recruitment of GPCR kinases (GRKs) and arrestins [540–543]. Therefore, the study of GPCRs in more native-like environments is highly desirable.

In addition to model membrane systems [544], significant progress has been made in developing and exploiting lipid-bilayer nanodiscs encapsulated by amphiphilic copolymers that directly extract membrane proteins together with their surrounding lipids from cellular membranes [250]. These native nanodiscs often preserve the structural and functional integrity of extracted proteins. One of the most commonly used copolymers is styrene/maleic acid polymer SMA(2:1), a negatively charged random polymer employed to purify membrane proteins from different cell types [370–372,374,375,545]. However, the efficiency of membrane-protein extraction by SMA(2:1) and the characterization of SMA-encapsulated proteins are restricted by a rather narrow buffer range, excluding lower pH values and even low concentrations of divalent cations such as Mg^{2+} and Ca^{2+} [379,380]. New strategies could overcome some of the limitations in terms of buffer compatibility [381,382], but the quantification of encapsulated proteins and several other biophysical experiments are hampered by SMA's strong absorption in the UV range, which is due to its aromatic styrene moieties. Diisobutylene/maleic acid (DIBMA) is an alternating copolymer that does not contain any aromatic groups but retains the ability to solubilize membrane proteins and lipids [383]. Thus, one of the significant advantages of DIBMA is its lower absorption in the UV range. Moreover, DIBMA exhibits only a gentle impact on the lipid acyl chain order and a high resistance against divalent cations [384]. DIBMA has been successfully used to extract a broad range of membrane proteins from different host cells, including rhomboid proteases [546], the membrane tether protein ZipA [547], the ATP Binding Cassette (ABC) transporter BmrA [547], the GPCRs adenosine A_{2A} receptor ($A_{2A}R$) [547] and calcitonin gene-related peptide receptor (CGRP) [547], as well as the mechanosensitive channel of small conductance (MscS)-like channel YnaI [548]. Nonetheless, the high charge densities carried by both SMA and DIBMA, which are due to their carboxylic acid pendant groups, can interfere with binding measurements using charged ligands through unspecific Coulombic interactions.

In this work, we describe a series of new amphiphilic copolymers, including Dab-DIBMA, Arg-DIBMA, Meg-DIBMA, and $mPEG_4$-DIBMA obtained from DIBMA via partial amidation with various biocompatible amines. The formation of nanodiscs by exposing large unilamellar vesicles (LUVs) to polymers, the morphology of the resulting nanodiscs, and the thermotropic phase behavior of the encapsulated lipid bilayers were examined with the aid of dynamic light scattering (DLS), transmission electron microscopy (TEM), and differential scanning calorimetry (DSC), respectively. Additionally, microfluidic diffusional sizing (MDS) was used to gauge potential unspecific interactions between peptide ligands and polymers. The efficacies of the new polymers in extracting a prototypical GPCR were assessed by using the human melanocortin 4 receptor (MC4R) expressed in insect cells. The results of our study demonstrate that all of the polymers examined are able to form lipid-bilayer nanodiscs with narrow size distributions. Furthermore, all polymers can extract MC4R into native nanodiscs, providing new tools for the structural and functional characterization of GPRCs. Notably, we found that $mPEG_4$-DIBMA does not display any unspecific interactions with a cationic peptide ligand and exhibits only low UV absorption. In addition, $mPEG_4$-DIBMA is highly water-soluble, readily solubilizes phospholipid vesicles, and efficiently extracts MC4R from insect membranes. Taken together, our study demonstrates that $mPEG_4$-DIBMA is an outstanding amphiphilic copolymer for investigating integral membrane proteins in their native lipid environment.

5.4 Methods

Materials. The zwitterionic, saturated phospholipid 1,2-dimyristoyl-*sn*-glycero-3-phosphocholine (DMPC) was obtained from Avanti Polar Lipids (Avanti, Alabaster, USA). DIBMA monomethyl ester was a kind gift from Glycon Biochemicals (Luckenwalde, Germany). Styrene/maleic acid (SMA(2:1)) copolymer was purchased from Orbiscope (Geleen, The Netherlands). *n*-Dodecyl-β-D-maltopyranoside (DDM) was from Glycon Biochemicals (Luckenwalde, Germany). L-Arginine was purchased from Carl Roth (Karlsruhe, Germany), meglumine from Fisher Scientific (Schwerte, Austria), and L-2,4-diaminobutyric acid dihydrochloride from Bachem (Bubendorf, Switzerland). Cholesteryl hemisuccinate (CHS), tris(hydroxymethyl)aminomethane hydrochloride (Tris-HCl), 2-(4-(2-hydroxyethyl)-1-piperazinyl)-ethanesulfonic acid (HEPES), $CaCl_2$, $MgCl_2$, and other chemicals were purchased from Sigma–Aldrich (Darmstadt, Germany).

Syntheses. The synthetic procedures for DIBMA amide derivatives followed the same general protocol previously published for Glyco-DIBMA [390]. Briefly, to DIBMA monomethyl ester (2 g, 15.6 mmol) dissolved in 80 mL MeOH was added an amine (15.6 mmol; see below) in 25 wt% sodium methoxide (4 mL diluted in 20 mL MeOH) under stirring at room temperature. The reaction mixture was refluxed overnight, and MeOH was removed by rotary evaporation. The identity of the resulting DIBMA amide product was confirmed by attenuated total reflection infrared (ATR-IR) spectroscopy. Arg-DIBMA: L-arginine was used as amine; ATR-IR: 2942 (C–H str), 1722 (C=O str), 1558 (C–N str/NH bend) cm^{-1}; Dab-DIBMA: L-2,4-diaminobutyric acid dihydrochloride was used as amine; ATR-IR: 3345, 3283, 3178 (N–H str), 2946 (C–H str), 1727 (C=O str), 1567 (C–N str/ NH bend) cm^{-1}; Meg-DIBMA: meglumine was used as amine; ATR-IR: 3296 (O–H str), 2943 (C–H str), 1726 (C=O str), 1575 (C–N str/NH bend) cm^{-1}; $mPEG_4$-DIBMA: tetraethyleneglycol monomethyl ether amine ($mPEG_4$-amine) was used as amine; ATR-IR: 2868 (C–H str), 1729 (C=O str), 1582 (C–N str/ NH bend) cm^{-1}.

Polymer stock solutions. Polymer powders used throughout this study were dissolved in 50 mM Tris-HCl or 50 mM HEPES, 200 mM NaCl unless noted otherwise, followed by incubation at 55 °C for 10–15 min with vortexing in an alternating fashion to yield a mass concentration of 50 mg/mL. The final pH value of polymer stock solutions was adjusted to 8.0 or 7.4, as indicated. All polymer stock solutions were then filtered through polycarbonate membranes with a pore size of 0.22 µm and stored at –4 °C.

Large unilamellar vesicles (LUVs). DMPC powder was dissolved in 50 mM Tris-HCl or HEPES, 200 mM NaCl, pH 8.0 to a final concentration of 20 mg/mL. The lipid suspension was incubated at 35 °C for 30–40 min with vortexing every 10 min in an alternating fashion. In order to increase the hydration efficiency, the lipid suspension was then immersed in liquid nitrogen followed by thawing in a ThermoMixer (Eppendorf, Germany) at 35 °C for 5–10 freeze–thaw cycles. Subsequently, the DMPC suspension was loaded into gas-tight syringes and extruded at 35 °C through a 100-nm Whatman polycarbonate membrane filter at least 20 times using a Mini-Extruder (Avanti, Alabaster, USA) to prepare LUVs.

Ultraviolet–visible (UV–vis) spectroscopy. The absorption spectra of polymers at 1 mg/mL dissolved in 50 mM Tris-HCl, 200 mM NaCl, pH 8.0 were recorded on a Jasco V-650 UV–vis spectrophotometer (JASCO

Germany). Measurements were performed at room temperature using a quartz cuvette with a 10-mm light path (Hellma Analytics, Germany) at a scan rate of 200 nm/min in the wavelength range of 220–600 nm.

Polymer/lipid nanodiscs. The DMPC LUVs suspension was added to the polymer stock solutions at different polymer/lipid mass ratios (m_P/m_L) and incubated at 35 °C for at least 16 h with shaking at 450 rpm to form polymer-encapsulated DMPC nanodiscs. All experiments were performed in aqueous buffer containing 50 mM Tris-HCl, 200 mM NaCl, pH 8.0.

Dynamic light scattering (DLS). Solubilization efficiencies of all polymers were confirmed and quantified with the aid of DLS using DMPC model membranes. A Zetasizer Nano S (Malvern Panalytical, UK) was used to perform DLS measurements in a 70-µL microcuvette (Brand, Wertheim, Germany) at a temperature of 25 °C. The DLS instrument was equipped with a He–Ne laser having a wavelength of 633 nm, and the detection scattering angle was 173°. The sample was thermostatted for 5 min at 35 °C prior to measurement.

Differential scanning calorimetry (DSC). DSC measurements were carried out using a MicroCal VP-DSC calorimeter (Malvern Panalytical, UK) to monitor the thermotropic behavior of DMPC lipids in the absence and presence of polymers. Samples were prepared in 50 mM Tris-HCl, 200 mM NaCl, pH 8.0 at various polymer/lipid mass ratios (m_P/m_L). Polymer/DMPC samples and reference buffer were first degassed and then measured in 5–10 heating and cooling cycles at a scan rate of 60 °C h^{-1} in the range of 2–80 °C. One representative curve was chosen from the closely overlaid scan traces, the buffer baseline was subtracted, and the data were normalized against the DMPC concentration (6 mM) using MicroCal Origin 7.0 software (OriginLab, Northampton, USA). The phase transition temperature (T_m) was determined as the temperature at which the excess molar isobaric heat capacity (C_p) reached its maximum value. The size of the cooperative unit (CU) was obtained as the ratio of the van't Hoff enthalpy, given by the shape of the melting peak, to the calorimetric enthalpy, given by the peak area [549].

Turbidity experiments. The colloidal stability of mPEG$_4$-DIBMA lipid particles in the presence of divalent cations was evaluated with turbidity experiments at 620 nm using a Tecan Spark 10M microplate reader (Tecan, Switzerland).

ζ-potential measurements. Samples containing 4 mg/mL DMPC LUVs, 8 mg/mL polymer, or polymer/DMPC nanodiscs at m_P/m_L = 2 were prepared in 50 mM Tris-HCl, 100 mM NaCl, pH 7.4. ζ-potential measurements were carried out on a Zetasizer Nano ZS (Malvern Panalytical, UK) using disposable folded capillary zeta cells DTS1070 (Malvern Panalytical, UK) at a detection scattering angle of 173° and a temperature of 25 °C. The diffusion barrier technique was used to prepare the sample cell for ζ-potential measurement [550]. The folded capillary cell was first filled with buffer before 100 µL of sample was pipetted directly into the cell bottom with the aid of a gel-loading tip, avoiding mixing of the sample with buffer during loading. The cell was capped and equilibrated for 300 s prior to measurement to reduce fluid motion induced by temperature gradients.

Adrenocorticotropic hormone peptide (ACTH). The human adrenocorticotropic hormone truncated construct ACTH (1-23)Cys was subcloned into pET-16b vector, including a 6xHis tag at N-terminus, followed by B1 domain of streptococcal protein G (GB1 fusion protein) and tobacco etch virus (TEV) cleavage site.

Escherichia coli strain BL21 (DE3) cells were used for peptide expression. Cells were cultured in 2xYT medium at 37 °C, 140 rpm in baffled flask, supplemented with 100 µg/mL ampicillin. The expression was inducted with 1 mM isopropyl-β-D-thiogalactopyranoside (IPTG) upon the optical density 600 (OD_{600}) reached 0.6–0.8. Cells were harvested by centrifugation at 6,000 *g*, 10 min, 4 °C after 5 h induction, flash-frozen in N_2 (l), and stored at –80 °C for future use. Cell pellets were resuspended in lysis buffer containing 50 mM sodium phosphate, pH 7.5, 300 mM NaCl, 1 mM dithiothreitol (DTT), supplemented with EDTA free cOmplete protease inhibitor cocktail tablet (Roche). The homogenate was sonicated on ice, and the lysate was centrifuged at 100,000 *g* for 25 min at 4 °C. The supernatant was incubated with Ni-NTA resin (Macherey-Nagel, Germany) at 4 °C overnight with gentle rotation. The resin was loaded onto a gravity column and washed with 10 column volumes (CVs) lysis buffer and 10 CVs lysis buffer supplemented with 20 mM imidazole. The peptide was eluted with 10 CVs lysis buffer supplemented with 250 mM imidazole. Fractions containing peptides were collected and dialyzed against lysis buffer using 3.5K MWCO SnakeSkin dialysis tubing (ThermoFisher) at 4 °C overnight. The fusion protein was removed by addition of home-made TEV protease. The cleaved peptide was further purified by size-exclusion chromatography (Superdex 16/600, 30 pg column; GE health) with a running buffer containing 20 mM ammonium bicarbonate. Peptide labeling with thiol-reactive ATTO-488 maleimide (ATTO-TEC, Germany) was carried out according to the manufacturer's instructions. The labeled peptide was further purified using high-performance liquid chromatography (HPLC) using a Zorbax SB300 C8 4.6 x 250 mm analytical column (Agilent Technologies).

Microfluidic diffusional sizing (MDS). ATTO 488-labeled human adrenocorticotropic hormone (ACTH) peptide was added to polymer/DMPC nanodiscs at $m_P/m_L = 4$ to a final peptide concentration of 20 nM. The final concentration of DMPC was 4 mg/mL. Interactions between peptide and polymer/DMPC nanodiscs were measured on a Fluidity One-W system (Fluidic Analytics, Cambridge, UK) by recording changes in hydrodynamic particle size [394,529]. Disposable MDS chips were used holding a total sample volume of 5 µL. All experiments were carried out in 50 mM HEPES, 200 mM NaCl, pH 7.4 or 8.0.

Negative-stain transmission electron microscopy (TEM). TEM specimens were prepared by spreading 4 µL $mPEG_4$-DIBMA/DMPC nanodiscs at $m_P/m_L = 4$ onto freshly glow-discharged copper grids (15 mA for 25 s at 0.39 mbar) coated with a carbon support film. Excess suspension was blotted off after ~5 s using filter paper. Grids were washed with 5 µL MilliQ water once, followed by staining with 5 µL 2% (*w*/*v*) aqueous uranyl acetate solution twice and blotted off after ~15 s with filter paper. After preparation, specimens were air-dried and examined on a Talos L120C transmission electron microscopy equipped with a 4k × 4K Ceta CMOS camera (Thermo Scientific).

Preparation of insect membranes and solubilization of MC4R. The wild-type human melanocortin 4 receptor (MC4R, UniProtKB-P32245) was codon-optimized and inserted into a mortified pFastbac1 vector, including an influenza virus hemagglutinin (HA) signal peptide followed by a Flag tag at the N-terminus as well as a human rhinovirus (HRV3C) cleavage site and a 10xHis tag at the C-terminus by using NcoI-EcoRI restriction endonucleases (New England Biolabs). The thermostabilized mutant MC4R construct was modified by introducing 5 mutations ($E49^{1.37}V$, $N97^{2.57}L$, $S99^{2.59}F$, $S131^{3.34}A$ and $D298^{7.49}N$, where superscript numbers correspond to the Ballesteros–Weinstein nomenclature [14]) containing the same tags as the wild type, a generous

gift of Prof. Dr. Raymond C. Stevens (iHuman Institute at ShanghaiTech University) [224]. The MC4R-eYFP construct was modified by introducing the eYFP gene between the HRV3C cleavage site and the 10xHis tag. Recombinant baculovirus production of MC4R-eYFP was generated by transfecting *Spodoptera frugiperda* (Sf9) cells grown in Sf-900 III SFM media (ThermoFisher) at 27 °C with Bacmid (Bac-to-Bac system, ThermoFisher) using FuGENE HD transfection reagent according to the manufacturer's instructions. Sf9 cells were infected at a density of 2 to 3 x 10^6 cells/mL with recombinant baculovirus. 72 h after infection, cells were harvested by centrifugation at 6000 *g*, 4 °C for 10 min and stored at –80 °C. Cellular membranes were prepared as described previously with slight modifications [224]. In brief, Sf9 cell pellets were resuspended in a hypotonic buffer containing 10 mM HEPES, 10 mM $MgCl_2$, 20 mM KCl, pH 7.8 and cOmplete EDTA-free protease inhibitor cocktail tablet (Roche) and then lysed by sonication on ice (Bandelin Sonorex, Germany). Cell membranes containing MC4R-eYFP were harvested by ultracentrifugation at 120,000 *g*, 4 °C for 30 min (Optima xpn-80 ultracentrifuge, Beckman Coulter, USA). The membrane pellet was resuspended in the same hypotonic buffer and disrupted with a Dounce homogenizer followed by ultracentrifugation at 120,000 *g*, 4 °C for 30 min. The above procedure was repeated twice. Further membrane purification was performed three times using hypotonic buffer supplemented with 1 M NaCl. Purified membrane pellets were washed once with 50 mM HEPES, 200 mM NaCl, pH 8.0, flash-frozen in liquid nitrogen, and stored at –80 °C. Polymers were added to 20 mg/mL (wet mass/volume) purified cellular membranes at different concentrations and incubated at 4 °C for either 4 h or 16 h with gentle rotation. Supernatants were collected after ultracentrifugation at 120,000 *g*, 4 °C for 30 min.

5.5 Results and discussion

Design and synthesis of copolymers. The goal of our synthetic approach was to reduce the charge density on the polymer backbone by derivatizing DIBMA through amidation of one of the two carboxylic acid groups in each repeating unit (Fig. 16). We have previously used the same strategy to produce Glyco-DIBMA, which offers several advantages over unmodified DIBMA, including a higher protein-extraction efficiency [390,551]. Here, we sought to explore a larger chemical space through amidation using a set of structurally diverse amines, including: α-amino acids such as L-arginine (Arg) and L-2,4-diaminobutyric acid (Dab); the hexosamine meglumine (Meg); and the oligo (ethylene oxide) tetraethyleneglycol monomethyl ether amine ($mPEG_4$). These compounds have in common that they contain at least one reactive amino group, are highly water-soluble, biocompatible, and net neutral once coupled to the polymer backbone through an amide linkage. We considered these properties important to reduce the charge density on the DIBMA polymer backbone while retaining its excellent water solubility. Four polymers were thus synthesized, henceforth referred to as Arg-DIBMA, Dab-DIBMA, Meg-DIBMA, and $mPEG_4$-DIBMA.

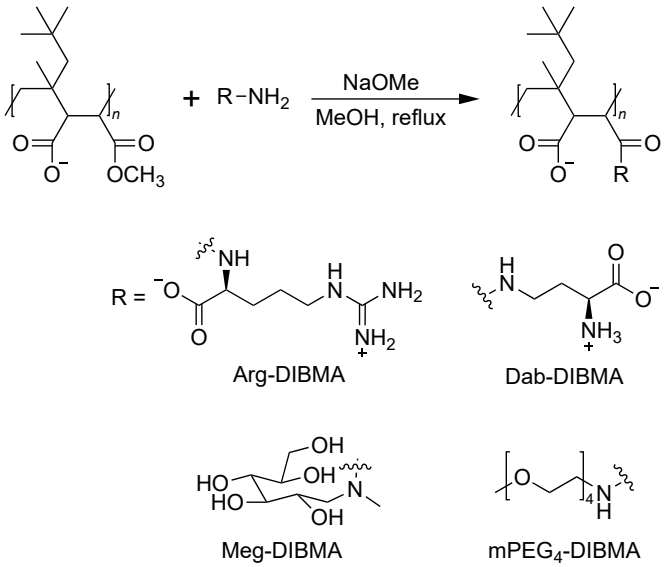

Fig. 16 General scheme for the synthesis of DIBMA-based amphiphilic copolymers that form lipid-bilayer nanodiscs.

Each polymer variant was subsequently tested for its key biophysical and nanodiscs-forming properties, including lipid extraction from synthetic vesicles as well as protein extraction from eukaryotic cells. First, we investigated the formation of polymer/DMPC nanodiscs and the solubilization efficiency of the new polymers. To this end, large unilamellar vesicles (LUVs) made from DMPC were incubated with each polymer at different polymer/lipid mass ratios, and particle size distributions were analyzed by dynamic light scattering (DLS). At a polymer/lipid mass ratio (m_P/m_L) of 2.0, the hydrodynamic particle sizes of all new nanodiscs were in the expected range of ~10 nm (Fig. 17a). By contrast, at a lower m_P/m_L of 0.5, substantial differences in hydrodynamic particle sizes were observed, reflecting differences in the solubilization efficiency among the polymers (Fig. 17b). A more systematic screening of m_P/m_L revealed that mass ratios of ~1 should be used for all new DIBMA variants to obtain the often-desired nanodisc diameter of ~10 nm (Fig. 17c, top panel). This minimal m_P/m_L ratio is considerably less than that observed for unmodified DIBMA but about a factor of two larger than for SMA(2:1) and Sulfo-DIBMA (Fig. 17c, lower panel). Sulfo-DIBMA is a recent electroneutral DIBMA variant that contains an imide ring [393], in contrast with the open amide linkage of the DIBMA variants reported here (Fig. 16).

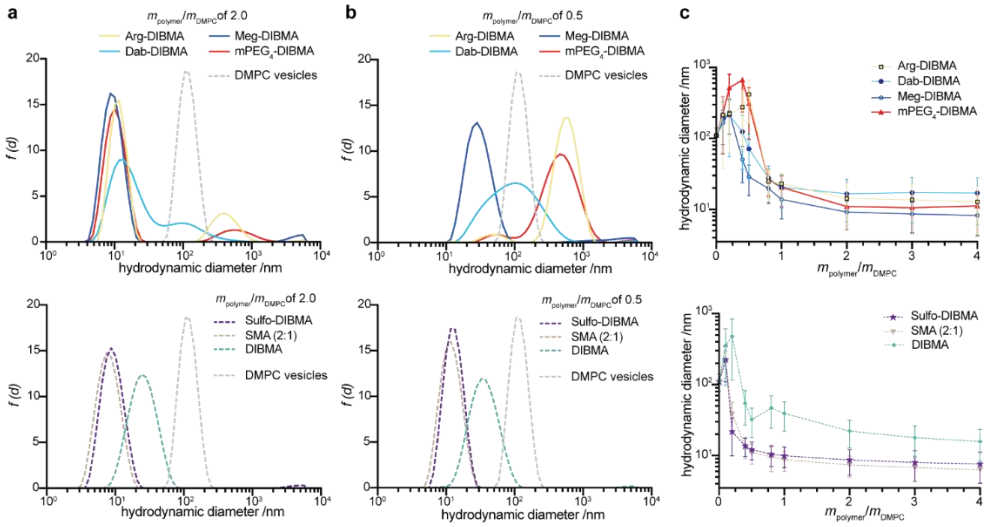

Fig. 17 Particle size analysis shows formation of homogenous nanodiscs for all polymers at polymer/lipid mass ratios >1. (a,b) Intensity-weighted particle size distributions of mixtures containing polymer and DMPC (4 mg/mL) at polymer/lipid mass ratios (m_P/m_L) of (a) 2.0 and (b) 0.5 as obtained from DLS. Upper panels show data for the new DIBMA variants, while lower panels serve as reference for established polymers. (c) z-Average particle diameters derived from DLS as functions of m_P/m_L. Vertical bars indicate size distribution widths defined as $\sigma = z * \sqrt{PDI}$, where PDI is the polydispersity index.

Next, we tested the suitability of each new polymer for characterizing interactions that are susceptible to charge effects. Most existing polymers, such as SMA and DIBMA, are incompatible with ligand binding assays for GPCRs because of unspecific interactions between the polyanionic polymer chains and the ligands [393]. To assess the new DIBMA variants for their suitability in such ligand–GPCRs interaction experiments, we performed microfluidic diffusional sizing (MDS) measurements with the binding fragment of the adrenocorticotropic hormone (ACTH), a potent agonist of the melanocortin 4 receptor (MC4R) [552]. MDS allows for the determination of the hydrodynamic particle size of bare ACTH and its increase resulting from unspecific interactions with nanodiscs [394,529]. To evaluate the interactions between the DIBMA variants and ACTH, we used polymer-encapsulated nanodiscs containing the zwitterionic phospholipid DMPC, a lipid known not to interact with ACTH [393]. Polymer/DMPC nanodiscs were prepared at m_P/m_L of 4 to obtain small nanodiscs, as confirmed by DLS (Fig. 17c and S4). In line with previous observations [393], our MDS results confirmed that the hydrodynamic particle size of ACTH remained unchanged upon addition of DMPC nanodiscs encapsulated by the electroneutral polymer Sulfo-DIBMA, indicating the absence of unspecific interactions between the polymer and the ligand (Fig. 18). In contrast with Sulfo-DIBMA, we observed an increase in hydrodynamic particle size when ACTH was exposed to nanodiscs encapsulated by DIBMA, Arg-DIBMA, Dab-DIBMA, or Meg-DIBMA, suggesting unspecific interactions between the cationic peptide ligand and the anionic polymers. In stark contrast, the hydrodynamic particle size of ACTH remained unchanged upon addition of nanodiscs encapsulated by the PEGylated polymer mPEG$_4$-DIBMA, even though mPEG$_4$-DIBMA still carries carboxylate groups (Fig. 16). For all polymers, the same interaction behaviors were found at two different pH values (pH 7.4, Fig. 18 and pH 8.0, Fig. S5), confirming that mPEG$_4$-DIBMA is of particular interest for studying the specific binding of ligands to nanodiscs-embedded membrane proteins under commonly applied buffer conditions.

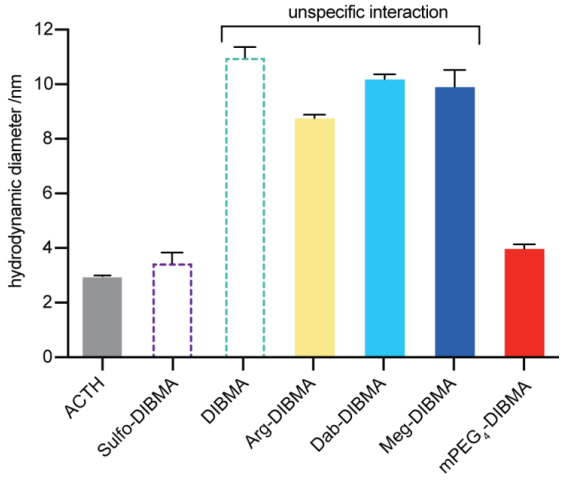

Fig. 18 Only mPEG$_4$-DIBMA shows reduced unspecific interactions with the cationic peptide ligand ACTH. Unspecific interactions between ACTH and polymer/DMPC nanodiscs at m_P/m_L of 4 were measured by means of microfluidic diffusional sizing (MDS). All experiments were carried out at 50 mM HEPES, 200 mM NaCl, pH 7.4. Error bars represent one standard deviation of two independent experiments, each repeated in triplicate.

Due to its promising features in ligand-binding assays, we carried out a more comprehensive characterization of mPEG$_4$-DIBMA. First, we investigated the origin of the reduced unspecific interactions with ACTH by determining the ζ-potential. Our results confirmed that unmodified DIBMA indeed has a strongly negative ζ-potential, which is only partly reduced by the mPEG$_4$ modification, in contrast with electroneutral Sulfo-DIBMA (Fig. 19a). Negative ζ-potentials were similarly detected in lipid-free polymer samples and for lipid-encapsulating nanodiscs. From this finding, we infer that unspecific binding to mPEG$_4$-DIBMA is not prevented by a lack of charged groups on the polymer but rather by the relatively bulky, strongly hydrated PEG chains, which sterically block access of the peptide to the polymer backbone. This interpretation is consistent with the expected Debye–Hückel screening length of <1 nm under the applied conditions, which indicates that Coulombic interactions in salty aqueous buffers decay steeply with the distance between two charged groups. Consequently, the unspecific interactions between the positively charged peptide and the negatively charged carboxylate groups may are much less prominent in mPEG$_4$-DIBMA because of their spatial separation by the hydrated PEG chains and the shielding effects of the buffer ions.

Next, we assessed the morphology of mPEG$_4$-DIBMA/DMPC nanodiscs with the aid of negative-stain transmission electron microscopy (TEM). TEM images demonstrated the presence of homogeneously sized nanodiscs with an average diameter of 10 nm (Fig. 19b), consistent with our DLS data (Fig. 17). Furthermore, absorbance measurements showed that mPEG$_4$-DIBMA has a very low absorbance in the ultraviolet (UV) spectral range, offering favorable properties for the photometric quantification of protein levels (Fig. 19c).

In order to evaluate the effects of divalent cations on the colloidal stability of nanodiscs, we measured the turbidity of mPEG$_4$-DIBMA/DMPC nanodiscs as a function of increasing concentrations of Mg^{2+} or Ca^{2+}. mPEG$_4$-DIBMA/DMPC nanodiscs began to precipitate at divalent ion concentrations of 10 mM Mg^{2+} or 5 mM Ca^{2+} (Fig. 19d and S6). Thus, mPEG$_4$-DIBMA/DMPC nanodiscs showed a rather modest colloidal stability in the presence of divalent cations, as expected for negatively charged nanodiscs. Nevertheless, this modest stability is still

sufficient for physiological concentrations of divalent cations and, thus, should enable activity studies of membrane proteins requiring typical concentrations of divalent cations.

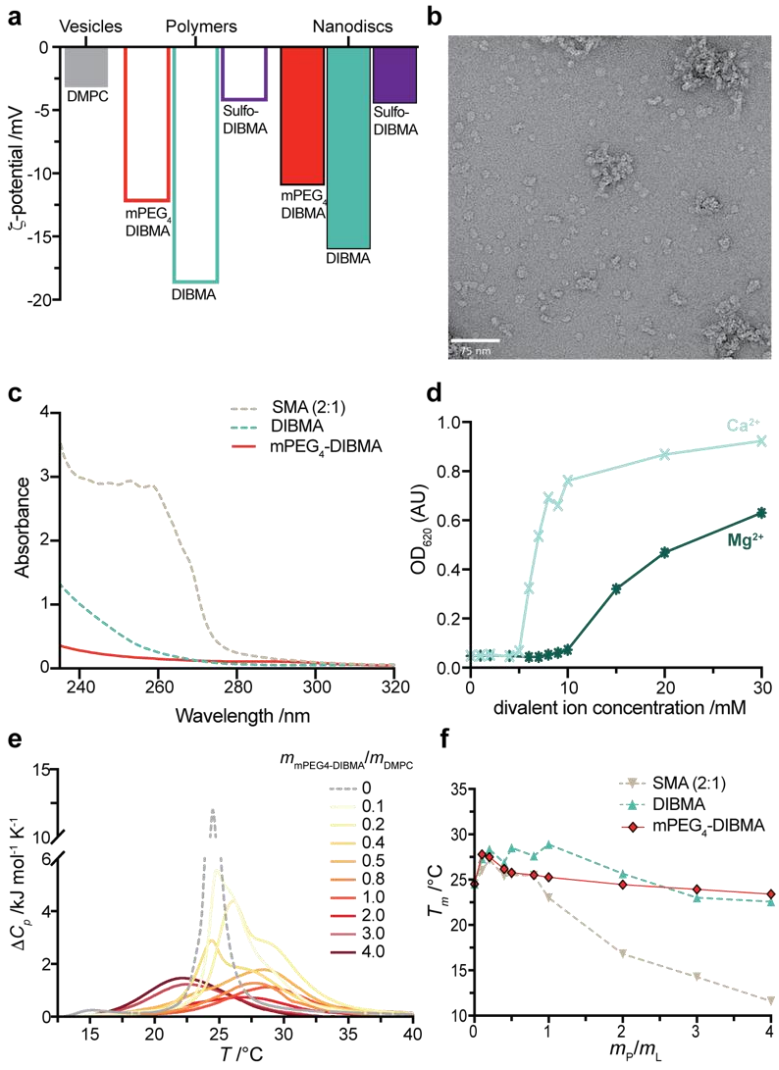

Fig. 19 Physicochemical properties of mPEG4-DIBMA. (a) ζ-potentials of mPEG4-DIBMA, DIBMA, Sulfo-DIBMA, and respective polymer-encapsulated DMPC nanodiscs. (b) Negative-stain transmission electron microscopy (TEM) image of mPEG4-DIBMA/DMPC nanodiscs at m_P/m_L of 4.(c) UV absorption spectra of mPEG4-DIBMA, DIBMA, and SMA(2:1). (d) Colloidal stability of mPEG4-DIBMA/DMPC nanodiscs at m_P/m_L of 4 as determined by turbidity in response to increasing concentration of Mg^2 or Ca^{2+}. (e) Differential scanning calorimetry (DSC) thermograms displaying the excess molar isobaric heat capacities (ΔC_p) of 4 mg/mL DMPC LUVs and mPEG4-DIBMA/DMPC nanodiscs at the indicated polymer/DMPC mass ratios, m_P/m_L. (f) Main phase transition temperature (T_m) as a function of the polymer/DMPC mass ratio, m_P/m_L.

To investigate the integrity of the nanodisc's lipid matrix, we measured the effect of mPEG4-DIBMA on the thermotropic behavior of the encapsulated lipid-bilayer patch using differential scanning calorimetry (DSC). DSC thermograms showed that the phase-transition peak became broader with increasing m_P/m_L (Fig. 19e). This observation confirms the formation of smaller lipid-bilayer nanoparticles upon addition of mPEG4-DIBMA to DMPC vesicles, which showed the expected highly cooperative gel-to-fluid transition at ~24.5 °C (Fig. 19e, grey). It is worth noting that multiple phase transition peaks were observed at low polymer/lipid mass ratios, where

nanodiscs coexist with vesicles (Fig. 19e and S7). Hence, it appears that a polymer/lipid mass ratio of ~1 is required for mPEG$_4$-DIBMA to fully solubilize DMPC vesicles, in agreement with our DLS data (Fig. 17c) and in contrast with SMA(2:1) (Fig. 19e and S7a). At higher polymer/lipid ratios, the mPEG$_4$-DIBMA nanodiscs revealed a moderate decrease in the phase transition temperature (T_m) to about 22 °C. We infer that the DMPC molecules along the perimeter of the nanodiscs were affected by mPEG$_4$-DIBMA, whereas the core of the DMPC bilayer in the nanodiscs was not significantly affected. Similar results were observed in DSC measurement of DIBMA/DMPC nanodiscs (Fig. 19f and S7b), in line with previous findings [383] . In contrast, SMA-encapsulated nanodiscs showed a steep drop in T_m with increasing polymer concentration down to 11.6 °C at m_P/m_L of 4 (Fig. 19f and S7a). This observation has been explained by a perturbation of the lipids' acyl chain packing by the polymer, which might be caused by the intercalation of the phenyl groups of SMA(2:1) [553]. Overall, our DSC data demonstrate that, in comparison with SMA(2:1), mPEG$_4$-DIBMA requires slightly elevated polymer/lipid mass ratios for complete solubilization. However, mPEG$_4$-DIBMA also has much milder effects on the lipid matrix under the conditions required to prepare small and homogenous nanodiscs, making it an ideal tool for subsequent biophysical or structural studies.

In addition to the solubilization of synthetic lipids, we tested the capacities of all new polymers to extract and encapsulate integral transmembrane proteins from cellular membranes into nanodiscs. For this purpose, we selected a prototypical GPCR comprising a thermostabilized mutant of the melanocortin 4 receptor (MC4R-eYFP) carrying an enhanced yellow fluorescent protein (eYFP) tag. We exposed crude membrane preparations from Sf9 insect cells to different concentrations of polymers and quantified the amounts of extracted MC4R by measuring the emission intensities of eYFP (Fig. 20). Interestingly, all four new DIBMA variants considerably enhanced the solubilization efficiency as compared with unmodified DIBMA (Fig. 20). Previous findings have shown that DIBMA carries higher negative charge densities than SMA(2:1) under similar conditions [384]. As a result, strong Coulombic repulsion may affect the interaction of DIBMA with the negatively charged cell membrane and hinder the extraction of membrane proteins into native nanodiscs. Our data show that the newly designed DIBMA variants indeed facilitate the cell-membrane fragmentation process, resulting in higher extraction efficiencies. With the exception of Dab-DIBMA, all new DIBMA variants also offered solubilization efficiencies comparable to or surpassing that of SMA(2:1) at polymer concentrations ≥ 1%. Again, mPEG$_4$-DIBMA displayed the best performance, approaching solubilization yields similar to the DDM/CHS system that was used as reference and generally serves as a gold standard for the extraction of GPCRs. In direct comparison with electroneutral Sulfo-DIBMA, the solubilization of MC4R was about 1.5-fold higher with mPEG$_4$-DIBMA, making this new DIBMA variant particularly interesting for studies where the amount of extracted membrane protein is a limiting factor. Noteworthily, many functional and structural studies of GPCRs suffer from limited stability of these labile receptors. Therefore, long incubation times of the cell pellet with the polymer may adversely affect subsequent *in vitro* studies. To address this important point, we finally tested the effects of reducing the incubation time (Fig. 20b, 4 h). These data largely reproduced the results obtained at longer incubation times (Fig. 20a, 16 h). The only exceptions were SMA(2:1) and Dab-DIBMA at low polymer concentrations, which displayed significantly lower extraction efficiencies at 4 h than at 16 h incubation. A more thorough analysis carried out for mPEG$_4$-DIBMA further suggested that even shorter incubation times, in the range of 20–60 min, can be used to efficiently extract MC4R (Fig. 20c).

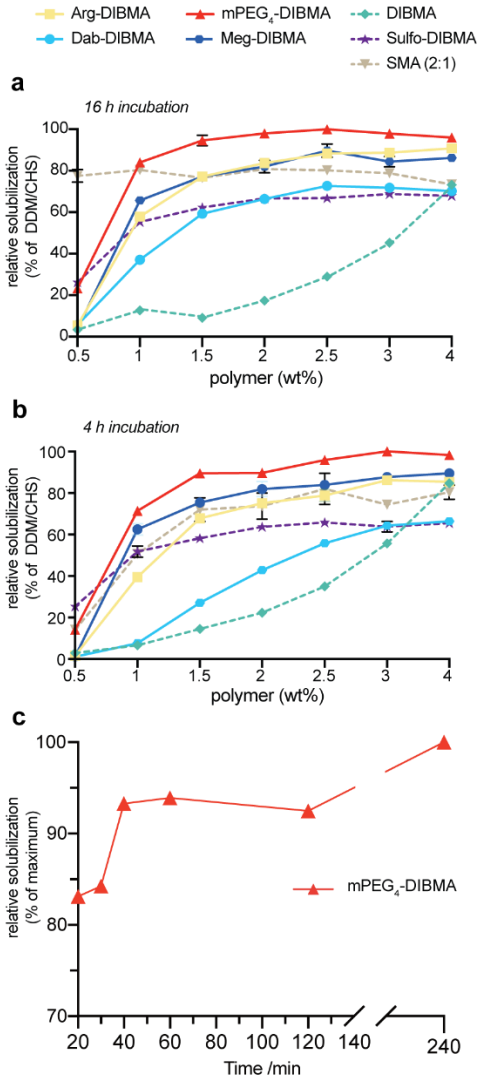

Fig. 20 All new DIBMA variants, in particular mPEG$_4$-DIBMA, efficiently extract the GPCR MC4R. (a,b) Polymer-mediated extraction of the melanocortin-4 receptor (MC4R-eYFP) from insect membranes. The extraction efficiencies of the different polymers in comparison with the frequently used DDM/CHS system (1% (*w/v*) DDM and 0.2% (*w/v*) cholesteryl hemisuccinate (CHS)) are plotted. The amount of solubilized receptor for each preparation was determined by eYFP fluorescence after incubation with the indicated polymers for either 16 h (a) or 4 h (b). (c) Solubilization efficiency of 2% (*w/v*) mPEG$_4$-DIBMA (normalized to maximum solubilization after 240 min) as a function of incubation time.

Taken together, we found that all new DIBMA variants can solubilize synthetic lipids and extract a GPCR from insect cells into native nanodiscs. Our MDS assay identified mPEG$_4$-DIBMA as a new member of the small set of polymers that avert unspecific Columbic interactions with a cationic peptide ligand, thus facilitating interaction studies using nanodisc-embedded membrane proteins. Furthermore, we observed an outstanding performance of mPEG$_4$-DIBMA in efficiently extracting MC4R from native cellular membranes. Paired with its decent Mg^{2+} and Ca^{2+} tolerance and its low UV absorbance, mPEG$_4$-DIBMA has a particularly high potential for future applications in membrane-protein research.

5.6 Conclusions

Polymer-encapsulated nanodiscs offer several advantages over other membrane mimetics, including the detergent-free extraction of target membrane proteins within their native lipid-bilayer environment. Several amphiphilic copolymers, such as SMA and DIBMA, have been successfully used in the purification of membrane proteins from different cells and the determination of membrane-protein structures [400,554,402,555] . In general, existing polymers differ in key features such as extraction efficiency, tolerance against divalent metal ions, UV absorbance, and charge density, a factor that often restricts interaction studies using polymer-encapsulated nanodiscs. Although all of the listed properties are essential for characterizing membrane proteins such as GPCRs, none of the currently available polymers can provide top performances in all properties, necessitating compromises to be made in the selection process. To overcome this limitation, we here introduced and tested a series of new DIBMA variants. All new polymers show promising features, in particular as regards their solubilization efficiency of a GPCR from insect membranes. A PEGylated polymer, $mPEG_4$-DIBMA, emerged as the top performer in all tested properties. $mPEG_4$-DIBMA overcomes some of the most serious limitations of SMA and DIBMA without sacrificing protein yields, highlighting its potential for the functional and structural characterization of membrane proteins in their native lipid-bilayer environment.

6. Conclusions and perspectives

Detergent micelles, MSP nanodiscs and polymer native membrane nanodiscs are three most commonly used membrane mimicking systems for the *in viro* studies of membrane proteins. In order to evaluate the influence of different environments on the function of MC4R, we performed the solubilization and purification of MC4R expressed in Sf9 cells using detergents, MSP1D1 nanodiscs and Sulfo-DIBMA native membrane nanodiscs, respectively. The results demonstrate that lipid bilayer, particularly the native lipid environment (Sulfo-DIBMA), is more effective in preserving the functional integrity of MC4R. Given the critical roles of divalent cations in the ligand binding and signal transduction of a number of GPCRs, we investigated the allosteric regulation of divalent cations on the ACTH (1-23) binding to MC4R embedded in detergent micelles, MSP1D1/POPC nanodiscs and Sulfo-DIBMA native membrane nanodiscs, respectively. Our results show that Ca^{2+} and Cu^{2+} enhances and inhibits the ligand binding of MC4R, respectively, in all membrane mimetics. Interestingly, the ligand binding affinity is reduced by the addition of Zn^{2+} when MC4R embedded in detergent micelles but increased in lipid bilayer. Therefore, the environments play a critical role in shaping the function of GPCRs, including their ligand binding properties in the absence or presence of extracellular modulators.

Generally, existing polymers differ in key features such as extraction efficiency, tolerance against divalent metal ions, UV absorbance, and charge density, a factor that often restricts interaction studies using polymer-encapsulated nanodiscs. Although all of the listed properties are essential for characterizing membrane proteins such as GPCRs, none of the currently available polymers can provide top performances in all properties, necessitating compromises to be made in the selection process. To overcome this limitation, we synthesized and tested a series of new DIBMA variants, including Arg-DIBMA, Dab-DIBMA, Meg-DIBMA and $mPEG_4$-DIBMA. All new polymers show promising features, in particular the solubilization efficiency of MC4R from insect membranes. Of note, $mPEG_4$-DIBMA overcomes some of the most serious limitations of SMA and DIBMA without sacrificing protein yields, and does not interfere with ligand-lipid interactions, emerging as the top performer in all tested properties and highlighting its potential for the functional and structural characterization of GPCRs in their native lipid-bilayer environment.

Taken together, this work contributes to a better understanding of the functional properties of MC4R and may pave the way for obtaining atomic-resolution insights into the structure and dynamics of MC4R in an environment that adequately preserves their functionally relevant conformation(s).

Supplementary Information

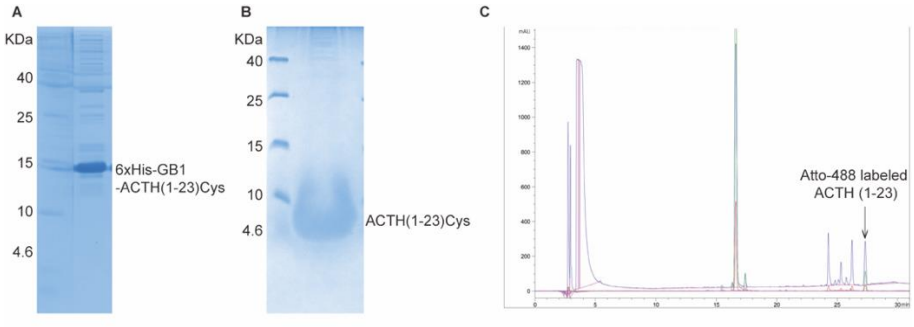

Fig. S1 Peptide purification. (A) Ni-NTA purification of ACTHA (1-23)Cys containing fusion peptide GB1. (B) SEC (Superdex 16/600, 30 pg column) purification of ACTH (1-23)Cys. (C) HPLC purification of dye labeled ACTH (1-23). HPLC program: 0-4 min (5-10% AcNcan, 0.1% TFA), 4-20 min (10-36% AcN, 0.1% TFA), 20-22 min (36-60% AcN, 0.1% TFA), 22-27 min (80% AcN, 0.1% TFA) and 27-31 min (5% AcN, 0.1% TFA). A214 colored blue, A280 colored red and A488 colored green.

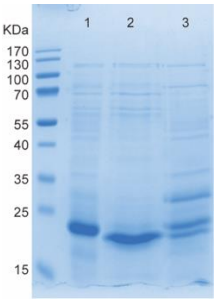

Fig. S2 Purification of MSP1D1. Line 1: Ni-NTA purification of 6xHis-TEV-MSP1D protein. Line 2: His-tag free MSP1D1 (Ni-NTA flow through). Line3: Eluted proteins from Ni-NTA column.

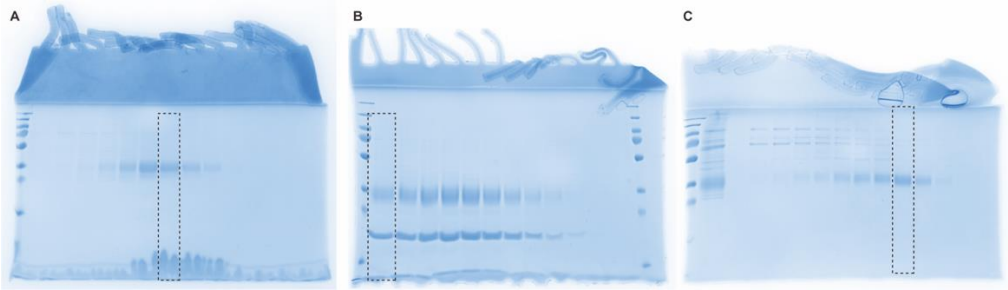

Fig. S3 Uncropped purification images of the SDS-PAGE gels. (A) Detergent micelles/MC4R, (B) MSP1D1/POPC/MC4R nanodiscs and (C) Sulfo-DIBMA/MC4R native membrane nanodiscs. The black dotted boxes indicate the portion of the gel that was presented earlier in Fig. 11C-E.

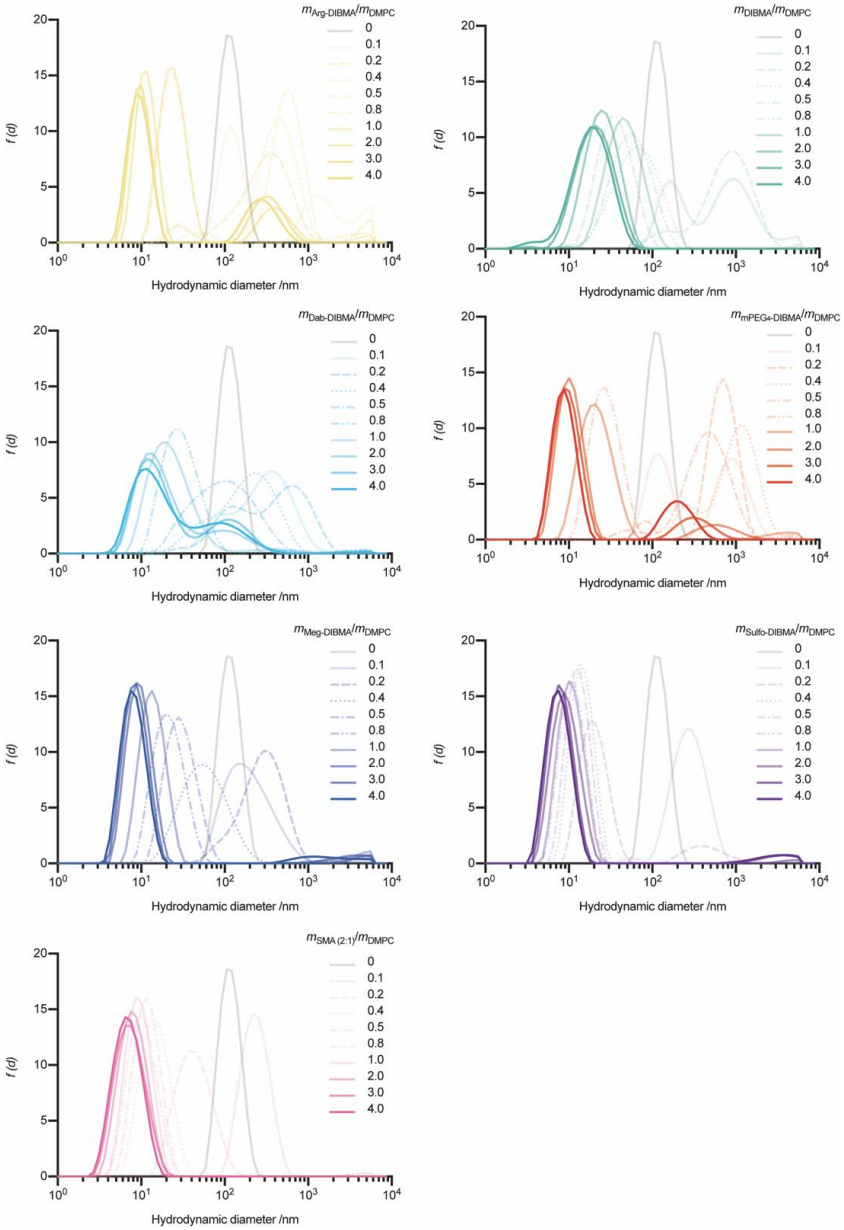

Fig. S4 Solubilization of DMPC vesicles and formation of polymer-encapsulated DMPC nanodiscs. Intensity-weighted particle size distributions of mixtures containing polymer and DMPC (4 mg/mL) at indicated polymer/lipid mass ratios (m_P/m_L).

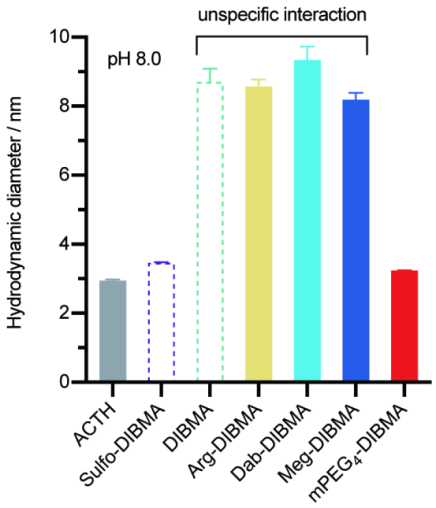

Fig. S5 Unspecific interactions between peptide and polymer/DMPC nanodiscs at m_P/m_L of 4 were measured by means of microfluidic diffusional sizing (MDS). All experiments were carried out at 50 mM HEPES, 200 mM NaCl, pH 8.0. Error bars indicate ± one standard deviation of two independent experiments, each repeated in triplicate.

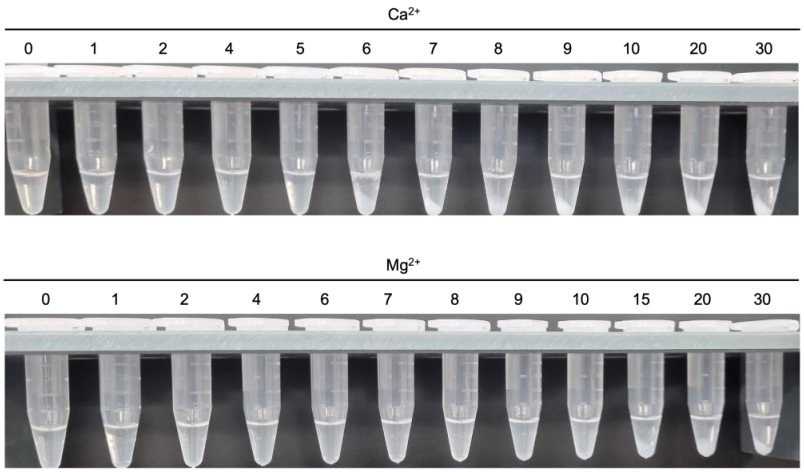

Fig. S6 Visual appearance of mPEG$_4$-DIBMA/DMPC nanodiscs at m_P/m_L of 4 in response to increasing concentration of Mg^{2+} or Ca^{2+}.

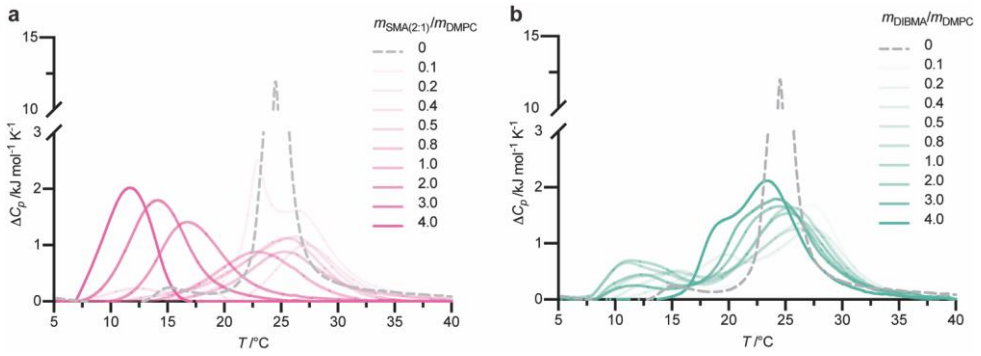

Fig. S7 DSC thermograms of polymer-encapsulated DMPC nanodiscs. DSC thermograms displaying excess molar isobaric heat capacities (ΔC_P) of SMA(2:1)/DMPC (a) and DIBMA/DMPC (b) at indicated polymer/DMPC mass ratios, m_P/m_L.

Materials. All starting materials were purchased from TCI (Eschborn, Germany), Fisher Scientific (Schwerte, Austria), Th. Geyer (Renningen, Germany), and Sigma–Aldrich (Darmstadt, Germany) and were used as received. The general synthetic procedure for preparing mPEG$_4$-amine [556–558] is shown below:

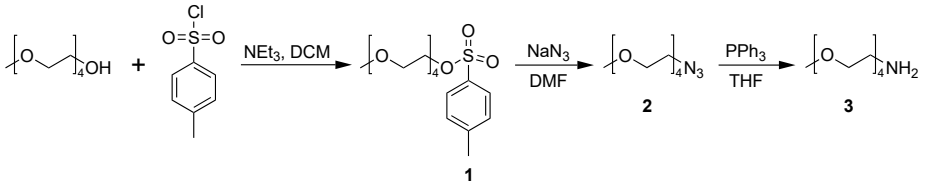

2,5,8,11-Tetraoxatridecan-13-yl 4-methylbenzenesulfonate (**1**)

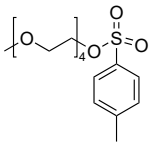

A solution of tetraethylene glycol monomethyl ether (9.15 g, 48 mmol, 1 eq.) in DCM (50 mL) was added dropwise over 30 min to a solution of *p*-toluenesulfonyl chloride (9.16 g, 48 mmol, 1 eq.) suspended in DCM (50 mL) while stirring at room temperature. Triethylamine (13.4 mL, 0.096 mmol, 2 eq.) was then added dropwise over 10 min and the reaction mixture was stirred at room temperature for 22 h. The solvent was evaporated under reduced pressure and the residue was diluted in DCM (70 mL) and washed with NaOH (1 M, 3 × 70 mL), followed by water (3 × 70 mL). The organic phase was dried over $MgSO_4$, filtered, and concentrated under reduced pressure. The resulting oil was purified by gravity column chromatography using ethyl acetate as eluent. The product was obtained as a yellowish oil in 73% yield. The identity of the resulting product was confirmed by NMR and attenuated total reflection infrared (ATR-IR) spectroscopy: ^{1}H-NMR (300 MHz, $CDCl_3$, 25°C): δ (ppm) = 2.39 (s, 3H, Ar–C*H*$_3$), 3.32 (s, 3 H, –OC*H*$_3$), 3.45–3.66 (m, 14 H, 3(–O–C*H*$_2$C*H*$_2$–O–), –OC*H*$_2$–), 4.10 (t, 2H, Ts–CH$_2$–, $^3J_{H–H}$ = 4.89 Hz), 7.29 (d, 2H, Ar–H, $^3J_{H–H}$ = 8.01 Hz), 7.74 (d, 2H, Ar–H, $^3J_{H–H}$ = 8.32 Hz); ^{13}C-NMR (75 MHz, $CDCl_3$, 25°C): δ (ppm) = 144.9, 133.1, 129.9, 128.1, 72.0, 70.8, 70.7, 70.6, 70.6, 70.6, 69.4, 68.8,

59.1, 21.7; ATR-IR[2,3] (cm^{-1}): 2874 (C–H str, aliphatic), 1452 (C=C str, aromatic), 1353 (S=O str, asym), 1189 (S=O str, sym), 1175 (C–C str, aliphatic), 1096 (C–O–C str).

13-Azido-2,5,8,11-tetraoxatridecane (**2**)

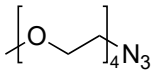

To a suspension of sodium azide (1.54 g, 23.4 mmol, 1.5 eq.) in DMF (40 mL), a solution of **1** (5.66 g, 15.6 mmol, 1.0 eq.) in DMF (25 mL) was added dropwise over 50 min and the reaction mixture was stirred at room temperature for 22 h. The mixture was diluted with water (130 mL) and washed with DCM (7 × 100 mL). The organic fractions were collected and washed further with water (2 × 100 mL), dried over $MgSO_4$, filtered, and concentrated under reduced pressure. DMF was removed by repeated distillation of the solution with toluene. The residue was purified by gravity column chromatography using 2:1 hexane/EtOAc as eluent. The product was obtained as a colorless oil in 86% yield. The identity of the resulting product was confirmed by NMR and attenuated total reflection infrared (ATR-IR) spectroscopy: ^{1}H-NMR (300 MHz, $CDCl_3$, 25°C): δ (ppm) = 3.27–3.41 (m, 5H, –OC*H*$_3$, –OCH$_2$–C*H*$_2$–N$_3$), 3.48–3.55 (m, 2H, –OC*H*$_2$–CH$_2$–N$_3$, 3.57–3.68 (m, 12H, 3 × –OC*H*$_2$–C*H*$_2$O–); ^{13}C-NMR (75 MHz, $CDCl_3$, 25°C): δ (ppm) = 72.1, 70.8, 70.8, 70.8, 70.8, 70.7, 70.2, 59.2, 50.8; ATR-IR[2,3] (cm^{-1}): 2870 (C–H str, aliphatic), 2098 (C–N$_3$), 1101 (C–O–C str).

2,5,8,11-Tetraoxatridecan-13-amine (**3**)

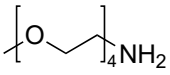

To a solution of **2** (3.0 g, 12.9 mmol, 1.0 eq.) in anhydrous THF (25 mL), triphenylphosphine (4.22 g, 16.1 mmol, 1.25 eq.) in anhydrous THF (15 mL) was added dropwise over 15 min under nitrogen atmosphere and the reaction mixture was stirred at room temperature for 5 h. Distilled water (20 mL) was then added and the solution was refluxed for 22 h. The solution was concentrated under reduced pressure and the residue was purified by gravity column chromatography using 9:1 DCM/MeOH (+1% Et_3N). The product was obtained as a yellowish oil in 97% yield. The identity of the resulting product was confirmed by NMR and attenuated total reflection infrared (ATR-IR) spectroscopy: ^{1}H-NMR (300 MHz, $CDCl_3$, 25°C): δ (ppm) = 2.82 (t, 2H, $^3J_{H–H}$ = 5.21 Hz, –CH$_2$–C*H*$_2$–NH$_2$), 3.33 (s, 3H, –OC*H*$_3$), 3.43–3.54 (m, 4H, –OCH$_2$–C*H*$_2$O–, –C*H*$_2$–CH$_2$–NH$_2$), 3.54–3.68 (m, 10H, 2× –OC*H*$_2$–C*H*$_2$O, –OC*H*$_2$–CH$_2$O–); ^{13}C-NMR (75 MHz, $CDCl_3$, 25°C): δ (ppm) = 73.3, 72.1, 70.7, 70.7 (2×), 70.6, 70.4, 59.2, 41.8; ATR-IR[2,3] (cm^{-1}): 3372 (N–H str), 2866 (C–H str, aliphatic), 1100 (C–O–C str).

Acknowledgments

I sincerely thank all the people who have shared his/her inspiring ideas, expertise, and guidance for this thesis. In particular:

Doctorate supervisor Dr. Manuel Etzkorn (Heinrich Heine University Düsseldorf) for giving me the opportunity to work in his lab, and for his fruitful supervision, discussions, and advice throughout the years.

Prof. Dr. Gunnar Schröder (Forschungszentrum Jülich) for agreeing to act as co-supervisor of this thesis, and for the fruitful discussions and advice with respect to the transmission electron microscopy data with the assistance of Simon Sommerhage (Forschungszentrum Jülich).

The collaboration partners Prof. Dr. Sandro Keller (University of Graz) for giving me the opportunity to visit his lab and perform the ζ-potential measurements with the assistance of Sarah Tutz (University of Graz) and providing the polymers used in this thesis synthesized by Dr. Carolyn Vargas (University of Graz), for their warm hospitality during my visit, and also for their fruitful discussions and advice throughout the years.

Prof. Dr. Georg Groth (Heinrich Heine University Düsseldorf) for granting access to perform the dynamic light scattering and microscale thermophoresis measurements in his lab.

Prof. Dr. Reza Ahmadian (Heinrich Heine University Düsseldorf) for providing the insect cells and opportunity to culture the cells in his lab.

Prof. Dr. Raymond C. Stevens (iHuman Institute at ShanghaiTech University) for providing us with the plasmids encoding the thermostabilized melanocortin 4 receptors.

Prof. Dr. Bernard Mouillac (University of montpellier) for providing us with the plasmids encoding human G protein subunits β_1 and γ_2.

Dr. Mohanraj Gopalswamy for his scientific and personal help throughout the years, and Dr. Marcel Falke, Dr. Sabine Schriek, Dr. Jan Borggräfe, Dr. Julian Victor, Dr. Fatima Escobedo and Dr. Tao Zhang for their support and discussions.

My friends (Qing-hai Tan, Long-long Liu, Guo Li, Zhong Huang, Cai-quan Huang, Ze-ju Shi, Yun-long Zhu, Xiao-hui Xiong, Ya-guang Wang, and Qi-rui Ma), especially my parents (Gen-chao Chu and Gui-lan Lin) and my brother (Xiao-guang Chu) for their tireless and continuous support.

Bibliography

[1] K. Sriram, P.A. Insel, G protein-coupled receptors as targets for approved drugs: How many targets and how many drugs?, Molecular Pharmacology, 93 (2018) 251–258.

[2] A.S. Hauser, S. Chavali, I. Masuho, L.J. Jahn, K.A. Martemyanov, D.E. Gloriam, M.M. Babu, Pharmacogenomics of GPCR Drug Targets, Cell, 172 (2018) 41-54.e19.

[3] X. Zhang, S. Dong, F. Xu, Structural and Druggability Landscape of Frizzled G Protein-Coupled Receptors, Trends in Biochemical Sciences, 43 (2018) 1033–1046.

[4] R.G. MacKenzie, Obesity-associated mutations in the human melanocortin-4 receptor gene, Peptides, 27 (2006) 395–403.

[5] J. Zhao, Y. Deng, Z. Jiang, H. Qing, G protein-coupled receptors (GPCRs) in Alzheimer's disease: A focus on BACE1 related GPCRs, Frontiers in Aging Neuroscience, 8 (2016) 1–15.

[6] D. Hilger, M. Masureel, B.K. Kobilka, Structure and dynamics of GPCR signaling complexes, Nature Structural and Molecular Biology, 25 (2018) 4–12.

[7] R.T. Dorsam, J.S. Gutkind, G-protein-coupled receptors and cancer, Nat Rev Cancer, 7 (2007) 79–94.

[8] V. Cherezov, D.M. Rosenbaum, M.A. Hanson, S.G.F. Rasmussen, S.T. Foon, T.S. Kobilka, H.J. Choi, P. Kuhn, W.I. Weis, B.K. Kobilka, R.C. Stevens, High-resolution crystal structure of an engineered human β2-adrenergic G protein-coupled receptor, Science, 318 (2007) 1258–1265.

[9] S.G.F. Rasmussen, H.J. Choi, D.M. Rosenbaum, T.S. Kobilka, F.S. Thian, P.C. Edwards, M. Burghammer, V.R.P. Ratnala, R. Sanishvili, R.F. Fischetti, G.F.X. Schertler, W.I. Weis, B.K. Kobilka, Crystal structure of the human β2 adrenergic G-protein-coupled receptor, Nature, 450 (2007) 383–387.

[10] D.M. Rosenbaum, V. Cherezov, M.A. Hanson, S.G.F. Rasmussen, S.T. Foon, T.S. Kobilka, H.J. Choi, X.J. Yao, W.I. Weis, R.C. Stevens, B.K. Kobilka, GPCR engineering yields high-resolution structural insights into β2-adrenergic receptor function, Science, 318 (2007) 1266–1273.

[11] J. Van Durme, F. Horn, S. Costagliola, G. Vriend, G. Vassart, GRIS: Glycoprotein-hormone receptor information system, Molecular Endocrinology, 20 (2006) 2247–2255.

[12] Q.R. Fan, W.A. Hendrickson, Structure of human follicle-stimulating hormone in complex with its receptor, Nature, 84 (2005) 1254.

[13] A. Brüser, A. Schulz, S. Rothemund, A. Ricken, D. Calebiro, G. Kleinau, T. Schöneberg, The activation mechanism of glycoprotein hormone receptors with implications in the cause and therapy of endocrine diseases, Journal of Biological Chemistry, 291 (2016) 508–520.

[14] J.A. Ballesteros, H. Weinstein, Integrated methods for the construction of three-dimensional models and computational probing of structure-function relations in G protein-coupled receptors, Methods in Neurosciences, 25 (1995) 366–428.

[15] R. Nygaard, T.M. Frimurer, B. Holst, M.M. Rosenkilde, T.W. Schwartz, Ligand binding and micro-switches in 7TM receptor structures, Trends in Pharmacological Sciences, 30 (2009) 249–259.

[16] S. Filipek, Molecular switches in GPCRs, Current Opinion in Structural Biology, 55 (2019) 114–120.

[17] A.S. Hauser, M.M. Attwood, M. Rask-Andersen, H.B. Schiöth, D.E. Gloriam, Trends in GPCR drug discovery: New agents, targets and indications, Nature Reviews Drug Discovery, 16 (2017) 829–842.

[18] D. Yang, Q. Zhou, V. Labroska, S. Qin, S. Darbalaei, Y. Wu, E. Yuliantie, L. Xie, H. Tao, J. Cheng, Q. Liu, S. Zhao, W. Shui, Y. Jiang, M.W. Wang, G protein-coupled receptors: structure- and function-based drug discovery, Signal Transduction and Targeted Therapy, 6 (2021).

[19] C. de Graaf, G. Song, C. Cao, Q. Zhao, M.W. Wang, B. Wu, R.C. Stevens, Extending the Structural View of Class B GPCRs, Trends in Biochemical Sciences, 42 (2017) 946–960.

[20] A. Andersen, A. Lund, F.K. Knop, T. Vilsbøll, Glucagon-like peptide 1 in health and disease, Nature Reviews Endocrinology, 14 (2018) 390–403.

[21] A. Jazayeri, M. Rappas, A.J.H. Brown, J. Kean, J.C. Errey, N.J. Robertson, C. Fiez-Vandal, S.P. Andrews, M. Congreve, A. Bortolato, J.S. Mason, A.H. Baig, I. Teobald, A.S. Doré, M. Weir, R.M. Cooke, F.H. Marshall, Crystal structure of the GLP-1 receptor bound to a peptide agonist, Nature, 546 (2017) 254–258.

[22] Y. Zhang, B. Sun, D. Feng, H. Hu, M. Chu, Q. Qu, J.T. Tarrasch, S. Li, T. Sun Kobilka, B.K. Kobilka, G. Skiniotis, Cryo-EM structure of the activated GLP-1 receptor in complex with a G protein, Nature, 546 (2017) 248–253.

[23] F. Wu, L. Yang, K. Hang, M. Laursen, L. Wu, G.W. Han, Q. Ren, N.K. Roed, G. Lin, M.A. Hanson, H. Jiang, M.W. Wang, S. Reedtz-Runge, G. Song, R.C. Stevens, Full-length human GLP-1 receptor structure without orthosteric ligands, Nature Communications, 11 (2020) 1–10.

[24] J. Hamann, G. Aust, D. Araç, F.B. Engel, C. Formstone, R. Fredriksson, R.A. Hall, B.L. Harty, C. Kirchhoff, B. Knapp, A. Krishnan, I. Liebscher, H.H. Lin, D.C. Martinelli, K.R. Monk, M.C. Peeters, X. Piao, S. Prömel, T. Schöneberg, T.W. Schwartz, et al., International union of basic and clinical pharmacology XCIV adhesion G protein-coupled receptors, Pharmacological Reviews, 67 (2015) 338–367.

[25] R.H. Purcell, R.A. Hall, Adhesion G Protein-Coupled Receptors as Drug Targets, Annual Review of Pharmacology and Toxicology, 58 (2018) 429–449.

[26] D. Araç, A.A. Boucard, M.F. Bolliger, J. Nguyen, S.M. Soltis, T.C. Südhof, A.T. Brunger, A novel evolutionarily conserved domain of cell-adhesion GPCRs mediates autoproteolysis, EMBO Journal, 31 (2012) 1364–1378.

[27] T.K. Bjarnadóttir, R. Fredriksson, P.J. Höglund, D.E. Gloriam, M.C. Lagerström, H.B. Schiöth, The human and mouse repertoire of the adhesion family of G-protein-coupled receptors, Genomics, 84 (2004) 23–33.

[28] H.M. Stoveken, A.G. Hajduczok, L. Xu, G.G. Tall, Adhesion G protein-coupled receptors are activated by exposure of a cryptic tethered agonist, Proceedings of the National Academy of Sciences of the United States of America, 112 (2015) 6194–6199.

[29] F. Bassilana, M. Nash, M.G. Ludwig, Adhesion G protein-coupled receptors: opportunities for drug discovery, Nature Reviews Drug Discovery, 18 (2019) 869–884.

[30] A.D. Bondarev, M.M. Attwood, J. Jonsson, V.N. Chubarev, V. V. Tarasov, H.B. Schiöth, Opportunities and challenges for drug discovery in modulating Adhesion G protein-coupled receptor (GPCR) functions, Expert Opinion on Drug Discovery, 15 (2020) 1291–1307.

[31] F.M. Hannan, Europe PMC Funders Group Calcium-sensing receptor in physiology and in calcitropic and non-calcitropic diseases Europe PMC Funders Author Manuscripts, Nat Rev Endocrinol, 15 (2019) 33–51.

[32] R. Thakker, Calcium-sensing receptor: Role in health and disease, Indian Journal of Endocrinology and Metabolism, 16 (2012) 213.

[33] N. Nuemket, N. Yasui, Y. Kusakabe, Y. Nomura, N. Atsumi, S. Akiyama, E. Nango, Y. Kato, M.K. Kaneko, J. Takagi, M. Hosotani, A. Yamashita, Structural basis for perception of diverse chemical substances by T1r taste receptors, Nature Communications, 8 (2017) 1–10.

[34] M. Kochem, Type 1 Taste Receptors in Taste and Metabolism, Annals of Nutrition and Metabolism, 70 (2017) 27–36.

[35] C.F. Heaney, J.W. Kinney, Role of GABAB receptors in learning and memory and neurological disorders, Neuroscience and Biobehavioral Reviews, 63 (2016) 1–28.

[36] B.M.T. Erunuma, Diversity of structure and function of GABA B receptors : a complexity of GABA B - mediated signaling, 94 (2018) 390–411.

[37] C.M. Niswender, P.J. Conn, Metabotropic glutamate receptors: Physiology, pharmacology, and disease, Annual Review of Pharmacology and Toxicology, 50 (2010) 295–322.

[38] C. Clemmensen, S. Smajilovic, P. Wellendorph, H. Bräuner-Osborne, The GPCR, class C, group 6, subtype A (GPRC6A) receptor: From cloning to physiological function, British Journal of Pharmacology, 171 (2014) 1129–1141.

[39] N. Kunishima, Y. Shimada, Y. Tsuji, T. Sato, M. Yamamoto, T. Kumasaka, S. Nakanishi, H. Jingami, K. Morikawa, Structural basis of glutamate recognition by a dimeric metabotropic glutamate receptor, Nature, 407 (2000) 971–977.

[40] T.C. Møller, D. Moreno-Delgado, J.-P. Pin, J. Kniazeff, Class C G protein-coupled receptors: reviving old couples with new partners, Biophysics Reports, 3 (2017) 57–63.

[41] C. Romano, W.L. Yang, K.L. O'Malley, Metabotropic glutamate receptor 5 is a disulfide-linked dimer, Journal of Biological Chemistry, 271 (1996) 28612–28616.

[42] K. Ray, B.C. Hauschild, P.J. Steinbach, P.K. Goldsmith, O. Hauache, A.M. Spiegel, Identification of the cysteine residues in the amino-terminal extracellular domain of the human Ca2+ receptor critical for dimerization Implications for function of monomeric Ca2+ receptor, Journal of Biological Chemistry, 274 (1999) 27642–27650.

[43] K. Ray, B.C. Hauschild, Cys-140 is critical for metabotropic glutamate receptor-1 dimerization, Journal of Biological Chemistry, 275 (2000) 34245–34251.

[44] L. Nørskov-Lauritsen, S. Jørgensen, H. Bräuner-Osborne, N-glycosylation and disulfide bonding affects GPRC6A receptor expression, function, and dimerization, FEBS Letters, 589 (2015) 588–597.

[45] Y. Tsuji, Y. Shimada, T. Takeshita, N. Kajimura, S. Nomura, N. Sekiyama, J. Otomo, J. Usukura, S. Nakanishi, H. Jingami, Cryptic dimer interface and domain organization of the extracellular region of metabotropic glutamate receptor subtype 1, Journal of Biological Chemistry, 275 (2000) 28144–28151.

[46] A. Koehl, H. Hu, D. Feng, B. Sun, Y. Zhang, M.J. Robertson, M. Chu, T.S. Kobilka, T. Laermans, J. Steyaert, J. Tarrasch, S. Dutta, R. Fonseca, W.I. Weis, J.M. Mathiesen, G. Skiniotis, B.K. Kobilka, GABAB receptors – the first 7TM heterodimers, Nature, 566 (2019) 79–84.

[47] C. Romano, J.K. Miller, K. Hyrc, S. Dikranian, S. Mennerick, Y. Takeuchi, M.P. Goldberg, K.L. O'Malley, Covalent and noncovalent interactions mediate metabotropic glutamate receptor mGlu5 dimerization, Molecular Pharmacology, 59 (2001) 46–53.

[48] J. Levitz, C. Habrian, S. Bharill, Z. Fu, R. Vafabakhsh, E.Y. Isacoff, Mechanism of Assembly and Cooperativity of Homomeric and Heteromeric Metabotropic Glutamate Receptors, Neuron, 92 (2016) 143–159.

[49] H. Brauner-Osborne, P. Wellendorph, A. Jensen, Structure, Pharmacology and Therapeutic Prospects of Family C G-Protein Coupled Receptors, Current Drug Targets, 8 (2006) 169–184.

[50] E. Doumazane, P. Scholler, J.M. Zwier, E. Trinquet, P. Rondard, J. Pin, A new approach to analyze cell surface protein complexes reveals specific heterodimeric metabotropic glutamate receptors, The FASEB Journal, 25 (2011) 66–77.

[51] M. Gassmann, B. Bettler, Regulation of neuronal GABAB receptor functions by subunit composition, Nature Reviews Neuroscience, 13 (2012) 380–394.

[52] F.H. Marshall, K.A. Jones, K. Kaupmann, B. Bettler, GABA(B) receptors - The first 7TM heterodimers, Trends in Pharmacological Sciences, 20 (1999) 396–399.

[53] M.M. Papasergi-Scott, M.J. Robertson, A.B. Seven, O. Panova, J.M. Mathiesen, G. Skiniotis, Structures of metabotropic GABAB receptor, Nature, 584 (2020) 310–314.

[54] J.P. Pin, J. Kniazeff, J. Liu, V. Binet, C. Goudet, P. Rondard, L. Prézeau, Allosteric functioning of dimeric class C G-protein-coupled receptors, FEBS Journal, 272 (2005) 2947–2955.

[55] R. Vafabakhsh, J. Levitz, E.Y. Isacoff, Conformational dynamics of a class C G-protein-coupled receptor, Nature, 524 (2015) 497–501.

[56] J.P. Pin, B. Bettler, Organization and functions of mGlu and GABA B receptor complexes, Nature, 540 (2016) 60–68.

[57] A. Ellaithy, J. Gonzalez-Maeso, D.A. Logothetis, J. Levitz, Structural and Biophysical Mechanisms of Class C G Protein-Coupled Receptor Function, Trends in Biochemical Sciences, 45 (2020) 1049–1064.

[58] G. Schulte, International Union of Basic and Clinical, Pharmacological Reviews, 62 (2010) 632–667.

[59] Y. Wang, H. Chang, A. Rattner, J. Nathans, Frizzled Receptors in Development and Disease, Elsevier Inc., 2016.

[60] C.M. Zeng, Z. Chen, L. Fu, Frizzled receptors as potential therapeutic targets in human cancers, International Journal of Molecular Sciences, 19 (2018).

[61] K. Alhosaini, A. Azhar, A. Alonazi, F. Al-Zoghaibi, GPCRs: The most promiscuous druggable receptor of the mankind, Saudi Pharmaceutical Journal, 29 (2021) 539–551.

[62] G. Schulte, S.C. Wright, Frizzleds as GPCRs – More Conventional Than We Thought!, Trends in Pharmacological Sciences, 39 (2018) 828–842.

[63] R.R. Neubig, M. Spedding, T. Kenakin, A. Christopoulos, International Union of Pharmacology Committee on Receptor Nomenclature and Drug Classification, International Union of Pharmacology Committee on Receptor Nomenclature and Drug Classification XXXVIII Update on terms and symbols in quantitative pharmacology, Pharmacol Rev, 55 (2003) 597–606.

[64] R. Nussinov, C.-J. Tsai, The different ways through which specificity works in orthosteric and allosteric drugs, Curr Pharm Des, 18 (2012) 1311–1316.

[65] S. Basith, M. Cui, S.J.Y. Macalino, J. Park, N.A.B. Clavio, S. Kang, S. Choi, Exploring G Protein-Coupled Receptors (GPCRs) Ligand Space via Cheminformatics Approaches: Impact on Rational Drug Design, Frontiers in Pharmacology, 9 (2018).

[66] Y. Zhang, F. Yang, S. Ling, P. Lv, Y. Zhou, W. Fang, W. Sun, L. Zhang, P. Shi, C. Tian, Single-particle cryo-EM structural studies of the β2AR–Gs complex bound with a full agonist formoterol, Cell Discov, 6 (2020) 1–5.

[67] A. Koehl, H. Hu, D. Feng, B. Sun, Y. Zhang, M.J. Robertson, M. Chu, T.S. Kobilka, T. Laeremans, J. Steyaert, J. Tarrasch, S. Dutta, R. Fonseca, W.I. Weis, J.M. Mathiesen, G. Skiniotis, B.K. Kobilka, Structural insights into the activation of metabotropic glutamate receptors, Nature, 566 (2019) 79–84.

[68] X. Zhang, F. Zhao, Y. Wu, J. Yang, G.W. Han, S. Zhao, A. Ishchenko, L. Ye, X. Lin, K. Ding, V. Dharmarajan, P.R. Griffin, C. Gati, G. Nelson, M.S. Hunter, M.A. Hanson, V. Cherezov, R.C. Stevens, W. Tan, H. Tao, et al., Crystal structure of a multi-domain human smoothened receptor in complex with a super stabilizing ligand, Nat Commun, 8 (2017) 15383.

[69] J. Wess, R.M. Eglen, D. Gautam, Muscarinic acetylcholine receptors: mutant mice provide new insights for drug development, Nat Rev Drug Discov, 6 (2007) 721–733.

[70] C.C. Felder, P.J. Goldsmith, K. Jackson, H.E. Sanger, D.A. Evans, A.J. Mogg, L.M. Broad, Current status of muscarinic M1 and M4 receptors as drug targets for neurodegenerative diseases, Neuropharmacology, 136 (2018) 449–458.

[71] A. Christopoulos, Allosteric binding sites on cell-surface receptors: novel targets for drug discovery, Nat Rev Drug Discov, 1 (2002) 198–210.

[72] L.T. May, K. Leach, P.M. Sexton, A. Christopoulos, Allosteric Modulation of G Protein–Coupled Receptors, Annu. Rev. Pharmacol. Toxicol., 47 (2007) 1–51.

[73] K. Leach, P.M. Sexton, A. Christopoulos, Allosteric GPCR modulators: taking advantage of permissive receptor pharmacology, Trends in Pharmacological Sciences, 28 (2007) 382–389.

[74] P. Jeffrey Conn, A. Christopoulos, C.W. Lindsley, Allosteric modulators of GPCRs: a novel approach for the treatment of CNS disorders, Nat Rev Drug Discov, 8 (2009) 41–54.

[75] T. Kenakin, L.J. Miller, Seven Transmembrane Receptors as Shapeshifting Proteins: The Impact of Allosteric Modulation and Functional Selectivity on New Drug Discovery, Pharmacol Rev, 62 (2010) 265–304.

[76] D.J. Foster, P.J. Conn, Allosteric Modulation of GPCRs: New Insights and Potential Utility for Treatment of Schizophrenia and Other CNS Disorders, Neuron, 94 (2017) 431–446.

[77] T.W. Schwartz, B. Holst, Ago-allosteric modulation and other types of allostery in dimeric 7TM receptors, J Recept Signal Transduct Res, 26 (2006) 107–128.

[78] T.W. Schwartz, B. Holst, Allosteric enhancers, allosteric agonists and ago-allosteric modulators: where do they bind and how do they act?, Trends in Pharmacological Sciences, 28 (2007) 366–373.

[79] Z. Cong, L.-N. Chen, H. Ma, Q. Zhou, X. Zou, C. Ye, A. Dai, Q. Liu, W. Huang, X. Sun, X. Wang, P. Xu, L. Zhao, T. Xia, W. Zhong, D. Yang, H. Eric Xu, Y. Zhang, M.-W. Wang, Molecular insights into ago-allosteric modulation of the human glucagon-like peptide-1 receptor, Nat Commun, 12 (2021) 3763.

[80] D. Wootten, A. Christopoulos, P.M. Sexton, Emerging paradigms in GPCR allostery: implications for drug discovery, Nat Rev Drug Discov, 12 (2013) 630–644.

[81] D.W. Engers, C.W. Lindsley, Allosteric modulation of Class C GPCRs: a novel approach for the treatment of CNS disorders, Drug Discovery Today: Technologies, 10 (2013) e269–e276.

[82] D.J. Luessen, P.J. Conn, Allosteric Modulators of Metabotropic Glutamate Receptors as Novel Therapeutics for Neuropsychiatric Disease, Pharmacol Rev, 74 (2022) 630–661.

[83] Z. Huang, L. Zhu, Y. Cao, G. Wu, X. Liu, Y. Chen, Q. Wang, T. Shi, Y. Zhao, Y. Wang, W. Li, Y. Li, H. Chen, G. Chen, J. Zhang, ASD: a comprehensive database of allosteric proteins and modulators, Nucleic Acids Res, 39 (2011) D663–D669.

[84] X. Liu, S. Lu, K. Song, Q. Shen, D. Ni, Q. Li, X. He, H. Zhang, Q. Wang, Y. Chen, X. Li, J. Wu, C. Sheng, G. Chen, Y. Liu, X. Lu, J. Zhang, Unraveling allosteric landscapes of allosterome with ASD, Nucleic Acids Research, (2019) gkz958.

[85] N. Nagano, Pharmacological and clinical properties of calcimimetics: Calcium receptor activators that afford an innovative approach to controlling hyperparathyroidism, Pharmacology & Therapeutics, 109 (2006) 339–365.

[86] C. Vahe, K. Benomar, S. Espiard, L. Coppin, A. Jannin, M.F. Odou, M.C. Vantyghem, Diseases associated with calcium-sensing receptor, Orphanet J Rare Dis, 12 (2017) 19.

[87] P. Harrington, C. Fotsch, Calcium Sensing Receptor Activators: Calcimimetics, CMC, 14 (2007) 3027–3034.

[88] Z. Saidak, M. Brazier, S. Kamel, R. Mentaverri, Agonists and Allosteric Modulators of the Calcium-Sensing Receptor and Their Therapeutic Applications, Mol Pharmacol, 76 (2009) 1131–1144.

[89] E.F. Nemeth, M.E. Steffey, L.G. Hammerland, B.C.P. Hung, B.C. Van Wagenen, E.G. DelMar, M.F. Balandrin, Calcimimetics with potent and selective activity on the parathyroid calcium receptor, Proc. Natl. Acad. Sci. U.S.A., 95 (1998) 4040–4045.

[90] G.A. Block, K.J. Martin, A.L.M. de Francisco, S.A. Turner, M.M. Avram, M.G. Suranyi, G. Hercz, J. Cunningham, A.K. Abu-Alfa, P. Messa, D.W. Coyne, F. Locatelli, R.M. Cohen, P. Evenepoel, S.M. Moe, A. Fournier, J. Braun, L.C. McCary, V.J. Zani, K.A. Olson, et al., Cinacalcet for Secondary Hyperparathyroidism in Patients Receiving Hemodialysis, N Engl J Med, 350 (2004) 1516–1525.

[91] J.S. Lindberg, B. Culleton, G. Wong, M.F. Borah, R.V. Clark, W.B. Shapiro, S.D. Roger, F.E. Husserl, P.S. Klassen, M.D. Guo, M.B. Albizem, J.W. Coburn, Cinacalcet HCl, an Oral Calcimimetic Agent for the Treatment of Secondary Hyperparathyroidism in Hemodialysis and Peritoneal Dialysis: A Randomized, Double-Blind, Multicenter Study, Journal of the American Society of Nephrology, 16 (2005) 800–807.

[92] G. Poon, Cinacalcet Hydrochloride (Sensipar), Baylor University Medical Center Proceedings, 18 (2005) 181–184.

[93] D.A. Bushinsky, G.M. Chertow, S. Cheng, H. Deng, N. Kopyt, K.J. Martin, A. Rastogi, P. Urena-Torres, M. Vervloet, G.A. Block, One-year safety and efficacy of intravenous etelcalcetide in patients on hemodialysis with secondary hyperparathyroidism, (n.d.).

[94] T. Kawata, S. Tokunaga, M. Murai, N. Masuda, W. Haruyama, Y. Shoukei, Y. Hisada, T. Yanagida, H. Miyazaki, M. Wada, T. Akizawa, M. Fukagawa, A novel calcimimetic agent, evocalcet (MT-4580/KHK7580), suppresses the parathyroid cell function with little effect on the gastrointestinal tract or CYP isozymes in vivo and in vitro, PLoS One, 13 (2018) e0195316.

[95] H. Miyazaki, Y. Ikeda, O. Sakurai, T. Miyake, R. Tsubota, J. Okabe, M. Kuroda, Y. Hisada, T. Yanagida, H. Yoneda, Y. Tsukumo, S. Tokunaga, T. Kawata, R. Ohashi, H. Fukuda, K. Kojima, A. Kannami, T. Kifuji, N. Sato, A. Idei, et al., Discovery of evocalcet, a next-generation calcium-sensing receptor agonist for the treatment of hyperparathyroidism, Bioorg Med Chem Lett, 28 (2018) 2055–2060.

[96] T. Akizawa, K. Ikejiri, Y. Kondo, Y. Endo, M. Fukagawa, Evocalcet: A New Oral Calcimimetic for Dialysis Patients With Secondary Hyperparathyroidism, Ther Apher Dial, 24 (2020) 248–257.

[97] Y. Gao, M.J. Robertson, S.N. Rahman, A.B. Seven, C. Zhang, J.G. Meyerowitz, O. Panova, F.M. Hannan, R.V. Thakker, H. Bräuner-Osborne, J.M. Mathiesen, G. Skiniotis, Asymmetric activation of the calcium-sensing receptor homodimer, Nature, 595 (2021) 455–459.

[98] A. Viola, A.D. Luster, Chemokines and Their Receptors: Drug Targets in Immunity and Inflammation, Annu. Rev. Pharmacol. Toxicol., 48 (2008) 171–197.

[99] P. Dorr, M. Westby, S. Dobbs, P. Griffin, B. Irvine, M. Macartney, J. Mori, G. Rickett, C. Smith-Burchnell, C. Napier, R. Webster, D. Armour, D. Price, B. Stammen, A. Wood, M. Perros, Maraviroc (UK-427,857), a Potent, Orally Bioavailable, and Selective Small-Molecule Inhibitor of Chemokine Receptor CCR5 with Broad-Spectrum Anti-Human Immunodeficiency Virus Type 1 Activity, Antimicrob Agents Chemother, 49 (2005) 4721–4732.

[100] W. Kromdijk, A.D. Huitema, J.W. Mulder, Treatment of HIV infection with the CCR5 antagonist maraviroc, Expert Opinion on Pharmacotherapy, 11 (2010) 1215–1223.

[101] C.M. Perry, Maraviroc: a review of its use in the management of CCR5-tropic HIV-1 infection, Drugs, 70 (2010) 1189–1213.

[102] Q. Tan, Y. Zhu, J. Li, Z. Chen, G.W. Han, I. Kufareva, T. Li, L. Ma, G. Fenalti, J. Li, W. Zhang, X. Xie, H. Yang, H. Jiang, V. Cherezov, H. Liu, R.C. Stevens, Q. Zhao, B. Wu, Structure of the CCR5 Chemokine Receptor–HIV Entry Inhibitor Maraviroc Complex, Science, 341 (2013) 1387–1390.

[103] H. Zhang, K. Chen, Q. Tan, Q. Shao, S. Han, C. Zhang, C. Yi, X. Chu, Y. Zhu, Y. Xu, Q. Zhao, B. Wu, Structural basis for chemokine recognition and receptor activation of chemokine receptor CCR5, Nat Commun, 12 (2021) 4151.

[104] D.L. Hay, A.A. Pioszak, RAMPs (Receptor-Activity Modifying Proteins): New Insights and Roles, Annu Rev Pharmacol Toxicol, 56 (2016) 469–487.

[105] A.A. Pioszak, D.L. Hay, RAMPs as allosteric modulators of the calcitonin and calcitonin-like class B G protein-coupled receptors, Adv Pharmacol, 88 (2020) 115–141.

[106] M.A. Hanson, V. Cherezov, M.T. Griffith, C.B. Roth, V.-P. Jaakola, E.Y.T. Chien, J. Velasquez, P. Kuhn, R.C. Stevens, A Specific Cholesterol Binding Site Is Established by the 28 Å Structure of the Human β2-Adrenergic Receptor, Structure, 16 (2008) 897–905.

[107] E.S. Levitt, M.J. Clark, P.M. Jenkins, J.R. Martens, J.R. Traynor, Differential Effect of Membrane Cholesterol Removal on μ- and δ-Opioid Receptors: A PARALLEL COMPARISON OF ACUTE AND CHRONIC SIGNALING TO ADENYLYL CYCLASE *, Journal of Biological Chemistry, 284 (2009) 22108–22122.

[108] M. Wang, Y. Yao, D. Kuang, D.R. Hampson, Activation of family C G-protein-coupled receptors by the tripeptide glutathione, J Biol Chem, 281 (2006) 8864–8870.

[109] G.K. Broadhead, H. Mun, V.A. Avlani, O. Jourdon, W.B. Church, A. Christopoulos, L. Delbridge, A.D. Conigrave, Allosteric modulation of the calcium-sensing receptor by gamma-glutamyl peptides: inhibition of PTH secretion, suppression of intracellular cAMP levels, and a common mechanism of action with L-amino acids, J Biol Chem, 286 (2011) 8786–8797.

[110] A.A. Kaczor, T.M. Wróbel, D. Bartuzi, Allosteric Modulators of Dopamine D2 Receptors for Fine-Tuning of Dopaminergic Neurotransmission in CNS Diseases: Overview, Pharmacology, Structural Aspects and Synthesis, Molecules, 28 (2022) 178.

[111] K.M. Olson, J.R. Traynor, A. Alt, Allosteric Modulator Leads Hiding in Plain Site: Developing Peptide and Peptidomimetics as GPCR Allosteric Modulators, Frontiers in Chemistry, 9 (2021).

[112] V. Petrucci, A. Chicca, S. Glasmacher, J. Paloczi, Z. Cao, P. Pacher, J. Gertsch, Pepcan-12 (RVD-hemopressin) is a CB2 receptor positive allosteric modulator constitutively secreted by adrenals and in liver upon tissue damage, Sci Rep, 7 (2017) 9560.

[113] K.E. Carlson, T.J. McMurry, S.W. Hunt, Pepducins: lipopeptide allosteric modulators of GPCR signaling, Drug Discovery Today: Technologies, 9 (2012) e33–e39.

[114] M.A. Skiba, A.C. Kruse, Autoantibodies as Endogenous Modulators of GPCR Signaling, Trends Pharmacol Sci, 42 (2021) 135–150.

[115] T. Hori, S. Yokoyama, Chapter 4 - Ions as GPCR allosteric modulators, in: R.B. Laprairie (Ed.), Allosteric Modulation of G Protein-Coupled Receptors, Academic Press, 2022: pp. 47–69.

[116] Allosteric coupling from G protein to the agonist-binding pocket in GPCRs | Nature, (n.d.).

[117] B. Zarzycka, S.A. Zaidi, B.L. Roth, V. Katritch, Harnessing Ion-Binding Sites for GPCR Pharmacology, Pharmacol Rev, 71 (2019) 571–595.

[118] W. Liu, E. Chun, A.A. Thompson, P. Chubukov, F. Xu, V. Katritch, G.W. Han, C.B. Roth, L.H. Heitman, A.P. IJzerman, V. Cherezov, R.C. Stevens, Structural Basis for Allosteric Regulation of GPCRs by Sodium Ions, Science, 337 (2012) 232–236.

[119] K.L. White, M.T. Eddy, Z.-G. Gao, G.W. Han, T. Lian, A. Deary, N. Patel, K.A. Jacobson, V. Katritch, R.C. Stevens, Structural Connection between Activation Microswitch and Allosteric Sodium Site in GPCR Signaling, Structure, 26 (2018) 259-269.e5.

[120] V. Katritch, G. Fenalti, E.E. Abola, B.L. Roth, V. Cherezov, R.C. Stevens, Allosteric sodium in class A GPCR signaling, Trends Biochem Sci, 39 (2014) 233–244.

[121] J.L. Miller-Gallacher, R. Nehmé, T. Warne, P.C. Edwards, G.F.X. Schertler, A.G.W. Leslie, C.G. Tate, The 21 Å Resolution Structure of Cyanopindolol-Bound β1-Adrenoceptor Identifies an Intramembrane Na+ Ion that Stabilises the Ligand-Free Receptor, PLOS ONE, 9 (2014) e92727.

[122] C. Zhang, Y. Srinivasan, D.H. Arlow, J.J. Fung, D. Palmer, Y. Zheng, H.F. Green, A. Pandey, R.O. Dror, D.E. Shaw, W.I. Weis, S.R. Coughlin, B.K. Kobilka, High-resolution crystal structure of human protease-activated receptor 1, Nature, 492 (2012) 387–392.

[123] G. Fenalti, P.M. Giguere, V. Katritch, X.-P. Huang, A.A. Thompson, V. Cherezov, B.L. Roth, R.C. Stevens, Molecular control of δ-opioid receptor signalling, Nature, 506 (2014) 191–196.

[124] F.M. Hannan, E. Kallay, W. Chang, M.L. Brandi, R.V. Thakker, Calcium-sensing receptor in physiology and in calcitropic and non-calcitropic diseases, Nat Rev Endocrinol, 15 (2018) 33–51.

[125] A.D. White, F. Fang, F.G. Jean-Alphonse, L.J. Clark, H.-J. An, H. Liu, Y. Zhao, S.L. Reynolds, S. Lee, K. Xiao, I. Sutkeviciute, J.-P. Vilardaga, Ca2+ allostery in PTH-receptor signaling, Proceedings of the National Academy of Sciences, 116 (2019) 3294–3299.

[126] B. Johansson, F.E. Parkinson, B.B. Fredholm, Effects of mono- and divalent ions on the binding of the adenosine analogue CGS 21680 to adenosine A2 receptors in rat striatum, Biochem Pharmacol, 44 (1992) 2365–2370.

[127] U. Burgmer, U. Schulz, C. Tränkle, K. Mohr, Interaction of Mg2+ with the allosteric site of muscarinic M2 receptors, Naunyn Schmiedebergs Arch Pharmacol, 357 (1998) 363–370.

[128] L. Ye, C. Neale, A. Sljoka, B. Lyda, D. Pichugin, N. Tsuchimura, S.T. Larda, R. Pomès, A.E. García, O.P. Ernst, R.K. Sunahara, R.S. Prosser, Mechanistic insights into allosteric regulation of the A2A adenosine G protein-coupled receptor by physiological cations, Nat Commun, 9 (2018) 1372.

[129] D.W. Christianson, Structural biology of zinc, Adv Protein Chem, 42 (1991) 281–355.

[130] C.E. Elling, K. Thirstrup, B. Holst, T.W. Schwartz, Conversion of agonist site to metal-ion chelator site in the β2-adrenergic receptor, Proceedings of the National Academy of Sciences, 96 (1999) 12322–12327.

[131] N.J. Pace, E. Weerapana, Zinc-Binding Cysteines: Diverse Functions and Structural Motifs, Biomolecules, 4 (2014) 419–434.

[132] T.A. Shuster, A.K. Nagy, D.C. Conly, D.B. Farber, Direct zinc binding to purified rhodopsin and disc membranes, Biochemical Journal, 282 (1992) 123–128.

[133] S.W. Tam, K.E. Wilber, F.W. Wagner, Light sensitive zinc content of protein fractions from bovine rod outer segments, Biochem Biophys Res Commun, 72 (1976) 302–309.

[134] A. Stojanovic, J. Stitham, J. Hwa, Critical Role of Transmembrane Segment Zinc Binding in the Structure and Function of Rhodopsin*♦, Journal of Biological Chemistry, 279 (2004) 35932–35941.

[135] G. Swaminath, J. Steenhuis, B. Kobilka, T.W. Lee, Allosteric modulation of beta2-adrenergic receptor by Zn(2+), Mol Pharmacol, 61 (2002) 65–72.

[136] G. Swaminath, T.W. Lee, B. Kobilka, Identification of an allosteric binding site for Zn2+ on the beta2 adrenergic receptor, J Biol Chem, 278 (2003) 352–356.

[137] L.O. Gerlach, J.S. Jakobsen, K.P. Jensen, M.R. Rosenkilde, R.T. Skerlj, U. Ryde, G.J. Bridger, T.W. Schwartz, Metal ion enhanced binding of AMD3100 to Asp262 in the CXCR4 receptor, Biochemistry, 42 (2003) 710–717.

[138] J.A. Schetz, D.R. Sibley, Zinc allosterically modulates antagonist binding to cloned D1 and D2 dopamine receptors, J Neurochem, 68 (1997) 1990–1997.

[139] J.A. Schetz, D.R. Sibley, The binding-site crevice of the D4 dopamine receptor is coupled to three distinct sites of allosteric modulation, J Pharmacol Exp Ther, 296 (2001) 359–363.

[140] Y. Liu, M.M. Teeter, C.J. DuRand, K.A. Neve, Identification of a Zn2+-binding site on the dopamine D2 receptor, Biochemical and Biophysical Research Communications, 339 (2006) 873–879.

[141] G. Satała, B. Duszyńska, K. Stachowicz, A. Rafalo, B. Pochwat, C. Luckhart, P.R. Albert, M. Daigle, K.F. Tanaka, R. Hen, T. Lenda, G. Nowak, A.J. Bojarski, B. Szewczyk, Concentration-Dependent Dual Mode of Zn Action at Serotonin 5-HT1A Receptors: In Vitro and In Vivo Studies, Mol Neurobiol, 53 (2016) 6869–6881.

[142] W. Jiang, S. Zheng, Structural insights into galanin receptor signaling, Proceedings of the National Academy of Sciences, 119 (2022) e2121465119.

[143] D.D. Markov, O.V. Dolotov, I.A. Grivennikov, The Melanocortin System: A Promising Target for the Development of New Antidepressant Drugs, International Journal of Molecular Sciences, 24 (2023) 6664.

[144] C. Girardet, A.A. Butler, Neural melanocortin receptors in obesity and related metabolic disorders, Biochimica et Biophysica Acta (BBA) - Molecular Basis of Disease, 1842 (2014) 482–494.

[145] B.L. Panaro, I.R. Tough, M.S. Engelstoft, R.T. Matthews, G.J. Digby, C.L. Møller, B. Svendsen, F. Gribble, F. Reimann, J.J. Holst, B. Holst, T.W. Schwartz, H.M. Cox, R.D. Cone, The Melanocortin-4 Receptor Is Expressed in Enteroendocrine L Cells and Regulates the Release of Peptide YY and Glucagon-like Peptide 1 In Vivo, Cell Metabolism, 20 (2014) 1018–1029.

[146] E.J.P. Anderson, I. Çakir, S.J. Carrington, R.D. Cone, M. Ghamari-Langroudi, T. Gillyard, L.E. Gimenez, M.J. Litt, 60 YEARS OF POMC: Regulation of feeding and energy homeostasis by α-MSH, Journal of Molecular Endocrinology, 56 (2016) T157–T174.

[147] M.J. Krashes, B.B. Lowell, A.S. Garfield, Melanocortin-4 receptor–regulated energy homeostasis, Nat Neurosci, 19 (2016) 206–219.

[148] L.A. Metherell, J.P. Chapple, S. Cooray, A. David, C. Becker, F. Rüschendorf, D. Naville, M. Begeot, B. Khoo, P. Nürnberg, A. Huebner, M.E. Cheetham, A.J.L. Clark, Mutations in MRAP, encoding a new interacting partner of the ACTH receptor, cause familial glucocorticoid deficiency type 2, Nat Genet, 37 (2005) 166–170.

[149] D.S. Jackson, S. Ramachandrappa, A.J. Clark, L.F. Chan, Melanocortin receptor accessory proteins in adrenal disease and obesity, Front. Neurosci., 9 (2015).

[150] A.A.J. Rouault, D.K. Srinivasan, T.C. Yin, A.A. Lee, J.A. Sebag, Melanocortin Receptor Accessory Proteins (MRAPs): Functions in the melanocortin system and beyond, Biochimica et Biophysica Acta (BBA) - Molecular Basis of Disease, 1863 (2017) 2462–2467.

[151] R. Branson, N. Potoczna, J.G. Kral, K.-U. Lentes, M.R. Hoehe, F.F. Horber, Binge Eating as a Major Phenotype of Melanocortin 4 Receptor Gene Mutations, N Engl J Med, 348 (2003) 1096–1103.

[152] K. Tan, I.D. Pogozheva, G.S.H. Yeo, D. Hadaschik, J.M. Keogh, C. Haskell-Leuvano, S. O'Rahilly, H.I. Mosberg, I.S. Farooqi, Functional Characterization and Structural Modeling of Obesity Associated Mutations in the Melanocortin 4 Receptor, Endocrinology, 150 (2009) 114–125.

[153] L.A. Lotta, J. Mokrosiński, E. Mendes de Oliveira, C. Li, S.J. Sharp, J. Luan, B. Brouwers, V. Ayinampudi, N. Bowker, N. Kerrison, V. Kaimakis, D. Hoult, I.D. Stewart, E. Wheeler, F.R. Day, J.R.B. Perry, C. Langenberg, N.J. Wareham, I.S. Farooqi, Human Gain-of-Function MC4R Variants Show Signaling Bias and Protect against Obesity, Cell, 177 (2019) 597-607.e9.

[154] L.H.T. Van der Ploeg, W.J. Martin, A.D. Howard, R.P. Nargund, C.P. Austin, X. Guan, J. Drisko, D. Cashen, I. Sebhat, A.A. Patchett, D.J. Figueroa, A.G. DiLella, B.M. Connolly, D.H. Weinberg, C.P. Tan, O.C. Palyha, S.-S. Pong, T. MacNeil, C. Rosenblum, A. Vongs, et al., A role for the melanocortin 4 receptor in sexual function, Proc. Natl. Acad. Sci. U.S.A., 99 (2002) 11381–11386.

[155] L.S. Tallam, A.A. da Silva, J.E. Hall, Melanocortin-4 Receptor Mediates Chronic Cardiovascular and Metabolic Actions of Leptin, Hypertension, 48 (2006) 58–64.

[156] J.R. Greenfield, Melanocortin Signalling and the Regulation of Blood Pressure in Human Obesity, Journal of Neuroendocrinology, 23 (2011) 186–193.

[157] A.A. da Silva, J.M. do Carmo, Z. Wang, J.E. Hall, Melanocortin-4 Receptors and Sympathetic Nervous System Activation in Hypertension, Curr Hypertens Rep, 21 (2019) 46.

[158] J.M. do Carmo, A.A. da Silva, Z. Wang, T. Fang, N. Aberdein, C.E. Perez de Lara, J.E. Hall, Role of the brain melanocortins in blood pressure regulation, Biochimica et Biophysica Acta (BBA) - Molecular Basis of Disease, 1863 (2017) 2508–2514.

[159] M.S. Thearle, Y.L. Muller, R.L. Hanson, M. Mullins, M. AbdusSamad, J. Tran, W.C. Knowler, C. Bogardus, J. Krakoff, L.J. Baier, Greater Impact of Melanocortin-4 Receptor Deficiency on Rates of Growth and Risk of Type 2 Diabetes During Childhood Compared With Adulthood in Pima Indians, Diabetes, 61 (2012) 250–257.

[160] M. Chrétien, M. Mbikay, 60 YEARS OF POMC: From the prohormone theory to pro-opiomelanocortin and to proprotein convertases (PCSK1 to PCSK9), Journal of Molecular Endocrinology, 56 (2016) T49–T62.

[161] R.D. Cone, Studies on the Physiological Functions of the Melanocortin System, Endocrine Reviews, 27 (2006) 736–749.

[162] T.K. Sawyer, P.J. Sanfilippo, V.J. Hruby, M.H. Engel, C.B. Heward, J.B. Burnett, M.E. Hadley, 4-Norleucine, 7-D-phenylalanine-alpha-melanocyte-stimulating hormone: a highly potent alpha-melanotropin with ultralong biological activity, Proc. Natl. Acad. Sci. U.S.A., 77 (1980) 5754–5758.

[163] J.G. Langendonk, M. Balwani, K.E. Anderson, H.L. Bonkovsky, A.V. Anstey, D.M. Bissell, J. Bloomer, C. Edwards, N.J. Neumann, C. Parker, J.D. Phillips, H.W. Lim, I. Hamzavi, J.-C. Deybach, R. Kauppinen, L.E. Rhodes, J. Frank, G.M. Murphy, F.P.J. Karstens, E.J.G. Sijbrands, et al., Afamelanotide for Erythropoietic Protoporphyria, N Engl J Med, 373 (2015) 48–59.

[164] Z.A. Abdel-Malek, Melanocortin receptors: their functions and regulation by physiological agonists and antagonists, CMLS, Cell. Mol. Life Sci., 58 (2001) 434–441.

[165] Y. Yang, C.M. Harmon, Molecular signatures of human melanocortin receptors for ligand binding and signaling, Biochimica et Biophysica Acta (BBA) - Molecular Basis of Disease, 1863 (2017) 2436–2447.

[166] Y. Yang, T.M. Fong, C.J. Dickinson, C. Mao, J.-Y. Li, M.R. Tota, R. Mosley, L.H.T. Van der Ploeg, I. Gantz, Molecular Determinants of Ligand Binding to the Human Melanocortin-4 Receptor, Biochemistry, 39 (2000) 14900–14911.

[167] C. Haskell-Luevano, R.D. Cone, E.K. Monck, Y.-P. Wan, Structure Activity Studies of the Melanocortin-4 Receptor by *in Vitro* Mutagenesis: Identification of Agouti-Related Protein (AGRP), Melanocortin Agonist and Synthetic Peptide Antagonist Interaction Determinants, Biochemistry, 40 (2001) 6164–6179.

[168] M. Chen, M. Cai, C.J. Aprahamian, K.E. Georgeson, V. Hruby, C.M. Harmon, Y. Yang, Contribution of the Conserved Amino Acids of the Melanocortin-4 Receptor in d-[Nle4,Phe7]-α-Melanocyte-stimulating Hormone Binding and Signaling, Journal of Biological Chemistry, 282 (2007) 21712–21719.

[169] S.A. Nickolls, M.I. Cismowski, X. Wang, M. Wolff, P.J. Conlon, R.A. Maki, Molecular Determinants of Melanocortin 4 Receptor Ligand Binding and MC4/MC3 Receptor Selectivity, J Pharmacol Exp Ther, 304 (2003) 1217–1227.

[170] K. Hogan, S. Peluso, S. Gould, I. Parsons, D. Ryan, L. Wu, I. Visiers, Mapping the Binding Site of Melanocortin 4 Receptor Agonists: A Hydrophobic Pocket Formed by I328(125), I332(129), and I742(291) Is Critical for Receptor Activation, J. Med. Chem., 49 (2006) 911–922.

[171] E.M. Haslach, J.W. Schaub, C. Haskell-Luevano, β-Turn secondary structure and melanocortin ligands, Bioorganic & Medicinal Chemistry, 17 (2009) 952–958.

[172] A. Zorzi, K. Deyle, C. Heinis, Cyclic peptide therapeutics: past, present and future, Current Opinion in Chemical Biology, 38 (2017) 24–29.

[173] A.A. Vinogradov, Y. Yin, H. Suga, Macrocyclic Peptides as Drug Candidates: Recent Progress and Remaining Challenges, J. Am. Chem. Soc., 141 (2019) 4167–4181.

[174] C. Bechtler, C. Lamers, Macrocyclization strategies for cyclic peptides and peptidomimetics, RSC Med. Chem., 12 (2021) 1325–1351.

[175] J.P.L. Gonçalves, D. Palmer, M. Meldal, MC4R Agonists: Structural Overview on Antiobesity Therapeutics, Trends in Pharmacological Sciences, 39 (2018) 402–423.

[176] F. Al-Obeidi, A.M. de L. Castrucci, M.E. Hadley, V.J. Hruby, Potent and prolonged-acting cyclic lactam analogs of .alpha-melanotropin: design based on molecular dynamics, J. Med. Chem., 32 (1989) 2555–2561.

[177] R.T. Dorr, V.J. Hruby, M.E. Hadley, EVALUATION OF MELANOTAN-II, A SIJPERPOTENT CYCLIC MELANOTROPIC PEPTIDE IN A PILOT PHASE-I CLINICAL STUDY, 58 (1996).

[178] M.J. Hansen, H.B. Schiöth, M.J. Morris, Feeding responses to a melanocortin agonist and antagonist in obesity induced by a palatable high-fat diet, Brain Research, 1039 (2005) 137–145.

[179] I. Côté, Y. Sakarya, N. Kirichenko, D. Morgan, C.S. Carter, N. Tümer, P.J. Scarpace, Activation of the central melanocortin system chronically reduces body mass without the necessity of long-term caloric restriction, Can. J. Physiol. Pharmacol., 95 (2017) 206–214.

[180] A.H. Clayton, S.E. Althof, S. Kingsberg, L.R. DeRogatis, R. Kroll, I. Goldstein, J. Kaminetsky, C. Spana, J. Lucas, R. Jordan, D.J. Portman, Bremelanotide for Female Sexual Dysfunctions in Premenopausal Women: A Randomized, Placebo-Controlled Dose-Finding Trial, Womens Health (Lond Engl), 12 (2016) 325–337.

[181] S. Dhillon, S.J. Keam, Bremelanotide: First Approval, Drugs, 79 (2019) 1599–1606.

[182] P. Roubert, B. Dubern, P. Plas, C. Lubrano-Berthelier, R. Alihi, F. Auger, D.B. Deoliveira, J.Z. Dong, A. Basdevant, C. Thurieau, K. Clément, Novel pharmacological MC4R agonists can efficiently activate mutated MC4R from obese patient with impaired endogenous agonist response, Journal of Endocrinology, 207 (2010) 177–183.

[183] K.G. Kumar, G.M. Sutton, J.Z. Dong, P. Roubert, P. Plas, H.A. Halem, M.D. Culler, H. Yang, V.D. Dixit, A.A. Butler, Analysis of the therapeutic functions of novel melanocortin receptor agonists in MC3R- and MC4R-deficient C57BL/6J mice, Peptides, 30 (2009) 1892–1900.

[184] K. Clément, C. Vaisse, N. Lahlou, S. Cabrol, V. Pelloux, D. Cassuto, M. Gourmelen, C. Dina, J. Chambaz, J.-M. Lacorte, A. Basdevant, P. Bougnères, Y. Lebouc, P. Froguel, B. Guy-Grand, A mutation in the human leptin receptor gene causes obesity and pituitary dysfunction, Nature, 392 (1998) 398–401.

[185] H. Krude, H. Biebermann, W. Luck, R. Horn, G. Brabant, A. Grüters, Severe early-onset obesity, adrenal insufficiency and red hair pigmentation caused by POMC mutations in humans, 19 (1998).

[186] K.Y. Chen, R. Muniyappa, B.S. Abel, K.P. Mullins, P. Staker, R.J. Brychta, X. Zhao, M. Ring, T.L. Psota, R.D. Cone, B.L. Panaro, K.M. Gottesdiener, L.H.T. Van der Ploeg, M.L. Reitman, M.C. Skarulis, RM-493, a Melanocortin-4 Receptor (MC4R) Agonist, Increases Resting Energy Expenditure in Obese Individuals, The Journal of Clinical Endocrinology & Metabolism, 100 (2015) 1639–1645.

[187] P. Kühnen, K. Clément, S. Wiegand, O. Blankenstein, K. Gottesdiener, L.L. Martini, K. Mai, U. Blume-Peytavi, A. Grüters, H. Krude, Proopiomelanocortin Deficiency Treated with a Melanocortin-4 Receptor Agonist, N Engl J Med, 375 (2016) 240–246.

[188] T.-H. Collet, B. Dubern, J. Mokrosinski, H. Connors, J.M. Keogh, E. Mendes de Oliveira, E. Henning, C. Poitou-Bernert, J.-M. Oppert, P. Tounian, F. Marchelli, R. Alili, J. Le Beyec, D. Pépin, J.-M. Lacorte, A. Gottesdiener, R. Bounds, S. Sharma, C. Folster, B. Henderson, et al., Evaluation of a melanocortin-4 receptor (MC4R) agonist (Setmelanotide) in MC4R deficiency, Molecular Metabolism, 6 (2017) 1321–1329.

[189] K. Clément, E. van den Akker, J. Argente, A. Bahm, W.K. Chung, H. Connors, K. De Waele, I.S. Farooqi, J. Gonneau-Lejeune, G. Gordon, K. Kohlsdorf, C. Poitou, L. Puder, J. Swain, M. Stewart, G. Yuan, M. Wabitsch, P. Kühnen, P. Pigeon-Kherchiche, A. Flaus-Furmaniuk, et al., Efficacy and safety of setmelanotide, an MC4R agonist, in individuals with severe obesity due to LEPR or POMC deficiency: single-arm, open-label, multicentre, phase 3 trials, The Lancet Diabetes & Endocrinology, 8 (2020) 960–970.

[190] S. Seo, D.-F. Guo, K. Bugge, D.A. Morgan, K. Rahmouni, V.C. Sheffield, Requirement of Bardet-Biedl syndrome proteins for leptin receptor signaling, Human Molecular Genetics, 18 (2009) 1323–1331.

[191] A. Markham, Setmelanotide: First Approval, Drugs, 81 (2021) 397–403.

[192] C.M. Trapp, M. Censani, Setmelanotide: a promising advancement for pediatric patients with rare forms of genetic obesity, Current Opinion in Endocrinology, Diabetes & Obesity, 30 (2023) 136–140.

[193] C. Haskell-Luevano, Å. Rosenquist, A. Souers, K.C. Khong, J.A. Ellman, R.D. Cone, Compounds That Activate the Mouse Melanocortin-1 Receptor Identified by Screening a Small Molecule Library Based upon the β-Turn, J. Med. Chem., 42 (1999) 4380–4387.

[194] I.K. Sebhat, W.J. Martin, Z. Ye, K. Barakat, R.T. Mosley, D.B.R. Johnston, R. Bakshi, B. Palucki, D.H. Weinberg, T. MacNeil, R.N. Kalyani, R. Tang, R.A. Stearns, R.R. Miller, C. Tamvakopoulos, A.M. Strack, E. McGowan, D.E. Cashen, J.E. Drisko, G.J. Hom, et al., Design and Pharmacology of *N* -[(3 *R*)-1,2,3,4-Tetrahydroisoquinolinium- 3-ylcarbonyl]-(1 *R*)-1-(4-chlorobenzyl)- 2-[4-cyclohexyl-4-(1 *H* -1,2,4-triazol- 1-ylmethyl)piperidin-1-yl]-2-oxoethylamine (**1**), a Potent, Selective, Melanocortin Subtype-4 Receptor Agonist, J. Med. Chem., 45 (2002) 4589–4593.

[195] B.L. Palucki, M.K. Park, R.P. Nargund, Z. Ye, I.K. Sebhat, P.G. Pollard, R.N. Kalyani, R. Tang, T. MacNeil, D.H. Weinberg, A. Vongs, C.I. Rosenblum, G.A. Doss, R.R. Miller, R.A. Stearns, Q. Peng, C. Tamvakopoulos, E. McGowan, W.J. Martin, J.M. Metzger, et al., Discovery of (2S)-N-[(1R)-2-[4-cyclohexyl-4-[[(1,1-dimethylethyl)amino]carbonyl]-1-piperidinyl]-1-[(4-fluorophenyl)methyl]-2-oxoethyl]-4-methyl-2-piperazinecarboxamide (MB243), a potent and selective melanocortin subtype-4 receptor agonist, Bioorganic & Medicinal Chemistry Letters, 15 (2005) 171–175.

[196] I. Mosialou, S. Shikhel, J.-M. Liu, A. Maurizi, N. Luo, Z. He, Y. Huang, H. Zong, R.A. Friedman, J. Barasch, P. Lanzano, L. Deng, R.L. Leibel, M. Rubin, T. Nickolas, W. Chung, L.M. Zeltser, K.W. Williams, J.E. Pessin, S. Kousteni, MC4R-dependent suppression of appetite by bone-derived lipocalin 2, Nature, 543 (2017) 385–390.

[197] R.D. Cone, Anatomy and regulation of the central melanocortin system, Nat Neurosci, 8 (2005) 571–578.

[198] B. Beck, Neuropeptide Y in normal eating and in genetic and dietary-induced obesity, Phil. Trans. R. Soc. B, 361 (2006) 1159–1185.

[199] C. Kienast, H.-C. Gunga, M. Steinach, Neuropeptide Y – Its role in human performance and extreme environments, REACH, 14–15 (2019) 100032.

[200] D.L. Marks, N. Ling, R.D. Cone, Role of the central melanocortin system in cachexia, Cancer Res, 61 (2001) 1432–1438.

[201] T. Vink, A. Hinney, A.A. van Elburg, S.H.M. van Goozen, L.A. Sandkuijl, R.J. Sinke, B.-M. Herpertz-Dahlmann, J. Hebebrand, H. Remschmidt, H. van Engeland, R.A.H. Adan, Association between an agouti-related protein gene polymorphism and anorexia nervosa, Mol Psychiatry, 6 (2001) 325–328.

[202] D.L. Marks, A.A. Butler, R. Turner, G. Brookhart, R.D. Cone, Differential Role of Melanocortin Receptor Subtypes in Cachexia, Endocrinology, 144 (2003) 1513–1523.

[203] M.J.H. Kas, G. van Dijk, A.J.W. Scheurink, R.A.H. Adan, Agouti-related protein prevents self-starvation, Mol Psychiatry, 8 (2003) 235–240.

[204] Y.-L. Ge, T. Ohta, D.J. Driscoll, R.D. Nicholls, S.P. Kalra, Anorexigenic melanocortin signaling in the hypothalamus is augmented in association with failure-to-thrive in a transgenic mouse model for Prader–Willi syndrome, Brain Research, 957 (2002) 42–45.

[205] J.R. Shutter, M. Graham, A.C. Kinsey, S. Scully, R. Lüthy, K.L. Stark, Hypothalamic expression of ART, a novel gene related to agouti, is up-regulated in obese and diabetic mutant mice, Genes Dev., 11 (1997) 593–602.

[206] M.M. Ollmann, B.D. Wilson, Y.-K. Yang, J.A. Kerns, Y. Chen, I. Gantz, G.S. Barsh, Antagonism of Central Melanocortin Receptors in Vitro and in Vivo by Agouti-Related Protein, Science, 278 (1997) 135–138.

[207] T.M. Fong, C. Mao, T. MacNeil, R. Kalyani, T. Smith, D. Weinberg, M.R. Tota, L.H.T. Van der Ploeg, ART (Protein Product of Agouti-Related Transcript) as an Antagonist of MC-3 and MC-4 Receptors, Biochemical and Biophysical Research Communications, 237 (1997) 629–631.

[208] C. Haskell-Luevano, E.K. Monck, Agouti-related protein functions as an inverse agonist at a constitutively active brain melanocortin-4 receptor, Regulatory Peptides, 99 (2001) 1–7.

[209] W.A.J. Nijenhuis, J. Oosterom, R.A.H. Adan, AgRP(83–132) Acts as an Inverse Agonist on the Human-Melanocortin-4 Receptor, Molecular Endocrinology, 15 (2001) 164–171.

[210] J.C. McNulty, D.A. Thompson, K.A. Bolin, J. Wilken, G.S. Barsh, G.L. Millhauser, High-Resolution NMR Structure of the Chemically-Synthesized Melanocortin Receptor Binding Domain AGRP(87−132) of the Agouti-Related Protein · Biochemistry, 40 (2001) 15520–15527.

[211] G.L. Millhauser, J.C. McNULTY, P.J. Jackson, D.A. Thompson, G.S. Barsh, I. Gantz, Loops and Links: Structural Insights into the Remarkable Function of the Agouti-Related Protein, Annals of the New York Academy of Sciences, 994 (2003) 27–35.

[212] P.J. Jackson, N.R. Douglas, B. Chai, J. Binkley, A. Sidow, G.S. Barsh, G.L. Millhauser, Structural and Molecular Evolutionary Analysis of Agouti and Agouti-Related Proteins, Chemistry & Biology, 13 (2006) 1297–1305.

[213] B.-X. Chai, R.R. Neubig, G.L. Millhauser, D.A. Thompson, P.J. Jackson, G.S. Barsh, C.J. Dickinson, J.-Y. Li, Y.-M. Lai, I. Gantz, Inverse agonist activity of agouti and agouti-related protein, Peptides, 24 (2003) 603–609.

[214] K.A. Fleming, M.D. Ericson, K.T. Freeman, D.N. Adank, M.M. Lunzer, S.L. Wilber, C. Haskell-Luevano, Structure–Activity Relationship Studies of a Macrocyclic AGRP-Mimetic Scaffold c[Pro-Arg-Phe-Phe-Asn-Ala-Phe-DPro] Yield Potent and Selective Melanocortin-4 Receptor Antagonists and Melanocortin-5 Receptor Inverse Agonists That Increase Food Intake in Mice, ACS Chem. Neurosci., 9 (2018) 1141–1151.

[215] M. Kojima, K. Kangawa, Ghrelin: Structure and Function, Physiological Reviews, 85 (2005) 495–522.

[216] Q. Tong, C.-P. Ye, J.E. Jones, J.K. Elmquist, B.B. Lowell, Synaptic release of GABA by AgRP neurons is required for normal regulation of energy balance, Nat Neurosci, 11 (2008) 998–1000.

[217] C.D. Morrison, G.J. Morton, K.D. Niswender, R.W. Gelling, M.W. Schwartz, Leptin inhibits hypothalamic *Npy* and *Agrp* gene expression via a mechanism that requires phosphatidylinositol 3-OH-kinase signaling, American Journal of Physiology-Endocrinology and Metabolism, 289 (2005) E1051–E1057.

[218] H. Dhillon, S.P. Kalra, P.S. Kalra, Dose-Dependent Effects of Central Leptin Gene Therapy on Genes That Regulate Body Weight and Appetite in the Hypothalamus, Molecular Therapy, 4 (2001) 139–145.

[219] C.M. Nasrallah, T.L. Horvath, Mitochondrial dynamics in the central regulation of metabolism, Nat Rev Endocrinol, 10 (2014) 650–658.

[220] E.T. van der Westhuizen, C. Valant, P.M. Sexton, A. Christopoulos, Endogenous allosteric modulators of G protein-coupled receptors, J Pharmacol Exp Ther, 353 (2015) 246–260.

[221] S. Urwyler, Allosteric Modulation of Family C G-Protein-Coupled Receptors: from Molecular Insights to Therapeutic Perspectives, Pharmacol Rev, 63 (2011) 59–126.

[222] A. Strasser, H.-J. Wittmann, E.H. Schneider, R. Seifert, Modulation of GPCRs by monovalent cations and anions, Naunyn Schmiedebergs Arch Pharmacol, 388 (2015) 363–380.

[223] S. Kopanchuk, S. Veiksina, R. Petrovska, I. Mutule, M. Szardenings, A. Rinken, J.E.S. Wikberg, Co-operative regulation of ligand binding to melanocortin receptor subtypes: evidence for interacting binding sites, Eur J Pharmacol, 512 (2005) 85–95.

[224] J. Yu, L.E. Gimenez, C.C. Hernandez, Y. Wu, A.H. Wein, G.W. Han, K. McClary, S.R. Mittal, K. Burdsall, B. Stauch, L. Wu, S.N. Stevens, A. Peisley, S.Y. Williams, V. Chen, G.L. Millhauser, S. Zhao, R.D. Cone, R.C. Stevens, Determination of the melanocortin-4 receptor structure identifies Ca2+ as a cofactor for ligand binding, Science, 368 (2020) 428–433.

[225] H. Zhang, L.-N. Chen, D. Yang, C. Mao, Q. Shen, W. Feng, D.-D. Shen, A. Dai, S. Xie, Y. Zhou, J. Qin, J.-P. Sun, D.H. Scharf, T. Hou, T. Zhou, M.-W. Wang, Y. Zhang, Structural insights into ligand recognition and activation of the melanocortin-4 receptor, Cell Res, 31 (2021) 1163–1175.

[226] N.A. Heyder, G. Kleinau, D. Speck, A. Schmidt, S. Paisdzior, M. Szczepek, B. Bauer, A. Koch, M. Gallandi, D. Kwiatkowski, J. Bürger, T. Mielke, A.G. Beck-Sickinger, P.W. Hildebrand, C.M.T. Spahn, D. Hilger, M. Schacherl, H. Biebermann, T. Hilal, P. Kühnen, et al., Structures of active melanocortin-4 receptor–Gs-protein complexes with NDP-α-MSH and setmelanotide, Cell Res, 31 (2021) 1176–1189.

[227] B. Holst, C.E. Elling, T.W. Schwartz, Metal Ion-mediated Agonism and Agonist Enhancement in Melanocortin MC1 and MC4 Receptors*, Journal of Biological Chemistry, 277 (2002) 47662–47670.

[228] M.C. Lagerström, J. Klovins, R. Fredriksson, D. Fridmanis, T. Haitina, M.K. Ling, M.M. Berglund, H.B. Schiöth, High affinity agonistic metal ion binding sites within the melanocortin 4 receptor illustrate conformational change of transmembrane region 3, J Biol Chem, 278 (2003) 51521–51526.

[229] B. Holst, T.W. Schwartz, Molecular mechanism of agonism and inverse agonism in the melanocortin receptors: Zn(2+) as a structural and functional probe, Ann N Y Acad Sci, 994 (2003) 1–11.

[230] R. Link, S. Veiksina, M.-J. Tahk, T. Laasfeld, P. Paiste, S. Kopanchuk, A. Rinken, The constitutive activity of melanocortin-4 receptors in cAMP pathway is allosterically modulated by zinc and copper ions, J Neurochem, 153 (2020) 346–361.

[231] Lifting the lid on GPCRs: the role of extracellular loops - PMC, (n.d.).

[232] Molecular signatures of G-protein-coupled receptors | Nature, (n.d.).

[233] M.J. Woolley, A.C. Conner, Understanding the common themes and diverse roles of the second extracellular loop (ECL2) of the GPCR super-family, Molecular and Cellular Endocrinology, 449 (2017) 3–11.

[234] S. Ma, Y. Chen, A. Dai, W. Yin, J. Guo, D. Yang, F. Zhou, Y. Jiang, M.-W. Wang, H.E. Xu, Structural mechanism of calcium-mediated hormone recognition and Gβ interaction by the human melanocortin-1 receptor, Cell Res, 31 (2021) 1061–1071.

[235] P. Luo, W. Feng, S. Ma, A. Dai, K. Wu, X. Chen, Q. Yuan, X. Cai, D. Yang, M.-W. Wang, H. Eric Xu, Y. Jiang, Structural basis of signaling regulation of the human melanocortin-2 receptor by MRAP1, Cell Res, 33 (2023) 46–54.

[236] G. Kleinau, N.A. Heyder, Y.-X. Tao, P. Scheerer, Structural Complexity and Plasticity of Signaling Regulation at the Melanocortin-4 Receptor, Int J Mol Sci, 21 (2020) 5728.

[237] W. Feng, Q. Zhou, X. Chen, A. Dai, X. Cai, X. Liu, F. Zhao, Y. Chen, C. Ye, Y. Xu, Z. Cong, H. Li, S. Lin, D. Yang, M.-W. Wang, Structural insights into ligand recognition and subtype selectivity of the human melanocortin-3 and melanocortin-5 receptors, Cell Discov, 9 (2023) 1–15.

[238] P. Tarnow, T. Schoneberg, H. Krude, A. Gruters, H. Biebermann, Mutationally induced disulfide bond formation within the third extracellular loop causes melanocortin 4 receptor inactivation in patients with obesity, J Biol Chem, 278 (2003) 48666–48673.

[239] I.L. Barsukov, D.E. Nolde, A.L. Lomize, A.S. Arseniev, Three-dimensional structure of proteolytic fragment 163-231 of bacterioopsin determined from nuclear magnetic resonance data in solution, Eur J Biochem, 206 (1992) 665–672.

[240] K.V. Pervushin, V.Yu. Orekhov, A.I. Popov, L.Yu. Musina, A.S. Arseniev, Three-dimensional structure of (1-71)bacterioopsin solubilized in methanol/chloroform and SDS micelles determined by 15N-1H heteronuclear NMR spectroscopy, Eur J Biochem, 219 (1994) 571–583.

[241] M.E. Girvin, V.K. Rastogi, F. Abildgaard, J.L. Markley, R.H. Fillingame, Solution Structure of the Transmembrane H^+-Transporting Subunit c of the F_1F_o ATP Synthase, Biochemistry, 37 (1998) 8817–8824.

[242] J. Yang, Y.-Q. Ma, R.C. Page, S. Misra, E.F. Plow, J. Qin, Structure of an integrin αIIbβ3 transmembrane-cytoplasmic heterocomplex provides insight into integrin activation, Proc. Natl. Acad. Sci. U.S.A., 106 (2009) 17729–17734.

[243] C. Tribet, R. Audebert, J.-L. Popot, Amphipols: Polymers that keep membrane proteins soluble in aqueous solutions, Proc. Natl. Acad. Sci. U.S.A., 93 (1996) 15047–15050.

[244] M. Zoonens, J.-L. Popot, Amphipols for Each Season, J Membrane Biol, 247 (2014) 759–796.

[245] R.M. Garavito, S. Ferguson-Miller, Detergents as Tools in Membrane Biochemistry, Journal of Biological Chemistry, 276 (2001) 32403–32406.

[246] A. Diller, C. Loudet, F. Aussenac, G. Raffard, S. Fournier, M. Laguerre, A. Grélard, S.J. Opella, F.M. Marassi, E.J. Dufourc, Bicelles: A natural 'molecular goniometer' for structural, dynamical and topological studies of molecules in membranes, Biochimie, 91 (2009) 744–751.

[247] M.A. McLean, M.C. Gregory, S.G. Sligar, Nanodiscs: A Controlled Bilayer Surface for the Study of Membrane Proteins, Annu. Rev. Biophys., 47 (2018) 107–124.

[248] B.B. Das, H.J. Nothnagel, G.J. Lu, W.S. Son, Y. Tian, F.M. Marassi, S.J. Opella, Structure Determination of a Membrane Protein in Proteoliposomes, J. Am. Chem. Soc., 134 (2012) 2047–2056.

[249] H. Nsairat, D. Khater, U. Sayed, F. Odeh, A. Al Bawab, W. Alshaer, Liposomes: structure, composition, types, and clinical applications, Heliyon, 8 (2022) e09394.

[250] A. Chen, E.J. Majdinasab, M.C. Fiori, H. Liang, G.A. Altenberg, Polymer-Encased Nanodiscs and Polymer Nanodiscs: New Platforms for Membrane Protein Research and Applications, Frontiers in Bioengineering and Biotechnology, 8 (2020).

[251] J. Birch, D. Axford, J. Foadi, A. Meyer, A. Eckhardt, Y. Thielmann, I. Moraes, The fine art of integral membrane protein crystallisation, Methods, 147 (2018) 150–162.

[252] R. Fernandez-Leiro, S.H.W. Scheres, Unravelling biological macromolecules with cryo-electron microscopy, Nature, 537 (2016) 339–346.

[253] W. Kühlbrandt, Forty years in cryoEM of membrane proteins, Microscopy, 71 (2022) i30–i50.

[254] K.R. Acharya, M.D. Lloyd, The advantages and limitations of protein crystal structures, Trends in Pharmacological Sciences, 26 (2005) 10–14.

[255] E. Chun, A.A. Thompson, W. Liu, C.B. Roth, M.T. Griffith, V. Katritch, J. Kunken, F. Xu, V. Cherezov, M.A. Hanson, R.C. Stevens, Fusion partner toolchest for the stabilization and crystallization of G protein-coupled receptors, Structure, 20 (2012) 967–976.

[256] A. Manglik, B.K. Kobilka, J. Steyaert, Nanobodies to Study G Protein–Coupled Receptor Structure and Function, Annu. Rev. Pharmacol. Toxicol., 57 (2017) 19–37.

[257] E. D'Imprima, W. Kühlbrandt, Current limitations to high-resolution structure determination by single-particle cryoEM, Q Rev Biophys, 54 (2021) e4.

[258] S. Pushpakom, F. Iorio, P.A. Eyers, K.J. Escott, S. Hopper, A. Wells, A. Doig, T. Guilliams, J. Latimer, C. McNamee, A. Norris, P. Sanseau, D. Cavalla, M. Pirmohamed, Drug repurposing: progress, challenges and recommendations, Nat Rev Drug Discov, 18 (2019) 41–58.

[259] I. Shimada, T. Ueda, Y. Kofuku, M.T. Eddy, K. Wüthrich, GPCR drug discovery: integrating solution NMR data with crystal and cryo-EM structures, Nat Rev Drug Discov, 18 (2019) 59–82.

[260] K. Takeuchi, Y. Kofuku, S. Imai, T. Ueda, Y. Tokunaga, Y. Toyama, Y. Shiraishi, I. Shimada, Function-Related Dynamics in Multi-Spanning Helical Membrane Proteins Revealed by Solution NMR, Membranes, 11 (2021) 604.

[261] N. Thakur, A.P. Ray, L. Sharp, B. Jin, A. Duong, N.G. Pour, S. Obeng, A.V. Wijesekara, Z.-G. Gao, C.R. McCurdy, K.A. Jacobson, E. Lyman, M.T. Eddy, Anionic phospholipids control mechanisms of GPCR-G protein recognition, Nat Commun, 14 (2023) 794.

[262] J. Oates, A. Watts, Uncovering the intimate relationship between lipids, cholesterol and GPCR activation, Current Opinion in Structural Biology, 21 (2011) 802–807.

[263] R. Dawaliby, C. Trubbia, C. Delporte, M. Masureel, P. Van Antwerpen, B.K. Kobilka, C. Govaerts, Allosteric regulation of G protein–coupled receptor activity by phospholipids, Nat Chem Biol, 12 (2016) 35–39.

[264] A.J.Y. Jones, F. Gabriel, A. Tandale, D. Nietlispach, Structure and dynamics of GPCRs in lipid membranes: physical principles and experimental approaches, Molecules, 25 (2020) 1–39.

[265] R. Baccouch, E. Rascol, K. Stoklosa, I.D. Alves, The role of the lipid environment in the activity of G protein coupled receptors, Biophysical Chemistry, 285 (2022) 106794.

[266] T.K.M. Nyholm, S. Özdirekcan, J.A. Killian, How Protein Transmembrane Segments Sense the Lipid Environment, Biochemistry, 46 (2007) 1457–1465.

[267] M. Zoonens, J.-L. Popot, Amphipols for Each Season, J Membrane Biol, 247 (2014) 759–796.

[268] H.J. Lee, H.S. Lee, T. Youn, B. Byrne, P.S. Chae, Impact of novel detergents on membrane protein studies, Chem, 8 (2022) 980–1013.

[269] J.M. Neugebauer, [18] Detergents: An overview, in: Methods in Enzymology, Elsevier, 1990: pp. 239–253.

[270] R. Nagarajan, Molecular Packing Parameter and Surfactant Self-Assembly: The Neglected Role of the Surfactant Tail, Langmuir, 18 (2002) 31–38.

[271] M. le Maire, P. Champeil, J.V. Møller, Interaction of membrane proteins and lipids with solubilizing detergents, Biochimica et Biophysica Acta (BBA) - Biomembranes, 1508 (2000) 86–111.

[272] T. Arnold, D. Linke, Phase separation in the isolation and purification of membrane proteins, BioTechniques, 43 (2007) 427–440.

[273] A.M. Seddon, P. Curnow, P.J. Booth, Membrane proteins, lipids and detergents: not just a soap opera, Biochimica et Biophysica Acta (BBA) - Biomembranes, 1666 (2004) 105–117.

[274] J. Gesell, M. Zasloff, S.J. Opella, Two-dimensional 1H NMR experiments show that the 23-residue magainin antibiotic peptide is an α-helix in dodecylphosphocholine micelles, sodium dodecylsulfate micelles, and trifluoroethanol/water solution, J Biomol NMR, 9 (1997) 127–135.

[275] S. Elter, T. Raschle, S. Arens, A. Viegas, V. Gelev, M. Etzkorn, G. Wagner, The Use of Amphipols for NMR Structural Characterization of 7-TM Proteins, J Membrane Biol, 247 (2014) 957–964.

[276] W. Ding, X. Qi, P. Li, Y. Maitani, T. Nagai, Cholesteryl hemisuccinate as a membrane stabilizer in dipalmitoylphosphatidylcholine liposomes containing saikosaponin-d, International Journal of Pharmaceutics, 300 (2005) 38–47.

[277] M. Bayrhuber, T. Meins, M. Habeck, S. Becker, K. Giller, S. Villinger, C. Vonrhein, C. Griesinger, M. Zweckstetter, K. Zeth, Structure of the human voltage-dependent anion channel, Proceedings of the National Academy of Sciences, 105 (2008) 15370–15375.

[278] M. Renault, O. Saurel, J. Czaplicki, P. Demange, V. Gervais, F. Löhr, V. Réat, M. Piotto, A. Milon, Solution State NMR Structure and Dynamics of KpOmpA, a 210 Residue Transmembrane Domain Possessing a High Potential for Immunological Applications, Journal of Molecular Biology, 385 (2009) 117–130.

[279] A. Gautier, H.R. Mott, M.J. Bostock, J.P. Kirkpatrick, D. Nietlispach, Structure determination of the seven-helix transmembrane receptor sensory rhodopsin II by solution NMR spectroscopy, Nat Struct Mol Biol, 17 (2010) 768–774.

[280] T.C. Edrington, E. Kintz, J.B. Goldberg, L.K. Tamm, Structural Basis for the Interaction of Lipopolysaccharide with Outer Membrane Protein H (OprH) from Pseudomonas aeruginosa, Journal of Biological Chemistry, 286 (2011) 39211–39223.

[281] I. Kucharska, P. Seelheim, T. Edrington, B. Liang, L.K. Tamm, OprG Harnesses the Dynamics of its Extracellular Loops to Transport Small Amino Acids across the Outer Membrane of Pseudomonas aeruginosa, Structure, 23 (2015) 2234–2245.

[282] F.M. Marassi, Y. Ding, C.D. Schwieters, Y. Tian, Y. Yao, Backbone structure of Yersinia pestis Ail determined in micelles by NMR-restrained simulated annealing with implicit membrane solvation, J Biomol NMR, 63 (2015) 59–65.

[283] B. Liang, L.K. Tamm, Structure of outer membrane protein G by solution NMR spectroscopy, Proc. Natl. Acad. Sci. U.S.A., 104 (2007) 16140–16145.

[284] M.J. Berardi, W.M. Shih, S.C. Harrison, J.J. Chou, Mitochondrial uncoupling protein 2 structure determined by NMR molecular fragment searching, Nature, 476 (2011) 109–113.

[285] B. OuYang, S. Xie, M.J. Berardi, X. Zhao, J. Dev, W. Yu, B. Sun, J.J. Chou, Unusual architecture of the p7 channel from hepatitis C virus, Nature, 498 (2013) 521–525.

[286] Ł. Jaremko, M. Jaremko, K. Giller, S. Becker, M. Zweckstetter, Structure of the Mitochondrial Translocator Protein in Complex with a Diagnostic Ligand, Science, 343 (2014) 1363–1366.

[287] D.A. Fox, P. Larsson, R.H. Lo, B.M. Kroncke, P.M. Kasson, L. Columbus, Structure of the Neisserial Outer Membrane Protein Opa $_{60}$: Loop Flexibility Essential to Receptor Recognition and Bacterial Engulfment, J. Am. Chem. Soc., 136 (2014) 9938–9946.

[288] S. Zhou, P. Pettersson, J. Huang, J. Sjöholm, D. Sjöstrand, R. Pomès, M. Högbom, P. Brzezinski, L. Mäler, P. Ädelroth, Solution NMR structure of yeast Rcf1, a protein involved in respiratory supercomplex formation, Proc. Natl. Acad. Sci. U.S.A., 115 (2018) 3048–3053.

[289] P. Strop, A.T. Brunger, Refractive index-based determination of detergent concentration and its application to the study of membrane proteins, Protein Sci, 14 (2005) 2207–2211.

[290] A. Stetsenko, A. Guskov, An Overview of the Top Ten Detergents Used for Membrane Protein Crystallization, Crystals, 7 (2017) 197.

[291] B. Lorber, J.B. Bishop, L.J. DeLucas, Purification of octyl β-d-glucopyranoside and re-estimation of its micellar size, Biochimica et Biophysica Acta (BBA) - Biomembranes, 1023 (1990) 254–265.

[292] D.J. Slotboom, R.H. Duurkens, K. Olieman, G.B. Erkens, Static light scattering to characterize membrane proteins in detergent solution, Methods, 46 (2008) 73–82.

[293] J. Cladera, J.L. Rigaud, J. Villaverde, M. Duñach, Liposome solubilization and membrane protein reconstitution using Chaps and Chapso, Eur J Biochem, 243 (1997) 798–804.

[294] V. Kotov, K. Bartels, K. Veith, I. Josts, U.K.T. Subhramanyam, C. Günther, J. Labahn, T.C. Marlovits, I. Moraes, H. Tidow, C. Löw, M.M. Garcia-Alai, High-throughput stability screening for detergent-solubilized membrane proteins, Sci Rep, 9 (2019) 10379.

[295] C.R. Sanders, J.P. Schwonek, Characterization of magnetically orientable bilayers in mixtures of dihexanoylphosphatidylcholine and dimyristoylphosphatidylcholine by solid-state NMR, Biochemistry, 31 (1992) 8898–8905.

[296] P. Ram, J.H. Prestegard, Magnetic field induced ordering of bile salt/phospholipid micelles: new media for NMR structural investigations, Biochimica et Biophysica Acta (BBA) - Biomembranes, 940 (1988) 289–294.

[297] C.R. Sanders, J.H. Prestegard, Magnetically orientable phospholipid bilayers containing small amounts of a bile salt analogue, CHAPSO, Biophysical Journal, 58 (1990) 447–460.

[298] R.R. Vold, R.S. Prosser, Magnetically Oriented Phospholipid Bilayered Micelles for Structural Studies of Polypeptides Does the Ideal Bicelle Exist?, Journal of Magnetic Resonance, Series B, 113 (1996) 267–271.

[299] K.J. Glover, J.A. Whiles, G. Wu, N. Yu, R. Deems, J.O. Struppe, R.E. Stark, E.A. Komives, R.R. Vold, Structural Evaluation of Phospholipid Bicelles for Solution-State Studies of Membrane-Associated Biomolecules, Biophysical Journal, 81 (2001) 2163–2171.

[300] S.J. Opella, F.M. Marassi, Structure Determination of Membrane Proteins by NMR Spectroscopy, Chem. Rev., 104 (2004) 3587–3606.

[301] R.S. Prosser, F. Evanics, J.L. Kitevski, M.S. Al-Abdul-Wahid, Current Applications of Bicelles in NMR Studies of Membrane-Associated Amphiphiles and Proteins · Biochemistry, 45 (2006) 8453–8465.

[302] É. Chartrand, A.A. Arnold, A. Gravel, S. Jenna, I. Marcotte, Potential role of the membrane in hERG channel functioning and drug-induced long QT syndrome, Biochimica et Biophysica Acta (BBA) - Biomembranes, 1798 (2010) 1651–1662.

[303] M. Lindberg, H. Biverståhl, A. Gräslund, L. Mäler, Structure and positioning comparison of two variants of penetratin in two different membrane mimicking systems by NMR: Structure and position of penetratin, European Journal of Biochemistry, 270 (2003) 3055–3063.

[304] J. Lind, A. Gräslund, L. Mäler, Membrane interactions of dynorphins, Biochemistry, 45 (2006) 15931–15940.

[305] E.V. Bocharov, M.L. Mayzel, P.E. Volynsky, M.V. Goncharuk, Y.S. Ermolyuk, A.A. Schulga, E.O. Artemenko, R.G. Efremov, A.S. Arseniev, Spatial Structure and pH-dependent Conformational Diversity of Dimeric Transmembrane Domain of the Receptor Tyrosine Kinase EphA1, Journal of Biological Chemistry, 283 (2008) 29385–29395.

[306] E.V. Bocharov, Y.E. Pustovalova, K.V. Pavlov, P.E. Volynsky, M.V. Goncharuk, Y.S. Ermolyuk, D.V. Karpunin, A.A. Schulga, M.P. Kirpichnikov, R.G. Efremov, I.V. Maslennikov, A.S. Arseniev, Unique Dimeric Structure of BNip3 Transmembrane Domain Suggests Membrane Permeabilization as a Cell Death Trigger, Journal of Biological Chemistry, 282 (2007) 16256–16266.

[307] E.V. Bocharov, K.S. Mineev, P.E. Volynsky, Y.S. Ermolyuk, E.N. Tkach, A.G. Sobol, V.V. Chupin, M.P. Kirpichnikov, R.G. Efremov, A.S. Arseniev, Spatial Structure of the Dimeric Transmembrane Domain of the Growth Factor Receptor ErbB2 Presumably Corresponding to the Receptor Active State, Journal of Biological Chemistry, 283 (2008) 6950–6956.

[308] T.-L. Lau, C. Kim, M.H. Ginsberg, T.S. Ulmer, The structure of the integrin αIIbβ3 transmembrane complex explains integrin transmembrane signalling, EMBO J, 28 (2009) 1351–1361.

[309] K. Koshiyama, M. Taneo, T. Shigematsu, S. Wada, Bicelle-to-Vesicle Transition of a Binary Phospholipid Mixture Guided by Controlled Local Lipid Compositions: A Molecular Dynamics Simulation Study, J. Phys. Chem. B, 123 (2019) 3118–3123.

[310] C. Dargel, Y. Hannappel, T. Hellweg, Heating-Induced DMPC/Glycyrrhizin Bicelle-to-Vesicle Transition: A X-Ray Contrast Variation Study, Biophysical Journal, 118 (2020) 2411–2425.

[311] J.-X. Lu, M.A. Caporini, G.A. Lorigan, The effects of cholesterol on magnetically aligned phospholipid bilayers: a solid-state NMR and EPR spectroscopy study, Journal of Magnetic Resonance, 168 (2004) 18–30.

[312] N.A. Nusair, E.K. Tiburu, P.C. Dave, G.A. Lorigan, Investigating fatty acids inserted into magnetically aligned phospholipid bilayers using EPR and solid-state NMR spectroscopy, Journal of Magnetic Resonance, 168 (2004) 228–237.

[313] J.M. Hutchison, K.-C. Shih, H.A. Scheidt, S.M. Fantin, K.F. Parson, G.A. Pantelopulos, H.R. Harrington, K.F. Mittendorf, S. Qian, R.A. Stein, S.E. Collier, M.G. Chambers, J. Katsaras, M.W. Voehler, B.T. Ruotolo, D. Huster, R.L. McFeeters, J.E. Straub, M.-P. Nieh, C.R. Sanders, Bicelles Rich in both Sphingolipids and Cholesterol and Their Use in Studies of Membrane Proteins, J. Am. Chem. Soc., 142 (2020) 12715–12729.

[314] T.H. Bayburt, Y.V. Grinkova, S.G. Sligar, Self-Assembly of Discoidal Phospholipid Bilayer Nanoparticles with Membrane Scaffold Proteins, Nano Letters, 2 (2002) 853–856.

[315] I.G. Denisov, Y.V. Grinkova, A.A. Lazarides, S.G. Sligar, Directed Self-Assembly of Monodisperse Phospholipid Bilayer Nanodiscs with Controlled Size, Journal of the American Chemical Society, 126 (2004) 3477–3487.

[316] A. Viegas, T. Viennet, M. Etzkorn, The power, pitfalls and potential of the nanodisc system for NMR-based studies, Biol Chem, 397 (2016) 1335–1354.

[317] T.K. Ritchie, Y.V. Grinkova, T.H. Bayburt, I.G. Denisov, J.K. Zolnerciks, W.M. Atkins, S.G. Sligar, Chapter 11 Reconstitution of Membrane Proteins in Phospholipid Bilayer Nanodiscs, Methods in Enzymology, 464 (2009) 211–231.

[318] T.H. Bayburt, S.G. Sligar, Self-assembly of single integral membrane proteins into soluble nanoscale phospholipid bilayers, Protein Science, 12 (2009) 2476–2481.

[319] T.H. Bayburt, Y.V. Grinkova, S.G. Sligar, Assembly of single bacteriorhodopsin trimers in bilayer nanodiscs, Archives of Biochemistry and Biophysics, 450 (2006) 215–222.

[320] T.H. Bayburt, A.J. Leitz, G. Xie, D.D. Oprian, S.G. Sligar, Transducin activation by nanoscale lipid bilayers containing one and two rhodopsins, Journal of Biological Chemistry, 282 (2007) 14875–14881.

[321] I.G. Denisov, B.J. Baas, Y.V. Grinkova, S.G. Sligar, Cooperativity in cytochrome P450 3A4: Linkages in substrate binding, spin state, uncoupling, and product formation, Journal of Biological Chemistry, 282 (2007) 7066–7076.

[322] Y.V. Grinkova, I.G. Denisov, S.G. Sligar, Engineering extended membrane scaffold proteins for self-assembly of soluble nanoscale lipid bilayers, Protein Engineering Design and Selection, 23 (2010) 843–848.

[323] F. Hagn, M. Etzkorn, T. Raschle, G. Wagner, Optimized phospholipid bilayer nanodiscs facilitate high-resolution structure determination of membrane proteins, Journal of the American Chemical Society, 135 (2013) 1919–1925.

[324] F. Hagn, M.L. Nasr, G. Wagner, Assembly of phospholipid nanodiscs of controlled size for structural studies of membrane proteins by NMR, Nature Protocols, 13 (2018) 79–98.

[325] X. Wang, Z. Mu, Y. Li, Y. Bi, Y. Wang, Smaller Nanodiscs are Suitable for Studying Protein Lipid Interactions by Solution NMR, Protein J, 34 (2015) 205–211.

[326] M.L. Nasr, D. Baptista, M. Strauss, Z.-Y.J. Sun, S. Grigoriu, S. Huser, A. Plückthun, F. Hagn, T. Walz, J.M. Hogle, G. Wagner, Covalently circularized nanodiscs for studying membrane proteins and viral entry, Nat Methods, 14 (2017) 49–52.

[327] I.G. Denisov, S.G. Sligar, Nanodiscs in Membrane Biochemistry and Biophysics, Chem. Rev., 117 (2017) 4669–4713.

[328] U. Günsel, F. Hagn, Lipid Nanodiscs for High-Resolution NMR Studies of Membrane Proteins, Chem. Rev., 122 (2022) 9395–9421.

[329] T. Viennet, M.M. Wördehoff, B. Uluca, C. Poojari, H. Shaykhalishahi, D. Willbold, B. Strodel, H. Heise, A.K. Buell, W. Hoyer, M. Etzkorn, Structural insights from lipid-bilayer nanodiscs link α-Synuclein membrane-binding modes to amyloid fibril formation, Commun Biol, 1 (2018) 1–12.

[330] N. Skar-Gislinge, J.B. Simonsen, K. Mortensen, R. Feidenhans'l, S.G. Sligar, B.L. Møller, T. Bjørnholm, L. Arleth, Elliptical Structure of Phospholipid Bilayer Nanodiscs Encapsulated by Scaffold Proteins: Casting the Roles of the Lipids and the Protein, J Am Chem Soc, 132 (2010) 13713–13722.

[331] N. Skar-Gislinge, S.A.R. Kynde, I.G. Denisov, X. Ye, I. Lenov, S.G. Sligar, L. Arleth, Small-angle scattering determination of the shape and localization of human cytochrome P450 embedded in a phospholipid nanodisc environment, Acta Crystallogr D Biol Crystallogr, 71 (2015) 2412–2421.

[332] I. Josts, J. Nitsche, S. Maric, H.D. Mertens, M. Moulin, M. Haertlein, S. Prevost, D.I. Svergun, S. Busch, V.T. Forsyth, H. Tidow, Conformational States of ABC Transporter MsbA in a Lipid Environment Investigated by Small-Angle Scattering Using Stealth Carrier Nanodiscs, Structure, 26 (2018) 1072-1079.e4.

[333] T.E. Cleveland, W. He, A.C. Evans, N.O. Fischer, E.Y. Lau, M.A. Coleman, P. Butler, Small angle X ray and neutron scattering demonstrates that cell free expression produces properly formed disc shaped nanolipoprotein particles, Protein Sci, 27 (2018) 780–789.

[334] R.G. Efremov, A. Leitner, R. Aebersold, S. Raunser, Architecture and conformational switch mechanism of the ryanodine receptor, Nature, 517 (2015) 39–43.

[335] Y. Gao, E. Cao, D. Julius, Y. Cheng, TRPV1 structures in nanodiscs reveal mechanisms of ligand and lipid action, Nature, 534 (2016) 347–351.

[336] R.G. Efremov, C. Gatsogiannis, S. Raunser, Lipid Nanodiscs as a Tool for High-Resolution Structure Determination of Membrane Proteins by Single-Particle Cryo-EM, Methods Enzymol, 594 (2017) 1–30.

[337] J.L. Syrjanen, K. Michalski, T.-H. Chou, T. Grant, S. Rao, N. Simorowski, S.J. Tucker, N. Grigorieff, H. Furukawa, Structure and assembly of calcium homeostasis modulator proteins, Nat Struct Mol Biol, 27 (2020) 150–159.

[338] M. Zhang, M. Gui, Z.F. Wang, C. Gorgulla, J.J. Yu, H. Wu, Z. yu J. Sun, C. Klenk, L. Merklinger, L. Morstein, F. Hagn, A. Plückthun, A. Brown, M.L. Nasr, G. Wagner, Cryo-EM structure of an activated GPCR–G protein complex in lipid nanodiscs, Nature Structural and Molecular Biology, 28 (2021) 258–267.

[339] T. Viennet, S. Bungert-Plümke, S. Elter, A. Viegas, C. Fahlke, M. Etzkorn, Reconstitution and NMR Characterization of the Ion-Channel Accessory Subunit Barttin in Detergents and Lipid-Bilayer Nanodiscs, Front Mol Biosci, 6 (2019) 13.

[340] T. Kolter, K. Sandhoff, Lysosomal degradation of membrane lipids, FEBS Letters, 584 (2010) 1700–1712.

[341] K. Popovic, J. Holyoake, R. Pomès, G.G. Privé, Structure of saposin A lipoprotein discs, Proc. Natl. Acad. Sci. U.S.A., 109 (2012) 2908–2912.

[342] J. Frauenfeld, R. Löving, J.-P. Armache, A.F.-P. Sonnen, F. Guettou, P. Moberg, L. Zhu, C. Jegerschöld, A. Flayhan, J.A.G. Briggs, H. Garoff, C. Löw, Y. Cheng, P. Nordlund, A saposin-lipoprotein nanoparticle system for membrane proteins, Nat Methods, 13 (2016) 345–351.

[343] A. Flayhan, H.D.T. Mertens, Y. Ural-Blimke, M. Martinez Molledo, D.I. Svergun, C. Löw, Saposin Lipid Nanoparticles: A Highly Versatile and Modular Tool for Membrane Protein Research, Structure, 26 (2018) 345-355.e5.

[344] N.X. Nguyen, J.-P. Armache, C. Lee, Y. Yang, W. Zeng, V.K. Mootha, Y. Cheng, X. Bai, Y. Jiang, Cryo-EM structure of a fungal mitochondrial calcium uniporter, Nature, 559 (2018) 570–574.

[345] D. Du, A. Neuberger, M.W. Orr, C.E. Newman, P.-C. Hsu, F. Samsudin, A. Szewczak-Harris, L.M. Ramos, M. Debela, S. Khalid, G. Storz, B.F. Luisi, Interactions of a Bacterial RND Transporter with a Transmembrane Small Protein in a Lipid Environment, Structure, 28 (2020) 625-634.e6.

[346] D.-M. Kehlenbeck, D.A.K. Traore, I. Josts, S. Sander, M. Moulin, M. Haertlein, S. Prevost, V.T. Forsyth, H. Tidow, Cryo-EM structure of MsbA in saposin-lipid nanoparticles (Salipro) provides insights into nucleotide coordination, FEBS J, 289 (2022) 2959–2970.

[347] I. Drulyte, A.R. Gutgsell, P. Lloris-Garcerá, M. Liss, S. Geschwindner, M. Radjainia, J. Frauenfeld, R. Löving, Direct cell extraction of membrane proteins for structure–function analysis, Sci Rep, 13 (2023) 1420.

[348] C.-T.H. Chien, L.R. Helfinger, M.J. Bostock, A. Solt, Y.L. Tan, D. Nietlispach, An Adaptable Phospholipid Membrane Mimetic System for Solution NMR Studies of Membrane Proteins, J. Am. Chem. Soc., 139 (2017) 14829–14832.

[349] G.M. Anantharamaiah, J.L. Jones, C.G. Brouillette, C.F. Schmidt, B.H. Chung, T.A. Hughes, A.S. Bhown, J.P. Segrest, Studies of synthetic peptide analogs of the amphipathic helix Structure of complexes with dimyristoyl phosphatidylcholine, J Biol Chem, 260 (1985) 10248–10255.

[350] V.K. Mishra, M.N. Palgunachari, J.P. Segrest, G.M. Anantharamaiah, Interactions of synthetic peptide analogs of the class A amphipathic helix with lipids Evidence for the snorkel hypothesis, J Biol Chem, 269 (1994) 7185–7191.

[351] M. Miyazaki, Y. Tajima, T. Handa, M. Nakano, Static and Dynamic Characterization of Nanodiscs with Apolipoprotein A-I and Its Model Peptide, J. Phys. Chem. B, 114 (2010) 12376–12382.

[352] V.K. Mishra, G.M. Anantharamaiah, J.P. Segrest, M.N. Palgunachari, M. Chaddha, S.W.S. Sham, N.R. Krishna, Association of a Model Class A (Apolipoprotein) Amphipathic α Helical Peptide with Lipid, Journal of Biological Chemistry, 281 (2006) 6511–6519.

[353] C. Anada, K. Ikeda, A. Egawa, T. Fujiwara, H. Nakao, M. Nakano, Temperature- and composition-dependent conformational transitions of amphipathic peptide–phospholipid nanodiscs, Journal of Colloid and Interface Science, 588 (2021) 522–530.

[354] S.R. Midtgaard, M.C. Pedersen, J.J.K. Kirkensgaard, K.K. Sørensen, K. Mortensen, K.J. Jensen, L. Arleth, Self-assembling peptides form nanodiscs that stabilize membrane proteins, Soft Matter, 10 (2014) 738–752.

[355] H. Kondo, K. Ikeda, M. Nakano, Formation of size-controlled, denaturation-resistant lipid nanodiscs by an amphiphilic self-polymerizing peptide, Colloids and Surfaces B: Biointerfaces, 146 (2016) 423–430.

[356] M.L. Carlson, J.W. Young, Z. Zhao, L. Fabre, D. Jun, J. Li, J. Li, H.S. Dhupar, I. Wason, A.T. Mills, J.T. Beatty, J.S. Klassen, I. Rouiller, F. Duong, The Peptidisc, a simple method for stabilizing membrane proteins in detergent-free solution, eLife, 7 (2018) e34085.

[357] Y.-C. Kuo, H. Chen, G. Shang, E. Uchikawa, H. Tian, X.-C. Bai, X. Zhang, Cryo-EM structure of the PlexinC1/A39R complex reveals inter-domain interactions critical for ligand-induced activation, Nat Commun, 11 (2020) 1953.

[358] K. Rantalainen, Z.T. Berndsen, A. Antanasijevic, T. Schiffner, X. Zhang, W.-H. Lee, J.L. Torres, L. Zhang, A. Irimia, J. Copps, K.H. Zhou, Y.D. Kwon, W.H. Law, C.A. Schramm, R. Verardi, S.J. Krebs, P.D. Kwong, N.A. Doria-Rose, I.A. Wilson, M.B. Zwick, et al., HIV-1 Envelope and MPER Antibody Structures in Lipid Assemblies, Cell Reports, 31 (2020) 107583.

[359] J.-X. Wu, R. Liu, K. Song, L. Chen, Structures of human dual oxidase 1 complex in low-calcium and high-calcium states, Nat Commun, 12 (2021) 155.

[360] A. Harris, M. Wagner, D. Du, S. Raschka, L.-M. Nentwig, H. Gohlke, S.H.J. Smits, B.F. Luisi, L. Schmitt, Structure and efflux mechanism of the yeast pleiotropic drug resistance transporter Pdr5, Nat Commun, 12 (2021) 5254.

[361] J.K. Demmer, B.P. Phillips, O.L. Uhrig, A. Filloux, L.P. Allsopp, M. Bublitz, T. Meier, Structure of ATP synthase from ESKAPE pathogen Acinetobacter baumannii, Sci Adv, 8 (n.d.) eabl5966.

[362] S. Itskanov, L. Wang, T. Junne, R. Sherriff, L. Xiao, N. Blanchard, W.Q. Shi, C. Forsyth, D. Hoepfner, M. Spiess, E. Park, A common mechanism of Sec61 translocon inhibition by small molecules, Nat Chem Biol, (2023) 1–9.

[363] P.W.K. Rothemund, Folding DNA to create nanoscale shapes and patterns, Nature, 440 (2006) 297–302.

[364] S.M. Douglas, J.J. Chou, W.M. Shih, DNA-nanotube-induced alignment of membrane proteins for NMR structure determination, Proc. Natl. Acad. Sci. U.S.A., 104 (2007) 6644–6648.

[365] S.M. Douglas, H. Dietz, T. Liedl, B. Högberg, F. Graf, W.M. Shih, Self-assembly of DNA into nanoscale three-dimensional shapes, Nature, 459 (2009) 414–418.

[366] F. Hong, F. Zhang, Y. Liu, H. Yan, DNA Origami: Scaffolds for Creating Higher Order Structures, Chem. Rev., 117 (2017) 12584–12640.

[367] Z. Zhao, M. Zhang, J.M. Hogle, W.M. Shih, G. Wagner, M.L. Nasr, DNA-Corralled Nanodiscs for the Structural and Functional Characterization of Membrane Proteins and Viral Entry, J. Am. Chem. Soc., 140 (2018) 10639–10643.

[368] T. Raschle, C. Lin, R. Jungmann, W.M. Shih, G. Wagner, Controlled Co-reconstitution of Multiple Membrane Proteins in Lipid Bilayer Nanodiscs Using DNA as a Scaffold, ACS Chem. Biol., 10 (2015) 2448–2454.

[369] K. Iric, M. Subramanian, J. Oertel, N.P. Agarwal, M. Matthies, X. Periole, T.P. Sakmar, T. Huber, K. Fahmy, T.L. Schmidt, DNA-encircled lipid bilayers, Nanoscale, 10 (2018) 18463–18467.

[370] M. Orwick-Rydmark, J.E. Lovett, A. Graziadei, L. Lindholm, M.R. Hicks, A. Watts, Detergent-free incorporation of a seven-transmembrane receptor protein into nanosized bilayer lipodisq particles for functional and biophysical studies, Nano Letters, 12 (2012) 4687–4692.

[371] S. Gulati, M. Jamshad, T.J. Knowles, K.A. Morrison, R. Downing, N. Cant, R. Collins, J.B. Koenderink, R.C. Ford, M. Overduin, I.D. Kerr, T.R. Dafforn, A.J. Rothnie, Detergent-free purification of ABC (ATP-binding-cassette) transporters, Biochemical Journal, 461 (2014) 269–278.

[372] M. Jamshad, J. Charlton, Y.P. Lin, S.J. Routledge, Z. Bawa, T.J. Knowles, M. Overduin, N. Dekker, T.R. Dafforn, R.M. Bill, D.R. Poyner, M. Wheatley, G-protein coupled receptor solubilization and purification for biophysical analysis and functional studies, in the total absence of detergent, Bioscience Reports, 35 (2015) 1–10.

[373] S.C. Lee, T.J. Knowles, V.L.G. Postis, M. Jamshad, R.A. Parslow, Y.P. Lin, A. Goldman, P. Sridhar, M. Overduin, S.P. Muench, T.R. Dafforn, A method for detergent-free isolation of membrane proteins in their local lipid environment, Nature Protocols, 11 (2016) 1149–1162.

[374] D.J.K. Swainsbury, S. Scheidelaar, N. Foster, R. van Grondelle, J.A. Killian, M.R. Jones, The effectiveness of styrene-maleic acid (SMA) copolymers for solubilisation of integral membrane proteins from SMA-accessible and SMA-resistant membranes, Biochimica et Biophysica Acta - Biomembranes, 1859 (2017) 2133–2143.

[375] S. Rehan, V.O. Paavilainen, V.P. Jaakola, Functional reconstitution of human equilibrative nucleoside transporter-1 into styrene maleic acid co-polymer lipid particles, Biochimica et Biophysica Acta - Biomembranes, 1859 (2017) 1059–1065.

[376] S. Scheidelaar, M.C. Koorengevel, J.D. Pardo, J.D. Meeldijk, E. Breukink, J.A. Killian, Molecular Model for the solubilization of membranes into nanodisks by styrene maleic acid copolymers, Biophysical Journal, 108 (2015) 279–290.

[377] M. Xue, L. Cheng, I. Faustino, W. Guo, S.J. Marrink, Molecular Mechanism of Lipid Nanodisk Formation by Styrene-Maleic Acid Copolymers, Biophysical Journal, 115 (2018) 494–502.

[378] M. Orwick Rydmark, M.K. Christensen, E.S. Köksal, I. Kantarci, K. Kustanovich, V. Yantchev, A. Jesorka, I. Gözen, Styrene maleic acid copolymer induces pores in biomembranes, Soft Matter, 15 (2019) 7934–7944.

[379] S. Scheidelaar, M.C. Koorengevel, C.A. van Walree, J.J. Dominguez, J.M. Dörr, J.A. Killian, Effect of Polymer Composition and pH on Membrane Solubilization by Styrene-Maleic Acid Copolymers, Biophysical Journal, 111 (2016) 1974–1986.

[380] A.H. Kopf, J.M. Dörr, M.C. Koorengevel, F. Antoniciello, H. Jahn, J.A. Killian, Factors influencing the solubilization of membrane proteins from Escherichia coli membranes by styrene–maleic acid copolymers, Biochimica et Biophysica Acta - Biomembranes, 1862 (2020) 183125.

[381] M.C. Fiori, W. Zheng, E. Kamilar, G. Simiyu, G.A. Altenberg, H. Liang, Extraction and reconstitution of membrane proteins into lipid nanodiscs encased by zwitterionic styrene-maleic amide copolymers, Scientific Reports, 10 (2020) 1–13.

[382] M.C. Fiori, Y. Jiang, G.A. Altenberg, H. Liang, Polymer-encased nanodiscs with improved buffer compatibility, Scientific Reports, 7 (2017) 1–10.

[383] A.O. Oluwole, B. Danielczak, A. Meister, J.O. Babalola, C. Vargas, S. Keller, Solubilization of Membrane Proteins into Functional Lipid-Bilayer Nanodiscs Using a Diisobutylene/Maleic Acid Copolymer, Angewandte Chemie - International Edition, 56 (2017) 1919–1924.

[384] A.O. Oluwole, J. Klingler, B. Danielczak, J.O. Babalola, C. Vargas, G. Pabst, S. Keller, Formation of Lipid-Bilayer Nanodiscs by Diisobutylene/Maleic Acid (DIBMA) Copolymer, Langmuir, 33 (2017) 14378–14388.

[385] S.C.L. Hall, C. Tognoloni, J. Charlton, É.C. Bragginton, A.J. Rothnie, P. Sridhar, M. Wheatley, T.J. Knowles, T. Arnold, K.J. Edler, T.R. Dafforn, An acid-compatible co-polymer for the solubilization of membranes and proteins into lipid bilayer-containing nanoparticles, Nanoscale, 10 (2018) 10609–10619.

[386] S. Lavington, A. Watts, Detergent-free solubilisation & purification of a G protein coupled receptor using a polymethacrylate polymer, Biochimica et Biophysica Acta (BBA) - Biomembranes, 1863 (2021) 183441.

[387] T. Ravula, N.Z. Hardin, J. Bai, S.-C. Im, L. Waskell, A. Ramamoorthy, Effect of polymer charge on functional reconstitution of membrane proteins in polymer nanodiscs, Chem. Commun., 54 (2018) 9615–9618.

[388] T. Ravula, N.Z. Hardin, S.K. Ramadugu, A. Ramamoorthy, pH Tunable and Divalent Metal Ion Tolerant Polymer Lipid Nanodiscs, Langmuir, 33 (2017) 10655–10662.

[389] M. Esmaili, C.J. Brown, R. Shaykhutdinov, C. Acevedo-Morantes, Y.L. Wang, H. Wille, R.D. Gandour, S.R. Turner, M. Overduin, Homogeneous nanodiscs of native membranes formed by stilbene–maleic-acid copolymers, Nanoscale, 12 (2020) 16705–16709.

[390] B. Danielczak, M. Rasche, J. Lenz, E.P. Patallo, S. Weyrauch, F. Mahler, M.T. Agbadaola, A. Meister, J.O. Babalola, C. Vargas, C. Kolar, S. Keller, A bioinspired glycopolymer for capturing membrane proteins in native-like lipid-bilayer nanodiscs, Nanoscale, 14 (2022) 1855–1867.

[391] S. Lindhoud, V. Carvalho, J.W. Pronk, M.-E. Aubin-Tam, SMA-SH: Modified Styrene–Maleic Acid Copolymer for Functionalization of Lipid Nanodiscs, Biomacromolecules, 17 (2016) 1516–1522.

[392] A.A.A. Smith, H.E. Autzen, B. Faust, J.L. Mann, B.W. Muir, S. Howard, A. Postma, A.J. Spakowitz, Y. Cheng, E.A. Appel, Lipid Nanodiscs via Ordered Copolymers, Chem, 6 (2020) 2782–2795.

[393] D. Glueck, A. Grethen, M. Das, O.P. Mmeka, E.P. Patallo, A. Meister, R. Rajender, S. Kins, M. Räschle, J. Victor, C. Chu, M. Etzkorn, Z. Köck, F. Bernhard, J.O. Babalola, C. Vargas, S. Keller, Electroneutral Polymer Nanodiscs Enable Interference-Free Probing of Membrane Proteins in a Lipid-Bilayer Environment, Small, 18 (2022) 2202492.

[394] T.W. Herling, D.J. O'Connell, M.C. Bauer, J. Persson, U. Weininger, T.P.J. Knowles, S. Linse, A Microfluidic Platform for Real-Time Detection and Quantification of Protein-Ligand Interactions, Biophysical Journal, 110 (2016) 1957–1966.

[395] C.J. Wienken, P. Baaske, U. Rothbauer, D. Braun, S. Duhr, Protein-binding assays in biological liquids using microscale thermophoresis, Nat Commun, 1 (2010) 100.

[396] M.M. Pierce, C.S. Raman, B.T. Nall, Isothermal Titration Calorimetry of Protein–Protein Interactions, Methods, 19 (1999) 213–221.

[397] A. Sultana, J.E. Lee, Measuring Protein-Protein and Protein-Nucleic Acid Interactions by Biolayer Interferometry, Current Protocols in Protein Science, 79 (2015) 19.25.1-19.25.26.

[398] D. Capelli, C. Parravicini, G. Pochetti, R. Montanari, C. Temporini, M. Rabuffetti, M.L. Trincavelli, S. Daniele, M. Fumagalli, S. Saporiti, E. Bonfanti, M.P. Abbracchio, I. Eberini, S. Ceruti, E. Calleri, S. Capaldi, Surface Plasmon Resonance as a Tool for Ligand Binding Investigation of Engineered GPR17 Receptor, a G Protein Coupled Receptor Involved in Myelination, Front. Chem., 7 (2020) 910.

[399] K. Janson, F.L. Kyrilis, C. Tüting, M. Alfes, M. Das, T.K. Träger, C. Schmidt, F. Hamdi, C. Vargas, S. Keller, A. Meister, P.L. Kastritis, Cryo-Electron Microscopy Snapshots of Eukaryotic Membrane Proteins in Native Lipid-Bilayer Nanodiscs, Biomacromolecules, 23 (2022) 5084–5094.

[400] V.J. Flegler, A. Rasmussen, S. Rao, N. Wu, R. Zenobi, M.S.P. Sansom, R. Hedrich, T. Rasmussen, B. Böttcher, The MscS-like channel YnaI has a gating mechanism based on flexible pore helices, Proceedings of the National Academy of Sciences, 117 (2020) 28754–28762.

[401] D.J.K. Swainsbury, F.R. Hawkings, E.C. Martin, S. Musiał, J.H. Salisbury, P.J. Jackson, D.A. Farmer, M.P. Johnson, C.A. Siebert, A. Hitchcock, C.N. Hunter, Cryo-EM structure of the four-subunit Rhodobacter sphaeroides cytochrome bc1 complex in styrene maleic acid nanodiscs, Proc Natl Acad Sci U S A, 120 (2023) e2217922120.

[402] J. Broecker, B.T. Eger, O.P. Ernst, Crystallogenesis of Membrane Proteins Mediated by Polymer-Bounded Lipid Nanodiscs, Structure, 25 (2017) 384–392.

[403] J. Radoicic, S.H. Park, S.J. Opella, Macrodiscs Comprising SMALPs for Oriented Sample Solid-State NMR Spectroscopy of Membrane Proteins, Biophysical Journal, 115 (2018) 22–25.

[404] T. Ravula, S.K. Ramadugu, G. Di Mauro, A. Ramamoorthy, Bioinspired, Size-Tunable Self-Assembly of Polymer-Lipid Bilayer Nanodiscs, Angew. Chem. Int. Ed., 56 (2017) 11466–11470.

[405] T. Ravula, A. Ramamoorthy, Magnetic Alignment of Polymer Macro-Nanodiscs Enables Residual-Dipolar-Coupling-Based High-Resolution Structural Studies by NMR Spectroscopy, Angewandte Chemie International Edition, 58 (2019) 14925–14928.

[406] S.H. Park, J. Wu, Y. Yao, C. Singh, Y. Tian, F.M. Marassi, S.J. Opella, Membrane proteins in magnetically aligned phospholipid polymer discs for solid-state NMR spectroscopy, Biochimica et Biophysica Acta (BBA) - Biomembranes, 1862 (2020) 183333.

[407] B. Bersch, J.M. Dörr, A. Hessel, J.A. Killian, P. Schanda, Proton-Detected Solid-State NMR Spectroscopy of a Zinc Diffusion Facilitator Protein in Native Nanodiscs, Angew Chem Int Ed Engl, 56 (2017) 2508–2512.

[408] V. Tugarinov, P.M. Hwang, J.E. Ollerenshaw, L.E. Kay, Cross-Correlated Relaxation Enhanced 1H−13C NMR Spectroscopy of Methyl Groups in Very High Molecular Weight Proteins and Protein Complexes, J. Am. Chem. Soc., 125 (2003) 10420–10428.

[409] R. Lichtenecker, M.L. Ludwiczek, W. Schmid, R. Konrat, Simplification of Protein NOESY Spectra Using Bioorganic Precursor Synthesis and NMR Spectral Editing, J. Am. Chem. Soc., 126 (2004) 5348–5349.

[410] R. Törner, R. Awad, P. Gans, B. Brutscher, J. Boisbouvier, Spectral editing of intra- and inter-chain methyl–methyl NOEs in protein complexes, J Biomol NMR, 74 (2020) 83–94.

[411] J. Wen, P. Zhou, J. Wu, Efficient acquisition of high-resolution 4-D diagonal-suppressed methyl-methyl NOESY for large proteins, J Magn Reson, 218 (2012) 128–132.

[412] H. Sun, L.E. Kay, V. Tugarinov, An Optimized Relaxation-Based Coherence Transfer NMR Experiment for the Measurement of Side-Chain Order in Methyl-Protonated, Highly Deuterated Proteins, J. Phys. Chem. B, 115 (2011) 14878–14884.

[413] V. Tugarinov, L.E. Kay, Relaxation Rates of Degenerate 1H Transitions in Methyl Groups of Proteins as Reporters of Side-Chain Dynamics, J. Am. Chem. Soc., 128 (2006) 7299–7308.

[414] Y. Mizukoshi, K. Takeuchi, M. Arutaki, Y. Tokunaga, T. Takizawa, H. Hanzawa, I. Shimada, Improvement of Ligand Affinity and Thermodynamic Properties by NMR-Based Evaluation of Local Dynamics and Surface Complementarity in the Receptor-Bound State, Angewandte Chemie International Edition, 55 (2016) 14606–14609.

[415] T. Yuwen, R. Huang, P. Vallurupalli, L.E. Kay, A Methyl-TROSY-Based 1H Relaxation Dispersion Experiment for Studies of Conformational Exchange in High Molecular Weight Proteins, Angewandte Chemie International Edition, 58 (2019) 6250–6254.

[416] G. Bouvignies, L.E. Kay, A 2D 13C-CEST experiment for studying slowly exchanging protein systems using methyl probes: an application to protein folding, J Biomol NMR, 53 (2012) 303–310.

[417] S.P. Behera, A. Dubey, W.-N. Chen, V.S. De Paula, M. Zhang, N.G. Sgourakis, W. Bermel, G. Wagner, P.W. Coote, H. Arthanari, Nearest-neighbor NMR spectroscopy: categorizing spectral peaks by their adjacent nuclei, Nat Commun, 11 (2020) 5547.

[418] P. Schanda, E. Kupce, B. Brutscher, SOFAST-HMQC experiments for recording two-dimensional heteronuclear correlation spectra of proteins within a few seconds, J Biomol NMR, 33 (2005) 199–211.

[419] P. Rößler, D. Mathieu, A.D. Gossert, Enabling NMR Studies of High Molecular Weight Systems Without the Need for Deuteration: The XL-ALSOFAST Experiment with Delayed Decoupling, Angewandte Chemie International Edition, 59 (2020) 19329–19337.

[420] N. Bolik-Coulon, A.I.M. Sever, R.W. Harkness, J.M. Aramini, Y. Toyama, D.F. Hansen, L.E. Kay, Less is more: A simple methyl-TROSY based pulse scheme offers improved sensitivity in applications to high molecular weight complexes, Journal of Magnetic Resonance, 346 (2023) 107326.

[421] P. Gans, O. Hamelin, R. Sounier, I. Ayala, M.A. Durá, C.D. Amero, M. Noirclerc-Savoye, B. Franzetti, M.J. Plevin, J. Boisbouvier, Stereospecific Isotopic Labeling of Methyl Groups for NMR Spectroscopic Studies of High-Molecular-Weight Proteins, Angewandte Chemie International Edition, 49 (2010) 1958–1962.

[422] V. Tugarinov, V. Kanelis, L.E. Kay, Isotope labeling strategies for the study of high-molecular-weight proteins by solution NMR spectroscopy, Nat Protoc, 1 (2006) 749–754.

[423] R. Linser, V. Gelev, F. Hagn, H. Arthanari, S.G. Hyberts, G. Wagner, Selective Methyl Labeling of Eukaryotic Membrane Proteins Using Cell-Free Expression, J. Am. Chem. Soc., 136 (2014) 11308–11310.

[424] M. Lazarova, F. Löhr, R.-B. Rues, R. Kleebach, V. Dötsch, F. Bernhard, Precursor-Based Selective Methyl Labeling of Cell-Free Synthesized Proteins, ACS Chem. Biol., 13 (2018) 2170–2178.

[425] R. Levin, F. Löhr, B. Karakoc, R. Lichtenecker, V. Dötsch, F. Bernhard, E coli “Stablelabel” S30 lysate for optimized cell-free NMR sample preparation, J Biomol NMR, 77 (2023) 131–147.

[426] R. Ali, L.D. Clark, J.A. Zahm, A. Lemoff, K. Ramesh, D.M. Rosenbaum, M.K. Rosen, Improved strategy for isoleucine 1H/13C methyl labeling in Pichia pastoris, J Biomol NMR, 73 (2019) 687–697.

[427] L. Clark, J.A. Zahm, R. Ali, M. Kukula, L. Bian, S.M. Patrie, K.H. Gardner, M.K. Rosen, D.M. Rosenbaum, Methyl labeling and TROSY NMR spectroscopy of proteins expressed in the eukaryote Pichia pastoris, J Biomol NMR, 62 (2015) 239–245.

[428] M. Miyazawa-Onami, K. Takeuchi, T. Takano, T. Sugiki, I. Shimada, H. Takahashi, Perdeuteration and methyl-selective (1)H, (13)C-labeling by using a Kluyveromyces lactis expression system, J Biomol NMR, 57 (2013) 297–304.

[429] T. Sugiki, I. Shimada, H. Takahashi, Stable isotope labeling of protein by Kluyveromyces lactis for NMR study, J Biomol NMR, 42 (2008) 159–162.

[430] L.D. Clark, I. Dikiy, K. Chapman, K.E. Rödström, J. Aramini, M.V. LeVine, G. Khelashvili, S.G. Rasmussen, K.H. Gardner, D.M. Rosenbaum, Ligand modulation of sidechain dynamics in a wild-type human GPCR, eLife, 6 (2017) e28505.

[431] T. Mizumura, K. Kondo, M. Kurita, Y. Kofuku, M. Natsume, S. Imai, Y. Shiraishi, T. Ueda, I. Shimada, Activation of adenosine A2A receptor by lipids from docosahexaenoic acid revealed by NMR, Science Advances, 6 (2020) eaay8544.

[432] M.P. Bokoch, Y. Zou, S.G.F. Rasmussen, C.W. Liu, R. Nygaard, D.M. Rosenbaum, J.J. Fung, H.-J. Choi, F.S. Thian, T.S. Kobilka, J.D. Puglisi, W.I. Weis, L. Pardo, R.S. Prosser, L. Mueller, B.K. Kobilka, Ligand-specific regulation of the extracellular surface of a G-protein-coupled receptor, Nature, 463 (2010) 108–112.

[433] R. Sounier, C. Mas, J. Steyaert, T. Laeremans, A. Manglik, W. Huang, B.K. Kobilka, H. Déméné, S. Granier, Propagation of conformational changes during μ-opioid receptor activation, Nature, 524 (2015) 375–378.

[434] Y. Kofuku, T. Ueda, J. Okude, Y. Shiraishi, K. Kondo, T. Mizumura, S. Suzuki, I. Shimada, Functional Dynamics of Deuterated β2-Adrenergic Receptor in Lipid Bilayers Revealed by NMR Spectroscopy, Angewandte Chemie International Edition, 53 (2014) 13376–13379.

[435] Y. Minato, S. Suzuki, T. Hara, Y. Kofuku, G. Kasuya, Y. Fujiwara, S. Igarashi, E. Suzuki, O. Nureki, M. Hattori, T. Ueda, I. Shimada, Conductance of P2X4 purinergic receptor is determined by conformational equilibrium in the transmembrane region, Proceedings of the National Academy of Sciences, 113 (2016) 4741–4746.

[436] R. Nygaard, Y. Zou, R.O. Dror, T.J. Mildorf, D.H. Arlow, A. Manglik, A.C. Pan, C.W. Liu, J.J. Fung, M.P. Bokoch, F.S. Thian, T.S. Kobilka, D.E. Shaw, L. Mueller, R.S. Prosser, B.K. Kobilka, The Dynamic Process of β2-Adrenergic Receptor Activation, Cell, 152 (2013) 532–542.

[437] J. Okude, T. Ueda, Y. Kofuku, M. Sato, N. Nobuyama, K. Kondo, Y. Shiraishi, T. Mizumura, K. Onishi, M. Natsume, M. Maeda, H. Tsujishita, T. Kuranaga, M. Inoue, I. Shimada, Identification of a Conformational Equilibrium That Determines the Efficacy and Functional Selectivity of the μ-Opioid Receptor, Angew Chem Int Ed Engl, 54 (2015) 15771–15776.

[438] Y. Kofuku, T. Yokomizo, S. Imai, Y. Shiraishi, M. Natsume, H. Itoh, M. Inoue, K. Nakata, S. Igarashi, H. Yamaguchi, T. Mizukoshi, E.-I. Suzuki, T. Ueda, I. Shimada, Deuteration and selective labeling of alanine methyl groups of β2-adrenergic receptor expressed in a baculovirus-insect cell expression system, J Biomol NMR, 71 (2018) 185–192.

[439] A. Dubey, N. Stoyanov, T. Viennet, S. Chhabra, S. Elter, J. Borggräfe, A. Viegas, R.P. Nowak, N. Burdzhiev, O. Petrov, E.S. Fischer, M. Etzkorn, V. Gelev, H. Arthanari, Local Deuteration Enables NMR Observation of Methyl Groups in Proteins from Eukaryotic and Cell-Free Expression Systems, Angewandte Chemie - International Edition, 60 (2021) 13783–13787.

[440] R.S. Prosser, T.H. Kim, Nuts and Bolts of CF3 and CH 3 NMR Toward the Understanding of Conformational Exchange of GPCRs, Methods Mol Biol, 1335 (2015) 39–51.

[441] A. Boeszoermenyi, S. Chhabra, A. Dubey, D.L. Radeva, N.T. Burdzhiev, C.D. Chanev, O.I. Petrov, V.M. Gelev, M. Zhang, C. Anklin, H. Kovacs, G. Wagner, I. Kuprov, K. Takeuchi, H. Arthanari, Aromatic 19F-13C TROSY: a background-free approach to probe biomolecular structure, function, and dynamics, Nat Methods, 16 (2019) 333–340.

[442] J.K. Watts, N. Martín-Pintado, I. Gómez-Pinto, J. Schwartzentruber, G. Portella, M. Orozco, C. González, M.J. Damha, Differential stability of 2′F-ANA•RNA and ANA•RNA hybrid duplexes: roles of structure, pseudohydrogen bonding, hydration, ion uptake and flexibility, Nucleic Acids Research, 38 (2010) 2498–2511.

[443] J.L. Kitevski-LeBlanc, M.S. Al-Abdul-Wahid, R.S. Prosser, A Mutagenesis-Free Approach to Assignment of 19F NMR Resonances in Biosynthetically Labeled Proteins, J. Am. Chem. Soc., 131 (2009) 2054–2055.

[444] M. Lu, R. Ishima, T. Polenova, A.M. Gronenborn, 19F NMR relaxation studies of fluorosubstituted tryptophans, J Biomol NMR, 73 (2019) 401–409.

[445] J.W. Peng, Cross-Correlated 19F Relaxation Measurements for the Study of Fluorinated Ligand–Receptor Interactions, Journal of Magnetic Resonance, 153 (2001) 32–47.

[446] J.H. Overbeck, W. Kremer, R. Sprangers, A suite of 19F based relaxation dispersion experiments to assess biomolecular motions, J Biomol NMR, 74 (2020) 753–766.

[447] M.T. Eddy, T. Didenko, R.C. Stevens, K. Wüthrich, β2-Adrenergic Receptor Conformational Response to Fusion Protein in the Third Intracellular Loop, Structure, 24 (2016) 2190–2197.

[448] R. Horst, J.J. Liu, R.C. Stevens, K. Wüthrich, β -adrenergic receptor activation by agonists studied with ^{19}F NMR spectroscopy, Angew Chem Int Ed Engl, 52 (2013) 10762–10765.

[449] J.J. Liu, R. Horst, V. Katritch, R.C. Stevens, K. Wüthrich, Biased signaling pathways in β2-adrenergic receptor characterized by 19F-NMR, Science, 335 (2012) 1106–1110.

[450] T.H. Kim, K.Y. Chung, A. Manglik, A.L. Hansen, R.O. Dror, T.J. Mildorf, D.E. Shaw, B.K. Kobilka, R.S. Prosser, The Role of Ligands on the Equilibria Between Functional States of a G Protein-Coupled Receptor, J. Am. Chem. Soc., 135 (2013) 9465–9474.

[451] L. Ye, S.T. Larda, Y.F. Frank Li, A. Manglik, R.S. Prosser, A comparison of chemical shift sensitivity of trifluoromethyl tags: optimizing resolution in ^{19}F NMR studies of proteins, J Biomol NMR, 62 (2015) 97–103.

[452] A. Manglik, T.H. Kim, M. Masureel, C. Altenbach, Z. Yang, D. Hilger, M.T. Lerch, T.S. Kobilka, F.S. Thian, W.L. Hubbell, R.S. Prosser, B.K. Kobilka, Structural Insights into the Dynamic Process of β2-Adrenergic Receptor Signaling, Cell, 161 (2015) 1101–1111.

[453] L. Ye, N. Van Eps, M. Zimmer, O.P. Ernst, R.S. Prosser, Activation of the A2A adenosine G-protein-coupled receptor by conformational selection, Nature, 533 (2016) 265–268.

[454] S.K. Huang, A. Pandey, D.P. Tran, N.L. Villanueva, A. Kitao, R.K. Sunahara, A. Sljoka, R.S. Prosser, Delineating the conformational landscape of the adenosine A2A receptor during G protein coupling, Cell, 184 (2021) 1884-1894.e14.

[455] D. Liu, K. Wüthrich, Ring current shifts in (19)F-NMR of membrane proteins, J Biomol NMR, 65 (2016) 1–5.

[456] L. Liu, I.-J.L. Byeon, I. Bahar, A.M. Gronenborn, Domain Swapping Proceeds via Complete Unfolding: A 19F- and 1H-NMR Study of the Cyanovirin-N Protein, J. Am. Chem. Soc., 134 (2012) 4229–4235.

[457] Y. Hou, W. Hu, X. Li, J.J. Skinner, D. Liu, K. Wüthrich, Solvent-accessibility of discrete residue positions in the polypeptide hormone glucagon by 19F-NMR observation of 4-fluorophenylalanine, J Biomol NMR, 68 (2017) 1–6.

[458] L.B.T. Pham, A. Costantino, L. Barbieri, V. Calderone, E. Luchinat, L. Banci, Direct Expression of Fluorinated Proteins in Human Cells for 19F In-Cell NMR Spectroscopy, J. Am. Chem. Soc., 145 (2023) 1389–1399.

[459] F. Yang, X. Yu, C. Liu, C.-X. Qu, Z. Gong, H.-D. Liu, F.-H. Li, H.-M. Wang, D.-F. He, F. Yi, C. Song, C.-L. Tian, K.-H. Xiao, J.-Y. Wang, J.-P. Sun, Phospho-selective mechanisms of arrestin conformations and functions revealed by unnatural amino acid incorporation and 19F-NMR, Nat Commun, 6 (2015) 8202.

[460] X. Wang, D. Liu, L. Shen, F. Li, Y. Li, L. Yang, T. Xu, H. Tao, D. Yao, L. Wu, K. Hirata, L.M. Bohn, A. Makriyannis, X. Liu, T. Hua, Z.-J. Liu, J. Wang, A Genetically Encoded F-19 NMR Probe Reveals the Allosteric Modulation Mechanism of Cannabinoid Receptor 1, J. Am. Chem. Soc., 143 (2021) 16320–16325.

[461] M.R. Elkins, J.K. Williams, M.D. Gelenter, P. Dai, B. Kwon, I.V. Sergeyev, B.L. Pentelute, M. Hong, Cholesterol-binding site of the influenza M2 protein in lipid bilayers from solid-state NMR, Proc Natl Acad Sci U S A, 114 (2017) 12946–12951.

[462] N. Tran, Y. Oh, M. Sutherland, Q. Cui, M. Hong, Cholesterol-Mediated Clustering of the HIV Fusion Protein gp41 in Lipid Bilayers, J Mol Biol, 434 (2022) 167345.

[463] A.A. Shcherbakov, G. Hisao, V.S. Mandala, N.E. Thomas, M. Soltani, E.A. Salter, J.H. Davis, K.A. Henzler-Wildman, M. Hong, Structure and dynamics of the drug-bound bacterial transporter EmrE in lipid bilayers, Nat Commun, 12 (2021) 172.

[464] M. Lu, M. Wang, I.V. Sergeyev, C.M. Quinn, J. Struppe, M. Rosay, W. Maas, A.M. Gronenborn, T. Polenova, 19F Dynamic Nuclear Polarization at Fast Magic Angle Spinning for NMR of HIV-1 Capsid Protein Assemblies, J. Am. Chem. Soc., 141 (2019) 5681–5691.

[465] K.K. Frederick, V.K. Michaelis, B. Corzilius, T.-C. Ong, A.C. Jacavone, R.G. Griffin, S. Lindquist, Sensitivity-Enhanced NMR Reveals Alterations in Protein Structure by Cellular Milieus, Cell, 163 (2015) 620–628.

[466] M. Kaplan, A. Cukkemane, G.C.P. van Zundert, S. Narasimhan, M. Daniëls, D. Mance, G. Waksman, A.M.J.J. Bonvin, R. Fronzes, G.E. Folkers, M. Baldus, Probing a cell-embedded megadalton protein complex by DNP-supported solid-state NMR, Nat Methods, 12 (2015) 649–652.

[467] N.T. Tran, F. Mentink-Vigier, J.R. Long, Dynamic Nuclear Polarization of Biomembrane Assemblies, Biomolecules, 10 (2020) 1246.

[468] A.P. Jagtap, M.-A. Geiger, D. Stöppler, M. Orwick-Rydmark, H. Oschkinat, S.T. Sigurdsson, bcTol: a highly water-soluble biradical for efficient dynamic nuclear polarization of biomolecules, Chem. Commun., 52 (2016) 7020–7023.

[469] D.J. Kubicki, G. Casano, M. Schwarzwälder, S. Abel, C. Sauvée, K. Ganesan, M. Yulikov, A.J. Rossini, G. Jeschke, C. Copéret, A. Lesage, P. Tordo, O. Ouari, L. Emsley, Rational design of dinitroxide biradicals for efficient cross-effect dynamic nuclear polarization, Chem. Sci., 7 (2015) 550–558.

[470] A. Lund, G. Casano, G. Menzildjian, M. Kaushik, G. Stevanato, M. Yulikov, R. Jabbour, D. Wisser, M. Renom-Carrasco, C. Thieuleux, F. Bernada, H. Karoui, D. Siri, M. Rosay, I.V. Sergeyev, D. Gajan, M. Lelli, L. Emsley, O. Ouari, A. Lesage, TinyPols: a family of water-soluble binitroxides tailored for dynamic nuclear polarization enhanced NMR spectroscopy at 188 and 211 T, Chem. Sci., 11 (2020) 2810–2818.

[471] T. Viennet, A. Viegas, A. Kuepper, S. Arens, V. Gelev, O. Petrov, T.N. Grossmann, H. Heise, M. Etzkorn, Selective Protein Hyperpolarization in Cell Lysates Using Targeted Dynamic Nuclear Polarization, Angew Chem Int Ed Engl, 55 (2016) 10746–10750.

[472] D. Gauto, O. Dakhlaoui, I. Marin-Montesinos, S. Hediger, G.D. Paëpe, Targeted DNP for biomolecular solid-state NMR, Chem. Sci., 12 (2021) 6223–6237.

[473] J. Heiliger, T. Matzel, E.C. Çetiner, H. Schwalbe, G. Kuenze, B. Corzilius, Site-specific dynamic nuclear polarization in a Gd(III)-labeled protein, Phys. Chem. Chem. Phys., 22 (2020) 25455–25466.

[474] M.A. Voinov, D.B. Good, M.E. Ward, S. Milikisiyants, A. Marek, M.A. Caporini, M. Rosay, R.A. Munro, M. Ljumovic, L.S. Brown, V. Ladizhansky, A.I. Smirnov, Cysteine-Specific Labeling of Proteins with a Nitroxide Biradical for Dynamic Nuclear Polarization NMR, J. Phys. Chem. B, 119 (2015) 10180–10190.

[475] L.B. Andreas, A.B. Barnes, B. Corzilius, J.J. Chou, E.A. Miller, M. Caporini, M. Rosay, R.G. Griffin, Dynamic Nuclear Polarization Study of Inhibitor Binding to the M218–60 Proton Transporter from Influenza A, Biochemistry, 52 (2013) 2774–2782.

[476] C. Fernández-de-Alba, H. Takahashi, A. Richard, Y. Chenavier, L. Dubois, V. Maurel, D. Lee, S. Hediger, G. De Paëpe, Matrix-free DNP-enhanced NMR spectroscopy of liposomes using a lipid-anchored biradical, Chemistry, 21 (2015) 4512–4517.

[477] D.B. Good, M.A. Voinov, D. Bolton, M.E. Ward, I.V. Sergeyev, M. Caporini, P. Scheffer, A. Lo, M. Rosay, A. Marek, L.S. Brown, A.I. Smirnov, V. Ladizhansky, A biradical-tagged phospholipid as a polarizing agent for solid-state MAS Dynamic Nuclear Polarization NMR of membrane proteins, Solid State Nucl Magn Reson, 100 (2019) 92–101.

[478] A.N. Smith, M.A. Caporini, G.E. Fanucci, J.R. Long, A method for dynamic nuclear polarization enhancement of membrane proteins, Angew Chem Int Ed Engl, 54 (2015) 1542–1546.

[479] R. Rogawski, I.V. Sergeyev, Y. Li, M.F. Ottaviani, V. Cornish, A.E. McDermott, Dynamic Nuclear Polarization Signal Enhancement with High-Affinity Biradical Tags, J Phys Chem B, 121 (2017) 1169–1175.

[480] M.-A. Sani, S. Zhu, V. Hofferek, F. Separovic, Nitroxide spin-labeled peptides for DNP-NMR in-cell studies, FASEB J, 33 (2019) 11021–11027.

[481] S. Zhu, E. Kachooei, J.R. Harmer, L.J. Brown, F. Separovic, M.-A. Sani, TOAC spin-labeled peptides tailored for DNP-NMR studies in lipid membrane environments, Biophysical Journal, 120 (2021) 4501–4511.

[482] S. Narasimhan, S. Scherpe, A. Lucini Paioni, J. van der Zwan, G.E. Folkers, H. Ovaa, M. Baldus, DNP-Supported Solid-State NMR Spectroscopy of Proteins Inside Mammalian Cells, Angewandte Chemie International Edition, 58 (2019) 12969–12973.

[483] R. Ghosh, R. Dumarieh, Y. Xiao, K.K. Frederick, Stability of the nitroxide biradical AMUPol in intact and lysed mammalian cells, Journal of Magnetic Resonance, 336 (2022) 107150.

[484] K.M. McCoy, R. Rogawski, O. Stovicek, A.E. McDermott, Stability of nitroxide biradical TOTAPOL in biological samples, Journal of Magnetic Resonance, 303 (2019) 115–120.

[485] B.J. Albert, C. Gao, E.L. Sesti, E.P. Saliba, N. Alaniva, F.J. Scott, S.Th. Sigurdsson, A.B. Barnes, Dynamic Nuclear Polarization Nuclear Magnetic Resonance in Human Cells Using Fluorescent Polarizing Agents, Biochemistry, 57 (2018) 4741–4746.

[486] R. Ghosh, Y. Xiao, J. Kragelj, K.K. Frederick, In-Cell Sensitivity-Enhanced NMR of Intact Viable Mammalian Cells, J. Am. Chem. Soc., 143 (2021) 18454–18466.

[487] R. Fredriksson, M.C. Lagerström, L.G. Lundin, H.B. Schiöth, The G-protein-coupled receptors in the human genome form five main families Phylogenetic analysis, paralogon groups, and fingerprints, Molecular Pharmacology, 63 (2003) 1256–1272.

[488] D. Hilger, The role of structural dynamics in GPCR mediated signaling, FEBS J, 288 (2021) 2461–2489.

[489] A.L. Aloia, R.V. Glatz, E.J. McMurchie, W.R. Leifert, GPCR Expression Using Baculovirus-Infected Sf9 Cells, in: W.R. Leifert (Ed.), G Protein-Coupled Receptors in Drug Discovery, Humana Press, Totowa, NJ, 2009: pp. 115–129.

[490] Y. Kofuku, T. Ueda, J. Okude, Y. Shiraishi, K. Kondo, M. Maeda, H. Tsujishita, I. Shimada, Efficacy of the β -adrenergic receptor is determined by conformational equilibrium in the transmembrane region, Nat Commun, 3 (2012) 1045.

[491] T. Warne, J. Chirnside, G.F.X. Schertler, Expression and purification of truncated, non-glycosylated turkey beta-adrenergic receptors for crystallization, Biochim Biophys Acta, 1610 (2003) 133–140.

[492] D.N. Wiseman, A. Otchere, J.H. Patel, R. Uddin, N.L. Pollock, S.J. Routledge, A.J. Rothnie, C. Slack, D.R. Poyner, R.M. Bill, A.D. Goddard, Expression and purification of recombinant G protein-coupled receptors: A review, Protein Expression and Purification, 167 (2020) 105524.

[493] E.H. Schneider, R. Seifert, Sf9 cells: a versatile model system to investigate the pharmacological properties of G protein-coupled receptors, Pharmacol Ther, 128 (2010) 387–418.

[494] A.D. Gossert, W. Jahnke, Isotope Labeling in Insect Cells, in: H.S. Atreya (Ed.), Isotope Labeling in Biomolecular NMR, Springer Netherlands, Dordrecht, 2012: pp. 179–196.

[495] A. Sitarska, L. Skora, J. Klopp, S. Roest, C. Fernández, B. Shrestha, A.D. Gossert, Affordable uniform isotope labeling with 2H, 13C and 15N in insect cells, Journal of Biomolecular NMR, 62 (2015) 191–197.

[496] B. Franke, C. Opitz, S. Isogai, A. Grahl, L. Delgado, A.D. Gossert, S. Grzesiek, Production of isotope-labeled proteins in insect cells for NMR, J Biomol NMR, 71 (2018) 173–184.

[497] R. Santos, O. Ursu, A. Gaulton, A.P. Bento, R.S. Donadi, C.G. Bologa, A. Karlsson, B. Al-Lazikani, A. Hersey, T.I. Oprea, J.P. Overington, A comprehensive map of molecular drug targets, Nature Reviews Drug Discovery, 16 (2016) 19–34.

[498] F. Mahler, A. Meister, C. Vargas, G. Durand, S. Keller, Self-Assembly of Protein-Containing Lipid-Bilayer Nanodiscs from Small-Molecule Amphiphiles, Small, 17 (2021) e2103603.

[499] S.R. Tonge, B.J. Tighe, Responsive hydrophobically associating polymers: a review of structure and properties, Adv Drug Deliv Rev, 53 (2001) 109–122.

[500] H.J. Lee, M. Ehsan, X. Zhang, S. Katsube, C.F. Munk, H. Wang, W. Ahmed, A. Kumar, B. Byrne, C.J. Loland, L. Guan, X. Liu, P.S. Chae, Development of 1,3-acetonedicarboxylate-derived glucoside amphiphiles (ACAs) for membrane protein study, Chem. Sci., 13 (2022) 5750–5759.

[501] T.J. Knowles, R. Finka, C. Smith, Y.-P. Lin, T. Dafforn, M. Overduin, Membrane proteins solubilized intact in lipid containing nanoparticles bounded by styrene maleic acid copolymer, J Am Chem Soc, 131 (2009) 7484–7485.

[502] J.M. Dörr, S. Scheidelaar, M.C. Koorengevel, J.J. Dominguez, M. Schäfer, C.A. van Walree, J.A. Killian, The styrene-maleic acid copolymer: a versatile tool in membrane research, Eur Biophys J, 45 (2016) 3–21.

[503] A. Olerinyova, A. Sonn-Segev, J. Gault, C. Eichmann, J. Schimpf, A.H. Kopf, L.S.P. Rudden, D. Ashkinadze, R. Bomba, L. Frey, J. Greenwald, M.T. Degiacomi, R. Steinhilper, J.A. Killian, T. Friedrich, R. Riek, W.B. Struwe, P. Kukura, Mass Photometry of Membrane Proteins, Chem, 7 (2021) 224–236.

[504] N.L. Pollock, J. Lloyd, C. Montinaro, M. Rai, T.R. Dafforn, Conformational trapping of an ABC transporter in polymer lipid nanoparticles, Biochem J, 479 (2022) 145–159.

[505] V.M. Luna, M. Vazir, A. Vaish, S. Chong, I. Chen, H.K. Yamane, Generation of membrane proteins in polymer-based lipoparticles as flow cytometry antigens, European Polymer Journal, 109 (2018) 483–488.

[506] H.A. Lashuel, C.R. Overk, A. Oueslati, E. Masliah, The many faces of α-synuclein: from structure and toxicity to therapeutic target, Nat Rev Neurosci, 14 (2013) 38–48.

[507] H. Gang, C. Galvagnion, G. Meisl, T. Müller, M. Pfammatter, A.K. Buell, A. Levin, C.M. Dobson, B. Mu, T.P.J. Knowles, Microfluidic Diffusion Platform for Characterizing the Sizes of Lipid Vesicles and the Thermodynamics of Protein-Lipid Interactions, Anal Chem, 90 (2018) 3284–3290.

[508] L. Macikova, V. Sinica, A. Kadkova, S. Villette, A. Ciaccafava, J. Faherty, S. Lecomte, I.D. Alves, V. Vlachova, Putative interaction site for membrane phospholipids controls activation of TRPA1 channel at physiological membrane potentials, FEBS J, 286 (2019) 3664–3683.

[509] M. Azouz, M. Gonin, S. Fiedler, J. Faherty, M. Decossas, C. Cullin, S. Villette, M. Lafleur, I. D Alves, S. Lecomte, A. Ciaccafava, Microfluidic diffusional sizing probes lipid nanodiscs formation, Biochim Biophys Acta Biomembr, 1862 (2020) 183215.

[510] P. Arosio, T. Müller, L. Rajah, E.V. Yates, F.A. Aprile, Y. Zhang, S.I.A. Cohen, D.A. White, T.W. Herling, E.J. De Genst, S. Linse, M. Vendruscolo, C.M. Dobson, T.P.J. Knowles, Microfluidic diffusion analysis of the sizes and interactions of proteins under native solution conditions, ACS Nano, 10 (2016) 333–341.

[511] M. Falke, J. Victor, M.M. Wördehoff, A. Peduzzo, T. Zhang, G.F. Schröder, A.K. Buell, W. Hoyer, M. Etzkorn, α-Synuclein-derived lipoparticles in the study of α-Synuclein amyloid fibril formation, Chemistry and Physics of Lipids, 220 (2019) 57–65.

[512] D. Sulzer, R.H. Edwards, The physiological role of α-synuclein and its relationship to Parkinson's Disease, J Neurochem, 150 (2019) 475–486.

[513] B.D. van Rooijen, M.M.A.E. Claessens, V. Subramaniam, Lipid bilayer disruption by oligomeric alpha-synuclein depends on bilayer charge and accessibility of the hydrophobic core, Biochim Biophys Acta, 1788 (2009) 1271–1278.

[514] G. Fusco, A. De Simone, T. Gopinath, V. Vostrikov, M. Vendruscolo, C.M. Dobson, G. Veglia, Direct observation of the three regions in α-synuclein that determine its membrane-bound behaviour, Nat Commun, 5 (2014) 3827.

[515] L. Fonseca-Ornelas, S.E. Eisbach, M. Paulat, K. Giller, C.O. Fernández, T.F. Outeiro, S. Becker, M. Zweckstetter, Small molecule-mediated stabilization of vesicle-associated helical α-synuclein inhibits pathogenic misfolding and aggregation, Nat Commun, 5 (2014) 5857.

[516] P.F. Verhallen, R.A. Demel, H. Zwiers, W.H. Gispen, Adrenocorticotropic hormone (ACTH)-lipid interactions Implications for involvement of amphipathic helix formation, Biochim Biophys Acta, 775 (1984) 246–254.

[517] A. Stevens, A. White, ACTH: cellular peptide hormone synthesis and secretory pathways, Results Probl Cell Differ, 50 (2010) 63–84.

[518] Z. Zhang, T.J. Melia, F. He, C. Yuan, A. McGough, M.F. Schmid, T.G. Wensel, How a G protein binds a membrane, J Biol Chem, 279 (2004) 33937–33945.

[519] T.S. Ulmer, A. Bax, N.B. Cole, R.L. Nussbaum, Structure and dynamics of micelle-bound human alpha-synuclein, J Biol Chem, 280 (2005) 9595–9603.

[520] M.C. Lagerström, H.B. Schiöth, Structural diversity of G protein-coupled receptors and significance for drug discovery, Nat Rev Drug Discov, 7 (2008) 339–357.

[521] A. Bernard, I.O. Naharros, X. Yue, F. Mifsud, A. Blake, F. Bourgain-Guglielmetti, J. Ciprin, S. Zhang, E. McDaid, K. Kim, M.V. Nachury, J.F. Reiter, C. Vaisse, MRAP2 regulates energy homeostasis by promoting primary cilia localization of MC4R, JCI Insight, 8 (2023).

[522] M. Ghamari-Langroudi, G.J. Digby, J.A. Sebag, G.L. Millhauser, R. Palomino, R. Matthews, T. Gillyard, B.L. Panaro, I.R. Tough, H.M. Cox, J.S. Denton, R.D. Cone, G-protein-independent coupling of MC4R to Kir71 in hypothalamic neurons, Nature, 520 (2015) 94–98.

[523] F. Hagn, M.L. Nasr, G. Wagner, Assembly of phospholipid nanodiscs of controlled size for structural studies of membrane proteins by NMR, Nature Protocols, 13 (2018) 79–98.

[524] X. Prasanna, M. Mohole, A. Chattopadhyay, D. Sengupta, Role of cholesterol-mediated effects in GPCR heterodimers, Chemistry and Physics of Lipids, 227 (2020) 104852.

[525] D. Glueck, A. Grethen, M. Das, O.P. Mmeka, E.P. Patallo, A. Meister, R. Rajender, S. Kins, M. Räschle, J. Victor, C. Chu, M. Etzkorn, Z. Köck, F. Bernhard, J.O. Babalola, C. Vargas, S. Keller, Electroneutral

Polymer Nanodiscs Enable Interference-Free Probing of Membrane Proteins in a Lipid-Bilayer Environment, Small, (2022).

[526] K. Gao, R. Oerlemans, M.R. Groves, Theory and applications of differential scanning fluorimetry in early-stage drug discovery, Biophys Rev, 12 (2020) 85–104.

[527] G. Chattopadhyay, R. Varadarajan, Facile measurement of protein stability and folding kinetics using a nano differential scanning fluorimeter, Protein Sci, 28 (2019) 1127–1134.

[528] S.A.I. Seidel, P.M. Dijkman, W.A. Lea, G. van den Bogaart, M. Jerabek-Willemsen, A. Lazic, J.S. Joseph, P. Srinivasan, P. Baaske, A. Simeonov, I. Katritch, F.A. Melo, J.E. Ladbury, G. Schreiber, A. Watts, D. Braun, S. Duhr, Microscale thermophoresis quantifies biomolecular interactions under previously challenging conditions, Methods, 59 (2013) 301–315.

[529] D.E. Otzen, A.K. Buell, H. Jensen, Microfluidics and the quantification of biomolecular interactions, Current Opinion in Structural Biology, 70 (2021) 8–15.

[530] M. Zhang, M. Gui, Z.-F. Wang, C. Gorgulla, J.J. Yu, H. Wu, Z.-Y.J. Sun, C. Klenk, L. Merklinger, L. Morstein, F. Hagn, A. Plückthun, A. Brown, M.L. Nasr, G. Wagner, Cryo-EM structure of an activated GPCR-G protein complex in lipid nanodiscs, Nat Struct Mol Biol, 28 (2021) 258–267.

[531] A.M. Knepp, A. Grunbeck, S. Banerjee, T.P. Sakmar, T. Huber, Direct Measurement of Thermal Stability of Expressed CCR5 and Stabilization by Small Molecule Ligands, Biochemistry, 50 (2011) 502–511.

[532] D.J. MacNeil, A.D. Howard, X. Guan, T.M. Fong, R.P. Nargund, M.A. Bednarek, M.T. Goulet, D.H. Weinberg, A.M. Strack, D.J. Marsh, H.Y. Chen, C.P. Shen, A.S. Chen, C.I. Rosenblum, T. MacNeil, M. Tota, E.D. MacIntyre, L.H.T. Van der Ploeg, The role of melanocortins in body weight regulation: opportunities for the treatment of obesity, European Journal of Pharmacology, 450 (2002) 93–109.

[533] K.Y. Chung, T.H. Kim, A. Manglik, R. Alvares, B.K. Kobilka, R.S. Prosser, Role of Detergents in Conformational Exchange of a G Protein-coupled Receptor, J Biol Chem, 287 (2012) 36305–36311.

[534] S. Lee, A. Mao, S. Bhattacharya, N. Robertson, R. Grisshammer, C.G. Tate, N. Vaidehi, How Do Short Chain Nonionic Detergents Destabilize G-Protein-Coupled Receptors?, Journal of the American Chemical Society, 138 (2016) 15425–15433.

[535] S. Lee, S. Ghosh, S. Jana, N. Robertson, C.G. Tate, N. Vaidehi, How Do Branched Detergents Stabilize GPCRs in Micelles?, Biochemistry, 59 (2020) 2125–2134.

[536] M. Zocher, C. Zhang, S.G.F. Rasmussen, B.K. Kobilka, D.J. Müller, Cholesterol increases kinetic, energetic, and mechanical stability of the human β2-adrenergic receptor, Proceedings of the National Academy of Sciences, 109 (2012) E3463–E3472.

[537] A.N. Naranjo, P.M. McNeely, J. Katsaras, A.S. Robinson, Impact of purification conditions and history on A2A adenosine receptor activity: The role of CHAPS and lipids, Protein Expr Purif, 124 (2016) 62–67.

[538] S. Inagaki, R. Ghirlando, J.F. White, J. Gvozdenovic-Jeremic, J.K. Northup, R. Grisshammer, Modulation of the interaction between neurotensin receptor NTS1 and Gq protein by lipid, Journal of Molecular Biology, 417 (2012) 95–111.

[539] D.Y. Zhao, M. Pöge, T. Morizumi, S. Gulati, N. Van Eps, J. Zhang, P. Miszta, S. Filipek, J. Mahamid, J.M. Plitzko, W. Baumeister, O.P. Ernst, K. Palczewski, Cryo-EM structure of the native rhodopsin dimer in nanodiscs, Journal of Biological Chemistry, 294 (2019) 14215–14230.

[540] R. Dawaliby, C. Trubbia, C. Delporte, M. Masureel, P. Van Antwerpen, B.K. Kobilka, C. Govaerts, Allosteric regulation of G protein-coupled receptor activity by phospholipids, Nature Chemical Biology, 12 (2016) 35–39.

[541] M.J. Strohman, S. Maeda, D. Hilger, M. Masureel, Y. Du, B.K. Kobilka, Local membrane charge regulates β2 adrenergic receptor coupling to Gi3, Nature Communications, 10 (2019) 1–10.

[542] K.E. Komolov, Y. Du, N.M. Duc, R.M. Betz, J.P.G.L.M. Rodrigues, R.D. Leib, D. Patra, G. Skiniotis, C.M. Adams, R.O. Dror, K.Y. Chung, B.K. Kobilka, J.L. Benovic, Structural and Functional Analysis of a β2-Adrenergic Receptor Complex with GRK5, Cell, 169 (2017) 407-421.e16.

[543] D.P. Staus, H. Hu, M.J. Robertson, A.L.W. Kleinhenz, L.M. Wingler, W.D. Capel, N.R. Latorraca, R.J. Lefkowitz, G. Skiniotis, Structure of the M2 muscarinic receptor–β-arrestin complex in a lipid nanodisc, Nature, 579 (2020) 297–302.

[544] Y.-H.M. Chan, S.G. Boxer, Model Membrane Systems and Their Applications State of the field, Current Opinion in Chemical Biology, 11 (2007) 581–587.

[545] Y. Liu, E.C.C.M. Moura, J.M. Dörr, S. Scheidelaar, M. Heger, M.R. Egmond, J. Antoinette Killian, T. Mohammadi, E. Breukink, Bacillus subtilis MraY in detergent-free system of nanodiscs wrapped by styrene-maleic acid copolymers, PLoS ONE, 13 (2018) 1–18.

[546] M. Barniol-Xicota, S.H.L. Verhelst, Stable and Functional Rhomboid Proteases in Lipid Nanodiscs by Using Diisobutylene/Maleic Acid Copolymers, Journal of the American Chemical Society, 140 (2018) 14557–14561.

[547] A.A. Gulamhussein, R. Uddin, B.J. Tighe, D.R. Poyner, A.J. Rothnie, A comparison of SMA (styrene maleic acid) and DIBMA (di-isobutylene maleic acid) for membrane protein purification, Biochimica et Biophysica Acta - Biomembranes, 1862 (2020) 183281.

[548] V.J. Flegler, A. Rasmussen, S. Rao, N. Wu, R. Zenobi, M.S.P. Sansom, R. Hedrich, T. Rasmussen, B. Böttcher, The MscS-like channel YnaI has a gating mechanism based on flexible pore helices, Proceedings of the National Academy of Sciences of the United States of America, 117 (2020) 28754–28762.

[549] P. Gill, T.T. Moghadam, B. Ranjbar, Differential scanning calorimetry techniques: Applications in biology and nanoscience, Journal of Biomolecular Techniques, 21 (2010) 167–193.

[550] J.C.W. Corbett, M.T. Connah, K. Mattison, Advances in the measurement of protein mobility using laser Doppler electrophoresis – the diffusion barrier technique, ELECTROPHORESIS, 32 (2011) 1787–1794.

[551] J. Lenz, A.H. Larsen, S. Keller, A. Luchini, Effect of Cholesterol on the Structure and Composition of Glyco-DIBMA Lipid Particles, Langmuir, 39 (2023) 3569–3579.

[552] M.J. Agulleiro, R. Cortés, B. Fernández-Durán, S. Navarro, R. Guillot, E. Meimaridou, A.J.L. Clark, J.M. Cerdá-Reverter, Melanocortin 4 receptor becomes an ACTH receptor by coexpression of melanocortin receptor accessory protein 2, Molecular Endocrinology, 27 (2013) 1934–1945.

[553] M. Jamshad, V. Grimard, I. Idini, T.J. Knowles, M.R. Dowle, N. Schofield, P. Sridhar, Y. Lin, R. Finka, M. Wheatley, O.R.T. Thomas, R.E. Palmer, M. Overduin, C. Govaerts, J.M. Ruysschaert, K.J. Edler, T.R. Dafforn, Structural analysis of a nanoparticle containing a lipid bilayer used for detergent-free extraction of membrane proteins, Nano Research, 8 (2015) 774–789.

[554] V. Postis, S. Rawson, J.K. Mitchell, S.C. Lee, R.A. Parslow, T.R. Dafforn, S.A. Baldwin, S.P. Muench, The use of SMALPs as a novel membrane protein scaffold for structure study by negative stain electron microscopy, Biochimica et Biophysica Acta - Biomembranes, 1848 (2015) 496–501.

[555] S.C. Lee, R. Collins, Y. pin Lin, M. Jamshad, C. Broughton, S.A. Harris, B.S. Hanson, C. Tognoloni, R.A. Parslow, A.E. Terry, A. Rodger, C.J. Smith, K.J. Edler, R. Ford, D.I. Roper, T.R. Dafforn, Nano-encapsulated Escherichia coli Divisome Anchor ZipA, and in Complex with FtsZ, Scientific Reports, 9 (2019) 1–16.

[556] A. Mattarei, M. Azzolini, M. Zoratti, L. Biasutto, C. Paradisi, N-Monosubstituted Methoxy-oligo(ethylene glycol) Carbamate Ester Prodrugs of Resveratrol, Molecules, 20 (2015) 16085–16102.

[557] B. Fateley, PUDDLE, in: D. Lin-Vien, N.B. Colthup, W.G. Fateley, J.G. Grasselli (Eds.), The Handbook of Infrared and Raman Characteristic Frequencies of Organic Molecules, Academic Press, San Diego, 1991: p. vi.

[558] G. Socrates, Infrared and Raman characteristic group frequencies: tables and charts, John Wiley & Sons, 2004.

Eidesstattliche Versicherung

Ich versichere an Eides Statt, dass die Dissertation von mir selbständig und ohne unzulässige fremde Hilfe unter Beachtung der Grundsätze zur Sicherung guter wissenschaftlicher Praxis an der Heinrich-Heine-Universität Düsseldorf erstellt worden ist.

Ich versichere, dass die eingereichte schriftliche Fassung der auf dem beigefügten Medium gespeicherten Fassung entspricht.

Düsseldorf 18.04.2024 — Datum, Ort

Ci Chu — Ci Chu